FLJ22318: A Novel Binding Partner of the NKX3-1 Homeodomain Protein in Prostate Cancer Cells

Linda Fiona Dawson

B.Sc. (Hons)

This thesis is presented for the degree of Doctor of Philosophy of Murdoch University, October 2006

School of Biological Sciences & Biotechnology, Murdoch University,
Perth, Western Australia

I declare that this thesis is my own account of my research and contains as its main content work which has not previously been submitted for a degree at any tertiary education institution.

.....

Linda Fiona Dawson

Thesis Summary

Prostate cancer is a frequently diagnosed malignancy which ranges from an indolent asymptomatic tumour to an aggressive, rapidly lethal systemic disease. Determination of chromosomal, genetic and epigenetic alterations associated with prostate carcinogenesis have led to the characterisation of functional consequences of these alterations, thereby elucidating pathways contributing to malignant growth that can be utilised clinically and therapeutically.

FLJ22318 is a novel hypothetical protein that was identified by yeast two-hybrid analysis to interact with the prostatic homeodomain protein, NKX3-1. Expression of NKX3-1 is largely restricted to epithelial cells of the adult prostate where it is involved in maintaining the prostatic phenotype, while NKX3-1 expression is reduced or absent in prostate tumours. In contrast, FLJ22318 expression is documented in cDNA libraries derived from a variety of human adult and foetal tissues including the prostate, suggesting that it may be ubiquitously expressed and that it potentially interacts with a number of proteins in addition to NKX3-1. FLJ22318 expression is undocumented in human prostate tumours.

Bioinformatic analyses have postulated multiple FLJ22318 mRNA transcripts however the proposed open reading frames encoded by these transcripts predict the FLJ22318 protein to contain three strong protein-protein interaction domains, a Lissencephaly type-1-like homology (LisH), a C-terminal to LisH (CTLH) and a CT11-RanBPM (CRA) domain. Of the 44 single nucleotide polymorphisms identified within the *FLJ22318* gene, none are located within the protein coding region suggesting that FLJ22318 may be critical for cell survival and/or function. Comparison of the amino acid sequence between human FLJ22318 and its orthologues in a diverse range of mammalian species identified >97% sequence homology, providing further strong evidence of the critical cellular function of FLJ22318.

To characterise the biological activity of FLJ22318 in prostate cancer cells, the FLJ22318 coding region was amplified by polymerase chain reaction (PCR) and ligated into mammalian and bacterial expression vectors to encode V5-, myc-, GFP-, HA-, and

GST-FLJ22318 fusion proteins. Interaction between FLJ22318 and NKX3-1 was confirmed using (reverse) yeast two-hybrid, GST pull-down and co-immunoprecipitation assays. These data were supported by confocal microscopy which demonstrated the perinuclear and nuclear co-localisation of FLJ22318 and NKX3-1 in prostate cancer cells. Northern blotting identified expression of ~2Kb and ~4Kb FLJ22318 mRNA's in prostate cancer cell lines, which was consistent with bioinformatic analyses of mRNA species. Transfection of prostate cancer cells to overexpress FLJ22318 did not alter endogenous NKX3-1 levels, however FLJ22318 exhibited transcriptional repressor function on an NKX3-1 responsive element and increased NKX3-1 transcriptional repressor activity on this element.

To further investigate FLJ22318 function, additional yeast two-hybrid analyses were performed in prostate cancer cells to identify potential FLJ22318 binding proteins. These studies isolated cDNA's encoding 33 different proteins involved in cell metabolism and apoptosis as well as transcriptional regulators associated with control of cellular proliferation. One of the candidate FLJ22318 interactors, protein kinase, interferon-inducible double stranded RNA dependent activator (PRKRA/PACT) was shown using confocal microscopy to extensively co-localise with FLJ22318 in the cytoplasm and perinuclear regions of prostate cancer cells. Preliminary co-immunoprecipitation and GST pull-down assays have provided additional evidence of the interaction of PRKRA and FLJ22318.

Results of this thesis have generated important information characterising the structure of the FLJ22318 gene and protein, the interaction between FLJ22318 and NKX3-1 and the potential functions of FLJ22318 in prostate cancer cells. As the FLJ22318 gene is located on 5q35, a chromosomal region frequently disrupted in a variety of tumours, future studies of the biological activity of FLJ22318 will clarify its normal cellular functions and its contribution to tumorigenesis or malignant progression in the prostate and in other tissues.

Table of Contents

Chapter Five – Characterisation of FLJ22318 Interaction with NKX3-1

Acknowledgments

I wish to thank and acknowledge all those who have given me their encouragement, support and assistance in helping me to complete my PhD. In particular, I would like to thank my supervisor Dr. Jacky Bentel, whose continuous support, belief and patience with me has made this possible. I would also like to extend my appreciation to Bob Mead at Murdoch for his support and to my lab buddies Marc, Diana, Darren, Ben and Priscilla for giving me lots of valuable advice, ideas and discussions on my project. More importantly I would like to thank them and all the other people who make up the Anatomical Pathology department at Royal Perth Hospital for making me feel welcome and for their friendship over the years.

Finally, a very special thank-you goes to my family, my children Andrew, Shane, Kaye and Mark and to my husband Neal, whose emotional and mental support and confidence in my abilities has given me the courage to reach and attain this goal, I could not have done this without you all.

Awards

During my PhD studies I have been the recipient of a Murdoch University Research Studentship and an Australian Postgraduate Award.

I was the recipient of the Scientific Section – Encouragement Award for my presentation "FLJ22318: A Novel Co-factor of NKX3.1" at The Merck Sharp & Dohme Young Investigators Meeting in September, 2004.

Publications

Abstracts

Fiona Baxter, **Linda Lawford**, Myles Hodgson, Jacqueline Bentel (2002) Identification of Novel Cofactors of the Prostate Specific Homeodomain Protein NKX3.1. 7th World Congress on Advances in Oncology / 5th International Symposium on Molecular Medicine, Crete, October, 2002 (poster presentation)

Linda Lawford, Fiona Baxter, Robert Mead, Jacqueline Bentel (2003) Characterisation of FLJ22318: A Novel NKX3.1 Binding Protein. Combined Biological Science Meeting (CBSM), Perth, August 2003 (poster presentation)

Linda Lawford, Fiona Baxter, Jacqueline Bentel (2003) Characterisation of FLJ22318, a Novel Co-factor of NKX3.1. Australian Society for Medical Research (ASMR) annual conference, Adelaide, November 2003 (poster presentation)

Linda Dawson, Fiona Baxter, Jacqueline Bentel (2004) FLJ22318: A Novel NKX3.1 Binding Protein. Australian Society for Medical Research (ASMR) Perth, June 2004 (oral presentation)

Linda Dawson, Fiona Baxter, Jacqueline Bentel (2004) FLJ22318: A Novel Co-factor of NKX3.1. The Merck Sharp & Dome 2004 Young Investigators Meeting, Perth, September 2004 (oral presentation)

Linda Dawson, Fiona Baxter, Jacqueline Bentel (2005) Characterisation of a novel protein FLJ22318 in prostate cancer cells. Australian Society for Medical Research (ASMR) Perth, June 2005 (oral presentation)

Linda Dawson, Fiona Baxter, Jacqueline Bentel (2005) Characterisation of FLJ22318 in Prostate Cancer Cells. Combined Biological Science Meeting (CBSM), Perth, August 2005 (poster presentation)

Linda Dawson, Fiona Baxter, Jacqueline Bentel (2005) Characterisation of FLJ22318 in Prostate Cancer Cells. The Endocrine Society of Australia, 48th Annual Scientific Meeting Perth, September 2005 (oral presentation)

Jacqueline Bentel, **Linda Dawson**, Fiona Baxter (2005) FLJ22318, a novel binding partner of the prostate cancer tumour suppressor, NKX3.1. 5th State Cancer Conference / The Cancer Council Western Australia Perth, October 2005 (oral presentation)

Linda Dawson, Jacqueline Bentel (2005) Characterisation of FLJ22318: A novel NKX3.1 binding protein in prostate cancer cells. The Merck Sharp & Dome 2005 Young Investigators Meeting, Perth, November 2005 (oral presentation)

Linda Dawson, Jacqueline Bentel (2006) Characterisation of FLJ22318: A novel NKX3-1 binding partner in prostate cancer cells. Australian Society for Medical Research (ASMR) Perth, June 2006 (oral presentation)

Linda Dawson, Jacqueline Bentel (2006) Characterisation of a novel protein FLJ22318 in prostate cancer cells. Combined Biological Science Meeting (CBSM), Perth, August 2006 (oral presentation)

Index to Figures

Chapter Four – Bioinformatic Analysis of FLJ22318

Chapter Five – Characterisation of FLJ22318 Interaction with NKX3-1

Index to Tables

Abbreviations

5αR	*5α-reductase inhibitor*
aa	*amino acids*
AD	*activation domain*
Ade	*adenine*
AES	*amino enhancer of split*
AF2	*activation function 2*
AI	*androgen independence*
Ald	*aldolase*
AMV	*avian myeloblastosis virus*
APS	*ammonium persulphate*
AR	*androgen receptor*
ARE	*androgen response element*
Arg	*arginine*
AS	*antisense*
Asn	*asparagine*
ATP	a*denosine 5'-triphosphate disodium salt*
BAC	*β-actin*
BD	*binding domain*
BLAST	*Basic Local Alignment Search Tool*
bp	*base pairs*
BPH	*benign prostatic hyperplasia*
BSA	*bovine serum albumin*
C	*carboxy*
CAB	*combined androgen blockade*
cDNA	*complementary deoxyribonucleic acid*
CDS	*coding domain sequence*
CIAP	*calf intestinal alkaline phosphatase*
CK	*cytokeratin*
CK2	*casein kinase 2*
CMV	*cytomegalovirus*
CNS	*central nervous system*

CO_2	*carbon dioxide*
CRA	*CT11-RanBPM*
CS	*charcoal stripped*
CT	*computed tomography*
CTLH	*C-terminal to lissencephaly type-1-like homology domain*
$CuSO_4$	*copper sulphate*
Da	*daltons*
dATP	*deoxyadenine triphosphate*
dCTP	*deoxycytosine triphosphate*
DCX	*doublecortin*
ddH_2O	*deionised distilled water*
DDO	*double dropout*
DEPC	*diethyl pyrocarbonate*
DES	*diethylstilbestrol*
dGTP	*deoxyguanine triphosphate*
DHT	5α-*dihydrotestosterone*
DMF	*dimethyl formamide*
DMSO	*dimethyl sulphoxide*
DNA	*deoxyribonucleic acid*
dNTP	*deoxynucleotide triphosphate*
DO	*dropout*
DRE	*digital rectal examination*
ds	*double stranded*
dT	*deoxythymidine*
DTT	*dithiothreitol*
dTTP	*deoxythymidine triphosphate*
Dyrk	*dual-specificity tyrosine phosphorylation-regulated kinases*
ECL	*enhanced chemiluminescence*
EDTA	*ethylenediaminetetra-acetic acid*
EHD	*extended homeodomain*
ER	*endoplasmic reticulum*
EST	*expressed sequence tag*
FBPase	*fructose-1,6-bisphosphatase*

FCS	*foetal calf serum*
FLJ	*full long Japanese*
FMR1	*fragile X mental retardation 1*
FTZ	*Fushi tarazu*
FTZ-1	*Fushi tarazu factor 1*
G	*gauge*
Gal	*galactosidase*
GFP	*green fluorescent protein*
GID	*glucose induced degradation*
GO	*gene ontology*
GR	*glucocorticoid receptor*
Gro	*groucho*
GST	*glutathione S-transferase*
GTF	*general transcription factors*
HA	*haemaglutinin*
HAT	*histone acetyl transferase*
HB	*homeobox*
HCl	*hydrochloric acid*
HD	*homeodomain*
HDAC	*histone deacetylase*
HECT	*homologous to E6-AP carboxyl terminus*
HES	*hairy enhancer of split*
HIPK	*homeodomain interacting protein kinase*
His	*histidine*
HnRNPs	*heterogeneous ribonucleoproteins*
HNRPAB	*heterogenous nuclear ribonucleoprotein A/B*
HP	*hexapeptide*
HPVs	*human papillomaviruses*
HRP	*horseradish peroxidase*
Ig	*immunoglobulin*
IPTG	*isopropyl-β-D-thiogalactoside*
Kb	*kilobase*
KCl	*potassium chloride*

kDa	*kilodaltons*
LB	*Luria Bertani*
LBD	*ligand binding domain*
LD	*long distance*
Leu	*leucine*
LH-RH	*luteinising hormone-releasing hormone*
LiAc	*lithium acetate*
LisH	*lissencephaly type-1-like homology*
LOH	*loss of heterozygosity*
Luc	*luciferase*
MAEA	*macrophage erythroblast attacher*
MCS	*multiple cloning site*
MGC	*mammalian gene collection*
$MgCl_2$	*magnesium chloride*
MGMT	*O^6-methyl-guanine-DNA methyltransferase*
$MgSO_4$	*magnesium sulphate*
MITOP	*mitochondrial proteome database*
MOPS	*3-[N-Morpholino]propanesulphonic acid*
MMLV	*Moloney Murine Leukaemia Virus*
mRNA	*messenger ribonucleic acid*
MS	*mass spectrometry*
N	*amino*
N4BP3	*Nedd4 binding protein 3*
NaCl	*sodium chloride*
NaOH	*sodium hydroxide*
NCBI	*National Center for Biotechnology Information*
NCI	*National Cancer Institute*
N-CoR	*nuclear receptor co-repressor*
NDE1	*nuclear distribution gene E homolog 1*
NDEL1	*NDE1-Like 1*
$(NH_4)_2SO_4$	*ammonium sulphate*
NK2-SD	*NK2-specific domain*
NLS	*nuclear localisation signal*
NOLA2	*nucleolar protein family A member 2*

NP-40	*nonidet P-40*
NPAT	*ataxia-telangiectasia locus protein*
NRB	*nuclear receptor box*
OD	*optical density*
OFD1	*oral-facial-digital syndrome type I*
OPN	*osteopontin*
ORC	*origin recognition complex*
ORF	*open reading frame*
PAFAH1B1	*platelet-activating factor acetylhydrolase, isoform 1b, alpha subunit*
PBS	*phosphate buffered saline*
p.c.	*post coitum*
PCD	*programmed cell death*
PCR	*polymerase chain reaction*
PDEF	*prostate derived Ets factor*
PEG	*polyethylene glycol*
PFK	*phosphofructokinase*
Pfu	*Pyrococcus furiosus*
Phe	*phenylalanine*
PIN	*prostatic intraepithelial neoplasia*
PIPES	piperazine-*N,N'*-bis *(2-ethanesulphonic acid)*
PKC	*protein kinase C*
PLB	*passive lysis buffer*
PMSF	*phenylmethylsulphonylfluoride*
P/S	*penicillin/streptomycin*
PSA	*prostate specific antigen*
QDO	*quadruple dropout*
RANBP9	*RAN-binding protein 9*
RAR	*retinoid acid receptor*
Rb	*retinoblastoma*
RING	*really interesting new gene*
RIPA	*radioimmunoprecipitation assay*
RNA	*ribonucleic acid*
rpm	*revolutions per minute*
rRNA	*ribosomal ribonucleic acid*

RT	*reverse transcription*
RXR	*retinoid X receptor*
S	*sense*
SAAB	*selection and amplification binding assay*
SDS	*sodium dodecyl sulphate*
siRNA	*small interfering RNA*
SMART	*simple modular architecture research tool*
SMGA	*smooth muscle gamma-actin*
SMRT	*silencing mediator of retinoid and thyroid hormone receptor*
SNP	*single nucleotide polymorphism*
SRF	*serum response factor*
ss	*single stranded*
SSC	*sodium chloride, sodium citrate*
TAE	*TRIS, [ethylenedinitrilo] tetra-acetic acid*
Taq	*Thermus aquaticus*
TBL1X	*transducin β-like 1X*
TBS	*TRIS buffered saline*
TBST	*TRIS buffered saline/TWEEN 20*
TCA	*tricarboxylic acid*
TGCTs	*testicular germ cell tumours*
TDO	*triple dropout*
TE	*TRIS/EDTA*
TEMED	*[N, N, N', N'-Tetra-methyl]-ethylenediamine*
TIF	*tagged image format*
TK	*thymidine kinase*
TLE	*transducin-like enhancer of split*
TNM	*tumour, node, metastases classification*
TR	*thyroid receptor*
TRIS	*tris(hydroxymethylaminomethane)*
Triton X-100	*Octylphenoxypolyethoxyethanol*
Trp	*tryptophan*
TRUS	*transrectal ultrasound*
TSG	*tumour suppressor gene*

TSS	*transcription start site*
UAS	*upstream activating sequence*
UTR	*untranslated region*
UV	*ultraviolet*
V	*volts*
WD	*tryptophan-asparagine*
X-Gal	*5-bromo-4 chloro-3-indolyl-β-D-galactopyranoside*
X-α-Gal	*5-bromo-4 chloro-3-indolyl-α-D-galactopyranoside*
Y2H	*yeast two-hybrid*
YPDA	*yeast peptone dextrose agar*

Chapter One

Chapter One – Introduction

1.1 The Prostate Gland

1.1.1 Anatomical Location and Development

The prostate is a small walnut-shaped gland that surrounds the urethra at the base of the bladder and functions by contributing secretory proteins to the seminal fluid (Figure 1.1; Abate-Shen and Shen, 2000). The prostate gland is comprised of epithelium composed of two layers, a secretory luminal layer that consists of tall columnar cells which produce the secretory proteins that make up part of the seminal fluid, and a basal layer composed of cuboidal epithelial cells (McNeal, 1988). The basal layer is thought to contain the proliferative cell populations of the prostatic epithelium and is lined by a basement membrane of extracellular matrix which separates the glandular epithelium from the surrounding fibromuscular stroma (de Carvalho and Line, 1996).

Within the prostate epithelium there are a spectrum of cell types that express a continuum of biological properties, differentiation markers and variable degrees of androgen independence (Figure 1.2). These include the stem cell, the neuroendocrine cell, the basal cell, the luminal cell and intermediate cells, a sub-population of heterogeneous cells that migrate from the basal layer into the luminal layer (Liu et al., 1999; van Leenders et al., 2000). Using well described epithelial and prostate markers, intermediate cells have been shown to exhibit phenotypes between the progenitor basal cells and the terminally differentiated secretory luminal cells (Figure 1.2; van Leenders et al., 2000).

Stem cells are thought to reside in the basal layer and are considered to be androgen independent for growth and survival. They express high levels of p63, low levels of the cytokeratins (CK) 14 and 18, and are the cell type from which all prostate epithelial cell types are thought to arise (Liu et al., 1999; Pellegrinni et al., 2001). Neuroendocrine cells are also thought to arise from stem cells (Bonkhoff et al., 1995) however there is evidence to suggest that they may be neuronal in origin (Aumuller et al., 1999). These cells are sparsely dispersed between the basal and luminal epithelial layers, are also androgen independent for growth and survival and are thought to be non-proliferating terminally differentiated cells that provide paracrine signals that support the growth and

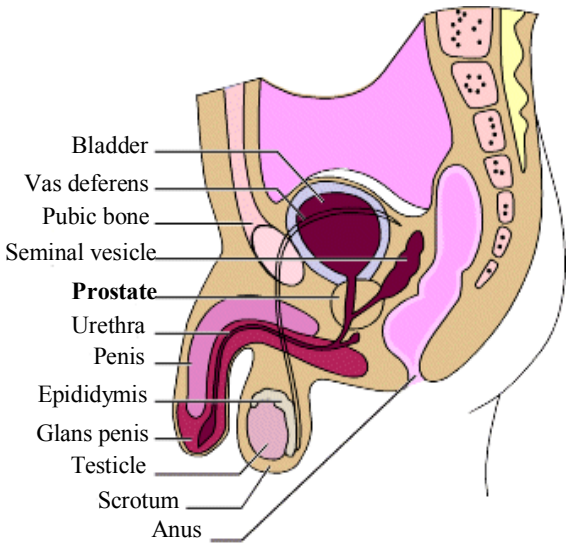

Figure 1.1 Anatomical location of the prostate gland at the base of the bladder and surrounding the urethra (Adapted from http://www.prostateline.com).

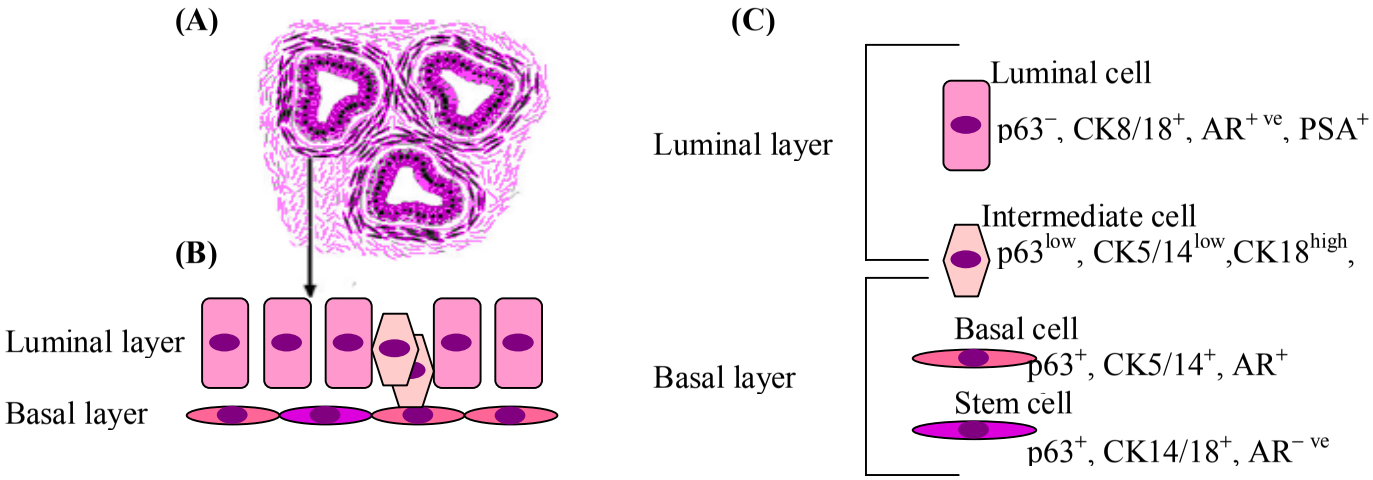

Figure 1.2 Schematic representation of epithelial cell differentiation in the human prostate. **(A)** Cross section of the prostate showing the glandular epithelium surrounded by fibromuscular stroma. **(B)** Depiction of the migration of differentiating epithelial cells from the basal layer to the luminal layer that forms the two layers of glandular epithelium. **(C)** Evolution of the cell phenotypes from a basal stem cell to a differentiated secretory luminal cell and the most common markers expressed by each cell type. (CK-cytokeratin, AR-androgen receptor, PSA-prostate specific antigen) (Adapted from Long et al., 2005)

differentiation of the developing prostate (di Sant`Agnese, 1998). Basal cells are non-secretory cells which are found between the luminal cells and the underlying basement membrane (Liu et al., 1999). These cells express p63 and a range of cytokeratins with CK5/14 being the most common, however androgen receptor (AR) expression can be either absent, weak or high and this may explain why basal cells are androgen independent for survival but androgen responsive for proliferation (Tokar et al., 2005). The intermediate cells are considered to be a transient population of cells that are either continually differentiating or quiescent cells and which terminally differentiate into secretory luminal cells only when required at precise times during prostate differentiation and growth (Long et al., 2005). These cells express low levels of p63 and CK5/14 but high levels of CK18 (Tokar et al., 2005). Intermediate cells are also androgen independent for growth and survival but in response to androgens exhibit increased AR and prostate specific antigen (PSA) expression and are thought to account for the finding in the basal layer of androgen dependent cells which express both the AR and PSA (Bonkhoff et al., 1994). Luminal cells are the predominant cell type found in prostate epithelium, they are androgen dependent for growth and express CK8/18, AR and secretory proteins such as prostate specific antigen (PSA) and prostatic acid phosphatase (Bonkhoff et al., 1994).

The prostate is endodermal in origin and forms during embryogenesis through epithelial budding from the urogenital sinus as a consequence of epithelial and mesenchymal interactions (Cunha et al., 1987). Initially androgens act on the mesenchyme and subsequently the epithelium during prostate development, indicating that androgens are required in the mesenchyme for prostate induction and growth, and later in the epithelium for the development and maintenance of the secretory function of differentiated cell types (Abate-Shen and Shen, 2000). The prostatic epithelial buds subsequently undergo extensive ductal outgrowth and branching into the surrounding mesenchyme as the prostate matures (Timms et al., 1994). In humans, this largely occurs during puberty in response to high levels of circulating androgens (Abate-Shen and Shen, 2000). In adult human males, the prostate is defined by three distinct morphological regions based upon their relationship to prostatic disease. These are the central zone, the transition zone where benign prostatic hyperplasia (BPH) mainly occurs and the peripheral zone where prostate cancer primarily arises (Figure 1.3; McNeal, 1988). For correct differentiation of prostate epithelium to be maintained, a

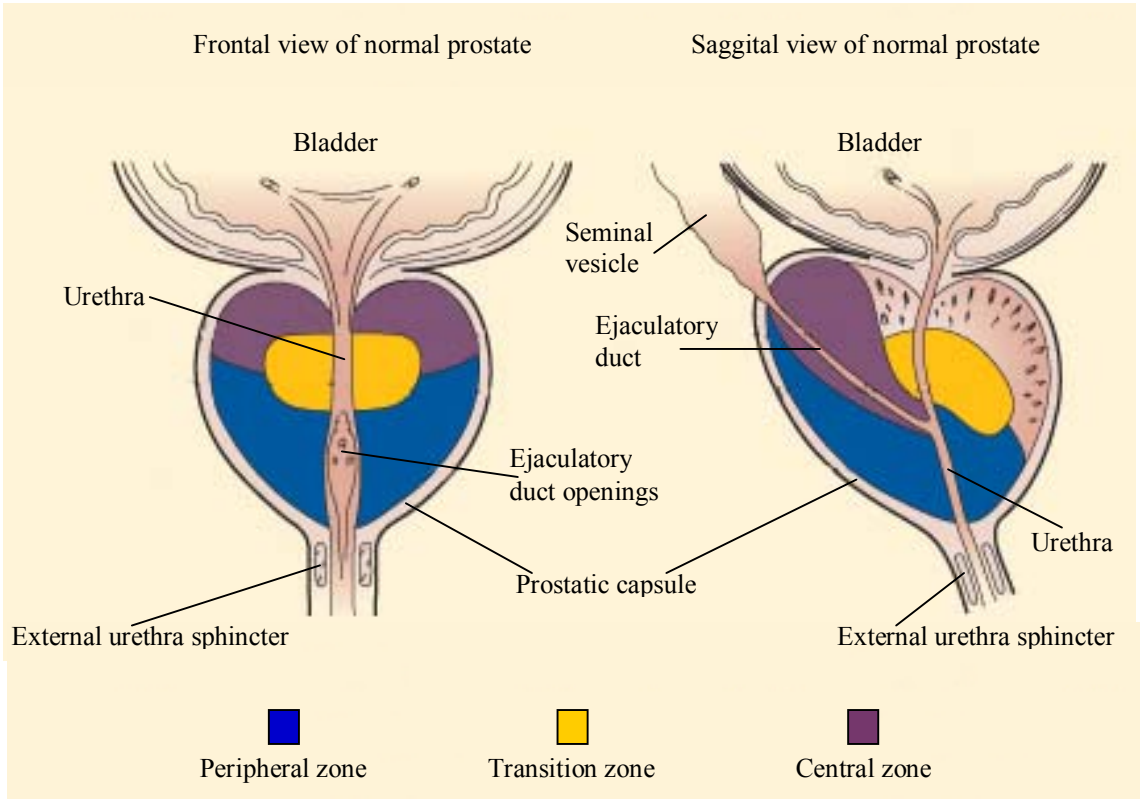

Figure 1.3 The three distinct morphological regions of the adult human prostate (Adapted from http://www.prostate-research.org.uk).

closely regulated balance between proliferation, differentiation and apoptosis is essential and this process involves androgens, the extracellular matrix and stromal growth factors (Long et al., 2005). As prostate cancer stroma differs from normal stroma, alterations in stromal growth factor signalling have been implicated in the development of prostate cancer (Lang et al., 2000). Although specific growth factors have not been definitively identified, it has been proposed that these aberrant signals result in the inappropriate differentiation of prostate epithelial cells (Long et al., 2005). However as cell lineage relationships in normal prostatic epithelium are not well characterised, the cell type(s) involved that give rise to prostate cancer remain unknown (Long et al., 2005; Tokar et al., 2005). It has been suggested that as prostate cancer cells express both basal and luminal cell characteristics, deregulation is most likely to occur during the differentiation of intermediate cells from androgen independent basal cells to androgen dependent luminal cells (Long et al., 2005).

1.2 Prostate Cancer

1.2.1 Prostate Cancer Incidence

Prostate cancer is the second leading cause of cancer death in men after lung cancer and is the most frequently diagnosed cancer of men in Australia, North America and Western Europe (AIHW and AACR, 2004; Gronberg, 2003). Although other factors such as diet, environment, ethnicity or family history also contribute, ageing represents the single most significant risk factor for the development of prostate cancer (Figure 1.4; Brothman, 2002). Studies at autopsy show that 15-30% of men over the age of 50 years have evidence of prostate cancer (Sakr et al., 1993), whereas by the age of 80 years this figure has risen to 60-70% (Brawley et al., 2000). Prostate tumours are not always fatal and men may die of other age associated diseases and not as a direct consequence of prostate cancer (Figure 1.4; Brothman, 2002). Nevertheless, prostate cancer is a heterogeneous condition and as such ranges from an indolent asymptomatic disease to an aggressive rapidly lethal systemic disease. At present there is no effective way of distinguishing between those prostate cancers which will remain indolent and those that will become aggressive (Hughes et al., 2005). In England and Wales, although the 5 year survival rates for prostate cancer have increased by 11% for men diagnosed during 1996-1999 as compared to those men diagnosed during 1991-1995, the increase in survival rates reflected the increased detection of early stage disease in

men who died from causes other than prostate cancer rather than improved treatment of the disease. For those men diagnosed with advanced prostate cancer, there are still no effective long term treatments (section 1.2.5-1.2.7; Hughes et al., 2005).

Prostatic intraepithelial neoplasia (PIN) describes precursor or premalignant prostate lesions that are thought to precede invasive cancer by at least 10 years and are primarily found in the peripheral zone, as is prostate cancer (Sakr et al., 1993). These lesions display architectural features found in early invasive cancers, such as disruption of the basal layer. PIN can be found in men in their twenties and are common in men in their fifties, affecting 1 man in 3 (Bostwick et al., 1993). PIN lesions occur as a continuum between low grade and high-grade forms, with high-grade PIN representing the immediate precursor of early invasive carcinoma (Bostwick, 1999). Prior to the age of 50, the diagnosis of prostate cancer is rare (Sakr et al., 1993), suggesting that although the changes associated with PIN lesions occur comparatively early in adulthood, the progression to cancer occurs as a consequence of ageing (Abate-Shen and Shen, 2000).

The incidence of prostate cancer in Australia is higher than in Western Europe, but is lower than the very high rates found in the United States of America (USA) and New Zealand. In the USA, the probability of being diagnosed with prostate cancer is 1 in 6 (Klotz, 2005), whereas in Australian men, the lifetime risk for the development of prostate cancer is 1 in 11. Between 1990 and 1994 the incidence of prostate cancer in Australia increased substantially as a result of the introduction of prostate specific antigen (PSA) screening in 1989, which increased the detection of the disease. From 1995 until 1997, prostate cancer incidence rates fell by 30% and have remained relatively unchanged from 1998 to 2001 (Figure 1.5; AIHW and AACR, 2004), although the number of new cases diagnosed is predicted to increase by 36% from 11,191 in 2001 to 15,202 in 2011 (AIHW et al., 2005). In 2001, prostate cancer accounted for approximately 23% of all invasive cancer diagnoses in Australian men (AIHW and AACR, 2004), compared to 31% for North American men (257,943 new cases) (Ferlay et al., 2004). Mortality rates are similar in Australia to that of North America, the United Kingdom and New Zealand with Australian men having a lifetime risk of prostate cancer mortality of 1 in 82, which is significantly lower than the incidence rate and has decreased 1.8% per year from 1991 to 2001 (AIHW and AACR, 2004). In 2001 prostate cancer accounted for 13% of all cancer deaths (2,718) of

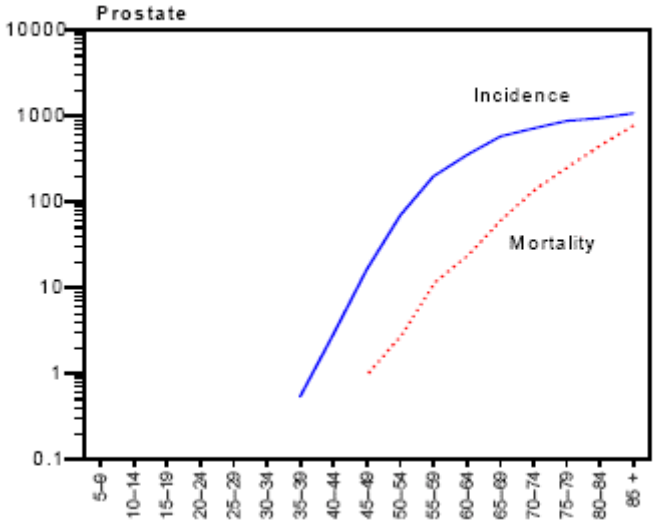

Figure 1.4 Age-specific incidence and mortality rates for cancer of the prostate in Australian men for 2001 (AIHW and AACR, 2004).

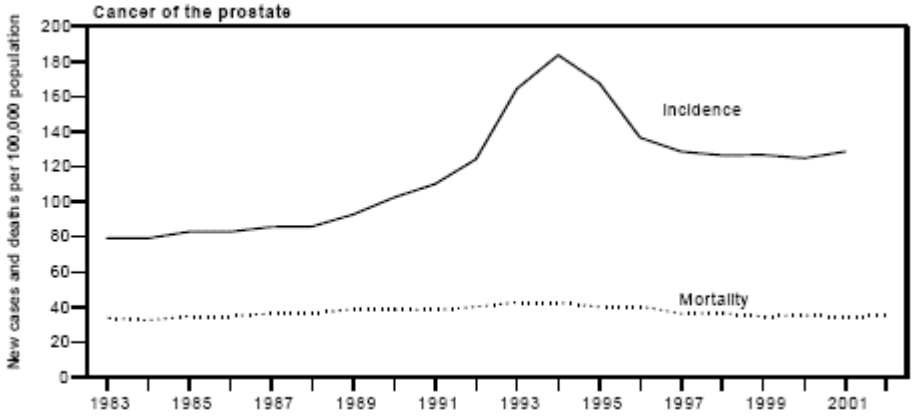

Figure 1.5 Age-standardised trend of the incidence and mortality rate for prostate cancer in Australian men from 1983 to 2002 (AIHW and AACR, 2004).

Australian men and 11% of all cancer deaths (36,447) of North American men (AIHW and AACR, 2004; Ferlay et al., 2004).

1.2.2 Aetiology

Familial prostate cancers, where there is evidence of the disease within a family, is proposed to account for approximately 25% of all prostate cancers but differs from hereditary prostate cancer which accounts for approximately 9% of all and 40% of early onset prostate cancers (age at diagnosis less than 55 years) (Bauer et al., 1998; Brothman, 2002). Hereditary cancer is defined as the incidence of prostate cancer in at least 3 first degree relatives, at least 3 successive generations or at least 2 relatives diagnosed prior to age 55 (Brothman, 2002). It is proposed in the majority of studies that prostate cancer is inherited by an autosomal dominant mode of inheritance although there is evidence to support autosomal recessive and X-linked modes of inheritance in specific families (Brothman, 2002). Few chromosomal regions are consistently identified as being linked to hereditary prostate cancer, possibly as the result of the existence of multiple, incompletely penetrant prostate cancer susceptibility genes (Xu et al., 2005). Nevertheless, candidate chromosomal regions and prostate cancer susceptibility genes have been identified by linkage analysis (Table 1.1; Brothman, 2002; Bussemakers et al., 1999; Cancel-Tassin and Cussenot, 2005; Chang et al., 2002; Dong et al., 2003; Xu et al., 2005; Zheng et al., 2006). To date, apart from NKX3-1, AR and RNAse L, the genes proposed to be involved in hereditary prostate tumours have not been investigated for their roles in sporadic prostate tumours (Brothman, 2002; Noonan-Wheeler et al., 2006).

It is also believed that endogenous steroid hormones contribute to prostate cancer risk, although studies examining the role of androgens in the aetiology of prostate cancer have shown conflicting results (Miyamoto et al., 2004). Among other factors associated with an increased risk of prostate cancer are ethnicity, occupation, diet and infections with high risk human papillomaviruses (HPVs). The highest incidence of prostate cancer in the world is among African-American men however it is believed this may result from a combination of factors involving diet, access to health care and genetic variations (Bostwick et al., 2004). Increased rates of prostate cancer have been observed in association with occupations such as welding, where there is exposure to cadmium (Waalkes and Rehm, 1994), which is considered a significant prostate cancer risk factor

Table 1.1 Chromosomal sites and putative susceptibility genes implicated to be involved in hereditary prostate cancer.

Chromosomal Locus	**Putative Susceptibility Gene**	**Observations**
1p36	CAPB	Associated with hereditary brain and prostate cancer
1q24-25	HPC1/RNASEL	Accounts for ~6% familial cancers
1q42.2-43	PCAP	Early age at onset
3p24	Not identified	
5q12	Not identified	
5q35	Not identified	
7q11-21	Not identified	
8p21	NKX3-1	Gene sequence variants found
8p22-23	PG1/MSR1	Gene sequence variants found
8q13	Not identified	
11q22	Not identified	
13q12-13	BRCA2	Associated with hereditary breast and prostate cancer
13q14	Not identified	
15q11	Not identified	
16p13	Not identified	
17p11	HPC2/ELAC2	Gene sequence variants found
17q21	BRCA1	Associated with hereditary breast and prostate cancer
17q22	Not identified	
20q13	HPC20	Late age at onset
22q12	CHEK2	Gene sequence variants found
Xq12	AR	Associated with AR allele <16 GGC repeats
Xq27-28	HPCX	No male-male inheritance

as it has been shown to stimulate the growth of prostate epithelial cells and promote their malignant transformation (Bostwick et al., 2004). Cadmium has also been implicated in the more aggressive and lethal forms of prostate cancer seen in smokers who have high levels of prostatic cadmium as compared to non-smokers (Drasch et al., 2005).

Studies have indicated that diets high in fat are also positively associated with an increased incidence of prostate cancer, with a recent report identifying important differences in the type of fat consumed rather than total dietary fat intake (Bidoli et al., 2005; Yip et al., 1999). A significant protective effect of polyunsaturated fatty acids was noted in this study whereas monounsaturated fat consumption was correlated with an increased risk of prostate cancer (Bidoli et al., 2005). Other studies of vitamins and minerals have concluded that high serum levels of vitamin D may reduce the risk of prostate cancer (Polek and Weigel, 2002), as may supplementing the diet with vitamin E (Giovannucci, 2000), selenium and lycopene (the red carotenoid pigment found in watermelon and tomatoes) (Chan et al., 2005; Drasch et al., 2005). In addition, a recent study has found an inverse relationship between serum PSA and serum lycopene levels and demonstrated the use of lycopene as an effective treatment for high grade PIN lesions (Mohanty et al., 2005). Although the role of HPV infection in prostate cancer incidence remains undecided, studies have shown that men who are serologically positive for the high risk HPV-16 or HPV-18 strains that are associated with cervical cancer, have a 2.4 to 2.6 fold increased risk of prostate cancer (Dillner et al., 1998). In addition, a higher incidence of HPV DNA in prostate cancers has been noted as compared to benign prostatic hyperplasias (Leiros et al., 2005; Serth et al., 1999).

1.2.3 Detection and Diagnosis

Early stage prostate cancer is usually asymptomatic, although along with other health problems it may cause some of the following symptoms (National Cancer Institute (NCI), 2002).

- A need to urinate frequently, especially at night
- Difficulty starting or stopping urination
- Weak or interrupted flow of urine
- Painful or burning urination

- Difficulty in having an erection
- Painful ejaculation
- Blood in the urine or semen
- Frequent pain or stiffness in the lower back, hips, or upper thighs

Early detection and diagnosis therefore, relies on screening of asymptomatic patients. Currently, screening for prostate cancer involves either a digital rectal examination (DRE) or a blood test for serum PSA levels. DRE has an overall poor sensitivity and specificity, as only ~30% of prostate cancers detected by DRE are organ confined. In contrast, where routine screening by measurement of serum PSA levels is carried out, ~90% of prostate cancers detected are organ confined and therefore potentially curable (Bast et al., 2000). However, as routine PSA screening results in the diagnosis of prostate cancer in many men who will not manifest clinical progression during their lifetime, the Australian Cancer Council, the Urological Society of Australasia and the Australian Prostate Cancer Collaboration do not recommend screening of asymptomatic men. Instead they advise that individual men aged 50-70 years with a life expectancy of at least 10 years who wish to be tested should be able to be screened by annual DRE and PSA test after discussion with their doctor (NHMRC (National Health and Medical Research Council), 2006). This view is supported by the American Urological Association and the American Cancer Society who adopted similar guidelines in 1997 to that seen in Australia (American Urological Association, 2000). However the Canadian T. F. Periodic Health Exam and the UK Health Care Evaluation Unit advise against PSA screening of asymptomatic men. In Canada and the UK, PSA testing is reserved to monitor disease activity in men with established prostate cancer, to give an indication of the progression of the cancer and to assess response to treatment (Public Health Agency of Canada (PHAC), 2004; Watson et al., 2002).

PSA is a protein that is found in both normal and cancerous cells. In men without prostate cancer, serum PSA levels generally range between 0 and 2.50ng/mL. Cancer will be detected in only 20-25% of men with serum PSA levels between 2.50ng/mL and 4.0ng/mL and in 30-35% of men with serum PSA levels between 4.0ng/mL and 10.0ng/mL (National Comprehensive Cancer Network (NCCN) and the American Cancer Society (ACS), 2005). If serum PSA levels are above 10.0ng/mL, prostate cancer is detected in 67% of cases however PSA measurement is not a definitive marker

of prostate cancer as PSA levels can also be increased in benign conditions such as benign prostatic hyperplasia (BPH) and infections of the prostate gland (prostatitis) (National Comprehensive Cancer Network (NCCN) and the American Cancer Society (ACS), 2005). If a man has symptoms of prostate disease, or a DRE or PSA level that is abnormal, a transrectal ultrasound (TRUS) guided needle biopsy will be performed to collect tissue samples from the peripheral and transition zones of the prostate. Histological analysis of these biopsies and the presence of malignant cells within the prostate will be confirmed before a diagnosis of prostate cancer is made (Bast et al., 2000).

1.2.4 Grading and Staging

Following a diagnosis of prostate cancer, further tests such as follow-up serum PSA levels, TRUS, computed tomography (CT) and radioisotope bone scans, and/or surgery will be used to evaluate the extent of disease. The cancer will be classified using the Tumour, Node, Metastasis (TNM) classification (Table 1.2; Greene et al., 2002). In addition, the cancer will be graded from biopsy samples using a system developed by Gleason (Gleason and Mellinger, 1974), which has recently been revised to incorporate the reporting of tertiary patterns of gland differentiation in needle biopsy specimens that were not recognised when Gleason proposed this system (Lopez-Beltran et al., 2005). The system uses two levels of scoring, assigning grades of 1-5 based on the degree of differentiation seen histologically in patterns of gland formation. The Gleason score is the sum of the grades assigned to the primary and secondary patterns of gland differentiation or the best and poorest patterns of gland differentiation where tertiary patterns are seen, and gives an indication of how fast the cancer is growing (Gleason and Mellinger, 1974; Lopez-Beltran et al., 2005). A Gleason score of 2-4 indicates a slow growing tumour, 5-7 is intermediate whereas a score of 8-10 would indicate an aggressively growing tumour (Gleason and Mellinger, 1974).

1.2.5 Treatment Options and Prognosis

Treatment options and prognosis of prostate cancer depend on the TNM classification, Gleason grade, the patient's age and general health. Once the T, N and M categories have been determined, they are assigned a stage number, expressed in Roman numerals from I (the least advanced) to IV (the most advanced), and used to determine treatment

Table 1.2 TNM classification of prostate cancer.

	Primary Tumour (T)
TX	Primary tumour cannot be assessed
T0	No evidence of primary tumour
T1	Clinically inapparent tumour not palpable or visible by imaging
T1a	Tumour incidental histological finding in 5% or less of tissue resected
T1b	Tumour incidental histological finding in more than 5% of tissue resected
T1c	Tumour identified by needle biopsy – elevated PSA
T2	Palpable tumour confined within prostate*
T2a	Tumour involves less than 50% of one lobe
T2b	Tumour involves more than 50% of one lobe
T2c	Tumour involves both lobes
T3	Tumour extends through the prostatic capsule**
T3a	Extracapsular extension (unilateral or bilateral)
T3b	Tumour invades seminal vesicle(s)
T4	Tumour is fixed or invades adjacent structures other than seminal vesicles, bladder neck, external sphincter, rectum, levator muscles, and/or pelvic wall.
	Regional Lymph Nodes (N)
NX	Regional lymph nodes cannot be assessed
N0	No metastasis to regional lymph node(s)
N1	Metastasis in regional lymph node(s)
	Distant Metastasis (M)* **
MX	Distant metastasis cannot be assessed
M0	No distant metastasis
M1	Distant metastasis
M1a	Non-regional lymph nodes
M1b	Bone(s)
M1c	Other site(s)

*Tumour found in one or both lobes by needle biopsy, but not palpable or reliably visible by imaging, is classified T1c.

**Invasion into the prostatic apex or into (but not beyond) the prostatic capsule is not classified as T3, but as T2.

***When more than one site of metastasis is present, the most advanced category is used.

and prognosis (Table 1.3; National Comprehensive Cancer Network (NCCN) and the American Cancer Society (ACS), 2005).

Conventionally, men with low-grade, small volume tumours are regarded as appropriate candidates for watchful waiting and one option in these cases is to carefully monitor the cancer but undertake no active treatment (National Comprehensive Cancer Network (NCCN) and the American Cancer Society (ACS), 2005). Where the cancer is confined to the prostate gland, a prostatectomy involving the complete surgical removal of the prostate may be recommended. However as there can be significant side effects from the surgery, watchful waiting is also an option, as men with these tumours have a 20 year 80-90% disease-free survival rate and are classified as having good-risk prostate cancer (Klotz, 2005). These cancers are generally defined as a Gleason score of 6 or less, PSA < 10, and T1c to T2a, and constitute approximately 50% of newly diagnosed cases. Nevertheless, some men with supposedly good-risk prostate cancer have a more aggressive phenotype than expected and a recent study has shown that those men who have a PSA doubling time of 3 years or less should be offered surgical intervention (Klotz, 2005). In addition, a PSA doubling time of less than 2 years indicated that the cancer was probably locally advanced (Klotz, 2005). Once the cancer has spread beyond the prostate, surgery is not normally an option as tumours that have already invaded surrounding tissues on diagnosis are generally incurable, as occult metastasis has already occurred (Freeman et al., 1995). For men diagnosed with these cancers, progression-free survival at 5 years was approximately 70% following hormone therapy (Lane et al., 2004). For men with metastatic prostate cancer, usually to the bone, there is no cure and treatment is palliative (Garnick and Fair, 1996; National Comprehensive Cancer Network (NCCN) and the American Cancer Society (ACS), 2005).

1.2.6 Androgen Deprivation and Hormonal Therapies

As androgens are required for the growth of the prostate, prostate cancer growth can also be manipulated with hormonal therapy. At present, the most common treatment for localised disease with a high risk of relapse, locally advanced disease, biochemical relapse following earlier treatment and metastatic disease is androgen deprivation treatment or hormonal therapy (Silvestris et al., 2005). Current hormonal treatments and their most commonly recognised advantages and disadvantages are listed in Table 1.4 (Miyamoto et al., 2004). The classical form of androgen deprivation is castration, either

Table 1.3 Treatment options for prostate cancer based on disease stage.

Stage	TNM Classification and Gleason Grade	Treatments
I	T1a-N0-M0-low Gleason score (2-4)	Watchful waiting Surgery Radiation therapy
II	T1a-N0-M0-intermediate or high Gleason score (5-10) T1b-N0-M0-any Gleason score (2-10) T1c-N0-M0-any Gleason score (2-10) T2-N0-M0-any Gleason score (2-10)	Watchful waiting Surgery Radiation therapy
III	T3-N0-M0-any Gleason score (2-10)	Surgery Radiation Therapy Hormonal Therapy
IV	T4-N0-M0-any Gleason score (2-10) Any T-N1-M0-any Gleason score (2-10) Any T-Any N-M1-any Gleason score (2-10)	Radiation Therapy Hormonal Therapy Chemotherapy

Table 1.4 Hormonal therapy treatment options for prostate cancer.

Method	Action	Advantages	Disadvantages
Surgical castration	Orchiectomy	Rapid decrease of testicular androgens	Non-reversible Psychological problems Impotence and loss of libido Anaemia and osteoporosis Depression Loss of muscle mass Impaired cognitive function Unaffected adrenal androgens
Medical castration	Oestrogens	Reversible	Adverse cardiovascular effects (oestrogens)
	LH-RH agonists	More acceptable than surgical castration	Flare phenomenom (agonists)
	LH-RH antagonists	Decrease of testicular androgen	Impotence and loss of libido Anaemia and osteoporosis Depression Loss of muscle mass Impaired cognitive function Unaffected adrenal androgens
Complete androgen blockade	Castration + antiandrogen	Decrease of testicular androgen Inhibition of adrenal androgens	Increased side-effects
Antiandrogen monotherapy	Non-steroidal antiandrogen	Inhibition of both testicular and adrenal androgens	May be less effective
		Less severe side effects No loss of libido	Painful enlarged breasts
	Steroidal antiandrogen	Complete androgen blockade effect	Painful enlarged breasts Adverse cardiovascular effects
Intermittent androgen blockade	Intermittent hormonal therapy	May increase time of progression to AI Reduced side effects	Under investigation
Triple androgen blockade	Intermittent complete androgen blockade + 5αR inhibitor	Better than intermittent androgen blockade	Under investigation
Sequential androgen blockade	5αR inhibitor + antiandrogen or LH-RH agonist	Better than intermittent androgen blockade	Under investigation

LH-RH – Luteinising hormone-releasing hormone, AI – androgen independence, 5αR – 5α-reductase inhibitor (Miyamoto et al., 2004).

surgically (orchiectomy) or medically by the use of oestrogens or luteinising hormone-releasing hormone (LH-RH) agonists and more recently LH-RH antagonists. Orchiectomy reduces circulating testicular androgens by over 90% within 24 hours (Maatman et al., 1985), however this treatment approach is unacceptable to many men as it causes considerable psychological problems (Miyamoto et al., 2004).

Diethylstilbestrol (DES) was the first oestrogen compound used for medical castration and has the advantage that it is reversible, however DES is no longer used as an initial treatment as it has serious adverse cardiovascular side-effects including deep vein thrombosis and transient ischemic attack. DES is now more commonly used as a treatment for hormone refractory prostate cancer sometimes in combination with antithrombotic drugs (section 1.2.7; Malkowicz, 2001). Medical castration by the use of LH-RH agonists or antagonists suppresses testicular androgen secretion by inhibiting pituitary release of gonadotropins. However LH-RH agonists cause an initial rise in gonadotropin levels and testosterone, which may cause a surge in prostate cancer growth (flare phenomenon) and has been associated with increased bone pain in 5-10% of cases of metastatic disease (Bast et al., 2000). With the use of LH-RH antagonists on the other hand, this flare response is eliminated (Stricker, 2001).

Men who undergo castration still produce adrenal androgens, therefore the basis of combined or total androgen blockade therapy is to use LH-RH agonists to inhibit testicular androgens in conjunction with either steroidal or non-steroidal antiandrogens to inhibit the effects of adrenal androgens (Miyamoto et al., 2004). Various studies of total androgen blockade therapy have suggested that this therapy only provides a minimal improvement in 5 year survival as compared to monotherapy (Schmitt et al., 2001) and side effects associated with antiandrogens used can include liver dysfunction and diarrhoea (Miyamoto et al., 2004). Nonetheless, the use of an antiandrogen prior to and during the first few weeks of LH-RH agonist treatment has been shown to prevent the risk of increased bone pain associated with the flare phenomenon (Bast et al., 2000).

The administration of antiandrogens as a monotherapy has been used as an alternative treatment to castration as antiandrogens preserve the testes therefore providing potential quality of life benefits especially in terms of potency and libido (Miyamoto et al., 2004).

Studies using the anti-androgen bicalutamide have shown equivalent survival rates to that of surgical or medical castration in men with metastatic disease (Iversen et al., 2000), however breast enlargement and pain are complications of this treatment (Miyamoto et al., 2004). Intermittent androgen blockade describes androgen deprivation treatments administered until maximum responses (PSA levels, clinical evidence of disease) are achieved, then cessation of treatment until symptomatic or asymptomatic (eg. increasing serum PSA levels) disease recurs. This form of treatment is reported to reduce the side effects seen in continuous androgen deprivation therapy and is proposed to delay the onset of androgen independent prostate cancer, however it is still being debated whether intermittent androgen blockade improves survival (Oefelein, 2003).

A useful form of androgen deprivation therapy that is used to treat benign prostatic hyperplasia has been 5α-reductase inhibitors such as finasteride, which inhibit the 5α-reductase mediated conversion of testosterone into the more biologically active 5α-dihydrotestosterone (DHT) (Miyamoto et al., 2004). Finasteride monotherapy in prostate cancer has not been investigated, but in conjunction with total androgen blockade (termed triple androgen blockade), where finasteride is administered along with an LH-RH agonist and an antiandrogen, or sequential androgen blockade, where finasteride maintenance therapy follows total androgen blockade treatment, were shown to substantially decrease PSA levels in men with metastatic disease (Kirby et al., 1999; Leibowitz and Tucker, 2001). Side effects of hormonal therapies can include osteoporosis, depression, anaemia, and loss of muscle mass and it has recently been reported that long term androgen deprivation treatment (> 1 year) can adversely affect cognitive function (Bast et al., 2000; Bussiere et al., 2005). Furthermore, androgen deprivation therapy is effective only in the short-term and often results in the recurrence of prostate cancer that is androgen independent (hormone refractory) with the median time to this disease progression being 14 to 30 months following initiation of androgen deprivation treatment (Sharifi et al., 2005).

1.2.7 Androgen Independent Prostate Cancer

The transition of prostate cancer to androgen independence is thought to occur through the growth selection of androgen-independent cells that may co-exist within an androgen dependent population (Abate-Shen and Shen, 2000). Multiple mechanisms for

the progression to androgen independence have been proposed, including alterations in the *AR* gene, *AR* gene amplification, and alterations in AR function and/or specificity. In prostate cancer, the AR is frequently mutated within the hormone-binding domain as well as throughout its coding region, which permits binding of other steroid hormones, overcoming the specific requirement for androgen (Tilley et al., 1996). Genetic alterations, especially in oncogenes or tumour suppressor genes which are involved in activation of the AR may also promote proliferation of prostate cancer cells in the absence of androgens (Scher and Sawyers, 2005).

Treatment options for androgen independent prostate cancer include palliative radiotherapy to reduce bone pain associated with individual metastases and more recently chemotherapy, which when used in combination with corticosteroids has shown a significant reduction in bone pain to that of corticosteroid use alone (Sonpavde et al., 2006). Recently, clinical trials of a new chemotherapeutic agent, docetaxel in combination with corticosteroids have shown a significant improvement in quality of life, pain and median survival (18.9 months) for men with androgen independent tumours (Tannock et al., 2004). Ongoing clinical trials are assessing docetaxel in combination with novel agents such as endothelin receptor antagonists and vaccines in an effort to further improve treatment outcomes (Sonpavde et al., 2006).

1.2.8 Chromosomal Anomalies in Prostate Cancer

The most frequent chromosomal/genetic alterations detected in both PIN and prostate cancer are gain of chromosome 7, in particular 7q31, loss of 8p, gain of 8q and losses of 10q, 13q, 16q and 18q (Bostwick et al., 2004). Gain of 8q is one of the most common chromosomal anomalies in prostate cancer lymph node metastases and is frequently detected in androgen independent cancer (Cher et al., 1996). Conversely 8p is one of the most frequently deleted regions in prostate cancer (von Knobloch et al., 2004) indicating that changes of this chromosome and/or tumour suppressor genes located within this chromosomal region may be critical for the progression of prostate cancer. Loss of 8p is detected in 29-50% of PIN, 32-69% of primary cancers, and in 65-100% of metastatic cancers (Cunningham et al., 1996) and along with loss of 13q shows the highest incidence of loss of heterozygosity (LOH) throughout all stages of prostate cancer (von Knobloch et al., 2004). In addition when loss of 8p and 13q occur in combination, a highly significant association with advanced tumour grade is seen,

suggesting that tumour suppressor genes residing at these loci are synergistically involved in the progression of prostate cancer (von Knobloch et al., 2004).

Frequently deleted 8p regions include 8p21 and 8p12 with loss of 8p12-21 observed in 21-63% of PIN lesions and in 69-91% of cancer tissue samples (Emmert-Buck et al., 1995; Haggman et al., 1997; Kagan et al., 1995). LOH at chromosomal locus 8p21.2 is also common and is detected in 75-90% of advanced prostate cancers where it is thought to occur at the same time as loss of androgen responsiveness and the associated loss of differentiation of the tumour (Vocke et al., 1996). Recently, mutations in the *MSR1* gene located at 8p22 were seen in families with hereditary prostate cancer suggesting that more than one tumour suppressor gene may be located on 8p and that inactivation of these genes may be important for the initiation of prostate cancer (Wiklund et al., 2003). Interestingly, loss of 8p22 is also associated with a poor prognosis after radical prostatectomy (Tsuchiya et al., 2002). Gain, deletion, and translocation of 7q22-q31 are common in prostate cancer with aneusomy of chromosome 7 frequently occurring and often associated with higher cancer grade and early patient death (Alcaraz et al., 1994). The frequency of trisomy 7 is also higher in prostate cancer than in PIN (Bandyk et al., 1994) and gain of 7q31 is strongly correlated with high Gleason grade (Jenkins et al., 1998), suggesting that overrepresentation of genes in this area may be important for the progression of prostate cancer.

Two regions on chromosome 10 are frequently deleted in prostate cancer, 10q23-24 and 10p11.2 (Gray et al., 1995). On chromosome 16, loss of 16q24.1-24.2 is seen in approximately 30% of clinically localised prostate cancers and is associated with cancer progression (Carter et al., 1990). Men that have prostate tumours with deletions of both 16q24 and 8p22 show an increased incidence of lymph node metastases (Matsuyama et al., 2003). LOH at chromosomal regions 18q22.1, 21q22.2-22.3 and 3p25-26 are detected in ~ 20-40% of cancers and other regions that show consistent LOH are 5q, 6q, 13q and 17p31 (Cunningham et al., 1996). LOH at 13q14.1 occurs with an incidence of 61% and shows a significant association with advanced tumour stage whereas loss of 5q is significantly associated with lymph node metastasis as is LOH at 9p. LOH at 18q12.2-12.3 is thought to be an early event in disease progression as approximately 52% of prostate cancers compared to 19% of PIN lesions show allelic imbalance at this region (Bostwick et al., 1998; von Knobloch et al., 2004). It would appear from these

studies that loss of 8p or 13q may be involved in the initiation of prostate cancer whereas in combination they promote the progression of prostate cancer. Further losses of 5q and 16q, and gains of 7q and 8q, are then required for metastatic disease to develop.

Although no genes have been conclusively identified to cause initiation of prostate cancer, several genes are located at frequently altered chromosomal regions in prostate cancers and have been implicated based on their functional properties (Abate-Shen and Shen, 2000). One such gene is the prostatic homeobox gene *NKX3-1* that maps to 8p21.2, a region implicated in both the initiation and progression of prostate cancer.

1.3 NKX3-1

1.3.1 Homeobox Genes

Homeobox genes are important regulatory genes that were first identified and described in *D. melanogaster* in 1984 as genes that encode the body plan during development (McGinnis et al., 1984). Following their discovery in *Drosophila,* homeobox genes have been identified in all metazoan species and are characterised by a 180bp DNA sequence known as the homeobox (Banerjee-Basu and Baxevanis, 2001). The homeobox encodes a 60 amino acid α-helix-turn-helix DNA binding motif referred to as the homeodomain in all homeobox genes except the TALE class where the homeodomain contains 63 amino acids (Holland and Takahashi, 2005).

1.3.1.1 Homeodomain Proteins

The DNA binding specificity of homeodomain proteins (homeoproteins) is conferred by sequence specific DNA motifs within the homeodomain and the N-terminal extension (Banerjee-Basu and Baxevanis, 2001). The homeodomain is comprised of three α-helices folded into a globular structure where helices I and II, which are separated by a conserved region, lie parallel to one another and interact with DNA in the minor groove. An N-terminal extension precedes helix I, and also binds specific DNA bases in the minor groove. The third helix, the recognition helix, binds in the major groove of DNA contacting both the phosphate backbone and specific bases (Figure 1.6; Gehring et al., 1994). Within the recognition helix are four consensus residues conserved in all known homeodomains, residues 48 (tryptophan) and 49 (phenylalanine) that are important for

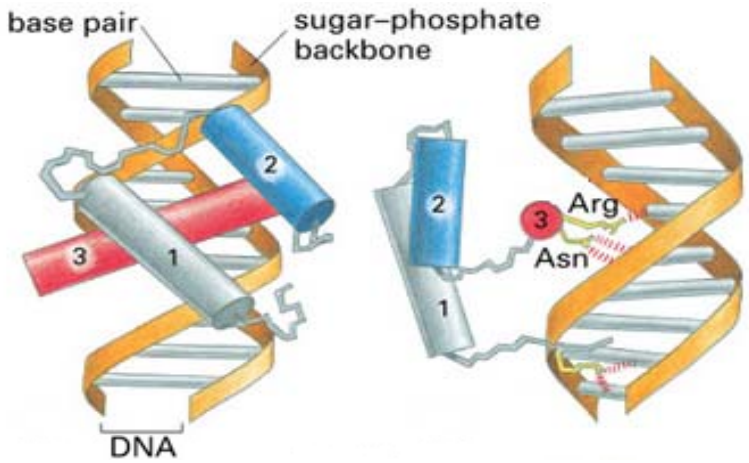

Figure 1.6 Schematic representation of the binding mode of the homeodomain. Helix 3 binds in the major groove of DNA contacting both the phosphate backbone and specific residues (Asn^{51} and Arg^{53}) which are conserved in all homeodomain proteins. The N-terminal arm lies in the minor groove and makes additional DNA contacts. (Adapted from Wolberger et al., 1991)

the integrity of the three α-helical structure, and residues 51 (asparagine) and 53 (arginine) that make essential contacts with the major groove of DNA (Banerjee-Basu and Baxevanis, 2001).

Within animal genomes, molecular phylogenetic analyses have revealed that homeobox genes can be segregated into 6 main classes based on their homeodomain sequence. Of these, the ANTP and PRD form 2 distinct classes whilst the remaining LIM, POU, SINE and TALE classes are more divergent (Holland and Takahashi, 2005). Based on chromosomal mapping and sequence specific residues located within the homeodomain (Banerjee-Basu and Baxevanis, 2001), the ANTP and PRD classes can be sub-divided into clades of Hox/ExHox, ParaHox and NK-related genes for the ANTP class and Paired-like (K_{50}), Paired-like (Q_{50}) and Pax (S_{50}) genes for the PRD class. These clades are then further divided into gene families comprising homeobox genes that contain a series of closely related genes (Table 1.5; Holland and Takahashi, 2005). However between classes of homeobox genes, there is considerable sequence diversity within homeodomains and within the N- and C-terminal regions that flank this domain. This is believed to contribute to the unique functional properties of individual homeodomain proteins as do additional conserved domains or motifs that occur in particular gene families (Banerjee-Basu and Baxevanis, 2001).

1.3.2 NK Homeobox Genes

The NK-related clade of homeobox genes is named after M. Nirenberg and Y. Kim who in 1989 identified 4 novel genes in *Drosophila* which they named *NK1* (*slouch*, *slo*), *NK2* (*ventral nervous system defective*, *vnd*) *NK3* (*bagpipe*, *bap*) and *NK4* (*tinman*, *tin*) (Kim and Nirenberg, 1989). Later, 3 other NK-related genes *C15* (*93Bal*), *ladybird early* (*lbe*) and *ladybird late* (*lbl*) were identified of which *lbe* and *lbl* represent gene duplications (Jagla et al., 2001). Of these *Drosophila* genes, all but *vnd* are clustered on chromosome 3 and are known as the 93D/E cluster (Jagla et al., 2001). Further studies in *A. gambiae* and amphioxus have identified 2 more genes, *NK5* and *Drop* (*Dr*) which belong to this cluster and provide evidence of an ancestral NK cluster comprised of 7 genes in the order *Dr*, *tin*, *bap*, *lbx* (ladybird), *C15*, *slo* and *NK5* which, like the Hox and ParaHox gene clusters then underwent duplication in early chordate evolution followed by gene loss (Garcia-Fernandez, 2005; Luke et al., 2003). However unlike the

Table 1.5 Classification of the homeobox genes. Based on phylogenetic analyses, chromosomal mapping and homeodomain sequence comparison, homeobox genes can be classified into 6 discrete classes (Holland and Takahashi, 2005).

ANTP			PRD			LIM	SINE	TALE	POU
Hox/ExHox	**ParaHox**	**NK-related**	**Paired-like (K_{50})**	**Paired-like (Q_{50})**	**Pax (S_{50})**				
Gbx	Cdx	NK1	Dmbx	Alx	Pax2/5/8	ISL	Six	Iro	Brn
En	Gsx	NK2	Gsc	Anf	Pax3/7	LIM		MEIS	Oct
Evx	Xlox	NK3	Otx	Arix	Pax4/6			Pbx	Pit
Mnx		NK4	Ptx	CVC				TGIF	
Mox		NK5		Dux					
		NK6		Mix					
		Dlx		Otp					
		Emx		PHOX					
		Hhex		Prx					
		Lbx		Rx					
		Msx		Shox					
		Tlx		Unc-4					

Holland, P.W. and Takahashi, T. (2005).

Hox and ParaHox gene clusters which have remained evolutionarily tightly linked in chordates but not in *Drosophila*, the NK-related gene cluster apart from *tin-bap* and *C15-lbx* has undergone breakage and dispersal in chordates but remains linked in *Drosophila* (Figure 1.7; Garcia-Fernandez, 2005). In the human genome, orthologues of the NK-related class of genes have also been identified (Table 1.6) however the only genes to have remained linked from the ancestral NK gene cluster are *NKX2-6/NKX3-1*, *TLX/LBX1* and *TLX2/LBX2* (Figure 1.7).

1.3.2.1 NK Homeodomain Proteins

Following the discovery of the *NK1-NK4* genes in *Drosophila*, the encoded proteins from these genes were classified into two new homeoprotein classes, NK-1 (containing NK1) and NK-2, (containing NK2, NK3, and NK4). The remainder of the NK-related homeoproteins have not been classified into classes. NK-2 class homeoproteins, of which there are 9 in humans (Table 1.6), have a tyrosine at position 54 of their homeodomain and this distinguishes class members from the NK-1 homeoproteins (Banerjee-Basu and Baxevanis, 2001). This conserved tyrosine also defines the DNA-binding specificity for a core DNA domain of CAAGTG, rather than a TAATGG core, which is preferentially bound by most other homeoproteins (Gruschus et al., 1997). Most of the NK-2 homeoproteins are further distinguished by an NK2-specific domain (NK2-SD) that is located 5' to the homeodomain and which is comprised of a hydrophobic core sequence 'VAVPVLV' flanked by basic amino acids that is believed to function as a transactivation regulator (Watada et al., 2000). In the human NK-2 class homeoproteins, the NK2-SD domain is present as 'V/IA/VVPVLV' in NK2 and NK4 orthologues and as VAVKVLV in the NK3 orthologue BAPX1 (NKX3-2), but is not present in the other NK3 orthologue NKX3-1.

NK-2 class homeoproteins generally show tissue specific expression patterns and were originally studied in *Drosophila* where it was shown that these genes are expressed in a sequential manner during development in early mesodermal patterning and in differentiation (Jagla et al., 2001). Members of the NK-2 class in humans are also expressed during embryonic development and in mesodermal derivatives, although they do not appear to be sequentially expressed. In contrast, NK-2 class paralogues appear to display an anteroventral pattern of expression in the chicken (Garcia-Fernandez, 2005). NK3 expression is required for the specification of *Drosophila* visceral mesoderm

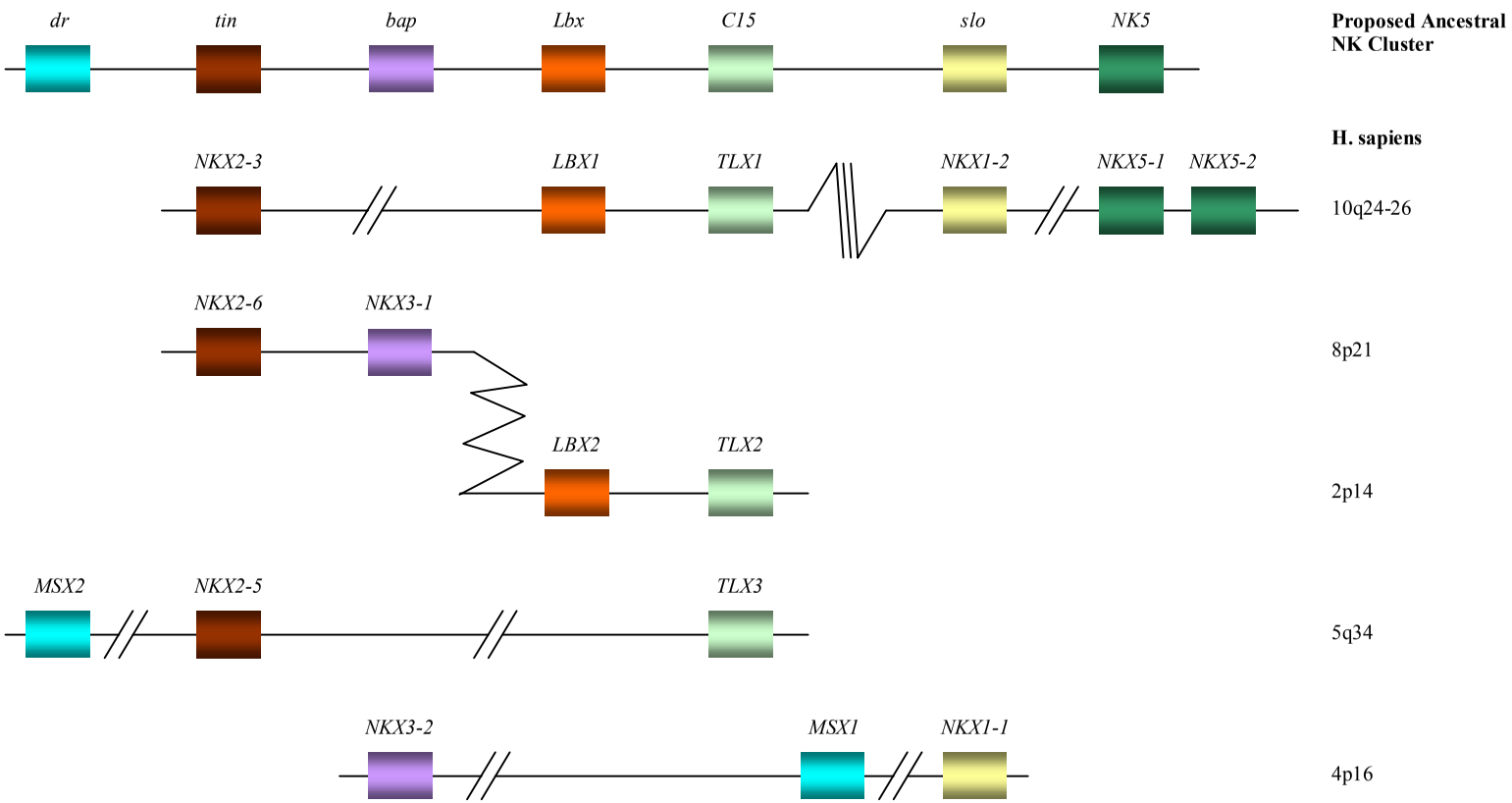

Figure 1.7 Comparison of the proposed ancestral NK cluster to the NK homeobox gene cluster of *Homo sapiens*. The complete NK cluster in the last common ancestor of protosomes and deuterosomes is proposed to have comprised of the genes *dr*, *tin*, *bap*, *Lbx*, *C15*, *slo* and *NK5*. Colour coding denotes orthologous genes and shows dispersal of the NK cluster in the human genome. Cluster breaks are denoted by // where intergenic distance is >1Mb and zigzags refers to a chromosomal transposition.

Table 1.6 Human orthologues of *Drosophila* NK-related genes

Drosophila	**H. sapiens**
slo (*NK1*)	*NKX1-1*
	C10orf121 (*NKX1-2*)
vnd (*NK2*)	*TITF1* (*NKX2-1*)
	NKX2-2
	NKX2-4
	NKX2-8
bap (*NK3*)	*NKX3-1*
	BAPX1 (*NKX3-2*)
tin (*NK4*)	*NKX2-3*
	NKX2-5
	NKX2-6
Hmx	*HMX2* (*NKX5-2*)
	HMX3 (*NKX5-1*)
HGTX	*NKX6-1*
	NKX6-2
NK7.1	*HHEX*
dll	*DLX1*
	DLX2
	DLX3
	DLX4
	DLX5
	DLX6
ems	*EMX1*
	EMX2
lbe, *lbl*	*LBX1*
	LBX2
dr	*MSX1*
	MSX2
C15	*TLX1*
	TLX2
	TLX3

during midgut musculature formation (Azpiazu and Frasch, 1993). In the mouse, Bapx1 is initially detected in the splanchnic mesoderm (Tribioli et al., 1997) and is associated with spleen and vertebral development (Lettice et al., 2001) while mouse Nkx3-1 is associated with the formation of the prostate and palantine salivary glands (Bhatia-Gaur et al., 1999; Tanaka et al., 2000). During vertebrate evolution, the appearance of the spleen is not well-defined but may have been present in lamprey. In contrast, the prostate is specific to mammals suggesting that the NK3 orthologues may have acquired new functions as a result of chromosomal duplication (Lettice et al., 2001), which is predicted to have occurred twice during vertebrate evolution (Pollard and Holland, 2000). It is proposed that Bapx1 and Nkx3-1 arose during one of these chromosomal duplications with Nkx3-1 appearing later in vertebrate evolution than Bapx1 as salivary glands only arose in vertebrates once tetrapods became land based feeders (Lettice et al., 2001).

1.3.3 The NKX3-1 Homeodomain Protein

1.3.3.1 The *NKX3-1* Gene

The human *NKX3-1* gene maps to chromosome 8p21.2 and spans 4223 bases pairs (bp) of genomic DNA with an open reading frame (ORF) divided between two exons, the second of which contains the homeobox. The gene produces a mRNA transcript of 3266bp comprised of a short 48bp 5' untranslated region (UTR) and an unusually long 2513bp 3' UTR, and encodes a protein of 234 amino acids (Figure 1.8; He et al., 1997). Of the *Drosophila* NK genes, *NKX3-1* shows 50% homology to the NK4 homeobox, 60% homology to the NK2 homeobox and 78% homology to the NK3 homeobox where it is identical within helix III of the homeodomain. However, outside of the homeodomain there is no strong homology with *Drosophila* NK3 (He et al., 1997). The mouse *Nkx3-1* and human *NKX3-1* genes represent mammalian orthologues of the *Drosophila NK3* gene and there is 100% homology between the homeodomains and 67% overall homology within the mouse *Nkx3-1* and human *NKX3-1* genes (Prescott et al., 1998). Following the discovery of the mouse *Nkx3-1* and human *NKX3-1* genes, homologous genes have been identified in the chimpanzee, dog and rat and in these genes there is 100% homology between the homeodomains except for the rat which differs at one position although this residue is still conserved (Figure 1.9).

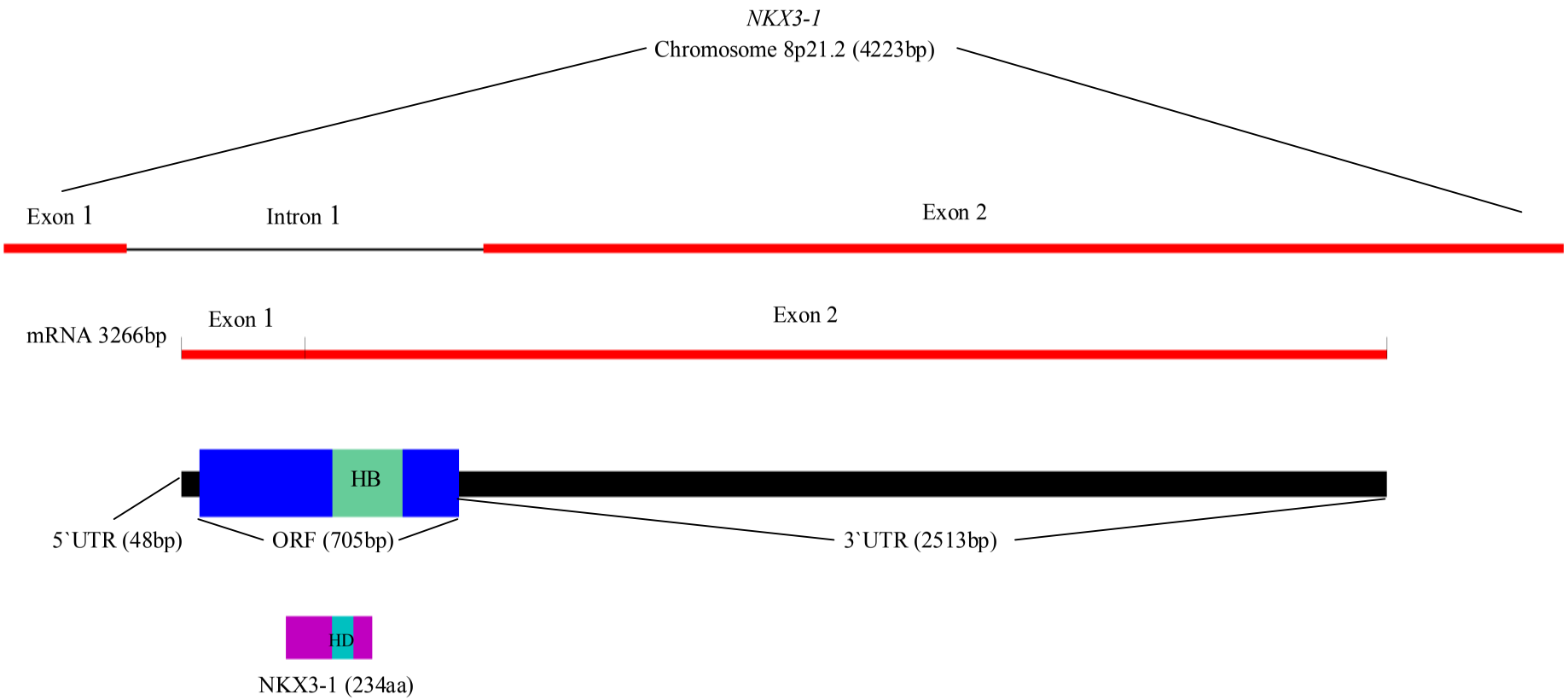

Figure 1.8 *NKX3-1* maps to 8p21.2 and spans 4223 base pairs (bp) of genomic DNA. This gene produces a mRNA transcript of 3266bp with an open reading frame (ORF) divided between two exons, the second of which contains the homeobox (HB). The NKX3-1 mRNA contains a short 48bp 5' untranslated region (UTR), an unusually long 2513bp 3' UTR and encodes a homeodomain (HD) protein of 234 amino acids (aa).

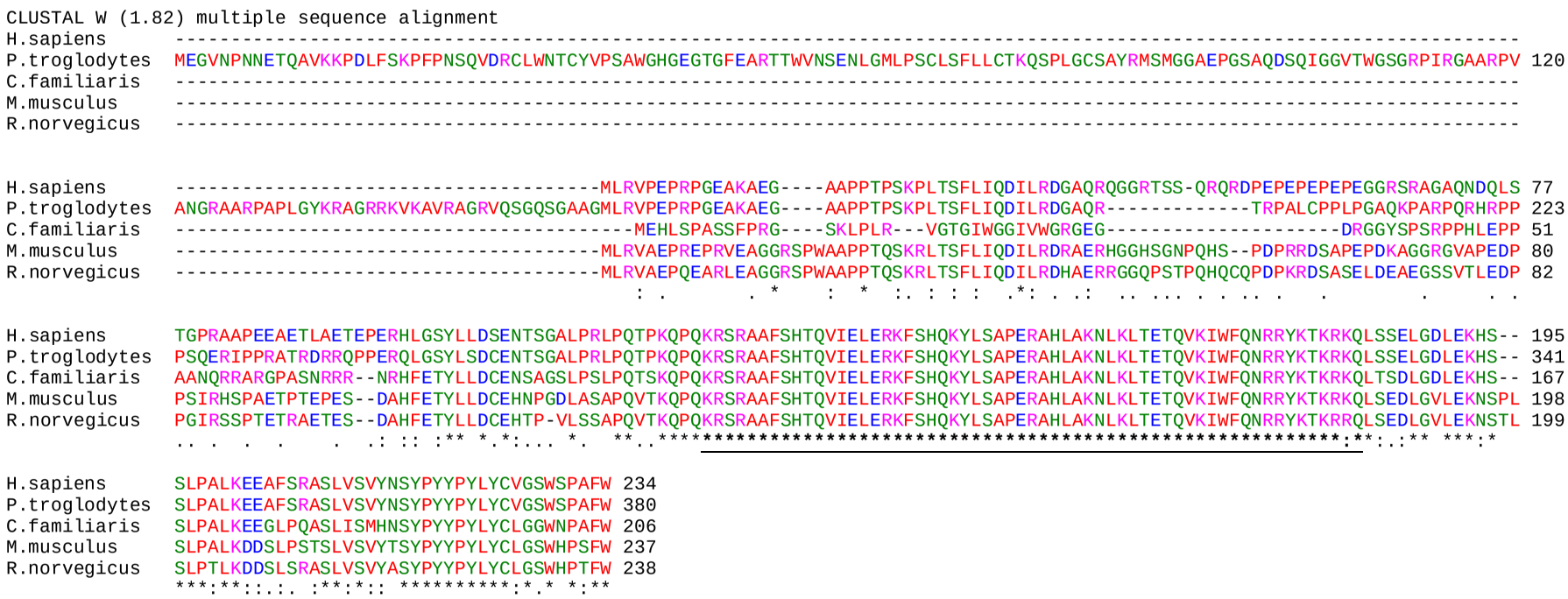

Figure 1.9 Sequence alignments of mammalian NKX3-1 proteins. Alignment of mammalian NKX3-1 homeoproteins using CLUSTALW (Thompson et al., 1994) indicates 100% homology between homeodomains (underlined). Conservation indicators (star, colon and dot) represent identical, conserved and semi-conserved amino acids respectively. Colouring indicates residue[1] property (red - small + hydrophobic including aromatic Y, blue – acidic, magenta – basic, green – hydroxyl + amine + basic Q).

[1] A – alanine, C – cysteine, D – aspartate, E – glutamate, F – phenylalanine,e G – glycine, H – histidine, I – isoleucine, K – lysine, L – leucine, M – methionine, N – asparagine, P – proline, Q – glutamine, R – arginine, S – serine, T – threonine, V – valine, W – tryphtophan, Y – tyrosine.

1.3.3.2 *Nkx3-1* Expression During Embryogenesis

In the mouse, *Nkx3-1* expression can be detected in developing embryos 7.5 days post coitum (p.c.) in the paraxial mesoderm adjacent to the neural fold. Expression proceeds caudally and at day 10.5 p.c. *Nkx3*-1 expression can only be detected in the most caudal somites (Kos et al., 1998; Tanaka et al., 1999), where in conjunction with *Bapx1* expression, regulation of the size and spatial organisation of the early sclerotomal compartment that gives rise to the vertebrae occurs (Herbrand et al., 2002). During this time, *Nkx3.1* expression is regulated by the notochord as well as the neural tube and expression is induced and maintained by sonic hedgehog. However, *Nkx3-1* expression in the sclerotome is only transient and from day 10.5 p.c. *Nkx3-1* expression can be down-regulated by the repression of sonic hedgehog following administration of forskolin (Herbrand et al., 2002; Kos et al., 1998). At this time, *Nkx3-1* expression is also be found in subpopulations of vascular smooth muscle cells (Tanaka et al., 1999).

During the later stages of gestation, *Nkx3-1* is expressed in the male urogenital sinus, prostatic buds, and testis. Expression in the prostatic buds is restricted to the leading edge in the urogenital sinus indicating that expression may occur in response to an inductive signal from the surrounding mesenchyme (Sciavolino et al., 1997). At this stage of development (14.5 p.c.) the urogenital sinus epithelium lacks functional AR, however functional AR are present in the urogenital sinus mesenchyme. At present, the role of urogenital sinus mesenchyme AR in controlling induction of *Nkx3-1* expression and early prostate duct formation is unknown (Bhatia-Gaur et al., 1999). Tissue recombinant experiments using urogenital sinus epithelium and urogenital sinus mesenchyme demonstrated that whilst urogenital sinus mesenchyme can induce *Nkx3-1* expression, functional AR is required in the urogenital sinus epithelium to maintain *Nkx3-1* expression, as tissue recombinants lacking functional AR failed to express *Nkx3-1* and prostate development did not proceed (Bhatia-Gaur et al., 1999).

At 17.5 days gestation, *Nkx3-1* expression becomes localised to the prostatic buds of the prospective lobes of the prostate, and to the medullary cords, which form the seminiferous tubules in the testes. In the 2-4 weeks following birth, *Nkx3-1* expression correlates with prostate ductal growth and differentiation. Upon reaching sexual maturity, *Nkx3-1* expression is upregulated in response to increased androgens (Sciavolino et al., 1997), and can be detected in all four lobes of the prostate gland, the

bulbourethral gland and at extremely low levels in the testes, salivary gland and brain (Bieberich et al., 1996). Expression of *Nkx3-1* was significantly reduced in adult mice following castration with expression levels decreasing 8-fold 2 days post castration and 10-fold 5 days post castration (Sciavolino et al., 1997). These studies suggest that during mouse embryogenesis *Nkx3-1* is involved in the development of the prostate while in the adult prostate it contributes to the androgen-regulated differentiated phenotype. In adult human males *NKX3-1* is also predominantly expressed in prostatic epithelium with lower levels detected in the testis (He et al., 1997). Human *NKX3-1* has also been shown to be androgen responsive as *NKX3-1* levels are regulated by androgens in the AR-expressing LNCaP prostate cancer cell line, whilst androgen independent prostate cancer cells, PC-3 and DU145 have exceedingly low levels of *NKX3-1* mRNA and do not express detectable levels of NKX3-1 protein (He et al., 1997).

1.3.3.3 *Nkx3-1* Knockout Mice

Nkx3-1 knockout mice exhibit abnormal prostatic differentiation, which is evident in neonates. The prostates of these mice are reduced in size compared to wild type mice and by 3 weeks of age show a significant reduction in the number of ductal tips and branch points although there is no overall decrease in prostate size (Bhatia-Gaur et al., 1999; Tanaka et al., 2000). By 6 months of age *Nkx3-1* knockout mice display prostatic epithelial hyperplasia, which increases in severity with age until 1 year but does not appear to increase in severity thereafter. In addition there is no evidence of prostate cancer in *Nkx3-1* knockout mice at 2 years of age (Tanaka et al., 2000). *Nkx3-1* is also expressed in mouse palatine salivary glands and *Nkx3-1* knockout mice demonstrate reduced ductal branching in these glands but with an increase in mucus producing cells and proliferating epithelial cells, suggesting that *Nkx3-1* is involved in regulating glandular morphogenesis (Tanaka et al., 2000). Although there is no evidence of prostate cancer in *Nkx3-1* knockout mice the prostatic epithelial hyperplasia and dysplasia displayed in these mice closely resembles human adult PIN lesions (Kim et al., 2002a). *Nkx3-1* knockout mice also display deregulated expression of several anti-oxidant and pro-oxidant proteins. This deregulation of expression occurs as early as 4 months of age, which is before the appearance of prostatic epithelial hyperplasia, and persists with aging (Ouyang et al., 2005). Compared to wild type mice, *Nkx3-1* knockout mice exhibit decreased expression of the anti-oxidants Gpx2 and Prdx6 in the

prostatic epithelium along with increased expression of the anti-oxidant Gpx3, which is thought to compensate for the reduction in Gpx2 and Prdx6 expression. Expression of the pro-oxidant Qscn6 is also elevated in these mice relative to wild type mice (Ouyang et al., 2005). This study suggested that Nkx3-1 maintains the prostatic phenotype by regulating genes involved in the oxidative response pathway and that loss of *Nkx3-1* expression accelerates aging of prostatic epithelium.

In *Nkx3-1*$^{+/-}$*/Pten*$^{+/-}$ and *Nkx3-1*$^{-/-}$*/Pten*$^{+/-}$ compound knockout mice, high-grade PIN lesions are seen by 6 months of age progressing to adenocarcinoma by 12 months of age (Kim et al., 2002b). In addition, *Nkx3-1*$^{-/-}$*/Pten*$^{+/-}$ knockout mice display further deregulation of the oxidative response pathway. In these mice, expression of Gpx2, Gpx3 and Prdx6 is barely detectable whilst expression of Qscn6 is further increased relative to *Nkx3-1* knockout mice (Ouyang et al., 2005). Expression of the anti-oxidant enzymes Mn SOD and Cu/Zn SOD are also reduced in these mice but only at the protein level, not at the mRNA level and only in older mice that have developed adenocarcinomas (Ouyang et al., 2005). Interestingly the *Nkx3-1*$^{+/-}$*/Pten*$^{+/-}$ compound heterozygotes, whilst retaining *Nkx3-1* mRNA, also displayed loss of Nkx3-1 protein expression without loss of the remaining *Nkx3-1* allele or mutation of its coding region (Kim et al., 2002b). This finding is in agreement with an analysis of the human *NKX3-1* gene, which found no mutations in the coding region and mRNA levels not significantly reduced in primary non-metastatic, androgen-dependent prostate cancers as compared to normal prostate (Ornstein et al., 2001; Xu et al., 2000). However, reduced NKX3-1 protein expression is observed in primary human prostate cancers with a recent study finding allelic deletion (LOH) to be the main genetic factor associated with reduced NKX3-1 expression (Asatiani et al., 2005).

Another gene which shows loss of protein expression in PIN and also co-operates with *Pten* to promote prostate cancer development is the cyclin-dependent kinase inhibitor *p27*^{KIP1} (Di Cristofano et al., 2001). In the prostates of *Nkx3-1*$^{-/-}$*/p27*$^{-/-}$; *Nkx3-1*$^{+/-}$*/p27*$^{-/-}$ and *Nkx3-1*$^{-/-}$*/p27*$^{+/-}$ compound knockout mice, extensive hyperplasia and dysplasia, increased nuclear crowding, nuclear elongation and hyperchromasia, and PIN lesions were seen by 24 weeks of age (Gary et al., 2004). However lesions were histopathologically similar in all mice. In addition, PIN lesions in *Nkx3-1*$^{+/-}$*/p27*$^{+/-}$ compound heterozygote knockout mice were phenotypically similar to those of *Nkx3-*

1$^{+/-}$*/p27*$^{+/+}$ and *Nkx3-1*$^{+/+}$*/p27*$^{+/-}$ mice, suggesting that unlike *Nkx3-1* and *Pten*, there was no co-operativity between *Nkx3-1* and *p27* in the induction of PIN (Gary et al., 2004). Nuclei from the prostatic lesions of *Nkx3-1*$^{-/-}$*/p27*$^{-/-}$ double knockout mice however, were significantly larger and had a higher DNA content. Moreover, in these mice there was a significant increase in the proliferation of prostate epithelial cells together with a reduction in apoptosis when compared to either *Nkx3-1*$^{+/+}$*/p27*$^{-/-}$ or *Nkx3-1*$^{+/-}$*/p27*$^{-/-}$ mice suggesting that loss of *Nkx3-1* expression suppresses apoptosis in *p27* deficient prostate cells (Gary et al., 2004).

NKX3-1 expression is reduced or absent in a proportion of both PIN lesions and advanced prostate cancers where loss of NKX3-1 expression correlates to disease progression (Bowen et al., 2000). As there is no significant loss of *NKX3-1* mRNA occurring, it has been suggested that *NKX3-1* haploinsufficiency is sufficient to promote loss of prostatic epithelial differentiation (Bhatia-Gaur et al., 1999). This proposal is consistent with the results seen in *Nkx3-1*$^{+/-}$ and *Nkx3-1*$^{-/-}$ knockout mice and is proposed to indicate that Nkx3-1 co-regulates the exit of androgen responsive proliferating luminal epithelial cells from the cell cycle. Deletion of one or both *Nkx3-1* alleles transiently extends the proliferative phase of regenerating prostate luminal epithelial cells resulting in prostatic epithelial hyperplasia (Magee et al., 2003). In addition gene expression profiling identified several genes that are co-regulated by androgens and Nkx3-1 in the prostate in a gene dosage-sensitive manner, and that the loss of one or both *Nkx3-1* alleles stochastically inactivated those genes that were normally activated by Nkx3-1 (Magee et al., 2003). Interestingly, this manner of regulation did not apply to genes that were normally repressed by Nkx3-1 suggesting the involvement of different regulatory mechanisms for activation and inhibition of Nkx3-1 targets.

1.3.3.4 Regulation of NKX3-1 Expression

NKX3-1 expression is also required for normal testis function with reduced NKX3-1 expression seen in testicular germ cell tumours (TGCTs) (Skotheim et al., 2003b). Unlike PIN lesions, NKX3-1 expression is not reduced in preinvasive testicular lesions indicating that loss of NKX3-1 expression is a later event in testicular carcinogenesis. In the testis, loss of NKX3-1 expression is also associated with tumour progression and is correlated with the expression of the DNA repair enzyme O^6-methyl-guanine-DNA

methyltransferase (MGMT) (Skotheim et al., 2003a; Skotheim et al., 2003b), which has been found to be epigenetically silenced in TGCTs through promoter hypermethylation (Koul et al., 2002). Although these results suggest that *NKX3-1* may also be epigenetically silenced through promoter hypermethylation, recent studies have found this is not the case in either testicular or prostate cancers (Lind et al., 2005). A G/A polymorphism 15 bases upstream from the coding sequence in the promoter region was detected however, and it was proposed that this may affect the transcriptional regulation of *NKX3-1* (Asatiani et al., 2005; Lind et al., 2005).

While inhibition of methylation or histone acetylation was found not to activate NKX3-1 expression in NKX3-1 non expressing DU145 and PC-3 prostate cancer cell lines (Asatiani et al., 2005), indicating that overall CpG methylation is not involved in regulation of NKX3-1 expression, the contribution of individually methylated CpG sites to the regulation of NKX3-1 expression is less clear. Methylation of individual CpG sites has been detected +1bp from the *NKX3-1* transcription start site (Lind et al., 2005) and at -921, -903 and -47bp of which the -47bp site is a potential Sp1 binding site (Asatiani et al., 2005). All 3 of the -921, -903 and -47 sites were found to be methylated in DU145 and PC-3 prostate cancer cell lines, but in the androgen responsive LNCaP cell line the -903 site was only partially methylated and not methylated at site -47. In prostate cancer tissue specimens, a greater degree of methylation was also observed at these sites compared to adjacent normal prostate tissue (Asatiani et al., 2005). Interestingly this study found that although LOH is the main determinant in reduced NKX3-1 expression, when the LOH occurred in conjunction with methylation at -921, -903 and -47 a further decrease in NKX3-1 expression was seen and this reduction in expression was proportional to the number of sites methylated (Asatiani et al., 2005). Although the significance of these findings is unclear it does suggest that methylation of individual CpG sites in the *NKX3-1* promoter maybe involved in the progression of prostate cancer.

Recently, sequencing analysis of the *NKX3-1* gene in prostate cancer families identified several germ-line mutations which significantly increased hereditary prostate cancer risk (Zheng et al., 2006). One of the mutations, a 1454A/G mutation was found to co-segregate with prostate cancer and resulted in a T146A amino acid substitution. This substitution corresponds to residue 41 of the homeodomain which is in the third

recognition helix and resulted in a less stable NKX3-1 protein that showed decreased binding affinity for its cognate sequence (Zheng et al., 2006). Interestingly, this residue is conserved in all but 2 of the human NK-related class of homeoproteins and is also the residue that in another NK-2 class protein (NKX2-5) is mutated in a family with hereditary heart defects (Kasahara and Benson, 2004). In that case, the DNA binding affinity of NKX2-5 was markedly reduced and mutant NKX2-5 was not able to activate the promoter of its target, atrial natriuretic factor (Kasahara and Benson, 2004). Of the remaining mutations that were found to have hereditary linkage with prostate cancer, 3 were found to be located in the *NKX3-1* promoter and 1 of these at -360bp G/A has been identified as being within a *NKX3-1* regulatory element with inhibitory function (Jiang et al., 2004).

These results provide further evidence that *NKX3-1* plays a critical role in the development and progression of prostate cancer, however the transcriptional mechanisms that regulate *NKX3-1* expression are not well characterised. Studies of a 32Kb genomic region of the *Nkx3-1* locus in mice have revealed that transcriptional control of *Nkx3-1* is complex and is mediated by multiple *cis*-acting elements (Chen et al., 2005). In the mouse, *Nkx3-1* expression in the somites and testes is regulated by a 2Kb sequence located 5Kb upstream of the *Nkx3-1* start codon, whereas expression in the prostate is regulated by enhancer elements contained in a 5Kb sequence originating 5Kb downstream from the *Nkx3-1* start codon (Chen et al., 2005). These data suggest that tissue specific expression of *Nkx3-1* may be controlled in a modular fashion by distinct regulatory elements (Chen et al., 2005) as is the case with *Nkx2-5*, which has a regulatory region containing 6 distinct activator and 3 distinct repressor elements (Schwartz and Olsen, 1999).

In the human *NKX3-1* gene, regulatory elements have also been located upstream of the *NKX3-1* gene in the promoter region. These include a positive *cis*-element of 16bp at -920 to -905bp (Jiang et al., 2005b) and a 20bp inhibitory element at -361 to -342bp (Jiang et al., 2004). When this inhibitory element was blocked by a decoy element, NKX3-1 expression in LNCaP prostate cancer cells was up-regulated resulting in decreased cellular proliferation (Jiang et al., 2005a), however factors that bind these regulatory regions have yet to be identified. Another positive *cis*-element of 16bp at -936 to 921bp has been shown to be responsive to 9-cis retinoic acid treatment, a

retinoid which activates retinoid X receptors (RXRs). Treatment of LNCaP prostate cells with 9-cis retinoic acid resulted in an increase in both NKX3-1 mRNA and protein levels and arrest of the LNCaP cells in the G_1 phase of the cell cycle. However, as the -936 to 921bp element does not contain a recognised RXR response element it was thought the RXR may be interacting indirectly with this element by binding to another as yet unidentified factor to upregulate *NKX3-1* expression (Jiang et al., 2006). Treatment of LNCaP cells with the retinoid acid receptor (RAR) ligand all-*trans* retinoic acid also leads to an increase in *NKX3-1* mRNA and protein levels and although several putative retinoic acid response elements (RAREs) were located within 2 kb of the *NKX3.1* proximal promoter and the 3`-UTR these were found not to be responsible for mediating retinoid responsiveness (Thomas et al., 2006).

An androgen response element (ARE) has been identified -3013bp upstream of the *NKX3-1* gene which, in the presence of androgens, was shown to bind the transcriptional co-repressors silencing mediator of retinoid and thyroid hormone receptor (SMRT) and nuclear receptor co-repressor (N-CoR), suppressing transcriptional activation of *NKX3-1* (Yoon and Wong, 2005). Knockdown of SMRT and/or N-CoR using small interfering RNA (siRNA) did not increase androgen receptor (AR) binding of the *NKX3-1* ARE but did result in increased binding of the co-activators SRC-1 and p300 leading to increased transcriptional activation of *NKX3-1* (Yoon and Wong, 2005). These results indicate that SMRT and N-CoR compete with SRC-1 and p300 for binding to ligand-bound AR and that the balance between co-repressors and co-activators determines the level of *NKX3-1* transcriptional activation. Transcriptional regulation of *NKX3-1*, mediated by androgens, was also found to occur through the *NKX3-1* 3`-UTR indicating the presence of additional AREs within this region (Thomas et al., 2006). However in contrast to the ARE located proximal to the *NKX3-1* gene which is involved in the transcriptional inhibition of *NKX3-1* in the presence of androgens, the *NKX3-1* 3`-UTR was shown to increase the transcriptional activity of *NKX3-1*. Several putative AREs have been identified in this region although the specific response element(s) involved in the upregulation of *NKX3-1* expression remain to be identified (Thomas et al., 2006).

1.3.3.5 NKX3-1 DNA-Binding Sites

Although some target genes of NKX3-1 have recently been identified (Magee et al., 2003), the NKX3-1 DNA-binding sites for these genes have not been mapped. Consensus DNA-binding elements have been identified using a selection and amplification binding assay. This assay determined the optimal DNA-binding sequence for NKX3-1 as 5`-TAAGTA-3` (Steadman et al., 2000), a similar motif to binding sequences of other NK-2 class homeoproteins including Nkx2-1 that binds 5`-CAAGTG-3` and Nkx2-5 that binds 5`-TNAAGTG-3` (Damante et al., 1994; Gehring et al., 1994). The preferential binding of NKX3-1 for T at the first position of the TAAGTA binding site is thought to be due to the variations in side chain volume, particularly amino acid residues 6 and 7 at the N-terminus of the homeodomain. The NKX3-1 homeodomain has alanine and phenylalanine at these positions whereas Nkx2-1 has leucine and phenylalanine at these positions (Steadman et al., 2000). Although NKX3-1 preferentially binds the TA dinucleotide following the TAAGT core binding sequence, competitive binding experiments revealed that NKX3-1 will also bind TAAGTG suggesting that the A and G nucleotides are interchangeable at this position. *In vitro* assays demonstrated that NKX3-1 expression repressed the transcriptional activity of a luciferase reporter gene construct containing 3 copies of the TAAGTA DNA-binding sequence and that the orientation of the TAAGTA sequence did not affect the transcriptional repression (Steadman et al., 2000). However like other homeoproteins such as Nkx2-1 and NK3, where phosphorylation and co-factor interactions have been shown to increase DNA-binding affinities respectively, it has been proposed that NKX3-1 binding *in vivo* would also be enhanced by post-translational modification and/or protein-protein interactions (Kim et al., 1998; Zannini et al., 1996).

1.3.3.6 NKX3-1 Co-Factors

The activity of transcriptional regulation is also modulated by co-regulatory proteins that act as either co-activators or co-repressors operating as part of a promoter or enhancer bound complex. Within this complex, co-regulators function by altering the chromatin template in a covalent or non-covalent manner thereby altering promoter usage to influence each other's activity or DNA-binding specificity (Courey, 2001). Currently, relatively few interacting partners of NKX3-1 have been identified. Serum response factor (SRF) and mouse Nkx3-1 have been shown to co-operatively bind

adjacent sites of the smooth muscle γ-actin (*SMGA*) promoter synergistically activating *SMGA* transcription (Carson et al., 2000), and in both normal and malignant prostate epithelial cells transcriptional activation of *SMGA* was shown to be dependent on Nkx3-1 expression (Fillmore et al., 2002). In co-immunoprecipitation assays, SRF was also shown to associate with Nkx3-1 independently of DNA binding indicating that these two proteins can form complexes via protein-protein interactions (Carson et al., 2000).

In contrast to the transcriptional activation activity of Nkx3-1 and SRF, human NKX3-1 inhibited activation of the prostate-specific antigen (*PSA*) promoter when complexed with a prostate-derived Ets factor (PDEF) (Chen et al., 2002). In this case however, NKX3-1 mediated inhibition of *PSA* transcription was not independent of DNA-binding (Chen and Bieberich, 2005). Interestingly, interactions between PDEF and NKX3-1 required the C-terminal portions of their respective DNA-binding domains together with additional sequences located downstream of these domains (Chen and Bieberich, 2005) and it was this region of Nkx3-1 that was identified as containing a repressor domain that was relieved by association with SRF (Carson et al., 2000).

Recently, co-transfection of mouse Nkx3-1 and Sp1, Sp3 or Sp4 was shown to inhibit Sp-induced *PSA* transcription whereas transfection of Nkx3-1 alone had little effect on the transcriptional activation of *PSA* (Simmons and Horowitz, 2006). In addition, the reduction of *PSA* transcription by Nkx3-1 was dependent on HDAC activity (Simmons and Horowitz, 2006). Also of interest was the finding that although Sp2 and Sp5 were unable to induce *PSA* gene transcription, they interacted more efficiently with NKX3-1 in *in vitro* binding assays than either Sp1 or Sp3. This suggested that Nkx3-1/Sp2 and/or Nkx3-1/Sp5 complexes may also affect transcriptional regulation. Target genes however, for Sp2 and Sp5 are unknown at present (Simmons and Horowitz, 2006).

Consistent with Nkx3-1 interactions with SRF and PDEF, Nkx3-1 interaction with Sp-family members also required portions of their respective DNA-binding domains as well as additional downstream sequences and, like the Nkx3-1/SRF interaction, these interactions were also independent of DNA-binding (Simmons and Horowitz, 2006). This would suggest that protein DNA-binding domains may also function as substrates for protein-protein interactions. More importantly, as Nkx3-1 DNA-binding activity was

not required for the Sp mediated inhibition of *PSA* transcription, these results demonstrated that the domains within Nkx3-1 that interact with the Sp-family members are also required for the repression of *PSA* transcription (Simmons and Horowitz, 2006). Moreover as neither Nkx3-1 nor the Sp-family members demonstrated DNA-binding when complexed, it would indicate that the Nkx3-1/Sp-family members form complexes with other factors which directly bind DNA (Simmons and Horowitz, 2006).

1.3.3.7 Isolation of NKX3-1 Co-Factors

Although several mouse Nkx3-1 co-factors have been identified (section 1.3.3.6), currently only two co-factors for human NKX3-1 are known. PDEF which was identified from a yeast two-hybrid (Y2H) screen of a normal prostate cDNA library (Chen et al., 2002) and HDAC1 which was recently identified as a NKX3-1 co-factor in prostate cancer (Lei et al., 2006). As NKX3-1 co-factors remain poorly characterised both in the normal prostate and in prostate cancer, a Y2H screen was used in this laboratory to identify NKX3-1 binding partners in LNCaP prostate cancer cells. Of the colonies isolated from this screen, 73 were selected for further analysis. Plasmid DNA was isolated from these clones and the cDNA inserts PCR amplified and sequenced. Basic Local Alignment Search Tool (BLAST) analysis of the resulting sequences identified cDNA inserts with homology to 31 different proteins, 4 of which were the novel hypothetical protein FLJ22318. This thesis describes the preliminary characterisation of FLJ22318 and its interaction with NKX3-1.

1.4 Summary and Statement of Aims

NKX3-1 is an androgen responsive homeodomain protein that is expressed in prostate epithelium where it is involved in maintaining the differentiated prostatic phenotype and in prostate cancer cells, where its function is unknown. *NKX3-1* has recently been linked to hereditary prostate cancer and maps to chromosome 8p21.2, a region that is implicated in both the initiation and progression of sporadic prostate tumours. However, regulation of NKX3-1 expression and function are not well understood with few NKX3-1 co-factors having been identified. To understand the role of NKX3-1 in normal prostate development and the consequences of its loss in prostate cancers, characterisation of NKX3-1 binding proteins such as FLJ22318 is essential. Because FLJ22318 has not been studied previously, its function in prostate cancer cells and the effects of its interaction on NKX3-1 are unknown. FLJ22318 expression has been reported in cDNA libraries derived from a range of different tissues, indicating that it is widely expressed and that it potentially interacts with a number of proteins in addition to NKX3-1. Therefore the aims of this project were:

1. The bioinformatic analysis of FLJ22318.
2. To characterise the interaction between FLJ22318 and NKX3-1 in prostate cancer cells.
3. To identify other binding partners of FLJ22318 in prostate cancer cells using a yeast two-hybrid analysis.

Chapter Two

Chapter Two – Materials

2.1 Reagents

2.1.1 Primers

Item	Supplier
BAC Sense	Geneworks, Australia
BAC Antisense	Geneworks, Australia
BGH Reverse Sequencing Primer	Invitrogen Technologies, Australia
EGFP1266 Sense	Geneworks, Australia
FLJ789 Sense	Geneworks, Australia
FLJBamHI Sense	Geneworks, Australia
FLJBamHI Antisense	Geneworks, Australia
FLJREV Antisense	Geneworks, Australia
FLJREV2 Antisense	Geneworks, Australia
FLJSalI Sense	Geneworks, Australia
FLJSalI Antisense	Geneworks, Australia
FLJTOPO Sense	Geneworks, Australia
FLJTOPO Antisense	Geneworks, Australia
Matchmaker 3′ AD LD-Insert Antisense	Clontech, California, USA
Matchmaker 5′ AD LD-Insert Sense	Clontech, California, USA
pCMV Sense Sequencing Primer	Clontech, California, USA
pGEX Sense Sequencing Primer	Geneworks, Australia
pGEX Antisense Sequencing Primer	Geneworks, Australia

2.1.2 PCR

Item	Supplier
Agarose	BioRad Laboratories, Australia
AMV Reverse Transcriptase 300U	Promega, Australia
AMV RT 5X Reaction Buffer	Promega, Australia
Big-Dye™ Terminator Mix	Applied Biosystems, California, USA
BSA Acetylated 10µg/µL	Promega, Australia
10X Buffer D	Promega, Australia
10X Buffer E	Promega, Australia

Calf Intestinal Alkaline Phosphatase 1U/µL	Promega, Australia
dATP, dCTP, dGTP, dTTP 40µL	Promega, Australia
*Hin*d III Restriction Enzyme 10U/µL	Promega, Australia
1 Kb Plus™ DNA Ladder 1µg/µL	Invitrogen Technologies, Australia
Not I Restriction Enzyme 10U/µL	Promega, Australia
50mM Magnesium Chloride	Invitrogen Technologies, Australia
Multi-Core™ 10X Buffer	Promega, Australia
Oligo(dT) Primer 20µg	Promega, Australia
Pfu DNA Polymerase 3U/µL	Promega, Australia
Pfu 10X Reaction Buffer with $MgSO_4$	Promega, Australia
Pst I Restriction Enzyme 10U/µL	Invitrogen Technologies, Australia
React 2 Buffer	Invitrogen Technologies, Australia
RNasin® 40U/µL	Promega, Australia
Sal I Restriction Enzyme 10U/µL	Promega, Australia
Taq DNA Polymerase 5U/µL	Invitrogen Technologies, Australia
Taq 10X PCR Buffer (minus Mg^{++})	Invitrogen Technologies, Australia

2.1.3 Plasmids

Item	**Supplier**
pcDNA3.1/V5-His-TOPO/l*ac*Z	Invitrogen Technologies, Australia
pCMV-Myc	Clontech, California, USA
pCMV-HA	Clontech, California, USA
pEGFPC2	Clontech, California, USA
pGEX-2TK	Amersham Pharmacia Biotech, Australia
pHc-GAPDH	Gift from Dr. P. Leedman, Medical Research Foundation, Perth, Australia
pRL-SV40 *Renilla*	Promega, Australia
pT109-NKX-TK-Luc	Gift from Dr. E. Gelmann, Lombardi Cancer Centre, Washington DC USA
pT109-TK-Luc	Gift from Dr. E. Gelmann, Lombardi Cancer Centre, Washington DC USA

2.1.4 Yeast Assays

Item	Supplier
Adenine	Sigma Chemical Company, USA
-His/-Leu/-Trp DO Supplement	Clontech, California, USA
L-Histidine HCl Monohydrate	Sigma Chemical Company, USA
L-Leucine	Sigma Chemical Company, USA
-Trp DO Supplement	Clontech, California, USA
N, N-Dimethyl Formamide (DMF)	Clontech, California, USA
Yeast Nitrogenbase	Sigma Chemical Company, USA
X-α-Gal	Clontech, California, USA

2.1.5 Tissue Culture

Item	Supplier
DU145 Cell Line	American Type Culture Collection, USA
LNCaP Cell Line	American Type Culture Collection, USA
Foetal Calf Serum	ICN Biomedicals Inc., USA
Charcoal Stripped Fœtal Calf Serum	ICN Biomedicals Inc., USA
LipofectAMINE™ 2000	Invitrogen Technologies, Australia
Penicillin/Streptomycin	ICN Biomedicals Inc., USA
RPMI 1640 Medium with L-Glutamine	Trace Biosciences, Australia
Trypsin/EDTA (1:250, pH7)	Thermo Trace, Melbourne, Australia

2.1.6 Western Blotting

Item	Supplier
Acrylamide	BioRad, Australia
Ammonium Persulphate	BioRad, Australia
Benchmark™ Prestained Protein Ladder	Invitrogen Technologies, Australia
Cronex Medical X-Ray Film	Sterling Diagnostic Imaging, USA
Donkey Anti-Goat IgG-HRP	Santa Cruz Biotechnology Inc, USA
ECL Detection Reagents	Amersham Pharmacia Biotech, Australia
ECL Plus Detection Reagents	Amersham Pharmacia Biotech, Australia
Goat Anti-Human Actin Ig	Santa Cruz Biotechnology Inc, USA
Goat Anti-Human PACT (N-20): sc-18768	Santa Cruz Biotechnology Inc, USA

Hybond-C Nitrocellulose Membrane	Amersham Pharmacia Biotech, Australia
Mouse Anti-GFP Ig (JL-8)	Clontech, California, USA
Mouse Anti-HA Ig	Covance Research Products, USA
Mouse Anti-Myc Ig	Cell Signaling Technology, USA
Mouse Anti-Nkx3.1 Ig	Zymed Laboratories, USA
Mouse Anti-V5 Ig	Invitrogen Technologies, Australia
Rabbit Anti-Myc Ig	Cell Signaling Technology, USA
Rabbit Anti-PACT Ig	Gift from Dr. P. Leedman, Medical Research Foundation, Perth, Australia
Sheep Anti-Mouse Ig-HRP Conjugated	Chemicon, Australia
Sheep Anti-Rabbit Ig-HRP Conjugated	Chemicon, Australia
Skim Milk Powder	Bonlac Foods Ltd, Australia
TEMED	BioRad, Australia
Whatman® 3MM paper	Whatman International, Australia

2.1.7 Immunocytochemistry

Item	**Supplier**
Antibody Diluent	Dako Corporation, USA
Biotinylated Anti-Goat, Anti-Mouse, Anti-Rabbit Ig	Dako Corporation, USA
Copper Sulphate	May & Baker Pty Ltd, Australia
DAB Reagent	Dako Corporation, USA
DEPX Mounting Medium	BDH Laboratory Systems, England
Haematoxylin	Sigma Chemical Company, USA
Streptavidin/HRP	Dako Corporation, USA

2.1.8 Immunoprecipitation

Item	**Supplier**
Complete Protease Inhibitor Cocktail Tablets	Roche Diagnostics GmbH, Germany
Nonidet P-40 (NP-40)	Sigma Chemical Company, USA
Phenylmethylsulphonylfluoride	Boehringer Mannheim Corp. USA
Protein A Sepharose	Amersham Pharmacia Biotech, Australia
Protein G Sepharose	Amersham Pharmacia Biotech, Australia
Sodium Deoxycholate	Sigma Chemical Company, USA

Sodium Fluoride	BDH Biochemicals, England
Sodium Orthovanadate	Sigma Chemical Company, USA

2.1.9 Confocal

Item	Supplier
Alexa Fluor® 488 A-11005 Donkey Anti-Goat IgG	Molecular Probes Inc, USA
Alexa Fluor® 488 A-11001 Goat Anti-Mouse IgG	Molecular Probes Inc, USA
Alexa Fluor® 546 A-11010 Goat Anti-Rabbit IgG	Molecular Probes Inc, USA
BSA Fraction V High-Grade Fatty Acid Free	Roche Diagnostics GmbH, Germany
Hoechst 33258	Sigma Chemical Company, USA
Horse Serum	Sigma Chemical Company, USA
Lab-Tek® 177402 Chamber Slide™	Nalge Nunc International, USA
Triton X-100	Sigma Chemical Company, USA

2.1.10 RNA Extraction and Northern Blotting

Item	Supplier
α-[^{32}P]-dCTP (3000Ci/mmol)	Amersham Pharmacia Biotech, Australia
Diethylpyrocarbonate	Sigma Chemical Company, USA
Formamide	Sigma Chemical Company, USA
Magna Nylon Transfer Membrane (0.45µ)	Osmonics Inc, USA
3-[N-Morpholino]Propanesulphonic Acid	Sigma Chemical Company, USA
Rapid-hyb™ Buffer	Amersham Pharmacia Biotech, Australia
Ultraspec™	Fisher Biotec, Australia

2.1.11 General Reagents

Item	Supplier
Acetic Acid (glacial)	Sigma Chemical Company, USA
Adenosine 5'-Triphosphate Disodium Salt	Sigma Chemical Company, USA
Agar (bacteriological)	Unipath, England
5α-Dihydrotestosterone	Sigma Chemical Company, USA
Ammonium Acetate	BDH Biochemicals, England

Ampicillin	CSL Limited, Australia
BL21 *E. coli* cells	Amersham Pharmacia Biotech, Australia
β-Mercaptoethanol	BDH Biochemicals, England
Calcium Chloride	Sigma Chemical Company, USA
Chlorobutanol	Sigma Chemical Company, USA
Chloroform	BDH Biochemicals, England
Co-enzyme A Lithium Salt	Sigma Chemical Company, USA
Coomassie Brilliant Blue	Amersham Pharmacia Biotech, Australia
DH5α *E. coli* Cells	Invitrogen Technologies, Australia
Dimethyl Formamide	Clontech, California, USA
Dimethyl Sulphoxide	Sigma Chemical Company, USA
Disodium Hydrogen Orthophosphate	BDH Biochemicals, England
Dithiothreitol	Sigma Chemical Company, USA
D-Luciferin Potassium Salt	Molecular Probes, USA
Ethylenediaminetetraacetic Acid	Sigma Chemical Company, USA
Ethanol	BDH Biochemicals, England
Ethidium Bromide	Sigma Chemical Company, USA
Formaldehyde	BDH Biochemicals, England
Glass Beads (425-600μm)	Sigma Chemical Company, USA
Glucose (dextrose)	Sigma Chemical Company, USA
Glutathione Sepharose 4B	Amersham Pharmacia Biotech, Australia
Glycerol	Sigma Chemical Company, USA
Glycine	BDH Biochemicals, England
Hydrochloric Acid	BDH Biochemicals, England
Isopropanol	BDH Biochemicals, England
Isopropyl-β-D-Thiogalactoside	Promega, Australia
Kanamycin	CSL Limited, Australia
Lithium Acetate	Sigma Chemical Company, USA
Lysozyme	Sigma Chemical Company, USA
Magnesium Chloride	BDH Biochemicals, England
Magnesium Sulphate	BDH Biochemicals, England
Methanol	BDH Biochemicals, England
PEG-3350	Sigma Chemical Company, USA

Peptone	Difco Laboratories, USA
Phenol 10mM Tris HCl pH 7.9 1mM EDTA	Sigma Chemical Company, USA
Phenol Red	Sigma Chemical Company, USA
PIPES	Sigma Chemical Company, USA
Polyvinyl Alcohol	Sigma Chemical Company, USA
Potassium Chloride	Sigma Chemical Company, USA
Potassium Dihydrogen Orthophosphate	BDH Biochemicals, England
RNaseA	Roche Diagnostics GmbH, Germany
Sodium Acetate	BDH Biochemicals, England
Sodium Azide	Sigma Chemical Company, USA
Sodium Bicarbonate	BDH Biochemicals, England
Sodium Chloride	Sigma Chemical Company, USA
Sodium Citrate	BDH Biochemicals, England
Sodium Dihydrogen Orthophosphate	BDH Biochemicals, England
Sodium Dodecyl Sulphate	BDH Biochemicals, England
Sodium Hydroxide	BDH Biochemicals, England
Sodium Phosphate	BDH Biochemicals, England
Sterile ddH_2O	Baxter Healthcare Pty Ltd., Australia
Sucrose	BDH Biochemicals, England
Tris Base	Sigma Chemical Company, USA
Tryptone	Sigma Chemical Company, USA
Tween 20	Sigma Chemical Company, USA
Yeast Extract	Unipath, England
X-Gal 50mg/mL	Promega, Australia

2.2 Commercial Kits

Item	**Supplier**
Concert™ High Purity Plasmid Maxiprep System	**Invitrogen Technologies, Australia**
Cell Lysis Solution E2	
Cell Suspension Buffer E1	
Elution Buffer E6	
Equilibration Buffer E4	
Maxi Columns	

Concert™ High Purity Plasmid Maxiprep System	**Invitrogen Technologies, Australia**
Neutralisation Buffer E3	
TE Buffer	
Wash Buffer E5	
Dual-Luciferase® Reporter Assay	**Promega, Australia**
Luciferase Assay Buffer II	
Luciferase Assay Substrate	
5X Passive Lysis Buffer	
Stop & Glo® Buffer	
Stop & Glo® Substrate	
Stop & Glo® Substrate Solvent	
LigaFast™ Rapid DNA Ligation System	**Promega, Australia**
2x Rapid Ligation Buffer	
T4 DNA Ligase	
Poly A Pure™ mRNA Purification Kit	**Ambion® Inc, USA**
5M Ammonium Acetate	
Glycogen 5mg/mL	
Oligo(dT) Cellulose (100mg aliquots)	
Lysis Solution	
Binding Buffer	
Wash Buffer	
Dilution Buffer	
Elution Buffer	
5M NaCl	
Elution Solution	
Microfuge Tubes	
Microfuge Tubes with Spin Columns	

BD Matchmaker™ Library Construction and Screening Kit	**Clontech, California, USA**
SMART III™ Oligo	
CDS III Primer	
MMLV Reverse Transcriptase	
RNase H (2 units/μL)	
5X First-Strand Buffer	
DTT	
Control Poly A^+ RNA	
dNTP Mix	
5' PCR Primer	
10X GC-Melt Solution	
3' PCR Primer	
CHROMA SPIN +TE400-Columns	
Sodium Acetate (3M pH4.8)	
pGBKT7 DNA-BD Cloning Vector	
pGADT7-Rec AD Cloning Vector	
pGBKT7-53 Control Vector	
pGBKT7-Lam Control Vector	
SV40 Large-T PCR Fragment	
S. cerevisiae strain AH109	
NaCl Solution (0.9%)	
-Ade/-His/-Leu/-Trp DO Supplement	
-Leu/ DO Supplement	
-Leu/-Trp DO Supplement	
10X Advantage® 2 PCR Buffer	
50X Advantage® 2 Polymerase Mix	
50X dNTP Mix	
Herring Testes Carrier DNA 10mg/mL	
YPD Liquid Medium Plus	

Original TA Cloning® Kit	**Invitrogen Technologies, Australia**
10X Ligation Buffer	
pCR®2.1 Linearised Expression Vector	
T4 DNA Ligase	
pcDNA3.1/V5-His-TOPO®TA Cloning Kit	**Invitrogen Technologies, Australia**
pcDNA3.1/V5-His-TOPO	
Salt Solution	
SOC Medium	
TOP10 *E. coli* Cells	
Prime-A-Gene® Labelling System	**Invitrogen Technologies, Australia**
BSA (10mg/mL)	
dATP (1.5mM)	
dCTP (1.5mM)	
dGTP (1.5mM)	
dTTP (1.5mM)	
DNA Polymerase I Klenow Fragment	
5X Labelling Buffer	
Nuclease-Free H_2O	
Wizard® SV Gel and PCR Clean-Up System	**Promega, Australia**
Membrane Binding Solution	
Membrane Wash Solution (concentrated)	
Nuclease-Free Water	
Wizard® SV Minicolumns	
Collection Tubes (2mL)	

2.3 Equipment

Item	**Supplier**
ABI 373 XL Automated Sequencer	Perkin Elmer Applied Biosystems, California, USA
AGFA CP-1000 Film Developer	AGFA-Gevaert NV, Belguim

Autoclave	Athertons, USA
Axiovert 100 Microscope	Zeiss, Germany
Beckman Avanti™ J-25I Centrifuge	Beckman Coulter, California, USA
Beckman TJ-6 Centrifuge	Beckman Coulter, California, USA
Beckman DU®-65 Spectrophotometer	Beckman Coulter, California, USA
Centrifuge 1-15	Sigma, USA
Centrifuge CR312	Jouan, St. Herblain, France
Centrifuge CR411	Jouan, St. Herblain, France
DNA Sub Cell™, Sub Cell GT™ and Mini Sub DNA Cell™ Electrophoresis Tanks	BioRad Laboratories, Australia
Dry Block Heater	Thermoline, Australia
Eppendorf 5415C Centrifuge	Eppendorf, Germany
Eppendorf 5415R Centrifuge	Eppendorf, Germany
Grant Water Heater	Grant Instruments, Cambridge, UK
Heidolph MR 1000 Magnetic Stirrer	John Morris Scientific Pty Ltd, Australia
HP Scanjet 5200C	Hewlett Packard, Australia
Hybridisation Oven Model 1000	Robbins Scientific Corp. USA
Improved Neubauer Hæmocytometer	Hawksley, UK
Laminar Flow Hood	Email-Westinghouse, Australia
Leica CV 5000 Cover Slip Mounter	Leica Microsystems Pty Ltd, Australia
Leica Jung Autostainer XL Machine	Leica Microsystems Pty Ltd, Australia
Mini-Protean II Electrophoresis and Transfer Apparatus	BioRad Laboratories, Australia
NanoDrop® ND-1000 Spectrophotometer	Biolab Australia, Australia
Needles 23G 1¼ TW	Becton Dickinson, Singapore
Nikon Digital Camera	Nikon, Japan
Nikon Phase Contrast Microscope	Nikon, Japan
Parafilm Laboratory Film	American National Can™, USA
PHM 83 AutoCal pH Meter	Radiometer, Copenhagen
Power Pac™ 300 and 1000	BioRad Laboratories, Australia
PTC-100™ Programmable Thermal Cycler	MJ Research Inc., Australia
Qualtex Water Heater	Watson Victor Ltd., Australia
Quantity One® Imaging and Quantitation Software	BioRad Laboratories, Australia
Ratek Orbital Mixer Incubator	Rowe Scientific, Australia

Ratek Orbital Shaker	Rowe Scientific, Australia
Ratek Suspension Mixer	Rowe Scientific, Australia
Red Rotor Orbital Shaker	Hoefer, Australia
Sanyo CO_2 Incubator	Sanyo Electric Co. Ltd., Japan
Sartorius Basic Scales	Selby Scientific, Perth, Australia
Series 900 Mini Monitor	Mini Instruments Ltd, UK
Sharp Microwave	Sharp, Australia
Sonifier™ 150	Branson Ultrasonics Corp, USA
Stratagene 1800 UV Crosslinker	Stratagene, USA
Syringes	Becton Dickinson, USA
Tissue Culture Dishes Cellstar®	Greiner Labortechnik, Germany
Tissue Culture Flasks	Sarstedt, USA
Tissue Culture Plates	Becton Dickinson, USA
UV Sterile Cabinet	Starkeys, Australia
UV Transilluminator	Hoefer, Australia
Wallac™ Victor 1420 Plate Reading Luminometer	Wallac™, Turku, Finland
Zx^3 Vortex	Velp, Scientifica, Italy

Chapter Three

Chapter Three – Methods

3.1 Polymerase Chain Reaction (PCR)

3.1.1 Primer Design

Oligonucleotide primers (Appendix 2) were designed to amplify the coding region of hypothetical gene *FLJ22318* which was obtained from the cDNA sequence published in NCBI (Accession No. NM_022762). The FLJTOPO sense primer contained a Kozak consensus sequence (G/ANN[2]), which is an optimal sequence for translation initiation. An ATT initiating codon was chosen as the Kozak sequence in order to maintain a GC content of 50% in the oligonucleotide (sense) primer. The stop codon was omitted from the FLJTOPO antisense primer as the PCR amplified product was to be cloned into the pcDNA3.1/V5-His-TOPO plasmid containing a C-terminal peptide (V5 epitope and polyhistidine tag). The FLJSalI sense, FLJSalI antisense and pCMV sense primers had *Sal* I restriction enzyme cleavage sites added at the 5' end, enabling the PCR amplified products to be cloned into the *Sal* I restriction enzyme sites in the pGBKT7, pCMV-Myc and pCMV-HA plasmids. An additional nucleotide 5' to the restriction site was also included to facilitate enzyme binding. To maintain the correct reading frame, two additional bases 3' to the restriction site and one additional base 3' to the restriction site were included in the FLJSalI sense and pCMV FWD sense primers, respectively. To facilitate cloning into pGEX2TK the FLJBamHI sense and FLJBamHI antisense primers had *BamH* I restriction enzyme cleavage sites added at the 5' end, enabling the PCR amplified products to be cloned into the *BamH* I restriction enzyme sites in the plasmid.

3.1.2 Reverse Transcription (RT)

One-3µL of target RNA (section 3.13.1) was diluted to 16.5µL with ddH_2O, incubated at 70°C for 5 minutes and placed on ice for two to five minutes to inhibit RNA renaturation. To each reaction, 5µL of 5X AMV RT buffer, 40U (1µL) RNasin® ribonuclease inhibitor, 0.5µg (1µL) oligo (dT) primer, 0.4mM (0.4µL) dNTPs[23] and 12.5U (0.5µL) of AMV RT were added to give a final volume of 25µL. Reactions were incubated at room temperature for 10 minutes to allow primer annealing, at 42°C for 60

[2] N equals A,T,G or C

minutes for DNA extension then at 95°C for 5 minutes to stop the reaction. cDNA samples were stored at -20°C.

3.1.3 Polymerase Chain Reaction

PCR reagents and conditions are summarised in Table 3.1 and all PCR amplifications were performed in sterile 0.5mL microcentrifuge tubes in PTC-100™ Programmable Thermal Cyclers. Amplification reactions using *Taq* polymerase contained 1.0-2.0mM $MgCl_2$, 5µL 5X PCR buffer[73] and 0.05U (0.1µL) *Taq* polymerase. Amplification reactions using *Pfu* polymerase contained 0.4mM (0.4µL) dNTPs[23], 2.5µL 10X PCR buffer[74] and 1U (0.3µL) *Pfu* polymerase. PCRs also contained 15ρmol (1µL) of forward and reverse primers except for reactions using FLJBamHI sense and FLJBamHI antisense primers which contained 5ρmol (1µL) of each primer, 1µL of target DNA and an appropriate volume of ddH_2O to give a final reaction volume of 25µL. Products amplified using *Pfu* polymerase were incubated, post PCR, with 1U (0.2µL) *Taq* polymerase at 72°C for 10 minutes to add 3' adenine overhangs required for ligation into the pCR®2.1 plasmid vector. Sequencing reactions amplified using the Advantage 2 PCR Kit (section 2.2) contained 1µL 50X Advantage® 2 Polymerase Mix, 5µL of 10X Advantage® 2 PCR Buffer, 1µL Polymerase Mix, 20ρmol of forward (5' ADLD) and reverse (3' ADLD) primers, 1µL 50X (10mM) dNTP mix, 2.8µg of plasmid DNA and an appropriate volume of ddH_2O for a final reaction volume of 50µL.

3.1.4 Agarose Gel Electrophoresis

DNA was electrophoresed in 1/2% (w/v) agarose gels[2]. An appropriate volume of 6X DNA loading dye[22] was added to samples, 5-15µL of sample was loaded into wells and each gel included a well containing 5µL of 1Kb Plus™ DNA Ladder[79]. Gels were electrophoresed in 1X TAE[134] at 100V for 30-60 minutes depending on gel size. Following electrophoresis, DNA bands were visualised and analysed using BioRad Quantity One® quantitation software.

3.1.5 Purification of PCR Products and Plasmids

PCR products and plasmids were purified using the Wizard® SV Gel and PCR Clean-Up System. DNA samples were diluted with an equal volume of Membrane Binding

Table 3.1 PCR Conditions

Amplifications using *Taq* Polymerase						
Primers (S/AS)	**[$MgCl_2$] (mM)**	**DNA denaturing time**	**Annealing temperature (°C)**	**Annealing time**	**Extension time**	**No. of cycles**
FLJTOPO	1.0	1 minute	65	1 minute	1 minute	40
FLJSalI	1.5	1 minute	65	1 minute	1 minute	45
FLJBamHI	1.0	1 minute	55	1 minute	1 minute	30
pGEX	2.0	1 minute	55	1 minute	1 minute	35
BAC	1.5	1 minute	55	1 minute	1 minute	35
Amplifications using *Pfu* Polymerase						
Primers (S/AS)		**DNA denaturing time**	**Annealing temperature (°C)**	**Annealing time**	**Extension time**	**No. of cycles**
FLJSalI		1 minute	65	1 minute	3 minutes	35
pCMV FWD		1 minute	65	1 minute	3 minutes	35
BAC		1 minute	55	1 minute	1 minute	35
Amplifications using 50X Advantage® 2 Polymerase Mix						
Primers (S/AS)	**DNA denaturing time**		**Annealing temperature (°C)**	**Annealing and Extension times**		**No. of cycles**
ADLD	30 seconds		68	3 minutes		29

solution[66] and loaded into spin columns containing a silica-based membrane that adsorbs double stranded DNA. The spin columns were placed into 2mL wash tubes and centrifuged at 13,000rpm for 1 minute. The flow through was discarded and 700µL of Membrane Wash solution[67] was added to the spin columns, which were centrifuged at 13,000rpm for 1 minute. The flow through was discarded and 500µL of Membrane Wash solution[67] was added to the spin columns, which were centrifuged at 13,000rpm for 5 minutes and the flow through again discarded. Spin columns were then centrifuged for an additional minute, the spin columns transferred to clean 2mL collection tubes and 50µL of nuclease-free water added directly to the centre of the membranes. Spin columns with collection tubes were incubated at room temperature for 1 minute then centrifuged at 13,000rpm for 1 minute to elute the DNA and the purified products were stored at -20°C.

3.1.6 Gel Purification of DNA

DNA to be gel purified was electrophoresed in an agarose gel[2] (section 3.1.4), the DNA was visualised using short wavelength UV transillumination, excised from the gel using a clean scalpel blade and dissolved in an equal volume (100µL/100mg of gel) of Membrane Binding solution[66] at 60°C for 10 minutes with mixing every 2 to 3 minutes. The samples were then purified using the Wizard® SV Gel and PCR Clean-Up System (section 3.1.5) and the purified products were stored at -20°C.

3.2 Cloning of FLJ22318

3.2.1 Plasmid Vectors

The plasmids used in this study were pCR®2.1 (Invitrogen), pcDNA3.1/V5-His-TOPO (Invitrogen), pGBKT7 (Clontech), pGADT7-Rec (Clontech), pCMV-Myc (Clontech), pCMV-HA (Clontech), pEGFP-C2 (Clontech) and pGEX-2TK (Amersham). The pCR®2.1 cloning vector was used for initial cloning of PCR amplified DNA as the TA cloning system permitted high efficiency ligation of unpurified PCR products (Figure 3.1). The pcDNA3.1/V5-His-TOPO (Figure 3.2), pCMV-Myc (Figure 3.3), pCMV-HA (Figure 3.4) and pEGFP-C2 (Figure 3.5) expression vectors were used to enable FLJ22318 expression following transfection into mammalian cells and the pGEX-2TK (Figure 3.6) vector enabled expression of FLJ22318 in bacterial cells. The yeast vectors, pGADT7-Rec and pGBKT7 were used for yeast two-hybrid analysis. The pGADT7-

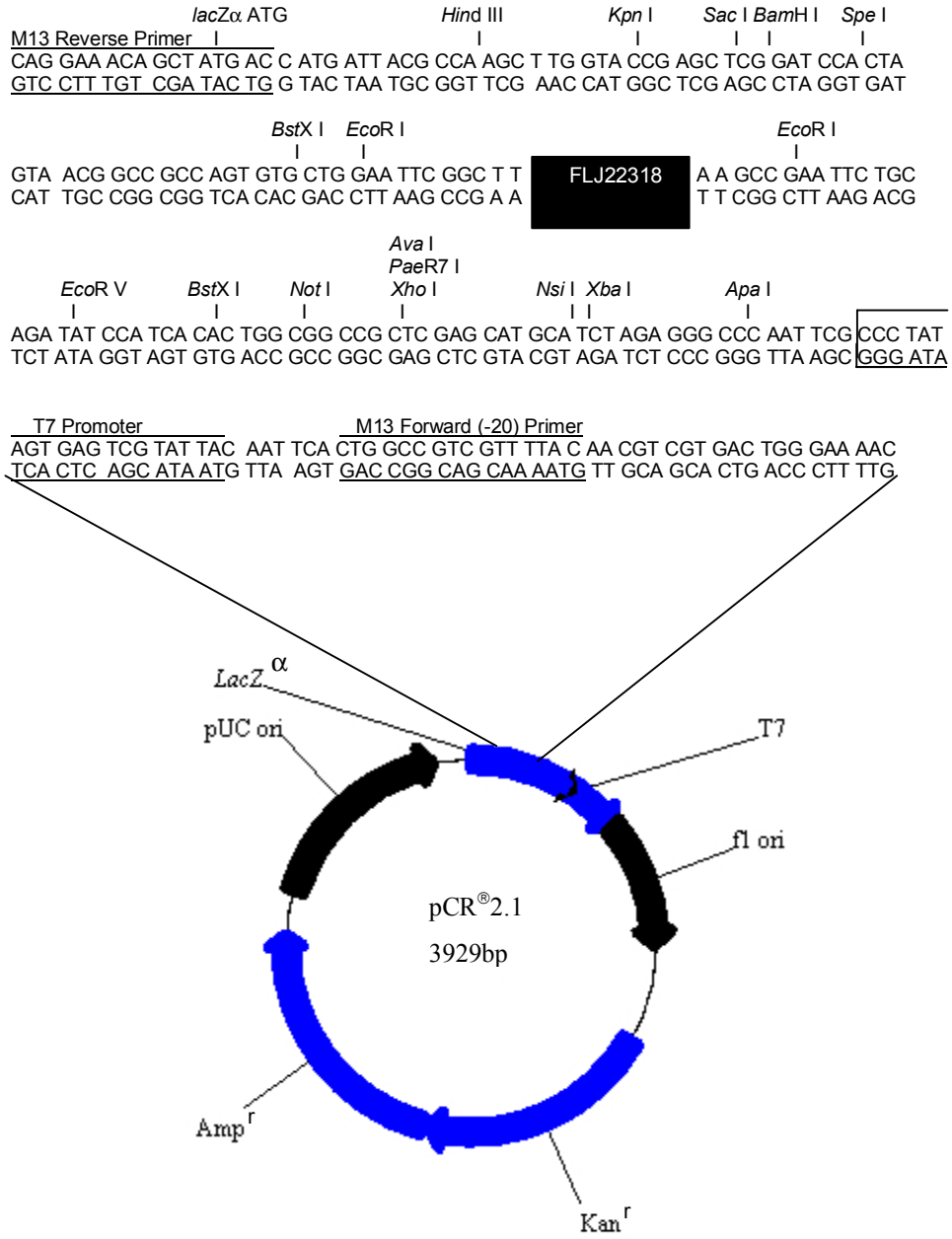

Figure 3.1 Map of the pCR®2.1 vector showing the multiple cloning site and site of FLJ22318 ligation following TA Cloning®. Insertion of FLJ22318 disrupts the *lacZ* gene enabling selection of bacterial colonies that contain plasmids with inserts (white as opposed to blue colonies) on LB Agar/X-Gal plates. The plasmid also contains ampicillin (Amp^r) and kanamycin (Kan^r) resistance genes for bacterial selection (adapted from http://www.invitrogen.com).

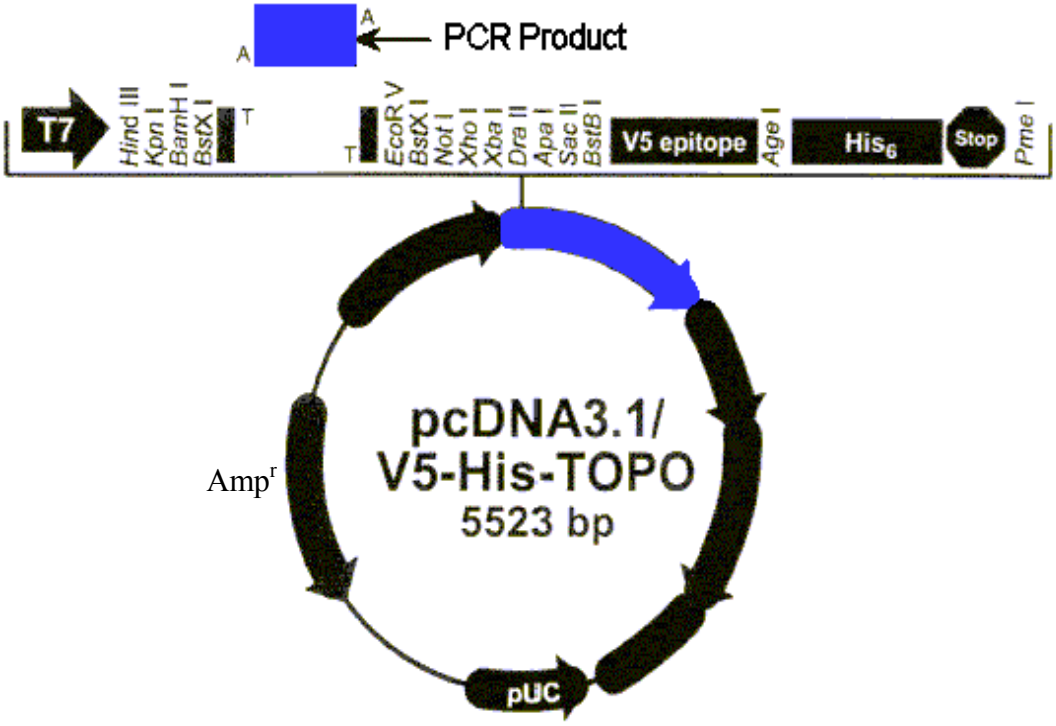

Figure 3.2 Map of the pcDNA3.1/V5-His-TOPO vector showing the TOPO® cloning site where PCR products are inserted. The pcDNA3.1/V5-His-TOPO vector expresses proteins containing C-terminal V5 and His epitope tags. The vector also contains an ampicillin resistance gene for selection in *E. coli* (http://www.invitrogen.com).

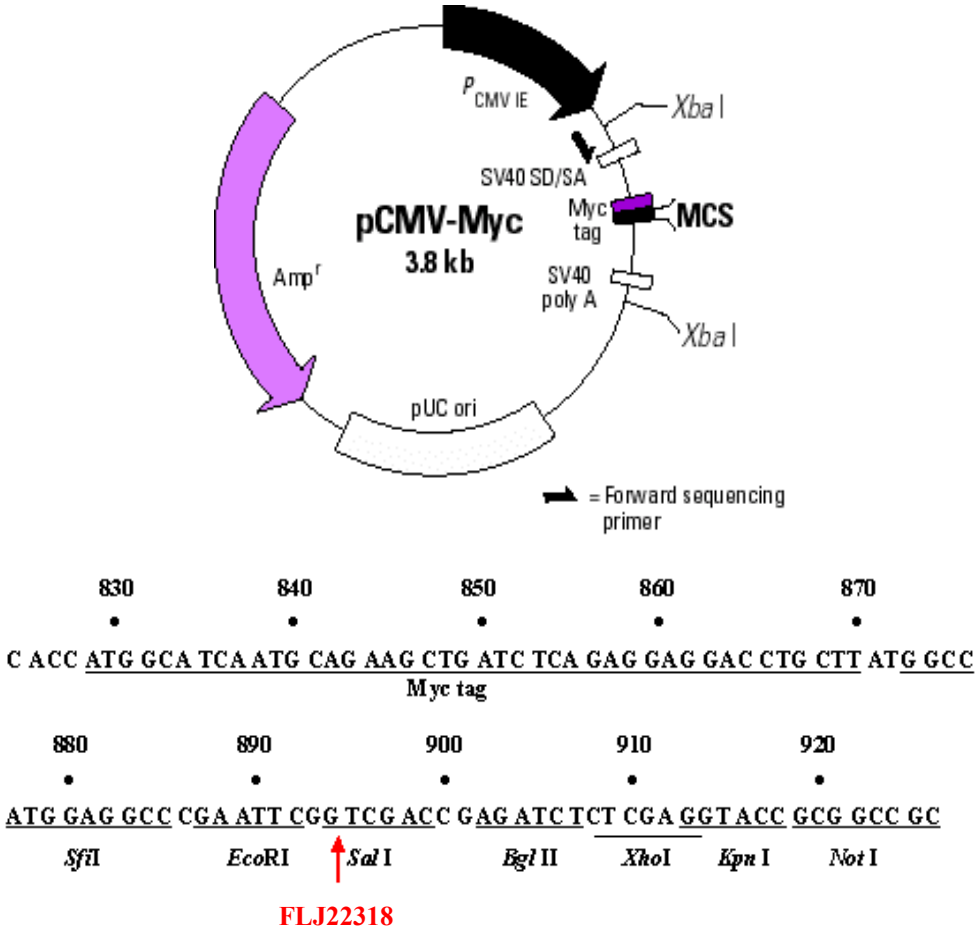

Figure 3.3 Map of the pCMV-Myc vector showing the multiple cloning site (MCS) and the *Sal* I FLJ22318 insert position. The pCMV-Myc vector expresses proteins as a fusion to an N-terminal c-Myc epitope tag. The vector also contains an ampicillin resistance gene for selection in *E. coli* (adapted from http://www.clontech.com).

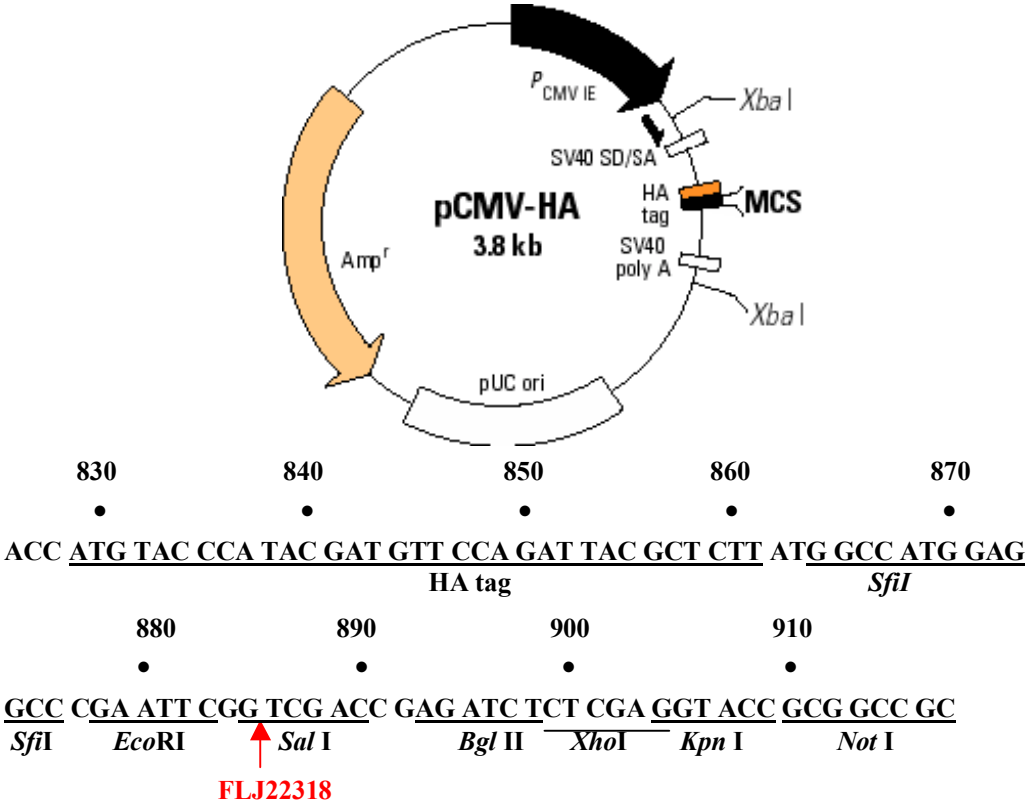

Figure 3.4 Map of the pCMV-HA vector showing the *Sal* I insert position for FLJ22318 within the multiple cloning site (MCS). The pCMV-HA vector contains an ampicillin resistance gene for selection in *E. coli* and in mammalian cells expresses proteins as a fusion to a N-terminal haemaglutinin (HA) epitope tag (adapted from http://www.clontech.com).

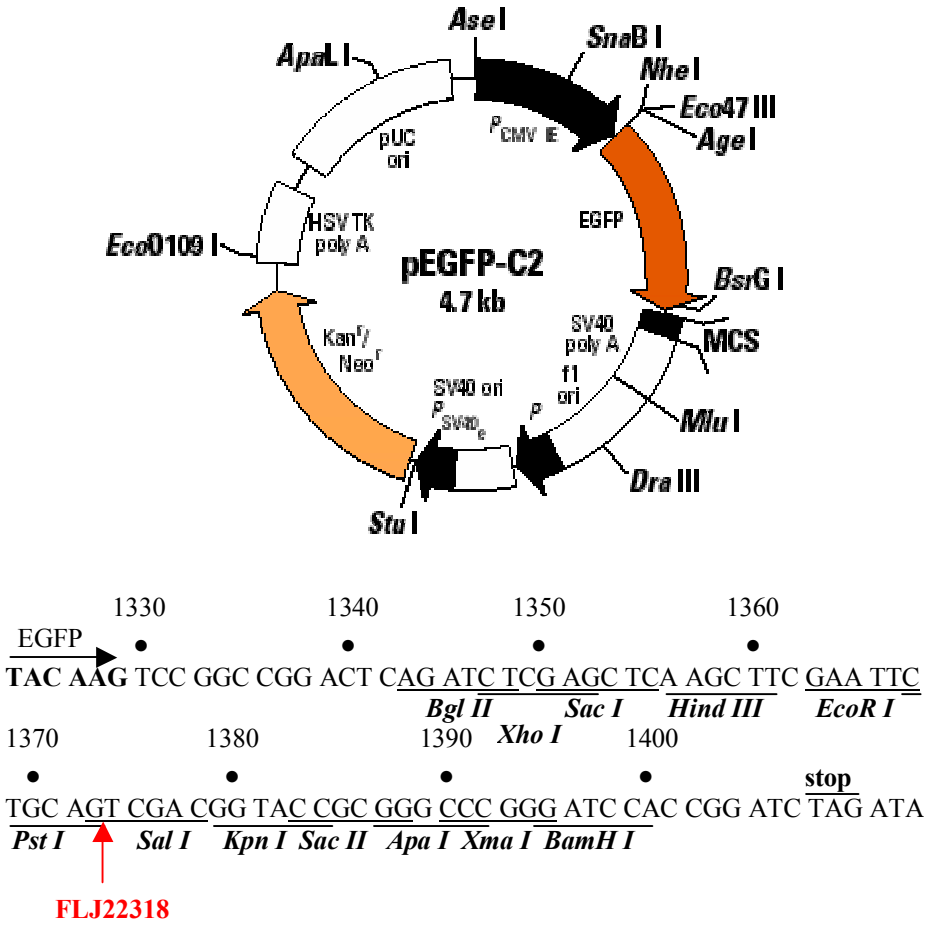

Figure 3.5 Map of the pEGFP-C2 vector showing the multiple cloning site (MCS) and *Sal* I FLJ22318 insert position. The pEGFP-C2 vector encodes a red-shifted variant of wild type GFP that fluoresces when excited at 488nm and emits light at 507nm. pEGFP-C2 expresses proteins as a fusion to the C terminus of EGFP in mammalian cells and contains a kanamycin resistance gene for selection in *E. coli* (adapted from http://www.clontech.com).

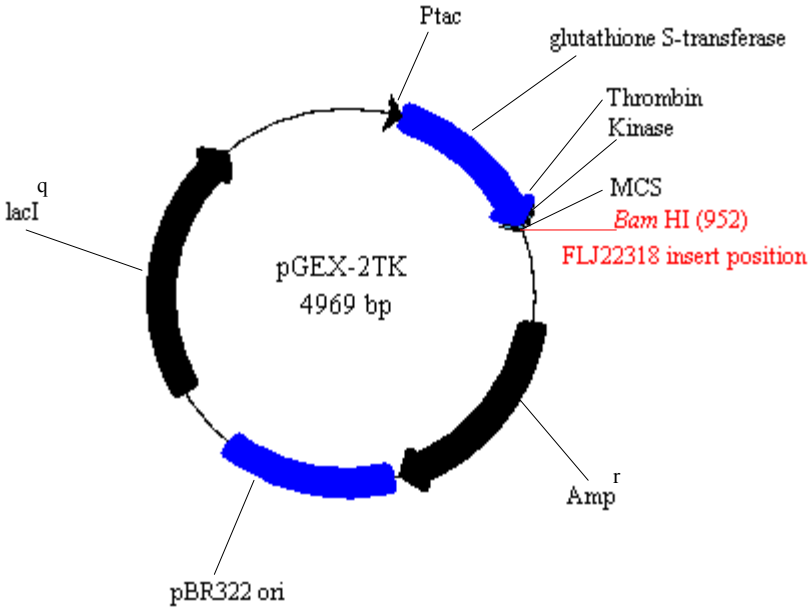

Figure 3.6 Map of the pGEX-2TK vector showing the multiple cloning site (MCS) and *BamH* I FLJ22318 insert position. Expression in *E. coli* yields a FLJ22318 fusion protein with a glutathione S-transferase (GST) moiety at the amino terminus. Expression in bacteria is under the control of the *tac* promoter, which is induced by the lactose analogue isopropyl β-D thiogalactoside (IPTG) (adapted from www5.amershambiosciences.com).

Rec plasmid expresses proteins fused to a GAL4 activation domain (AD) with a HA (haemagglutinin) epitope (Figure 3.7) and the pGBKT7 plasmid expresses proteins fused to a GAL4 DNA binding domain (BD) with a c-Myc epitope (Figure 3.8). When both fusion proteins interact in AH109 yeast cells (containing a GAL upstream activator sequence), the DNA-BD and AD are brought into close proximity and activate transcription of the *MEL1*, *lacZ*, *ADE2*, and *HIS3* yeast reporter genes that permit growth of AH109 yeast on selective media (section 3.5).

3.2.2 Restriction Enzyme Digestion

Plasmid DNA (1µg) was incubated at 37°C for 2-16 hours with 5U of the appropriate restriction enzyme, 0.2µL BSA (0.1µg/µL), 2µL of the appropriate 10X buffer (section 2.1.2) and ddH_2O to give a final reaction volume of 20µL.

3.2.3 Calf Intestinal Alkaline Phosphatase Treatment

Linearised plasmid DNA was treated with calf intestinal alkaline phosphatase (CIAP) to remove the 5' phosphate groups, thereby preventing re-circularisation of the plasmid. Each reaction containing linearised plasmid DNA (section 3.2.2), 5µL CIAP 10X reaction buffer, 5µL CIAP (0.01U/µL) and ddH_2O to 50µL was incubated at 37°C for 30 minutes. A further 5µL CIAP was added and the reaction was incubated for a further 30 minutes at 37°C. To terminate reactions, 0.5µL 0.5M EDTA[34] was added to each tube and tubes were incubated at 75°C for 10 minutes. CIAP treated plasmids were purified (section 3.1.5) and stored at -20°C.

3.2.4 Ligation of PCR Products into Plasmid Vectors

The concentration of PCR amplified DNA to be ligated into plasmids was determined following agarose gel electrophoresis (section 3.1.4) with the amount (x) of insert required for ligation into the plasmids calculated using the following formula:

$$x(ng)_{insert} = \frac{50ng_{vector} \times y(kb)_{insert}}{z(kb)_{vector}}$$

This formula calculates a molar ratio of 1:1 (vector:insert) and was adjusted appropriately for 1:2 and 1:3 molar ratios when using the LigaFast™ Rapid DNA

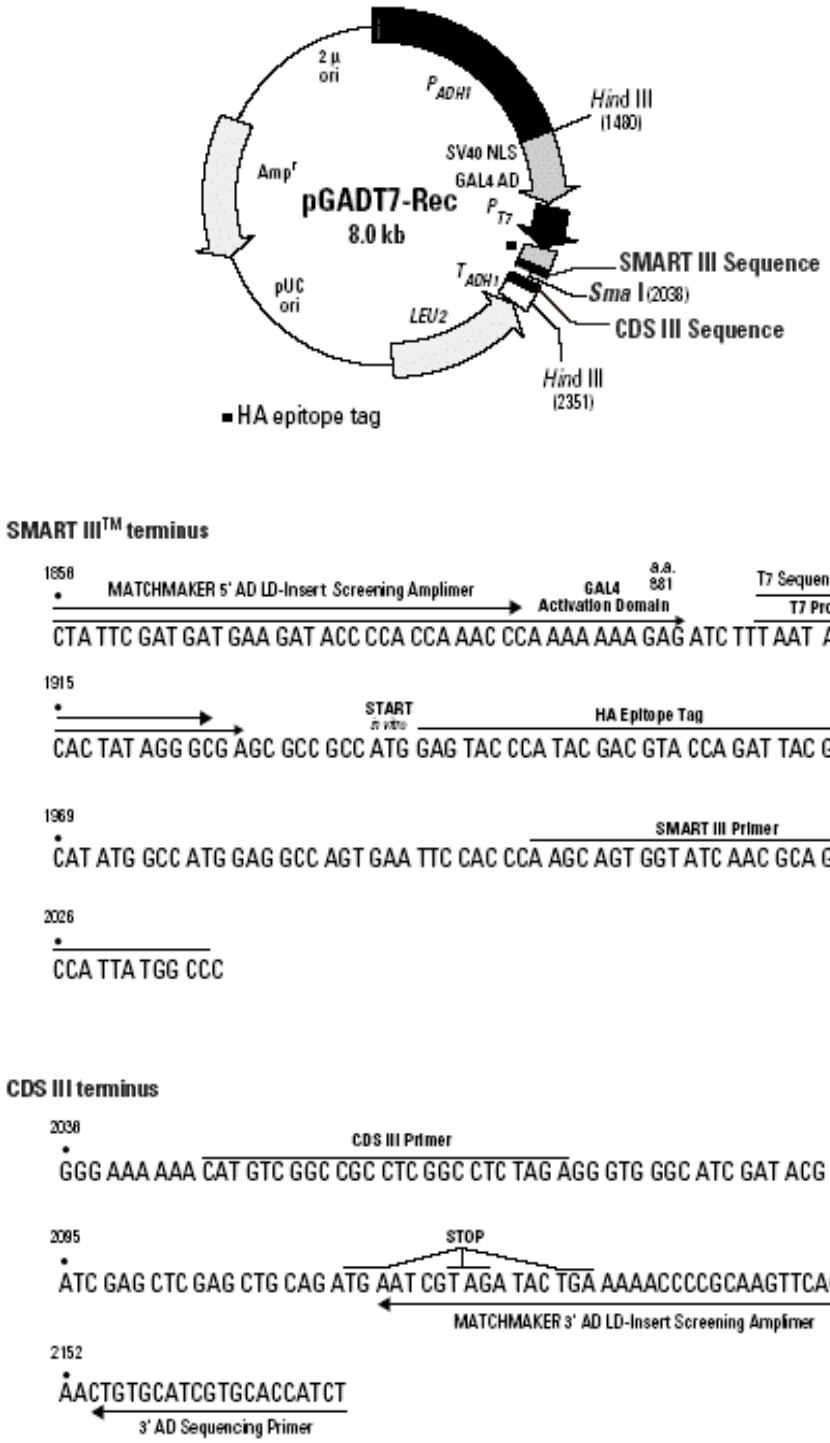

Figure 3.7 Map of the pGADT7-Rec vector. In yeast, pGADT7-Rec expresses proteins as a GAL4 activation domain (GAL4 AD) fusion with a haemagglutinin (HA) epitope tag. Transcription begins from the *ADH1* promoter (P_{ADH1}) and ends at the *ADH1* termination signal (T_{ADH1}). The vector also carries the *LEU2* marker for selection in yeast (adapted from http://www.clontech.com).

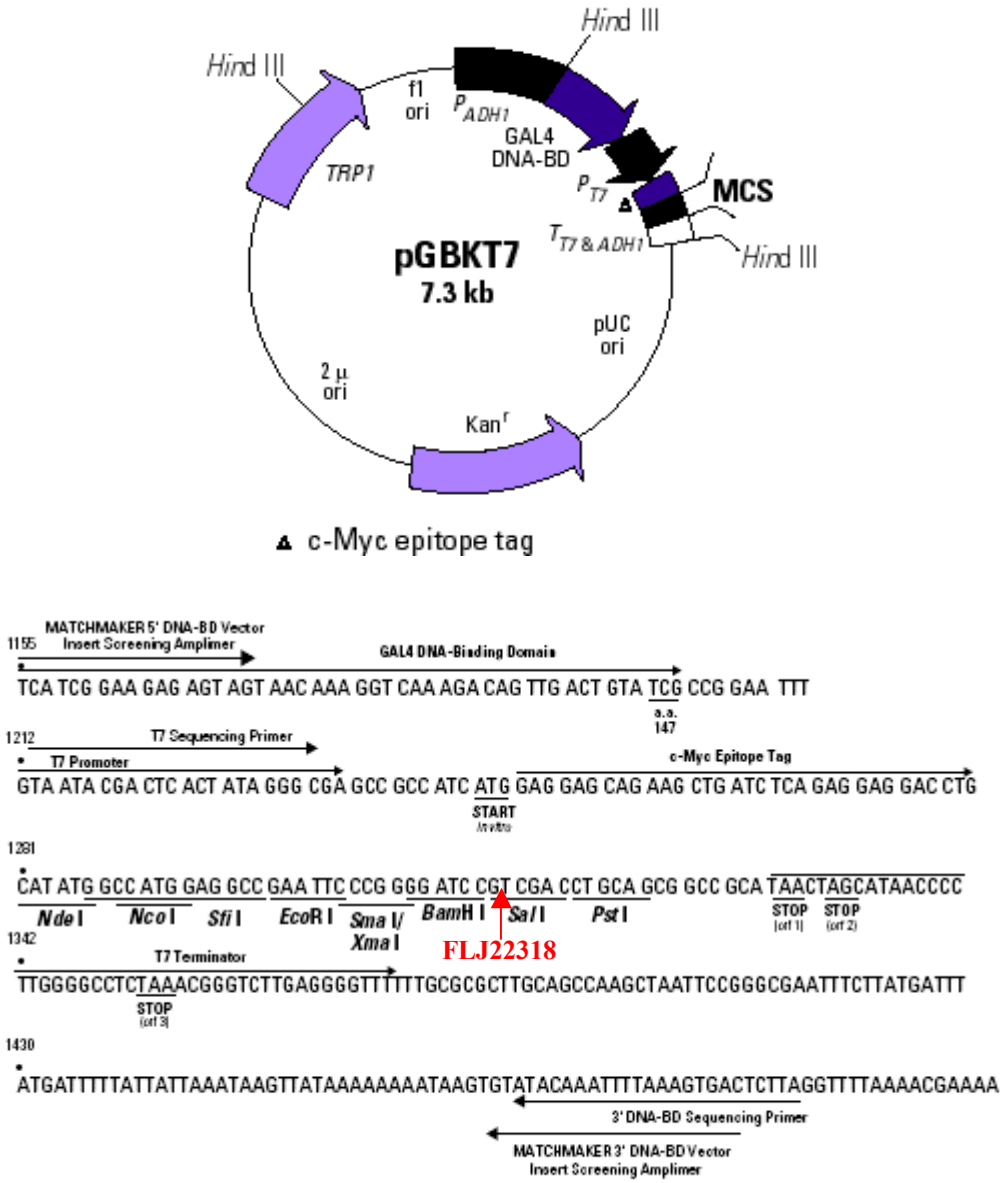

Figure 3.8 Restriction map of the pGBKT7 vector showing the GAL4 DNA-BD, multiple cloning site (MCS) and *Sal* I FLJ22318 insert position. In yeast, the pGBKT7 vector expresses FLJ22318 fused to the (N-terminal) GAL4 DNA binding domain and c-Myc epitope tag for detection of fusion proteins. pGBKT7 contains a kanamycin resistance gene for selection in *E. coli* and the *TRP1* marker for selection in yeast (adapted from http://www.clontech.com).

Ligation System. All LigaFast™ reactions comprised 100ng vector, 3U T4 DNA ligase, 5µL 2X Rapid Ligation Buffer, *x*ng DNA insert and an appropriate volume of ddH_2O for a final volume of 10µL. Reactions were incubated for 5 minutes at room temperature and used immediately for bacterial transformation. For all other ligation reactions, each reaction comprised 50ng vector, 4U T4 DNA ligase, 1µL 10X ligation buffer, *x*ng DNA insert and an appropriate volume of ddH_2O for a final volume of 10µL. These reactions were incubated overnight at 14°C and then used for bacterial transformation or stored at -20°C.

Ligation of purified DNA products into the pcDNA3.1/V5-His-TOPO cloning plasmid is dependent upon vector bound topoisomerase I that facilitates thymine-adenine base pairing between vector and insert. This allowed direct insertion of *Taq* polymerase amplified FLJ22318 product into the vector without the need for DNA ligase. Each reaction comprised 10ng vector, 1µL salt solution (1.2M NaCl; 0.06M $MgCl_2$) and 4µL of PCR product. Reactions were incubated for 5 minutes at 22°C and used immediately for bacterial transformation.

3.2.5 Preparation of Competent Bacterial Cells

DH5α bacterial cells were grown from frozen stocks (-80°C; section 3.2.7), streaked onto LB/agar plates[49] and incubated at 37°C overnight. A single DH5α colony was inoculated into 10mL of LB broth[53], vortexed and incubated at 37°C overnight at 225rpm. The following day, 1mL of this culture was transferred to a 250mL flask containing 100mL of LB broth[53], incubated at 37°C for 3-5 hours at 225rpm until the OD_{600} was 0.4-0.5, then transferred to pre-chilled 50mL tubes and the bacteria pelleted by centrifugation at 4000rpm for 10 minutes at 4°C. The supernatants were removed and bacterial pellets resuspended and pooled in 40mL of ice-cold glycerol buffer[45] then incubated for 30 minutes on ice. Following incubation the bacteria were pelleted by centrifugation at 4000rpm for 10 minutes at 4°C, supernatants were removed and bacterial pellets were resuspended in 4mL ice-cold glycerol buffer[45]. Bacterial cells were now considered competent and stored in 200µL aliquots at -80°C until required for transformation.

BL21 bacterial cells were grown from frozen stocks (-80°C), streaked onto LB/agar plates[49] and incubated at 37°C for 18 hours overnight. Single BL21 colonies were inoculated into 50mL of pre-warmed LB broth[53], vortexed and incubated at 37°C for 3-5 hours at 250rpm until the OD_{600} was 0.4-0.5. Cultures were transferred to pre-chilled 50mL tubes and bacteria pelleted by centrifugation at 2500 x g for 15 minutes at 4°C. The supernatants were removed and bacterial pellets were resuspended in 5mL of ice-cold transformation solution[148] then placed on ice. Bacterial cells were now considered competent and used within 2-3 hours for transformation.

3.2.6 Bacterial Transformation

Ligation reactions were transformed into competent DH5α, BL21 (section 3.2.5) or TOP10 *E. coli* (section 2.2). For DH5α and TOP10 transformations, 2-5μL of the ligation reaction was added to the competent cells which were mixed gently then placed on ice for 30 minutes, heat shocked at 42°C for 30-90 seconds and returned to ice for 2 minutes. SOC medium (250μL; section 2.2) was added and the cells were incubated at 37°C for 1 hour with shaking at 225rpm. Transformed bacteria were plated onto LB/agar/ampicillin/X-Gal plates[51], enabling blue/white colour selection of bacteria transformed with pCR®2.1. For selection of bacteria transformed with pcDNA3.1/V5-His-TOPO, pCMV-Myc, pCMV-HA and pGEX-2TK, LB/agar/ampicillin plates[50] were used and for transformations with pEGFP-C2 and pGBKT7, LB/agar/kanamycin plates[52] were used. For each transformation, 50μL and 100μL aliquots of transformed cells were spread onto agar plates, the plates were inverted, incubated overnight at 37°C then stored at 4°C.

Ligation reactions were transformed into competent BL21 cells (section 3.2.5) by the addition of 2μL of ligation reactions to 1mL competent cells in pre-chilled 1.5mL tubes. Cells were mixed gently, then incubated on ice for 45 minutes and heat shocked at 42°C for 2 minutes. Bacteria were chilled on ice then 100μL of the transformation mixture was transferred to clean 1.5mL tubes containing 900μL pre-warmed (37°C) LB broth[53] and incubated for 60 minutes at 37°C with shaking at 250rpm. One hundred μL aliquots of transformed cells were spread onto LB/agar/ampicillin plates[50], which were inverted and incubated overnight at 37°C then stored at 4°C wrapped in parafilm.

3.2.7 Preparation of Bacterial/Glycerol Stocks

Ten mL DH5α and TOP10 bacterial cultures were grown overnight under appropriate antibiotic selection (section 3.3.1), centrifuged for 10 minutes at 2500rpm and the supernatants removed. Pellets were resuspended in 1mL LB broth containing 10% glycerol[56], transferred to 2mL cryotubes and stored at -80°C.

To cryopreserve BL21 cultures, 100µL of diluted transformed bacterial cultures were inoculated into 1mL LB broth/ampicillin[54] and incubated for 30 minutes at 37°C with shaking at 250rpm. Following incubation, cultures were diluted with 200µL 80% glycerol[44], transferred to 2mL cryotubes and stored at -80°C.

3.3 Plasmid Purification

3.3.1 Small-Scale Isolation of Plasmid DNA

Transformed bacterial colonies were individually inoculated into 3mL of LB broth[53] with appropriate antibiotics and incubated overnight at 37°C with shaking at 225rpm. Following overnight growth, 1.5mL of each culture was transferred to a microcentrifuge tube and centrifuged at 14000rpm for 30 seconds at 4°C to pellet the bacteria. Supernatants were removed and the bacterial pellets were resuspended in 100µL of ice-cold Solution I[122] by vigorous vortexing. The cells were then lysed by the addition of 200µL of freshly prepared Solution II[123], and the tubes inverted 6 times to ensure all surfaces of the tubes were contacted. 150µL of ice-cold Solution III[124] was added to neutralise the reaction, tubes were immediately inverted and vortexed briefly 3 times, stored on ice for 5 minutes and centrifuged at 14000rpm for 5 minutes at 4°C. The supernatants (~450µL) were transferred to clean 1.5mL microcentrifuge tubes, an equal volume of phenol:chloroform was added, the tubes vortexed briefly, centrifuged at 14000rpm for 2 minutes at 4°C and the supernatants transferred to clean 1.5mL tubes. To precipitate recovered plasmid DNA, two volumes (~900µL) of 100% ethanol was added to each tube and the tubes were vortexed then incubated for 2 minutes at room temperature. Precipitated plasmid DNA was pelleted by centrifugation at 14000rpm for 5 minutes at 4°C and the supernatants discarded. Pellets were then washed with 600µL of 70% ethanol[37], centrifuged at 14000rpm for 5 minutes at 4°C and the supernatants discarded. Tubes were inverted and incubated at room temperature for 20 minutes to

allow the plasmid DNA pellets to dry. Pellets were then resuspended in 30µL of ddH_2O, 1µL (20µg) RNase[88] was added and tubes were incubated at 37°C for >60 minutes. Plasmid DNA was stored at -20°C.

3.3.2 Large-Scale Isolation of Plasmid DNA

Large-scale preparations of plasmid DNA were performed using the Concert™ High Purity Plasmid Maxiprep System (section 2.2). Frozen bacterial cultures containing the required plasmid (section 3.2.7) were inoculated into 10mL LB broth[53] containing the appropriate antibiotic and incubated at 37°C for 8 hours at 225rpm. Cultures were diluted with fresh LB broth[53] (250mL) containing the appropriate antibiotic and incubated at 37°C for 12-16 hours at 225rpm. Bacterial cultures were centrifuged for 10 minutes at 4500rpm, the supernatants decanted and pellets re-suspended in 10mL of Cell Suspension Buffer (E1)[26]. Cell suspensions were lysed by the addition of 10mL of Cell Lysis Solution (E2)[27], and tubes were inverted gently 5 times then incubated at room temperature for 5 minutes. The pH was neutralised by the addition of 10mL of Neutralisation Buffer (E3)[28], and the tubes were immediately inverted 5 times then centrifuged at room temperature for 10 minutes at 15000rpm to pellet cell debris. The supernatants were transferred to purification columns that had been pre-equilibrated with 30mL of Equilibration Buffer (E4)[29] that had been allowed to drain by gravity flow. The bacterial supernatants were allowed to drain through the columns, binding plasmid DNA to the column. The columns were then washed with 60mL of Wash Buffer (E5)[30], again drained by gravity flow and the flow throughs discarded. Plasmid DNA was eluted from the column by the addition of 15mL of Elution Buffer (E6)[31]. Following elution, the supernatants containing the plasmid DNA were transferred to sterile corex tubes and the DNA was precipitated by the addition of 10.5mL of isopropanol. Tubes were then centrifuged at 4°C for 30 minutes at 15000rpm and the supernatants discarded, pellets were washed with 5mL of 70% ethanol[37] then centrifuged at 15000rpm, 4°C for 5 minutes. The ethanol was decanted and the pellets were air dried at room temperature for 10-15 minutes. Purified plasmid DNA pellets were re-suspended in 500µL of TE Buffer[140] (TE) and stored at -20°C.

3.3.3 Spectrophotometric Quantitation of DNA/RNA

The concentration of RNA, and DNA isolated from plasmid preparations (section 3.3.2) was determined spectrophotometrically. The optical density (OD) of 1µL samples was measured at 260nm using a NanoDrop® ND-1000 spectrophotometer with ddH_2O as the background reading. An absorbance of 1.0 at OD_{260} was estimated to equal a RNA concentration of 40µg/mL and a DNA concentration of 50µg/mL. The concentration in µg/µL was then calculated from these spectrophotometric readings.

3.4 DNA Sequencing

3.4.1 Sequencing Reactions

DNA was sequenced by the dideoxy chain termination method and reactions were performed in 0.5mL microcentrifuge tubes. Each reaction comprised 2µL Big Dye™ Terminator Mix V3.1, 4µL Big Dye™ Terminator Sequencing Buffer V3.1, 3ρmol of the appropriate primer except for the ADLD primers where 4ρmol was used (Appendix 2), 200-500ng purified plasmid or ~90ng of purified PCR product and an appropriate volume of ddH_2O for a final reaction volume of 20µL. Reactions were amplified in PTC-100™ Programmable Thermal Cyclers and comprised 25 cycles of: DNA denaturation at 96°C for 15 seconds, primer annealing at 50°C for 10 seconds and primer extension at 60°C for 4 minutes.

3.4.2 Precipitation of Sequencing Reactions

Upon completion of sequencing the reaction mixtures were transferred to 1.5mL microcentrifuge tubes containing 2µL 3M sodium acetate[112] (pH4.6) and 50µL of 95% ethanol[38]. The tubes were vortexed and placed on ice for 10 minutes to precipitate the DNA, then centrifuged at 4°C for 30 minutes at 13000rpm to pellet the DNA. The supernatants were removed by pipetting and the pellets washed with 250µL 70% ethanol[37] then centrifuged for a further 5 minutes at 13000rpm and 4°C. The supernatants were gently removed and the DNA pellets air-dried for approximately 15-20 minutes at room temperature. The West Australian Genome Resource Centre at Royal Perth Hospital performed the gel analysis of precipitated sequencing reactions using an ABI 373 XL Automated Sequencer and the results were presented in DNA sequence and chromatograph formats.

3.5 Yeast Two-hybrid Analysis

3.5.1 Polyadenylated RNA Extraction and cDNA Synthesis

3.5.1.1 Polyadenylated RNA Extraction

Isolation of polyadenylated [poly(A)] RNA was performed using the Poly (A) Pure™ mRNA Purification Kit (section 2.2). LNCaP cells (8 x 10^7) were cultured in 175cm^2 cell culture flasks and trypsinised when confluent (section 3.6.1). Cells were pelleted by centrifuging at 4°C for 5 minutes at 1100rpm and the supernatants removed, then washed once in 2mL PBS[72] and centrifuged as above. Cells were lysed by the addition of 1mL of Lysis Solution[62] per 2 x 10^7 cells, the cell lysates were transferred to 15mL Corex tubes and homogenised by vigorous pipetting. Homogenates were diluted with 2 volumes of Dilution Buffer[20] to reduce the concentration of guanidine thiocyanate, providing the optimum salt concentration for poly(A) RNA/oligo(dT) hybridisation, mixed by swirling then centrifuged at 4°C at 12000 x g for 15 minutes to pellet cell debris. The supernatants were transferred to clean 15mL tubes, a vial of oligo(dT) cellulose was added and the solution was mixed by inversion to resuspend the resin. Tubes were incubated for 60 minutes at room temperature with gentle shaking to allow binding of poly(A) RNA to the oligo(dT) cellulose, centrifuged at 2500 x g for 3 minutes at room temperature to pellet the oligo(dT) cellulose and the supernatants were removed. To remove non-specifically bound material and ribosomal RNA the oligo(dT) cellulose pellets were washed 3X with 10mL Binding Buffer[8], centrifuging in between at 2500 x g for 3 minutes at room temperature and the supernatants removed. To provide a more stringent wash and remove additional ribosomal RNA the oligo(dT) cellulose pellets were further washed 3X with 10mL Wash Buffer[149], centrifuging in between at 2500 x g for 3 minutes at room temperature and the supernatants removed.

Following washes the oligo(dT) cellulose pellets were resuspended in 600µL Wash Buffer[149] and transferred to spin columns. The spin columns were placed into 2mL tubes and centrifuged at 5000 x g for 10 seconds at room temperature. The flow through was discarded, 500µL of Wash Buffer[149] was added to each spin column, the columns were centrifuged at 5000 x g for 10 seconds at room temperature, the flow through again discarded and a further 500µL of Wash Buffer[149]. Columns were centrifuged at 5000 x g for 10 seconds at room temperature and the OD_{260} of the flow through confirmed to be <0.05, at which time spin columns were transferred to clean 2mL

collection tubes and 200µL of pre-warmed Elution Buffer[36] (65°C) was added to the resin. Spin columns with collection tubes were centrifuged at 5000 x g for 10 seconds at room temperature to elute the RNA from the oligo(dT) cellulose. A further 200µL of pre-warmed Elution Buffer[36] was added to the resin which was centrifuged at 5000 x g for 10 seconds at room temperature to elute any remaining poly(A) RNA.

In order to perform a second round of oligo(dT) cellulose selection, the 400µL of recovered RNA was transferred to a clean 1.5mL tube, the salt concentration adjusted to 0.45M by the addition of 40µL 5M sodium chloride[116], then tubes were incubated at 65°C for 5 minutes and chilled on ice for one minute. The used spin column was placed into the previously used 2mL collection tube, 500µL Binding Buffer[8] was added and the tubes were centrifuged at 5000 x g for 10 seconds at room temperature to equilibrate the column for hybridisation. The flow through was discarded and the RNA sample was slowly added to the resin then centrifuged at 5000 x g for 10 seconds at room temperature. The flow through was reapplied to the column and the tubes were centrifuged at 5000 x g for 10 seconds at room temperature, such that the RNA sample had passed through the column 3 times. The flow through was transferred to clean 1.5mL tubes and stored at -80°C until subsequent recovery of poly(A) RNA was confirmed.

Columns were washed 3X with 500µL of Binding Buffer[8], centrifuging in between at 5000 x g for 10 seconds at room temperature, then washed similarly 3X with 500µL of Wash Buffer[149]. RNA was eluted from the oligo(dT) column as described above. Following elution, the RNA was precipitated by the addition of 40µL 5M ammonium acetate[5], 2µL glycogen and 1.1mL of absolute ethanol. The precipitation mixture was incubated at -80°C for 60 minutes then centrifuged at 4°C for 20 minutes at 12000 x g and the supernatants discarded. Pellets were washed with 1.3mL of 70% ethanol[37] then centrifuged at 12000 x g for 10 minutes at 4°C. The ethanol was decanted and the pellets were resuspended in 20µL of Elution Buffer[36] and stored at -80°C.

3.5.1.2 First-Strand cDNA Synthesis

For first-strand cDNA synthesis, 2µL of poly A^+ RNA (section 3.5.1.1), was combined with 1µL (1µM) CDS III primer and 1µL ddH_2O in a sterile 0.5mL microcentrifuge tube. Reactions were incubated at 72°C for 2 minutes, placed on ice for 2 minutes to inhibit RNA renaturation and spun briefly. Following denaturation, 2µL of 5X First-Strand buffer, 1µL (20mM) DTT, 1µL (10mM) dNTP mix and 1µL of MMLV Reverse Transcriptase (BD Matchmaker™ Library Construction and Screening Kit; section 2.2) were added to give a final volume of 9µL. Reactions were mixed gently by tapping, spun briefly and incubated at 42°C for 10 minutes. 1µL (1µM) SMART™ III Oligonucleotide was added and tubes were incubated at 42°C for 60 minutes for DNA extension. To terminate first-strand synthesis, reactions were incubated at 75°C for 10 minutes, cooled to room temperature, 1µL (2 units) RNase H was added and tubes were incubated at 37°C for 20 minutes. cDNA's were stored at -20°C.

3.5.2 cDNA Library Construction

3.5.2.1 Long Distance-PCR (LD-PCR)

LD-PCR's using the Advantage 2 PCR Kit (section 2.2) were performed in duplicate in pre-chilled sterile 0.5mL microcentrifuge tubes each containing 1µL 50X Advantage® 2 Polymerase Mix, 5µL of 10X Advantage® 2 PCR Buffer, 0.2µM of forward 5' PCR and reverse 3' PCR primers, 5µL of 10X GC-Melt Solution, 1µL (10mM) 50X dNTP mix, 1µL of first-strand cDNA (section 3.5.1.2) and an appropriate volume of ddH_2O for a final volume of 50µL. Reactions were mixed gently, centrifuged briefly then transferred to a pre-heated (95°C) PTC-100™ Programmable Thermal Cycler and heated for 10 seconds to denature DNA followed by primer annealing and DNA extension at 68°C for 6 minutes initially, increasing in 5 second increments to 7 minutes 35 seconds over 20 cycles.

3.5.2.2 LD-PCR Product Purification

LD-PCR products were combined and a 5µL aliquot visualised in agarose gels (section 3.1.4) then purified using CHROMA SPIN+TE-400 Columns (Clontech). Immediately prior to purification, columns were centrifuged at 700 x g for 5 minutes at room temperature to purge the equilibration buffer from the column and to re-establish the

matrix bed. Columns were then transferred to clean 2mL collection tubes, ~95µL cDNA samples (section 3.5.2.1) were applied to the centre of the gel bed and the columns were centrifuged at 700 x g for 5 minutes at room temperature to elute the purified DNA. Purified DNA products were combined in a single 1.5mL tube, to which was added 0.1 volumes 3M sodium acetate pH 4.6[112] and 2.5 volumes 95% ethanol[38]. Tubes were mixed gently, incubated at -20°C for 1-2 hours to precipitate the DNA, then centrifuged at room temperature for 20 minutes at 13000rpm to pellet the DNA. Supernatants were removed and the DNA pellets air-dried for approximately 10 minutes at room temperature, resuspended in 20µL ddH_2O then stored at -20°C.

3.5.3 Preparation of Competent Yeast Cells

Frozen stocks of AH109 *S. cerevisiae* yeast cells or AH109/pGBKT7-FLJ22318 transformed yeast cells (section 3.5.7) were streaked onto YPDA/agar[159] or SD/-Trp agar plates[106] and incubated at 30°C for 3-5 days until yeast colonies had reached ~2mm in diameter. To prepare competent cells for simultaneous transformations, several AH109 colonies (2-3mm in diameter) were inoculated into 1mL of YPDA medium[160], vortexed for 5 minutes and transferred to a 250mL flask containing 50mL of YPDA medium[160]. For sequential transformations, several AH109/pGBKT7-FLJ22318 colonies were inoculated into 1mL of SD/-Trp medium[107], vortexed for 5 minutes and transferred to a 250mL flask containing 50mL of SD/-Trp medium[107] supplemented with 0.2% adenine[3]. Cultures were incubated at 30°C for 16-20 hours at 230rpm until the OD_{600} was >1.5 for YPDA cultures or >1.0 for SD cultures. Following overnight incubation the yeast cultures were diluted into fresh YPDA medium[160] to give an OD_{600} of 0.2-0.3 and incubated at 30°C for ~3 hours at 230rpm until the OD_{600} had reached 0.4-0.6. Yeast cells were then pelleted by centrifugation at 1500rpm for 5 minutes at room temperature, supernatants were discarded and the cell pellets were resuspended in 25mL of ddH_2O. Following centrifugation at 1500rpm for 5 minutes at room temperature, supernatants were removed and yeast pellets were resuspended in 1mL of freshly prepared 1X TE/LiAc[143]. Yeast cells were now considered competent and were used immediately for transformation.

3.5.4 Small Scale LiAc Yeast Transformation

Competent AH109 yeast cells (50µL) were combined with 625ng of plasmid DNA, 5µg denatured herring testes carrier DNA[46] plus 500µL of PEG/LiAc/TE[76] in pre-chilled 1.5mL microcentrifuge tube. Tubes were gently vortexed then incubated at 30°C for 30 minutes at 230rpm. Twenty µL of DMSO was added to the yeast, the tubes were mixed by inversion, cells were heat shocked at 42°C for 20 minutes then centrifuged at 14000rpm for 15 seconds at room temperature. The supernatants were removed, yeast pellets were resuspended in 1mL of YPD Plus Liquid Medium[161] and incubated at 30°C for 90 minutes at 230rpm then centrifuged at 14000rpm for 15 seconds at room temperature. The supernatants were removed and yeast pellets were resuspended in 1mL of 0.9% NaCl[114]. To determine the cotransformation efficiency, 100µL of 1:10, 1:100 and 1:1000 dilutions of the transformation mixture was plated onto SD/-Leu/-Trp[104] agar plates. To select for cotransformed yeast expressing interacting proteins, 100µL of 1:10, 1:100 and 1:1000 dilutions of the transformation mixtures were plated onto SD/-Ade/-His/-Leu/-Trp-X-α-Gal[97] agar plates. Plates were incubated inverted at 30°C for 2-4 days until colonies appeared.

3.5.5 Large Scale LiAc Yeast Transformation

Competent AH109 yeast cells (100µL) were combined with 0.2µg of plasmid DNA, plus 100µg denatured herring testes carrier DNA[46] in a pre-chilled 1.5mL microcentrifuge tube. Six hundred µL of PEG/LiAc/TE[76] solution was added and tubes were gently vortexed for 10 seconds then incubated at 30°C for 30 minutes at 230rpm. Seventy µL of DMSO was added to the yeast, the tubes were mixed by inversion, cells were heat shocked at 42°C for 15 minutes then centrifuged at 14000rpm for 15 seconds at room temperature. The supernatants were removed and yeast pellets were resuspended in 1mL of 1X TE[143]. To select for yeast transformed with pGBKT7 or pGADT7 plasmids, 200µL of the transformation mixture was plated onto SD/-Trp[106] or SD/-Leu[102] agar plates. To select for sequentially transformed yeast, 200µL of transformation mixture was plated onto SD/-Ade/-His/-Leu/-Trp-X-α-Gal[97], SD/-His/-Leu/-Trp[99] and SD/-Leu/-Trp[104] agar plates. Plates were incubated inverted at 30°C for 2-4 days until colonies appeared.

3.5.6 Library Scale LiAc Yeast Transformation

Competent AH109/pGBKT7-FLJ22318 yeast cells (600µL) were combined with 20µL purified cDNA (section 3.5.3; section 3.5.2.2), 3µg of pGADT7-Rec plasmid DNA, plus 200µg denatured herring testes carrier DNA[46] in pre-chilled 15mL microcentrifuge tubes. PEG/LiAc/TE[76] solution (2.5mL) was added and tubes were gently vortexed for 10 seconds then incubated at 30°C for 45 minutes at 230rpm. DMSO (160µL) was added to the yeast, the tubes were mixed by inversion, cells were heat shocked at 42°C for 20 minutes with mixing every 10 minutes then centrifuged at 1500rpm for 5 minutes at room temperature. The supernatants were removed and yeast pellets were resuspended in 3mL of YPD Plus Liquid Medium[161] and incubated at 30°C for 90 minutes at 230rpm then centrifuged at 1500rpm for 5 minutes at room temperature. The supernatants were discarded and yeast pellets were suspended in 6mL 0.9% NaCl[114]. To select for pGADT7/pGBKT7 transformants expressing interacting proteins, 100µL aliquots of the transformation mixture was plated onto SD/-Ade/-His/-Leu/-Trp-X-α-Gal[97] and SD/-His/-Leu/-Trp-X-α-Gal[100] agar plates. To determine the transformation efficiency a 30µL aliquot of transformation mixture was diluted with 720µL of 0.9% NaCl[114] and 100µL plated onto duplicate SD/-Leu/-Trp[104] and SD/-Leu[102] agar plates. Plates were incubated inverted at 30°C for 2-4 days until colonies appeared. To provide transformation controls a small scale yeast transformation (section 3.5.4) was performed in parallel with the library screen.

3.5.7 Preparation of Yeast/Glycerol Stocks

To prepare glycerol stock cultures, single yeast colonies were inoculated into 500µL of the appropriate medium (Table 3.2), vortexed vigorously for 1 minute to disperse the cells and 500µL 50% glycerol[43] was added. Glycerol stock cultures were mixed by inversion and stored at -80°C in 2mL cryotubes.

Table 3.2 Yeast medium for glycerol stock preparation

AH109	pGBKT7-AH109	pGADT7-AH109	pGBKT7/pGADT7-AH109
YPDA	SD/-Trp[106]	SD/-Leu[102]	SD/-Leu/-Trp[104]

3.5.8 Plasmid Isolation from Yeast

Transformed yeast (section 3.5.6) were plated onto SD/-Ade/-His/-Leu/-Trp/agar[96] plates and incubated at 30°C for 3-5 days. Yeast colonies of 2-4mm in diameter were individually inoculated into 500µL SD/-Ade/-His/-Leu/-Trp[95] medium, vortexed for 1 minute, transferred into 4.5mL SD/-Ade/-His/-Leu/-Trp[95] medium and incubated overnight at 30°C with shaking at 250rpm. Following overnight growth, yeast cells were pelleted by centrifuging at 2500rpm for 5 minutes, the supernatants were removed and yeast cells were lysed by re-suspending in 300µL yeast lysis buffer[158] with 100µL 425-600µm glass beads. Plasmid DNA was recovered by the addition of 300µL phenol:chloroform (1:1). Cells were vortexed for 4 minutes then centrifuged at 14000rpm for 1 minute and the upper aqueous phase transferred to clean 1.5mL tubes. To precipitate plasmid DNA, 0.1 volume of 3M sodium acetate[112] and 2.5 volumes of absolute ethanol were added to the tubes. Tubes were vortexed briefly, incubated at room temperature for 2 minutes, centrifuged at 14000rpm for 5 minutes and the supernatants decanted. Pellets were then washed with 500µL of 70% ethanol[37], centrifuged at 14000rpm for 5 minutes and the supernatants discarded. Purified plasmid DNA pellets were air dried at room temperature for ~5-10 minutes then resuspended in 20µL of ddH_2O and stored at -20°C.

3.5.9 Transcriptional Activation of DNA-BD Fusion Construct

To ensure that the DNA-BD construct was not able to self-activate transcription of the reporter genes and could be used in Y2H screens, AH109 yeast cells transformed with pGBKT7 or pGBKT7 containing an insert were streaked onto SD/-Trp/X-α-Gal agar[109], SD/-His/-Trp/X-α-Gal agar[101] and SD/-Ade/-Trp/X-α-Gal agar[98] plates. Plates were incubated inverted at 30°C for 3-5 days, viewed, photographed where appropriate then stored at 4°C wrapped in parafilm.

3.5.10 Toxicity of DNA-BD Fusion Construct

To ensure that the DNA-BD construct was not toxic to AH109 yeast cells, pGBKT7 transformed AH109 yeast cells were streaked onto SD/-Trp agar[106] plates and incubated at 30°C for 3-5 days until colonies reached 2-3mm in diameter. Single large colonies were inoculated into 1mL of SD/-Trp medium[107], vortexed for 5 minutes and transferred

to a 250mL flask containing 50mL of SD/-Trp/Kan medium[108]. Cultures were incubated at 30°C for 16-24 hours at 220rpm and the OD_{600} measured.

3.5.11 Preparation of Yeast Protein Extracts

Stocks of pGBKT7 transformed yeast cells were streaked onto SD/-Trp/agar[106] plates, and incubated at 30°C for 3-5 days. Yeast colonies of 2-4mm in diameter were individually inoculated into 1mL SD/-Trp[107] medium, vortexed for approximately 2 minutes to disperse cell clumps and transferred to 4mL SD/-Trp[107] medium. As a negative control a 5mL culture of untransformed AH109 *S. cerevisiae* yeast cells was also prepared from frozen stocks, streaked onto YPDA/agar[159] plates, and inoculated into 5mL YPDA[160] medium. Cultures were incubated overnight at 30°C with shaking at 250rpm then centrifuged at 2500rpm for 5 minutes at room temperature. The supernatants were removed and yeast were incubated at -80°C for 10 minutes, resuspended in 100µL western lysis buffer[153] and the cell suspensions transferred to clean 1.5mL microcentrifuge tubes containing 100µL of glass beads. Cell suspensions were incubated at 70°C for 10 minutes, vortexed for 1 minute, centrifuged at 14000rpm for 5 minutes at room temperature and the supernatants transferred to clean 0.5mL centrifuge tubes. Ten µL aliquots were then diluted with an equal volume of 2X sample buffer[93], incubated for 5 minutes at 95°C and electrophoresed in 12% polyacrylamide gels (section 3.7.2). Following electrophoresis, proteins were transferred to nitrocellulose membranes and immunoblotted with antibodies to the c-Myc epitope encoded by the pGBKT7 plasmid (section 3.7.4).

3.6 Tissue Culture

3.6.1 Cell Culture Conditions

LNCaP and DU145 prostate cancer cells were routinely cultured at 37°C/5%CO_2 in RPMI 1640 medium[92] containing 10% foetal calf serum (FCS), 100µg/mL penicillin and 100U/mL streptomycin (PS). Medium was replaced every 2-3 days and LNCaP cells were passaged at a dilution of 1:5 with DU145 cells passaged at a dilution of 1:10 when 90-95% confluent. To passage cells, medium was aspirated, cells were rinsed with 1mL of PBS[72], the PBS[72] aspirated, 1-2mL of trypsin/EDTA (section 2.1.5) was then added to each flask and the flasks were incubated at 37°C for approximately 2 minutes until cells had detached from the culture surface. Culture medium was then added to

flasks to inactivate the trypsin, cells were dispersed by pipetting and the appropriate volume of cell suspensions was transferred to fresh flasks or plates.

3.6.2 Transfection of Cells

Transient transfection of LNCaP and DU145 prostate cancer cells with expression plasmids was performed using LipofectAMINE™ 2000 and according to the manufacturer's protocols (Invitrogen). Cells were passaged according to Table 3.3 and cultured overnight in RPMI/10% FCS[91] at 37°C/5% CO_2 to allow adhesion of cells to the culture surface.

Table 3.3 DU145 and LNCaP cell passage numbers

	DU145 Cells	LNCaP Cells
96 Well Plates	2.5×10^4	-
8 Well Chamber Slides	6.0×10^4	-
24 Well Plates	1.0×10^5	1.5×10^5
Microscope Slides	-	1.5×10^5
Microscope Slide Coverslips	-	3.75×10^5
6 Well Plates	5.0×10^5	7.5×10^5
10cm Petri Dishes	3.0×10^6	4.2×10^6

For each transfection, LipofectAMINE™ 2000 was added to an aliquot of RPMI 1640 medium[89] and incubated at room temperature for 5 minutes (Table 3.4). The plasmid DNA was added to another aliquot of RPMI 1640 medium[89] and the diluted LipofectAMINE™ 2000 and DNA solutions were combined and incubated at room temperature for 20 minutes to allow the formation of DNA/LipofectAMINE™ 2000 complexes. The DNA/LipofectAMINE™ 2000 solution was then added drop-wise to cultures and cells were incubated for 24-48 hours at 37°C/5% CO_2 to allow for plasmid uptake and expression.

3.6.3 Cryopreservation of Cell Cultures

Cell cultures to be cryopreserved were grown to confluency in T75 flasks, trypsinised (section 3.6.1), then centrifuged at 4°C for 5 minutes at 245 x g. The medium was

Table 3.4 Transfection details

96 Well Plates			
LipofectAMINE™ 2000 (µL)	**Medium (µL)**	**Plasmid DNA (µg)**	**Medium (µL)**
2	25	3	25
8 Well Chamber Slides			
LipofectAMINE™ 2000 (µL)	**Medium (µL)**	**Plasmid DNA (µg)**	**Medium (µL)**
2	40	1	40
24 Well Plates			
LipofectAMINE™ 2000 (µL)	**Medium (µL)**	**Plasmid DNA (µg)**	**Medium (µL)**
2	50	1	50
Microscope Slide Coverslips			
LipofectAMINE™ 2000 (µL)	**Medium (µL)**	**Plasmid DNA (µg)**	**Medium (µL)**
4	100	1.6	100
6 Well Plates			
LipofectAMINE™ 2000 (µL)	**Medium (µL)**	**Plasmid DNA (µg)**	**Medium (µL)**
10	250	5	250
10cm Petri Dishes			
LipofectAMINE™ 2000 (µL)	**Medium (µL)**	**Plasmid DNA (µg)**	**Medium (µL)**
40	1000	16	1000

aspirated, cells were resuspended in 4.5mL of fresh RPMI/10% FCS/PS[92] medium containing 10% DMSO, divided into 3 cryotubes, stored at -80°C for 24 hours before being transferred to liquid nitrogen.

3.6.4 DHT Treatment of Cells

LNCaP cells were cultured at 37°C/5%CO_2 in RPMI stock medium[92] until 80% confluent (or as required). The medium was then replaced with RPMI 1640 containing 5% charcoal stripped fœtal calf serum (CS-FCS) and PS[90] and cells were incubated for a further 48 hours prior to replacement of the medium with fresh medium containing 5% CS-FCS[90] and 10^{-9}M DHT[19] for the appropriate length of time. Control cultures contained the same volume (0.1% v/v) of ethanol (vechicle).

3.7 Western Blotting

3.7.1 Protein Extraction

To harvest cells, medium was aspirated, cells were rinsed with PBS[72] then lysed by the addition of western lysis buffer[153] (250-500µL per well of 24 well plates). Lysates were transferred to sterile 1.5mL microcetrifuge tubes and protein solutions, which were viscous due to the presence of genomic DNA in the samples, were repeatedly drawn through a 23G needle to decrease their viscosity. Protein extracts were stored at -20°C.

3.7.2 Polyacrylamide Gel Electrophoresis

The Mini Protean II™ polyacrylamide gel electrophoresis apparatus (BioRad) was assembled according to the manufacturer's instructions and 12% separating gels[81] were pipetted into the gel spaces to ~0.5cm below the level of the wells. Gels were overlaid with ddH_2O, covered and left to polymerise at room temperature for 45-60 minutes. After 1 hour, the ddH_2O was drained, the gel spaces were rinsed with 6% stacking gel solution[82], and separating gels were overlaid with 6% stacking gel solution[82]. Well combs were inserted, the apparatus covered and stacking gels left to polymerise at room temperature for 45-60 minutes. Following gel polymerisation, well combs were removed, wells were rinsed with ddH_2O and the apparatus was assembled and filled with 1X western running buffer[154]. Protein extracts (section 3.7.1) were diluted with 0.1 volumes of 10X sample buffer[94], 10-20µL aliquots (per well) were denatured at 95°C for 8 minutes, cooled to room temperature then loaded into wells. In addition, each gel

included a well containing 5µL of Benchmark™ Prestained Protein Ladder molecular weight markers. Gels were electrophoresed at 200V for approximately 45 minutes until the dye front had migrated to the end of the gel.

3.7.3 Western Transfer

Following polyacrylamide gel electrophoresis the apparatus was disassembled and gels were placed in western transfer buffer[156]. Transfer cassettes were assembled as follows, with all reagents pre-wetted in transfer buffer[156]. A scourer was placed on the black ("negative") side of the cassette, followed by two pieces of Whatman® 3MM paper, the gel, a piece of nitrocellulose filter, two pieces of Whatman® 3MM paper and another scourer. Cassettes were closed, placed in the transfer apparatus along with an ice block and a magnetic stirrer and the proteins were transferred to nitrocellulose filters overnight at 30V with stirring.

3.7.4 Western Blotting

Following transfer of proteins, the apparatus was disassembled and nitrocellulose membranes were cut to size according to the molecular weight of the proteins of interest. All incubations for western blotting were carried out at room temperature on a horizontal shaker and dilutions of primary and secondary antibodies are detailed in Table 3.5. Membranes were blocked in TBS-3% Blotto[137] for 1-1.5 hours then incubated with primary antibodies diluted in TBST-1% Blotto[139] for 1-1.5 hours. Membranes were washed in TBST[138] (3 x 10 minutes), incubated with secondary antibodies diluted in TBST-1% Blotto[139] for 1-1.5 hours then washed in TBST[138] (3 x 10 minutes). Immunoreactivity was detected by incubation of filters for 1 minute with ECL Detection Reagent[32] or for 5 minutes with ECL Plus Detection Reagent[33]. Filters were wrapped in plastic film, placed in an autoradiography cassette and exposed to X-Ray film for 10 seconds-10 minutes as required. Films were developed in an AGFA CP-1000 Film Developer, scanned and images stored in .TIF format.

Table 3.5 Primary (1°) and secondary (2°) antibody dilutions

1° Antibody	Dilution	2° Antibody	Dilution
Goat anti-human actin Ig	1:2000	Donkey anti-goat IgG	1:1000
Goat anti-PACT Ig	1:500	Donkey anti-goat Ig	1:2000
Mouse anti-GFP Ig	1:3000	Sheep anti-mouse Ig	1:2000
Mouse anti-HA Ig	1:2000	Sheep anti-mouse Ig	1:2000
Mouse anti-Myc Ig	1:1000	Sheep anti-mouse Ig	1:2000
Mouse anti-Nkx3.1	1:250	Sheep anti-mouse Ig	1:2000
Mouse anti-V5 Ig	1:5000	Sheep anti-mouse Ig	1:2000
Rabbit anti-Myc Ig	1:1000	Sheep anti-rabbit Ig	1:2000
Rabbit anti-PACT Ig	1:500	Sheep anti-rabbit Ig	1:2000

3.8 GST Pull-Down Assays

3.8.1 Small-Scale Production of GST Fusion Proteins

Transformed BL21 bacterial cells were streaked onto LB/agar/ampicillin[50] plates and incubated at 37°C overnight. Following overnight growth bacterial colonies were individually inoculated into 2mL of LB broth/ampicillin[54] and incubated at 37°C for 3-5 hours until the OD_{600} had reached 0.5. Fusion protein production was then induced by the addition of 2µL 100mM IPTG[47] and cells were incubated for 1-2 hours at 30°C with shaking at 250rpm. Following induction, the OD_{600} was recorded and 1mL of each culture was transferred to 1.5mL tubes, which were centrifuged at 13000rpm for 5 seconds at room temperature and the supernatants removed. Bacterial pellets were resuspended in western lysis buffer[153] using the formula:

$$x\mu L = 1000 \times \frac{OD_{600}}{8}$$

Owing to the presence of genomic DNA in the samples, bacterial lysates were repeatedly drawn through a 23G needle to decrease their viscosity and 20µL aliquots were transferred to clean 0.5mL tubes. Samples were diluted with 0.1 volumes of 10X sample buffer[94], incubated at 95°C for 5 minutes and 10µL aliquots were electrophoresed in 12% polyacrylamide gels[81] (section 3.7.2). Following electrophoresis, gels were stained with Coomassie blue staining solution[13] (section 3.8.2) to verify GST-fusion protein production.

3.8.2 Coomassie Blue Staining of Gels

Following electrophoresis, polyacrylamide gels were rinsed in ddH_2O, immersed in Coomassie blue staining solution[13] and incubated at room temperature with gentle agitation overnight. Following staining, gels were rinsed in ddH_2O, incubated 3X 30 minutes in Coomassie de-staining solution[14] with gentle agitation, rinsed in ddH_2O then wrapped in wet cellophane and clipped to a glass plate to prevent shrinkage. Gels were dried at room temperature for 3-4 days then scanned and the images stored in .TIF format.

3.8.3 Large-Scale Production and Purification of GST Fusion Proteins

Single bacterial colonies of transformed BL21 cells were individually inoculated into 5mL of LB broth/ampicillin[54] and incubated for 18 hours overnight at 37°C with shaking at 250rpm. Following 18 hours' incubation, cultures were diluted with 100mL fresh LB broth/ampicillin[54] and incubated at 37°C for ~3 hours at 250rpm until the OD_{600} had reached 0.5-2.0. To induce fusion protein production, 100µL of 100mM IPTG[47] was added to bacterial cultures and cells were incubated at 30°C for 3-4 hours with shaking at 250rpm. Bacterial cultures were centrifuged for 15 minutes at 3000rpm at 4°C, supernatants were decanted and pellets were placed on ice then re-suspended in 5mL of sonication buffer[125] and 50µL lysozyme[63] added. After incubating on ice for 15 minutes, 36µL 200mM PMSF[80], 12.5µL 0.5M EDTA[34], 5µL 1M DTT[25], 50µL 1M magnesium chloride[64] and 500µL 10% Triton X-100[147] was added to cultures to aid solubilisation of fusion proteins. Cell suspensions were lysed by sonicating at 5 second intervals (Branson sonifier™ 150, setting 3) with alternate 5 second incubations on ice, then lysates were incubated for 30 minutes at 4°C with gentle rotation. Lysates were pelleted at 3000rpm for 15 minutes at 4°C, the supernatants (~5mL) were transferred to clean 15mL tubes and 200µL of 50% Glutathione Sepharose 4B[42] was added to each tube. Samples were incubated with slow rotation for 15 minutes at 4°C to precipitate GST-fusion proteins. Beads were collected by centrifugation at 300rpm for 5 minutes at 4°C and the supernatants were discarded. Beads were washed 3X with 1.5mL ice-cold PBS[72] centrifuging in between at 300rpm for 5 minutes at 4°C and discarding the supernatants. Beads were resuspended in 100µL ice-cold PBS[72] and stored at 4°C. To confirm GST-fusion protein purification, 30µL aliquots of 50% Glutathione-fusion protein suspensions were centrifuged at 300rpm for 5 minutes at 4°C, the supernatants

were removed, beads were resuspended in 15µL 2X sample buffer[93] and incubated for 5 minutes at 95°C to dissociate proteins from beads. Protein samples were then centrifuged at 300rpm for 5 minutes at 4°C and 10µL aliquots were separated in 12% polyacrylamide gels[81] (section 3.7.2). Following electrophoresis, purified GST fusion proteins were visualised by Coomassie blue staining solution[13] (section 3.8.2).

3.8.4 GST Pull-Down Assays

Untransfected or transfected cells (LNCaP or DU145) were grown in 6 well plates, with cells harvested 24 hours following transfection to allow expression of fusion proteins (section 3.6.2). Medium was aspirated from the cells, 500µL per well ice-cold PBS[72] was added, and plates were gently rocked to wash the cells. PBS[72] was aspirated and cells were lysed by the addition of 500µL RIPA buffer[85] directly to the wells. Cell lysates were transferred to pre-chilled 1.5mL tubes, then incubated for 20 minutes at 4°C with slow rotation to ensure complete cell lysis. Protein solutions were centrifuged at 8000rpm for 10 minutes at 4°C to pellet cell debris, then 50µL of the lysates was removed and stored at -20°C. An additional 300µL of each lysate was transferred to clean pre-chilled 1.5mL tubes and samples were incubated overnight at 4°C with slow rotation with 60µL of the purified 50% Glutathione-GST-fusion proteins (section 3.8.3). Following overnight incubation, beads were collected by centrifugation at 1000rpm for 2 minutes at 4°C and supernatants were discarded. Beads were washed 3X with 300µL ice-cold PBS[72] centrifuging in between at 1000rpm for 2 minutes at 4°C and discarding supernatants, then the beads were resuspended in 25µL 2X sample buffer[93]. To dissociate fusion proteins from the beads, samples were incubated for 5 minutes at 95°C, centrifuged at 1000rpm for 2 minutes at 4°C and 15µL of each supernatant was transferred to clean 0.5mL tubes. Ten µL aliquots were separated in 12% polyacrylamide gels (section 3.7.2) together with 10µL of stored lysates (above) which had been diluted with 10µL of 2X sample buffer[93] and incubated for 5 minutes at 95°C. Following electrophoresis, protein samples were transferred to nitrocellulose membranes and immunoblotted (sections 3.7.3; 3.7.4).

3.9 Immunocytochemistry

3.9.1 Slide Preparation

To prepare glass microscope slides for immunocytochemistry, a circle of approximately 2cm diameter was drawn on each slide using a wax pen. The slides were then washed in ddH_2O followed by 70% ethanol[37], placed in open 10cm petri dishes and exposed to UV light for 1 hour to sterilise the culture surface. Following UV irradiation, 500µL of RPMI stock medium[92] was added to each slide, petri dishes were closed to maintain sterility and slides were incubated overnight at 37°C/5% CO_2. This procedure facilitated cell adherence to the culture surface. Cells were passaged onto the slides the following day (section 3.6.1) then transfected (section 3.6.2) 24 hours later if required.

3.9.2 Immunocytochemistry

Twenty-four hours post-transfection, slides were removed from petri dishes, washed in PBS[72] and fixed in 95% ethanol[38] for 5 minutes then washed in PBS[72] for a further 5 minutes and transferred to a humidifier tray. Goat anti-PACT primary antibody was diluted 1:750, 1:1000 and 1:1500 in antibody diluent (section 2.1.7), 500µL was added drop wise to slides and the slides were incubated at room temperature for 1 hour. Slides were then washed in PBS[72] for 3X 5 minutes and replaced in the humidifier tray. To detect the primary antibody, 5 drops of 'Link' (Biotinylated anti-goat/anti-mouse/anti rabbit IgG) were added to the slides, which were incubated at room temperature for 15 minutes, washed in PBS[72] for 3X 5 minutes then replaced in the humidifier tray. Five drops of 'Label' (Streptaviden/HRP) were added to slides and the slides were incubated at room temperature for 15 minutes, washed in PBS[72] for 5 minutes and replaced in the humidifier tray. Slides were covered in DAB[15] staining reagent, incubated at room temperature for 15 minutes then washed in PBS[72] for 5 minutes and replaced in the humidifier tray. Fifty µL of $CuSO_4$ (section 2.1.7) was added drop wise to the slides, which were then incubated for 5 minutes at room temperature, washed in PBS[72] for 5 minutes, then counterstained with weak haematoxylin in a Leica Jung Autostainer XL. For counterstaining, slides were sequentially immersed for 30 seconds each in ddH_2O, weak (1/10) haematoxylin, ddH_2O, acid alcohol, Scotts tap water, ddH_2O, 95% ethanol, absolute ethanol (2X) and xylene (3X). Upon completion of counterstaining, slides were mounted using a Leica CV 5000 Cover Slip Mounter and DEPX mounting medium.

3.10 Immunoprecipitation Assays

For immunoprecipitation assays, plasmids encoding the appropriate fusion protein were transfected into cells and the cultures were incubated for 24 hours (section 3.6.2). To harvest proteins, medium was aspirated from the culture dishes, 1mL ice-cold PBS[72] per well was added, and plates were rocked to gently wash cells. PBS[72] was aspirated, 1mL of RIPA buffer[85] per well was added to the dishes and cell lysates were transferred to pre-chilled 1.5mL tubes. Tubes were incubated for 20 minutes at 4°C with slow rotation to ensure complete cell lysis then centrifuged at 8000rpm for 10 minutes at 4°C to precipitate nuclei and cell debris. A 50µL aliquot of each lysate was stored at -20°C and ~1mL of each supernatant was transferred to clean pre-chilled 1.5mL tubes. To pre-clear samples, 50µL of 50% Protein G or Protein A sepharose[84] was added to each tube and the samples were incubated with slow rotation for 60 minutes at 4°C. Protein beads were pelleted by centrifugation at 1000rpm for 2 minutes at 4°C, 2 x 500µL aliquots of supernatant were transferred to clean pre-chilled 0.5mL tubes and primary antibody (Table 3.6) added to one of each set of two tubes. All samples were incubated overnight at 4°C with slow rotation. Following overnight incubation, 50µL of 50% Protein G or Protein A sepharose[84] was added to each tube and the samples were incubated with slow rotation for 2 hours at 4°C to precipitate immunocomplexes. Beads were collected by centrifugation at 1000rpm for 2 minutes at 4°C and the supernatants were discarded. Beads were washed 3X with 400µL ice-cold PBS[72], centrifuging in between at 1000rpm for 2 minutes at 4°C, supernatants were discarded, and the beads were resuspended in 50µL 2X sample buffer[93]. To dissociate immunocomplexes from the beads, samples were incubated for 5 minutes at 95°C, centrifuged at 1000rpm for 2 minutes at 4°C and 40µL of each supernatant was transferred to clean 0.5mL tubes. Ten µL aliquots were electrophoresed in 12% polyacrylamide gels (section 3.7.2) together with 10µL of the stored lysates (above) which had been diluted with 10µL of 2X sample buffer[93] and incubated for 5 minutes at 95°C. Following polyacrylamide gel electrophoresis, protein samples were transferred onto nitrocellulose membranes and immunoblotted (section 3.7.3; 3.7.4).

Table 3.6 Antibody dilutions for immunoprecipitation assays

1° Antibody	Dilution
Mouse anti-GFP Ig	1:100
Mouse anti-HA Ig	1:100
Mouse anti-Myc Ig	1:1000
Mouse anti-V5 Ig	1:250
Rabbit anti-Myc Ig	1:25
Rabbit anti-PACT Ig	1:25

3.11 Confocal Microscopy

3.11.1 Immunofluorescence

Following transfection (section 3.6.2) and one hour prior to fixing of cells, medium was aspirated from 8 well chamber slides and replaced with 500µL fresh RPMI medium[91] containing 0.5µL (10mg/mL) Hoechst 33258 nuclear stain. Cells were then incubated in the dark at 37°C /5% CO_2 for one hour to allow uptake of the Hoechst 33258 dye and staining of cell nuclei. Following this incubation, medium was removed and slides were gently washed 2X with 400µL PBS[72]. PBS[72] was aspirated and cells were fixed by the addition of 400µL 4% formaldehyde[40] directly to the wells, cells were incubated for 15 minutes at room temperature, then washed 3X with 400µL PBS[72] for 5 minutes at room temperature. Cells were permeabilised by the addition of 400µL 0.2% Triton X-100[146] for 5 minutes at room temperature then washed 3X with 400µL PBS[72] for 5 minutes at room temperature. PBS[72] was aspirated, 400µL of confocal blocking buffer[12] was added and the cells were incubated for 30 minutes at room temperature then washed 3X 5 minutes with 400µL PBS[72] at room temperature. Primary antibody (Table 3.7) was diluted in 1% BSA/PBS[9], 100µL was added drop-wise to each well and the chamber slides incubated at 4°C overnight in a humidifier tray shielded from light. The next morning, slides were washed 3X 5 minutes in PBS[72] and replaced in the humidifier tray. To detect primary antibody, secondary antibody (Table 3.7) was diluted in low light in 1% BSA/PBS[9], 100µL was added drop-wise to each well and the chamber slides were incubated at room temperature for 1 hour. Wells were washed 3X 5 minutes in PBS[72] then the chamber and gaskets were removed. Upon completion of staining, slides were mounted using ~15µL of low fade mounting media[60] and sealed around the edges of the cover slips with clear nail polish prior to viewing (section 3.11.2).

Table 3.7 Immunofluorescence antibody dilutions

Primary Antibody	Dilution	Secondary Antibody	Dilution
Mouse anti-V5 Ig	1:500	Goat anti-mouse IgG Alexa Fluor® 488	1:400
Rabbit anti-Myc Ig	1:500	Goat anti-rabbit IgG Alexa Fluor® 546	1:400
Goat anti-PACT Ig	1:1000	Donkey anti-goat IgG Alexa Fluor® 546	1:400

3.11.2 Confocal Microscopy

The confocal scanning microscope creates an image by scanning a finely focused laser light across a sample and recording the light emitted from a scanned point using a light detector (photomultiplier tube). The recorded emissions are then digitised and displayed on a computer screen as a grey shaded image with 256 levels of grey. In these studies the main advantage of using confocal microscopy over conventional fluorescence microscopy was that different proteins could be labelled with fluorochrome-antibody conjugates and imaged simultaneously. These images could be aligned, artificially coloured then merged to demonstrate the localisation and co-localisation of proteins within cells.

Confocal microscopy was performed using a BioRad MCR 1000/1024 UV Laser Scanning Confocal Microscope equipped with Argon ion and Helium/Neon lasers. The 250mW Argon UV laser, which excites light at a wavelength of 350nm, was used to detect the nuclei of cells which had been incubated with the Hoechst 33258 DNA stain. The 100mW Argon laser, which excites blue light at a wavelength of 488nm, and the Helium/Neon laser, which excites green light at wavelength of 543nm, were used to detect the localisation of cells incubated with the Alexa Fluor® 488 and Alexa Fluor® 546 fluorochrome-antibody conjugates, respectively. A 40X Plan-Apo oil immersion lens with a numerical aperture of 1.3 was used for all images.

To minimise cellular damage and photobleaching, the lasers were used at low power with a 1-3% intensity level for the Argon laser and 30-100% intensity level for the Helium/Neon, which has a much lower power output. To optimise the quality of the images collected, the level of signal amplification and the black level were adjusted and the images collected in normal scan rate using a Kalman collection filter set at 5 to average out noise. Images were viewed and artificially coloured using Confocal Assistant 4.02 (Todd Clark Brelje) software.

To determine protein localisation, images exhibiting fluorescence due to the Alexa Fluor® 546 fluorochrome-antibody conjugate were coloured red, whereas images exhibiting fluorescence due to the Alexa Fluor® 488 fluorochrome-antibody conjugate were coloured green. Co-localisation of proteins was determined from image overlays which produced a yellow colour where co-localisation had occurred.

3.12 Luciferase Reporter Assays

For luciferase reporter assays, cells were transfected in 96 well plates (section 3.6.2) with 1µg luciferase reporter plasmid (TK-Luc or NKX-TK-Luc; section 2.1.3) and combinations of NKX3-1-pcDNA3.1/V5-His-TOPO, FLJ22318-pcDNA3.1/V5-His-TOPO and pCMV-Myc-FLJ22318 expression plasmids (sections 5.2.1.1; 5.2.1.4). To ensure DNA concentrations were equal in all wells transfected, *lac*Z-pcDNA3.1/V5-His-TOPO plasmid (Figure 3.9) was added to give a final DNA concentration of 3µg per well. In addition, to control for variation in transfection efficiency, 10ng pRL-SV40-*Renilla* plasmid (Figure 3.10) was included in all transfections. Twenty-four hours post transfection, luciferase activity was determined as follows: medium was aspirated from the wells and cells were rinsed with PBS[72] then lysed by the addition of 20µL of 1X Passive Lysis Buffer[71] (PLB) to each well. Plates were gently rocked for 15 minutes at room temperature to facilitate cell lysis. Firefly luciferase activity was assayed by dispensing 50µL of Luciferase buffer[61] into each well and the resulting luminescence read in a Wallac™ plate-reading luminometer. *Renilla* luciferase activity was then assayed by dispensing 80µL of Stop & Glo® Reagent[130] into each well and luminescence was again measured.

3.13 Northern Blotting

3.13.1 RNA Extraction

To harvest cells, medium was aspirated from culture dishes and cells were lysed by the addition of 1mL Ultraspec™ to each dish, the cells were scraped from the culture surface and transferred to pre-chilled 1.5mL microcentrifuge tubes and incubated on ice for 5 minutes. Homogenates were diluted with 200µL chloroform with vigorous mixing, samples were incubated on ice for 5 minutes then centrifuged at 12000 x g for 15 minutes at 4°C and the upper aqueous phase (~600µL) transferred to clean 1.5mL

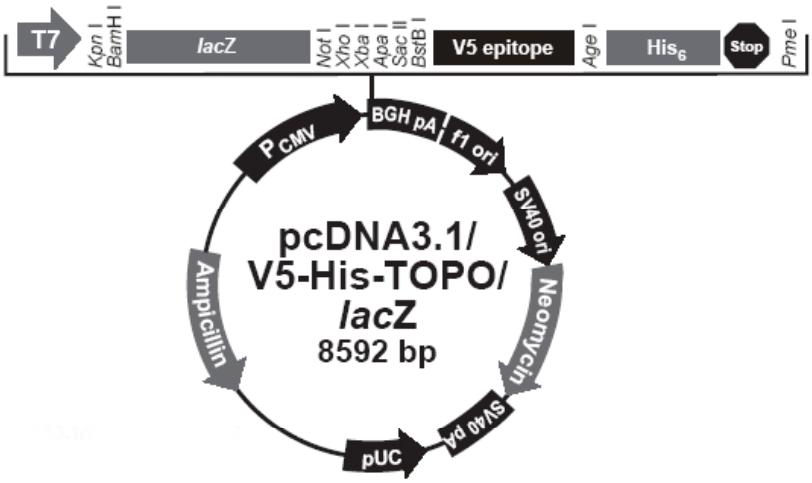

Figure 3.9 Map of the pcDNA3.1/V5-His-TOPO/*lacZ* vector which constitutively expresses β-galactosidase from the CMV promoter when transfected into mammalian cells. This plasmid was used to equalise DNA concentrations in luciferase assays (http://www.clontech.com).

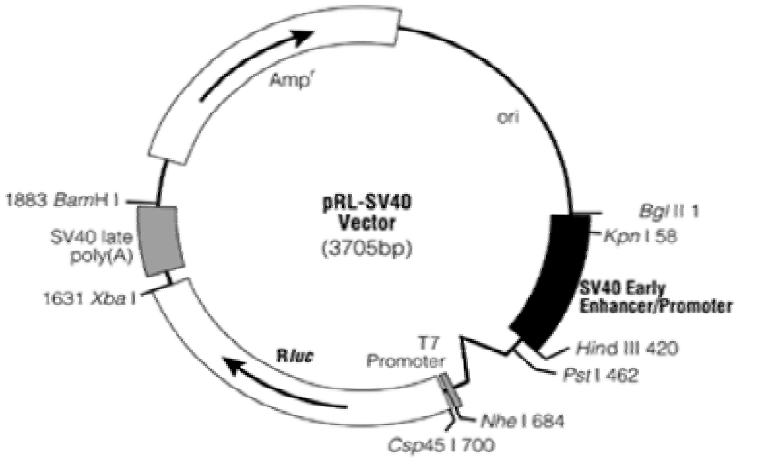

Figure 3.10 Map of the pRL-SV40 vector. The pRL-SV40 vector produces constitutive expression of *Renilla* luciferase in transfected mammalian cells from the SV40 enhancer and early promoter elements and was used in luciferase assays as an internal control to estimate and normalise results for variation in transfection efficiency (http://www.promega.com).

tubes. An equal volume of isopropanol was added and the samples were incubated on ice for 10 minutes followed by centrifugation at 12000 x g for 10 minutes at 4°C and the supernatants discarded. RNA pellets were washed 2X with 1mL 70% ethanol[37], centrifuged at 7600 x g for 5 minutes at 4°C, the ethanol decanted and the pellets air-dried for 5-10 minutes. Pellets were resuspended in 20-50µL DEPC-H_2O[16], vortexed briefly and stored at -80°C.

3.13.2 RNA Gel Electrophoresis

For Northern blotting, 8µg of RNA was made to 2.3µL with DEPC-H_2O[16], 7.7µL of RNA buffer[86] was added to each sample and samples were incubated at 65°C for 15 minutes then placed on ice for 5 minutes. 1.5µL RNA loading dye[87] was added to each sample and samples were loaded in 1% MOPS/formaldehyde/agarose[70] gels. Following electrophoresis in 1X MOPS[68] buffer at 100V for approximately 2 hours, RNA bands were visualised under UV transillumination prior to northern transfer (section 3.13.3).

3.13.3 Northern Transfer

To transfer RNA from gels to nylon membranes, northern gels were inverted onto two pieces of Whatman® 3MM filter paper that had been pre-soaked in 20X SSC-DEPC[128] and placed over a plastic support to form a wick. Nylon membranes were cut to the size of the gel, equilibrated in DEPC-H_2O[16] then 20X SSC-DEPC[128] and placed on top of the gel followed by another two pieces of Whatman® 3MM filter paper, also cut to the size of the gel and pre-soaked in 20X SSC-DEPC[128]. A 10cm stack of paper towels, a perspex plate and a 500g weight were placed on top of the gel to assist capillary transfer and plastic wrap was placed around the base of the gel over the support to prevent wicking. Following overnight transfer of RNA at room temperature, nylon membranes were rinsed in 1X SSC-DEPC[126], UV crosslinked in a Stratagene 1800UV Crosslinker, placed in Whatman® 3MM filter paper, wrapped in aluminium foil and stored in the dark at room temperature.

3.13.4 Labelling of DNA Probes

Purified cDNA probes were labelled by random priming with α-[^{32}P]-dCTP using the Prime-A-Gene® Labelling System (section 2.2). Twenty-five ng of DNA was made to 30µL with ddH_2O, then denatured at 95°C for 2 minutes and placed on ice. Two µL

dNTPs[24], 2µL (10µg/µL) BSA, 10µL 5X Labelling Buffer, 5µL α-[^{32}P]-dCTP (3000Ci/mmol) and 1µL DNA polymerase I Klenow fragment were added to each reaction and reactions were incubated at room temperature for 60 minutes. To stop the reaction, tubes were heated to 95°C for 2 minutes then 2µL 0.5M EDTA (pH 8.0)[34] was added to each tube to inactivate the DNA polymerase. Tubes were placed on ice until required.

3.13.5 Northern Hybridisation

Nylon membranes were pre-hybridised in 8mL of preheated Rapid-hyb™ buffer for 1 hour at 65°C with rotation in a Robbins hybridisation incubator. Following pre-hybridisation, 50µL of labelled probe (section 3.13.4) was added and membranes were hybridised for 2 hours at 65°C with rotation. Membranes were then washed at 65°C with rotation for 20 minutes each in Wash buffer I[150] then Wash buffer II[151], and finally in Wash buffer III[152] for 15 minutes. All wash buffers were pre-heated to 65°C. Membranes were then wrapped in plastic film and exposed to X-Ray film for 24-72 hours at -80°C. Following exposure, films were developed, scanned and images were stored in .TIF format.

Chapter Four

Chapter Four – Bioinformatic Analysis of FLJ22318

4.1 Introduction

FLJ22318 was originally identified through the National Institutes of Health, Mammalian Gene Collection (MGC) program, (Clone MGC2688, NCBI Accession BC00991; Strausberg et al., 2002). No phenotype has been reported for *FLJ22318*, however several features of this gene make it an appealing candidate for further study.

The *FLJ22318* gene is expressed at a very high level, 4 times the average gene (Thierry-Mieg et al., 2005) and according to the National Center for Biotechnology Information (NCBI) UniGene database (Hs.519804) is found in cDNA libraries from a wide range of normal and malignant tissues in both the foetus and adult. In addition, the 5'-flanking region of the *FLJ22318* locus and the region encompassing the first two exons of the *FLJ22318* gene has a high percentage (24.7%) of a C (cytosine) base followed immediately by a G (guanine) base (CpG) which is relatively rare unless there is selective pressure to keep it as such for regulation of gene expression (Figure 4.1). CpG islands are common near transcription start sites where they are present at significantly higher levels than is typical for the genome as a whole. Hypermethylation of CpG islands has been associated with transcriptional silencing, however it has been noted that CpG islands often surround the promoters of constitutively expressed (housekeeping) genes, particularly in vertebrates (Gardiner-Garden and Frommer, 1987). As such, the latter function of the CpG island is most consistent with the high level and widespread detection of FLJ22318 expression in human cDNA libraries.

FLJ22318 has an important cytogenetic location which is on the long arm of chromosome 5 at 5q35.3. This region frequently undergoes loss of heterozygosity (LOH) in both lung squamous cell carcinomas and lung adenocarcinomas (Mendes-da-Silva et al., 2000) as well as in neuroblastomas (Mosse et al., 2005). Deletions, additions and translocations of 5q35 have also been reported in haematological malignancies, as well as ovarian and breast cancers (Mitelman et al., 2005; Mosse et al., 2005) and recently this region has been linked to hereditary prostate cancer (Xu et al., 2005a).

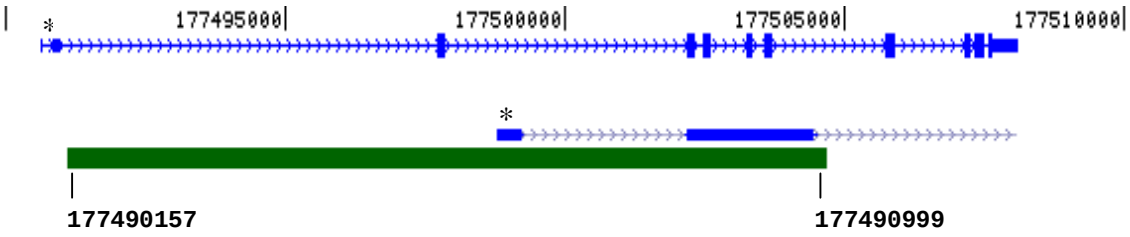

cgaggccggtgcgcacctagcccagccactgcccctcacggcccccgcgccgccctcactgagcaggg
cgggcagcgctgtaagcgtaaccacttggggcttggggcttctgacccgggagtcgggtgctgggttg
agtgcgaggccgacgcctctgccgggtggggaacccgcccgccggcgaggagcggtcgcggccagggg
cttccgccgactgggaggcccggggccgggccggagggactcggaacctggaaacgaccaggcgcgac
ccccagaggactacaggcgcggcttttctggccgccgcccggttcccgcgggcgactccactcggcat
gcgcggcggggagcctcggcggtgaggcgcaaagccgcgggctcgtgggacggccacccctccgcaaa
accgccaatgggcgggcccgggccgccgatcgcccgccgcggcttccggttccgatgacagtggcgcc
gGAAGCCGGGGCCGGGGCTGCGGGGCGAGgtgagagcgggcgggcttgggagccggcaggtgcgggcc
gagggcgggcacagcggccggcggagctgaggcgcgcggcggggaaagctcggccggcctcccgggcc
ccagccttctccagaacccctgctacccacgactaagccccgaacaatctgcccttgggcttgttctc
ttcgcagTTGTCGGCCCTGGGCCGGGAGCTGGAGTCCCAGACTCATAGGTCCCGGCCCAGCCCCCGAA
GAGCCGCCTCAGCCGGGGGGAGTTGCTCGGACTCAAACGTCCAGTCCTCGTGCGACCGCGCTGGGTCG
GAAGTGAGCAGgtgcgcaccgggctcg

Figure 4.1 CpG island surrounding the FLJ22318 transcription start site. Schematic representation of the 843 base CpG rich (24.7%; green) region encompassing the 5'-flanking region of the *FLJ22318* locus and exons 1 and 2 (∗ blue) of the *FLJ22318* gene (Adapted from http://genome.ucsc.edu/cgi-bin/hgTracks).

At present the *in vivo* function of FLJ22318 has not been determined, however the presence of several interesting putative protein-protein interaction motifs, including a lissencephaly type-1- like homology motif (LisH), a C-terminal to LisH (CTLH) motif, and a CT11-RanBPM (CRA) domain suggest that the protein is involved in multiple cellular functions as these domains are found in proteins with diverse biological activities (Letunic et al., 2006).

The LisH motif is a 33 amino acid motif composed of two α-helices that form a rare asymmetric homodimer that has a tightly packed hydrophobic core (Kim et al., 2004b; Figure 4.2). This motif is present in archaea, bacteria and eukaryotic proteins including human proteins (Letunic et al., 2006) and is based on the N-terminal sequence of the platelet-activating factor acetylhydrolase, isoform 1b, alpha subunit (PAFAH1B1; LIS1) protein which is involved in disorders of neural development (Emes and Ponting, 2001).

Mutations in the *PAFAH1B1* gene which encodes the non-catalytic alpha subunit of the intracellular 1B isoform of acetylhydrolase result in lissencephaly associated with Miller-Dieker lissencephaly syndrome. In this syndrome, the neurons fail to migrate to the cortex during cerebral development resulting in disorganised cortical layers which cause severe mental retardation and early death (Hattori et al., 1993; Reiner et al., 1993). Studies have shown that PAFAH1B1 is required for the movement of the dynein/dynactin complex along microtubules and it is also thought to regulate division of neuronal progenitor cells in the developing brain (Faulkner et al., 2000; Smith et al., 2000). In addition, Caspi et al., (2000) found that PAFAH1B1 interacts with doublecortin (DCX) in the developing cortex to enhance tubulin polymerisation, suggesting that interaction of these proteins is required for correct microtubule function. Kitagawa et al., (2000) demonstrated that PAFAH1B1 bound to platelet-activating factor acetylhydrolase, isoform 1b, beta subunit (PAFAH1B2) and the mitotic spindle assembly protein nuclear distribution gene E homolog 1 (NDE1) in a competitive manner whilst Tarricone et al., (2004) showed that PAFAH1B1 competed for binding to PAFAH1B2 with NDE1-Like 1 (NDEL1). NDE1 has recently been reported to be critical for normal cortical development (Feng and Walsh, 2004), whilst NDEL1 is required for regulation of dynein activity (Shu et al., 2004). These data indicate that

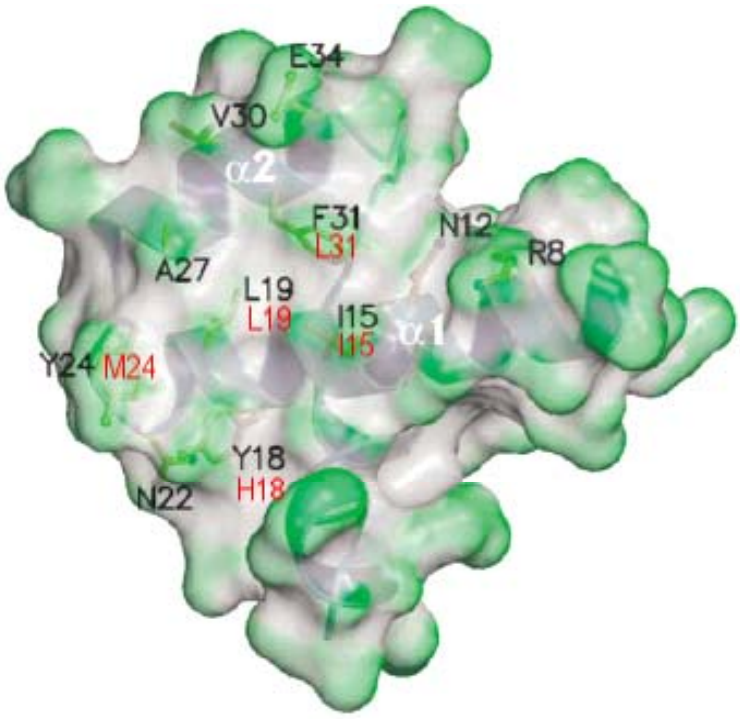

Figure 4.2 Schematic representation of the two α-helices that form the LisH motif. Model shows the LisH motif from the platelet-activating factor acetylhydrolase, isoform Ib, alpha subunit (PAFAH1B1;LIS1) protein with the tightly packed hydrophobic core residues[iii] in black and the corresponding hydrophobic core residues for FLJ22318 in red (Adapted from Kim et al., 2004).

[iii] A – alanine, E – glutamate, F – phenylalanine, I – isoleucine, L – leucine, M – methionine, N – asparagine, R – arginine, V – valine, Y – tyrosine

PAFAH1B1 is required for microtubule organisation, nuclear translocation, and neuronal positioning.

Homodimerisation of the N-terminal portion of PAFAH1B1 containing the LisH motif and a coiled-coil region is required for its biological activity. The mutant PAFAH1B1 protein is no longer able to bind PAFAH1B2 and studies in mice lacking the LisH region of PAFAH1B1 show a lissencephaly phenotype (Cahana et al., 2001). More recently, the LisH motif has been shown to affect protein turnover and cellular localisation as mutations to the PAFAH1B1 LisH motif resulted in a significantly reduced protein half-life and localisation of PAFAH1B1 to actin filaments rather than the cytoplasm (Gerlitz et al., 2005).

The LisH motif is also present in other proteins that are implicated in human neural developmental disorders including transducin β-like 1X (TBL1X) which is implicated in ocular albinism with late-onset sensorineural deafness and oral-facial-digital syndrome type I (OFD1) protein (Bassi et al., 1999; Ferrante et al., 2001). TBL1X and PAFAH1B1 contain WD40 repeat-containing β-propeller domains following the LisH motif whilst the OFD1 protein has several coiled-coil domains following the LisH motif. Other characterised human proteins containing a LisH motif include the ataxia-telangiectasia locus protein (NPAT) and RAN-binding protein 9 (RANBP9 ; Letunic et al., 2006).

TBL1X is a nuclear protein involved in the recruitment of the ubiquitin/19S proteasome complex to nuclear receptor-regulated transcription units. It plays an essential role in transcriptional activation mediated by nuclear receptors and is an integral component of the nuclear receptor co-repressor 1-histone deactylase 3 (NCOR-HDAC3) complex (Perissi et al., 2004; Zhang et al., 2002). Interaction between TBL1X and NCOR occurs through the N-terminal domain of TBL1X encompassing the LisH motif, which is also required for TBL1X binding to histones H2B and H4 (Yoon et al., 2003). Characterised mutations within the LisH motif of TBL1X result in the protein no longer localising to the nucleus (Gerlitz et al., 2005).

OFD1 syndrome is an X-linked dominant male lethal disease that in females is characterised by malformations of the hands, face and skull, and mental retardation (Ferrante et al., 2001). OFD1 localises to the centriole of the cell and is a core component of the centrosome throughout the cell cycle where it is believed to be involved in the differentiation of metanephric precursor cells and microtubule organisation and assembly (Keller et al., 2005; Romio et al., 2004). It is widely expressed during development in the metanephros, brain, tongue, limbs and during mesenchymal-epithelial transition associated with nephrogenesis (Romio et al., 2004; Romio et al., 2003). Recent studies in *OFD1* knock-out mice show failure of left-right axis specification in mutant male embryos in addition to impaired patterning of the neural tube and altered expression of the 5' *Hoxa* and *Hoxd* genes in the limb buds (Ferrante et al., 2006). Mutations of the LisH motif in *OFD1* result in aberrant OFD1 protein localisation to the Golgi apparatus and in some cases the nucleus (Gerlitz et al., 2005).

The nuclear protein NPAT is a ubiquitously expressed housekeeping gene that promotes cell cycle progression through histone H4 gene regulation at the G1/S phase cell cycle transition (Imai et al., 1996; Ye et al., 2003). Apart from the LisH motif, NPAT has no other domains, but unlike PAFAH1B1, TBL1X and OFD1, point mutations in the LisH motif of NPAT do not affect its localisation to nuclear Cajal bodies but instead block histone H4 transcriptional activity (Wei et al., 2003).

RANBP9 is a protein of 729 amino acids that is identical in sequence within the first 500 amino acids of the human, mouse and hamster proteins and shares 96% sequence similarity overall between the human and mouse proteins (Nishitani et al., 2001). RANBP9 has 4 protein-protein interaction motifs including a splA RyR (SPRY) domain, originally identified in mammalian ryanodine receptor proteins (Ponting et al., 1997) that is a protein-interacting module which recognises a specific individual partner protein based on protein conformation rather than a consensus sequence motif (Wei et al., 2003). Similar to FLJ22318, RANBP9 also contains a LisH motif, a CTLH domain and a C-terminal CRA domain (Menon et al., 2004).

RANBP9 is a multi-functional protein that is found in both the cytoplasm and nucleus of the cell, and in association with the plasma membrane when phosphorylated (Denti et

al., 2004; Nishitani et al., 2001). It has been shown to activate the Ras/Erk signalling pathway by binding and up-regulating MET, a protein that is overexpressed in many human cancers leading to enhanced cell motility and tumour invasion (Wang et al., 2002). In addition, RANBP9 has also been shown to bind and up-regulate both the androgen receptor (AR) and the glucocorticoid receptor (GR) in the presence of their ligands when transiently over expressed in prostate cancer cell lines (Rao et al., 2002). Conversely, RANBP9 binds and inhibits the co-activators, dual-specificity tyrosine phosphorylation-regulated kinases 1A (Dyrk1A) and Dyrk1B that are involved in epithelial cell migration (Zou et al., 2003) and increases the proapoptotic activity of p73 by inhibiting its ubiquitination (Kramer et al., 2005). The binding of RANBP9 to MET, AR and GR was found to occur through the SPRY domain whereas the transcriptional inhibition of Dyrk1A and Dyrk1B required both the SPRY domain and the LisH motif (Zou et al., 2003).

The CTLH domain is also predicted to be an α-helical domain that is found adjacent to the LisH motif in a number of proteins but is also found in some proteins in the absence of the LisH motif. This domain does not occur in archaea, bacteria or viruses and is found only in eukaryotes where the motif is present in all metazoans, indicating evolutionary conservation (Letunic et al., 2006). The function of the CTLH domain has not yet been characterised. Of the 326 proteins listed in the simple modular architecture research tool (SMART) database (Schultz et al., 1998) that contain a CTLH domain, only one which contains just this domain has been characterised and this is the proposed FLJ22318 orthologue, RMD5 from *S. cerevisiae*. RMD5 functions as a negative regulator of gluconeogenesis and is required for the proteasome-dependent catabolite degradation of fructose-1,6-bisphosphatase (FBPase) where it is specifically required for the ubiquitination of FBPase (Regelmann et al., 2003). Interestingly, yeast nutritional starvation induces sporulation and meiosis, and RMD5 has also been shown to be an *IME1* inducible protein that is essential for sporulation and meiotic nuclear division (Enyenihi and Saunders, 2003). Recently it has been shown that α-helical coiled-coil segments following the LisH motif are required for protein stability and that this region is necessary for an open or supercoiled conformation of the protein. It has been suggested that these coiled-coil segments in conjunction with LisH motifs have an

important biological activity and that the CTLH domain may have a similar function (Mateja et al., 2006).

The CRA domain was initially identified in RANBP9 as a C-terminal protein-protein interaction domain required for binding to the fragile X mental retardation 1 protein (FMR1). Fragile X syndrome is characterised by moderate to severe mental retardation, macroorchidism, large ears, prominent jaw, and high-pitched jovial speech with mental retardation being the most common feature (Mandel and Biancalana, 2004). This syndrome is associated with mutations in the *FMR1* gene with affected individuals having reduced FMR1 protein expression which has recently been shown to result in the early and abnormal differentiation of neuronal stem cells (Castren et al., 2005; Tassone and Hagerman, 2003). In unaffected individuals, neurons, dividing epithelial tissues and spermatogonia in adult testis show the highest levels of FMR1 expression while glial cells contain very low levels (Devys et al., 1993). Within the cell, FMR1 functions as a translational repressor RNA-binding protein that forms a messenger ribonucleoprotein complex that shuttles between the cytoplasm and nucleus of cells (Laggerbauer et al., 2001; Tamanini et al., 1999). Binding of RANBP9 to FMR1 was shown to modulate FMR1 binding to RNA. As the CRA domain of RANBP9 was able to significantly decrease the binding of the MAP1B RNA, an RGG box-binding partner of FMR1, it would suggest that RANBP9 functions as an RGG box-binding protein through its CRA domain (Menon et al., 2004).

The function of the hypothetical protein FLJ22318 is unknown and initial studies in this thesis sought to use bioinformatics analysis of its gene and protein sequences in order to characterise structural features of FLJ22318 that may be useful for investigating its biological activity.

4.2 Results

4.2.1 *FLJ22318* Gene Structure

The *FLJ22318* gene as annotated in the NCBI Entrez Gene database (Gene ID 64777) spans 17.4 kilo base pairs (kb) of genomic DNA with an ORF encoded by 11 exons and 10 introns. Examination of the FLJ22318 sequence demonstrates that all introns have 5'-GT and 3'-AG splice donor and acceptor sites. Transcription of the *FLJ22318* gene

produces a mRNA transcript of 1825bp comprising a 180bp 5' untranslated region (UTR), 1182bp coding region and 464bp 3' UTR and encodes a protein of 393 amino acids (Reference Sequence NP_073599). The start methionine of the 393 amino acid protein is within exon 3, with the stop codon in exon 11 (Figure 4.3).

According to AceView however, alternative splicing of this gene can produce 16 transcript variants (Figure 4.4) putatively encoding 14 different protein isoforms (Table 4.1; Thierry-Mieg et al., 2005). The NCBI published sequence (Accession No. NM_022762), differs in transcript size to the AceView data, although variants b, c and d all encode a protein of 393aa with a molecular weight of 44.4kDa as nucleotide differences are confined to the UTRs and do not affect the translated amino acid composition. Transcript variants a, e, f, g, h, i, j, k, l, m and o all encode putative proteins that contain portions of the 393aa reference sequence, although transcript variants a, h, i and o also comprise additional amino acid sequences. Transcript variants n and p are proposed to encode proteins of 103 and 77aa that are completely different to the reference sequence. Interestingly, several of the proposed FLJ22318 isoforms may localise to the nucleus of the cell (Table 4.1) whilst the remainder are proposed to be cytoplasmic.

4.2.1.1 Mammalian Gene Homologues of *FLJ22318*

A search of the NCBI HomoloGene database (www.ncbi.nlm.nih.gov/entrez/query.fcgi?db=homologene) revealed the presence of mammalian *FLJ22318* gene homologues for the chimpanzee, mouse, rat and dog. Sequence alignment of the genes from these species against human *FLJ22318* indicated that there is more than 80% nucleotide homology between these species within the coding exons. There is less homology evident within the 5' and 3'-UTRs of the genes, although immediately prior to the translation start site and following the stop codon there are segments of 5-7 homologous nucleotides that have been conserved and these may represent regulatory regions (Figure 4.5).

Further evidence of a common ancestral gene comes from analysis of the genomic sequences for these 5 species based on a phylogenetic hidden Markov model (phastCons). The phastCons program computes conservation scores based on a type of probabilistic model that describes both the process of DNA substitution at each site in a

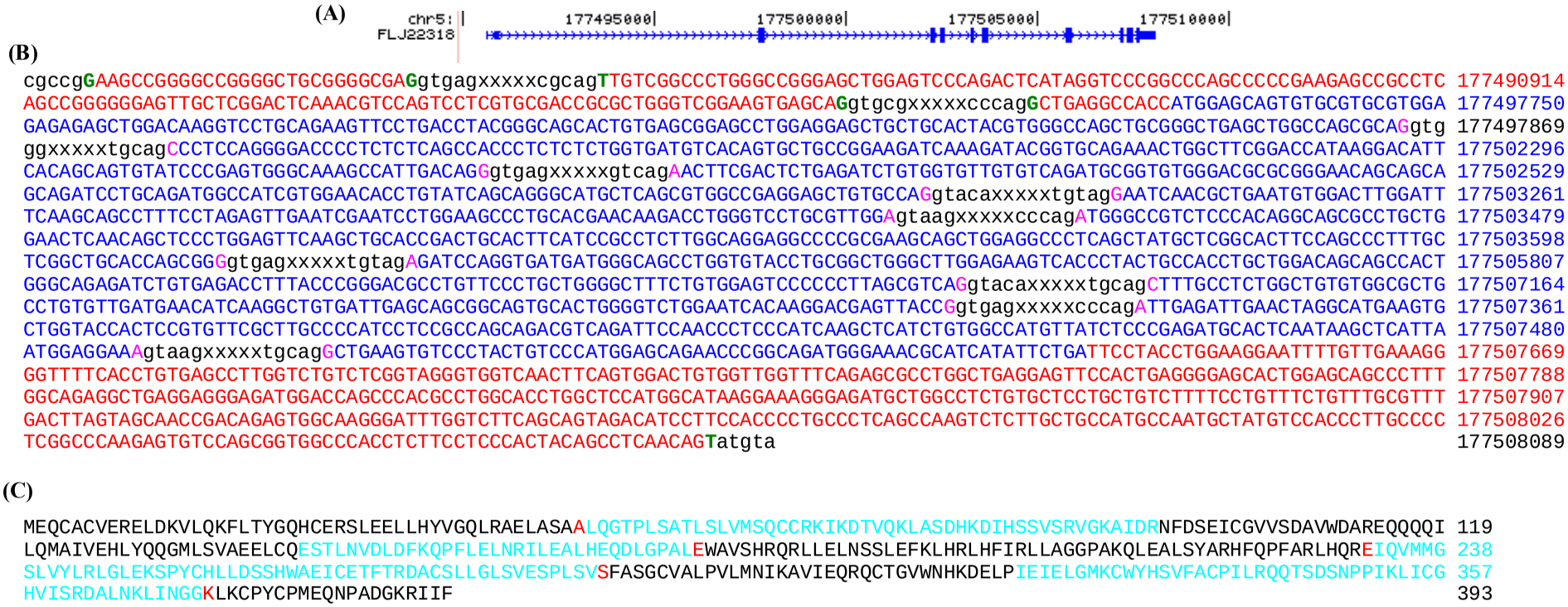

Figure 4.3 Genomic organisation of *FLJ22318*. **(A)** The *FLJ22318* gene spans 17.4kb of genomic DNA on chromosome 5q35.3: 177490634-177508084 and has an ORF divided between 11 exons and 10 introns. **(B)** Alignment of *FLJ22318* with the genomic sequence (black) demonstrates that all introns have 5'-GT and 3'-AG splice donor and acceptor sites (pink:coding or green:UTR) and produces a mRNA transcript of 1825bp comprising 1182bp coding region (dark blue), 180bp 5'-UTR and 464bp 3'-UTR (red) with the start ATG codon within exon 3 and the stop TGA codon in exon 11. **(C)** FLJ22318 protein of 393aa indicating exons 3 to 11 that comprise the coding region (alternating black:blue) and the amino acids that are encoded across a splice junction (red).

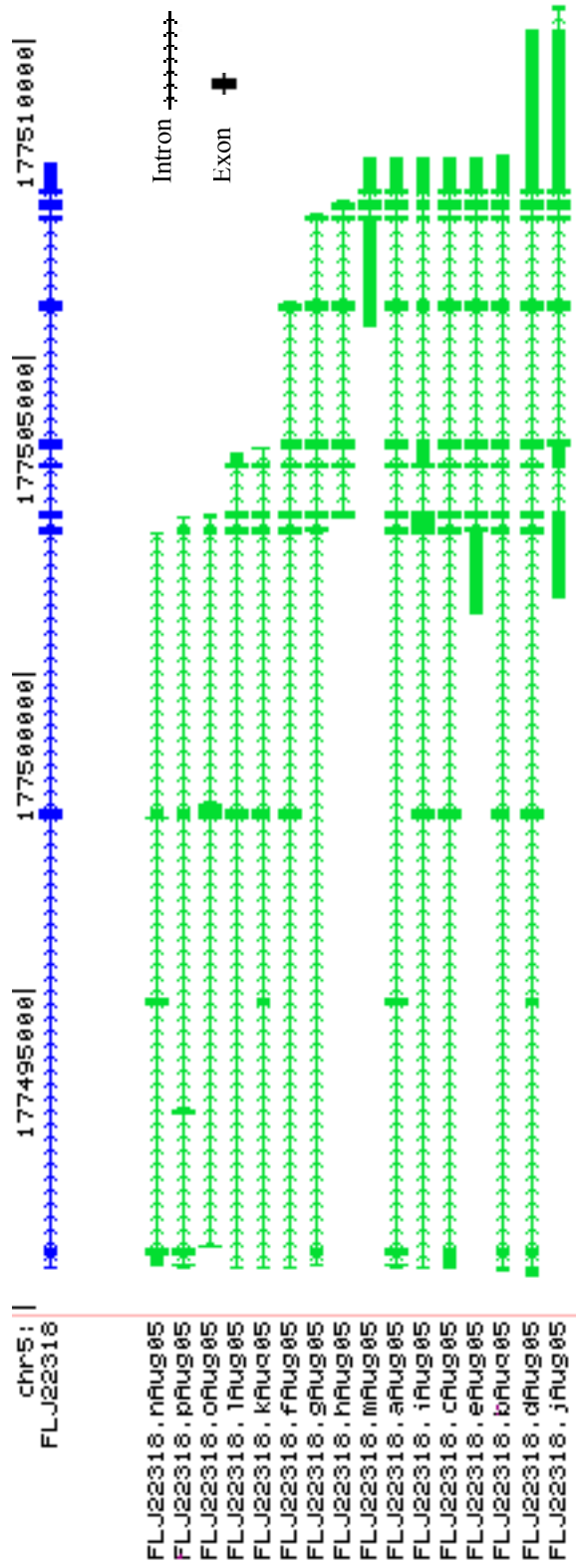

Figure 4.4 Proposed alternatively spliced transcripts of FLJ22318. Alignment of the alternatively spliced transcripts of FLJ22318 (green) as proposed by AceView in relation to the FLJ22318 reference sequence (blue) as published by NCBI (NM_022762; Adapted from http://genome.ucsc.edu/cgi-bin/hgTracks).

Table 4.1 AceView proposed transcript and protein variants of FLJ22318

AceView Transcript Variant	Genomic DNA (kb)	mRNA (bp)	5′ UTR (bp)	3′ UTR (bp)	Exons	Introns	Protein (aa)	MW (kDa)	Predicted Subcellular Location[iv]
aAug05	17.54	1884	32	517	11	10	444	49.4	Nucleus
bAug05	17.59	1945	218	545	11	10	393	44.4	Cytoplasm
cAug05	17.53	2067	364	521	10	9	393	44.4	Cytoplasm
dAug05	19.67	4170	455	2533	12	11	393	44.4	Cytoplasm
eAug05	7.23	2820	1284	534	8	7	333	37.7	Cytoplasm
fAug05	15.25	894	52	Truncated	7	6	280	31.8	Cytoplasm
gAug05	16.58	961	183	Truncated	8	7	259	29.4	Cytoplasm
hAug05	5.01	810	Truncated	Truncated	6	5	269	30.6	Cytoplasm
iAug05	17.54	2092	56	1383	8	7	217	24.4	Cytoplasm
jAug05	9.35	4988	1749	2611	7	5	209	23.5	Cytoplasm
kAug05	12.94	733	193	Truncated	7	6	180	20.2	Cytoplasm
lAug05	12.89	760	41	188	5	4	176	19.8	Cytoplasm
mAug05	2.68	2501	1971	42	3	2	95	10.8	Nucleus
nAug05	11.59	676	155	209	4	3	103	10.8	Nucleus
oAug05	11.60	555	Truncated	272	4	3	93	10.4	Cytoplasm
pAug05	11.89	653	29	390	6	5	77	7.9	Nucleus

[iv] Nakai, K. *PSORT II analysis.* http://psort.nibb.ac.jp, (Accessed 23.02.06)

```
CLUSTAL W (1.82) multiple sequence alignment
H. sapiens      ----------------------------------------------------------------------------------------------------
P. troglodytes  ----------------------------GAGGGCGGGCACAGCGGCCGGCGGAGCTGAGGCGCGCGGCGGGGAAAGCTCGGCCGGCCTCCCGGGCCCCAGC 73
M. musculus     GAACGATTCATTCGGCATTCCTTGCAAAGCCGCGGGCGAGACACACTGTCTCCCCACGCTCCGCGACACCACGCATGGGCGAGCCCGGACCCACCCGAGA 100
R. norvegicus   GAACGATTCATTCGGCATTCCATGCAAAGCCGCGGGCGAGGCAGACGGTCTCCCCACGCTCCGCGACACGGCGCATGGGCGAGCCCGGACCCACCCGAGG 100
C. familiaris   ----------------------------------------------------------------------------------------------------

H. sapiens      ----------------------------------------GAAGCCGGGGCCGGGGCTG--CGGGGCG---AGTTGTCGGCCCTGGG--CCGGGAGCTG 52
P. troglodytes  CTTCTCCAGAACCCCTGCTACCCACGACTAAGCC--CCGAACAATCTGCCCTTGGGCTTGTTCTCTTCGC--AGTTGTCGGCCCTGGG--CCGGGAGCTG 167
M. musculus     GGCAACCGCCGCGCCTTCCGGTTCCGATGACAGCGGCGCCGGAAGCGGGCTGAGCTGCAAGACTAGGTGACAGCCTGCCGGCTCCCGGTCCCGGGGTGCG 200
R. norvegicus   GGCAACCGCCGCGCCTTCCGGTTCCGATGACAGCGGCGCCGGAAGCCGGCTGGGCTGCAAGACTAGGTGACAGCCTGTGAGCTCCGGGTACCGGGGTGCG 200
C. familiaris   ------------------AAGTGGATGCACCATTTAATCAGCAAGCATTGGCTGAACACACACTGTGGACCAGGCCGTAGGCTGCGCGCTGTGGGGAGAG 82
                                                ** *       *        *             *   **     *    ***     *

H. sapiens      GAGTCCCAGACTCATAGGTCCCGGCCCAGCCCCCGA--AGAGCCGCCTCAGCCGGGGGGAGTTGCTCGGACTCAAACGTCCAGTCCTCGTGCGACCGCGC 150
P. troglodytes  GAGTCCCAGACTCATAGGTCCCGGCCCAGCCCCCGA--AGAGCCGCCTCAGCCGGGGGGAGTTGCTCGGACTCAAACGTCCAGTCCTCGTGCGACCGCGC 265
M. musculus     GGGCGCCCCGACCAAAG--CCTGGAGCAGTCGTCGGCCACACCCTCCAAGGGCTGGTGGAGTCGCCCGGACTCCGACGTCCCGTCCTAGTGC-ACCTGAC 297
R. norvegicus   GGGCGCCCCGACCAAAG--CCTGGAGAAATTGTCGGCCACACCCTCCAAGGGCTGGTGGAGTCGCCCGGACTCAGACGTCCCATTTTAGTGC-ACCTGAC 297
C. familiaris   AGAGGACAAGAC--TGGTCTCTAGCCCTGA-ACTGCTCACCGTCTC-----GTTGGGGGAG--ACCTGAAGACAGAC----AGTTATTGTGCCACCGTGC 168
                      *        *   *  *          *   *    * *       ** ****   *  * *  *  **      *  * **** ***   *

H. sapiens      TGGGTCGGAAG----------------------------TGAGCAGGCTGAGGCCACCATGGAGCAGTGTGCGTGCGTGGAGAGAGAGCTGGACAAGGTCC 223
P. troglodytes  TGGGTCGGAAG----------------------------TGAGCAGGCTGAGGCCACCATGGAGCAGTGTGCGTGCGTGGAGAGAGAGCTGGACAAGGTCC 338
M. musculus     TGAGTCAGAGGATCCACACTGGCCTGACCCAGTTGACATCACCAGGCAGAGGCCGCCATGGAGCAGTGTGCCTGTGTGGAGAGGGAGCTGGACAAGGTCC 397
R. norvegicus   TGGGTCAGAGGATCCACACTGGCCTAATCCAGTTGACATCACTAGGCAGAGGCCACCATGGAGCAGTGCGCATGTGTGGAGAGGGAGCTCGACAAGGTCC 397
C. familiaris   CAAG---GACT-------------------------------CAGGCAGAGGCCACAATGGAGCAGTGTGCAAGTGTGGAGAGAGAGGTGGACAAGGTCC 234
                   *   **                                 **** ****** * ********** **  * ******** *** * **********

H. sapiens      TGCAGAAGTTCCTGACCTACGGGCAGCACTGTGAGCGGAGCCTGGAGGAGCTGCTGCACTACGTGGGCCAGCTGCGGGCTGAGCTGGCCAGCGCAGCCCT 323
P. troglodytes  TGCAGAAGTTCCTGACCTACGGGCAGCACTGTGAGCAGAGCCTGGAGGAGCTGCTGCACTACGTGGGCCAGCTGCGGGCTGAGCTGGCCAGCGCAGCCCT 438
M. musculus     TGCACAAGTTCCTAACCTACGGGCAGCATTGCGAGCAGAGTCTGGAGGAGCTGCTGCACTCCGTGGGCCAGCTGAGAGCCGAGCTGGCCAGTGCAGCTCT 497
R. norvegicus   TGCACAAGTTCCTGACCTATGGGCAACATTGTGAGCAGAGCCTGGAGGAGCTGCTGCACTACGTGGGCCAGTTGAGAGCTGAACTGGCCAGTGCAGCTCT 497
C. familiaris   TGCAGAAGTTCCTGACCTATGGGCAACACTGTGAGCAGAGCTTGGAGGAGCTGCTGCGTTACGTGGGCCAGCTGCGGGCTGAGCTGGCTGGAACAGCCCT 334
                **** ******** ***** ***** ** ** **** ***  ***************  * ********** ** * ** ** *****  *  ***** **

H. sapiens      CCAGGGGACCCCTCTCTCAGCCACCCTCTCTCTGGTGATGTCACAGTGCTGCCGGAAGATCAAAGATACGGTGCAGAAACTGGCTTCGGACCATAAGGAC 423
P. troglodytes  CCAGGGGACCCCTCTTTCAGCCACCCTCTCTCTGGTGATGTCACAGTGCTGCCGGAAGATCAAAGATACGGTGCAGAAACTGGCTTCGGACCATAAAGAC 538
M. musculus     CCAGGGCACCCCTCTCTCAGCCACGCTGTCCCTTGTGATGTCCCAGTGCTGTCGGAAGATCAGAGACACAGTCCAGAAACTGGCTTCCGACCATAAGGAC 597
R. norvegicus   CCAGGGGACCCCTCTCTCAGCCACGCTGTCCCTAGTAATGTCCCAGTGCTGTCGGAAGATCAAAGACACAGTCCAGAAGCTGGCTTCCGACCATAAGGAC 597
C. familiaris   CCAGGGGACCCCTCTGTCAGCCACCCTCTCCCTGGTGATGTCTCAGTGCTGCCGGAAGATCAAAGACACCGTGCAGAAACTGGCTTCAGACCACAAGGAC 434
                ****** ******** ******** ** ** ** ** ***** ******** ********** *** ** ** ***** ******** ***** ** ***
```


H. sapiens ATTCACAGCAGTGTATCCCGAGTGGGCAAAGCCATTGACAGGAACTTCGACTCTGAGATCTGTGGTGTTGTGTCAGATGCGGTGTGGGACGCGCGGGAAC 523
P. troglodytes ATTCACAGCAGTGTATCCCGAGTGGGCAAAGCCATTGACAGGAACTTCGACTCTGAGATCTGTGGTGTTGTGTCAGATGCGGTGTGGGACGCGCGGGAAC 638
M. musculus ATTCACAGCAGCGTCTCTCGAGTGGGCAAAGCCATTGACAGGAACTTCGACTCTGAGATCTGCGGCGTGGTCTCGGATGCTGTGTGGGACTCCCGTGAGA 697
R. norvegicus ATTCACAGCAGCGTCTCCCGAGTGGGCAAAGCCATTGACCGGAACTTTGACTCTGAGATCTGCGGCGTGGTCTCAGATGCTGTGTGGGACTCCCGTGAGA 697
C. familiaris ATACACAGCAGTGTCTCCCGAGTGGGCAAAGCCATTGACAGGAACTTCGACTCTGAGATCTGCGGAGTGGTCTCTGATGCAGTGTGGGACTCACGGGAGA 534
H. sapiens AGCAGCAGCAGATCCTGCAGATGGCCATCGTGGAACACCTGTATCAGCAGGGCATGCTCAGCGTGGCCGAGGAGCTGTGCCAGGAATCAACGCTGAATGT 623
P. troglodytes AGCAGCAGCAGATCCTGCAGATGGCCATCGTGGAACACCTGTACCAGCAGGGCATGCTCAGCGTGGCCGAGGAGCTGTGCCAGGAATCAACACTGAATGT 738
M. musculus AGCAGCAGCAGATCCTGCAGATGGCCATCGTAGAGCACCTGTACCAGCAAGGCATGCTCAGTGTAGCGGAGGAGCTGTGCCAGGAATCGACATTGAATGT 797
R. norvegicus AGCAGCAGCAGATCCTGCAGATGGCCATTGTCGAGCACCTGTACCAGCAGGGCATGCTCAGCGTAGCTGAGGAGCTGTGCCAGGAATCAACATTGAATGT 797
C. familiaris AGCAGCAGCAGATCCTGCAGATGGCCATCGTGGAGCACCTGTATCAGCAGGGCATGCTTAGCGTTGCCGAGGAGCTGTGCCAGGAATCAACACTGAATGT 634
H. sapiens GGACTTGGATTTCAAGCAGCCTTTCCTAGAGTTGAATCGAATCCTGGAAGCCCTGCACGAACAAGACCTGGGTCCTGCGTTGGAATGGGCCGTCTCCCAC 723
P. troglodytes GGACTTGGATTTCAAGCAGCCTTTCCTAGAGTTGAATCGAATCCTGGAAGCCCTGCACGAACAAGACCTGGGTCCTGCGTTGGAATGGGCCGTCTCCCAC 838
M. musculus GGACCTGGACTTCAAGCAGCCCTTCTTGGAGTTGAATCGGATCTTGGAAGCTCTGCACGAGCAAGACCTAGGACCTGCGCTGGAATGGGCTGTATCTCAC 897
R. norvegicus GGACCTGGACTTCAAGCAGCCCTTCTTGGAGTTGAATCGGATCTTGGAGGCTCTGCATGAGCAAGACCTAGGACCTGCACTGGAATGGGCCGTTTCCCAC 897
C. familiaris GGACTTGGACTTTAAGCAGCCTTTCCTCGAGTTGAATCGAATCCTGGAAGCTCTGCACGAACAAGACCTAGGGCCAGCACTGGAATGGGCCGTCTCCCAC 734
H. sapiens AGGCAGCGCCTGCTGGAACTCAACAGCTCCCTGGAGTTCAAGCTGCACCGACTGCACTTCATCCGCCTCTTGGCAGGAGGCCCCGCGAAGCAGCTGGAGG 823
P. troglodytes AGGCAGCGCCTGCTGGAACTCAACAGCTCCCTGGAGTTCAAGCTGCACCGACTGCACTTCATCCGCCTCTTGGCAGGAGGCCCCGCGAAGCAGCTGGAGG 938
M. musculus AGGCAGCGCCTGCTGGAGCTCAACAGCTCGCTGGAGTTCAAGCTGCACCGGCTGCACTTTATCCGCCTCCTAGCTGGGGGCCCCGAGAAGCAGCTGGAGG 997
R. norvegicus AGGCAGCGCCTGCTGGAGCTCAACAGCTCACTGGAGTTCAAGCTGCACCGGCTGCACTTTATCCGCCTCCTAGCTGGTGGCCCGGAGAAGCAGCTGGAGG 997
C. familiaris AGGCAGCGCCTGCTCGAGCTCAACAGCTCCCTAGAGTTCAAGCTGCACCGCCTACACTTTATCCGCCTCCTGGCCGGTGGCCCTGAGAAGCAGCTGGAGG 834
H. sapiens CCCTCAGCTATGCTCGGCACTTCCAGCCCTTTGCTCGGCTGCACCAGCGGGAGATCCAGGTGATGATGGGCAGCCTGGTGTACCTGCGGCTGGGCTTGGA 923
P. troglodytes CCCTCAGCTATGCTCGGCACTTCCAGCCCTTTGCTCGGCTGCACCAGCGGGAGATCCAGGTGATGATGGGCAGCCTGGTGTACCTGCGGCTGGGCTTGGA 1038
M. musculus CCCTCAGCTATGCTCGGCACTTCCAGCCTTTTGCTAGGCTACACCAGAGAGAGATCCAGGTGATGATGGGCAGTCTGGTGTACCTGCGGCTGGGCTTGGA 1097
R. norvegicus CCCTCAGCTATGCCCGACACTTCCAGCCTTTTGCTCGGCTACACCAGAGAGAGATCCAGGTGATGATGGGCAGTCTGGTGTACCTGCGGCTGGGCTTGGA 1097
C. familiaris CCCTCAGCTACGCTCGGCACTTTCAGCCCTTTGCGCGGCTGCACCAGCGAGAGATCCAGGTGATGATGGGCAGTCTGGTGTACCTGCGGCTGGGCTTGGA 934
H. sapiens GAAGTCACCCTACTGCCACCTGCTGGACAGCAGCCACTGGGCAGAGATCTGTGAGACCTTTACCCGGGACGCCTGTTCCCTGCTGGGGCTTTCTGTGGAG 1023
P. troglodytes GAAGTCACCCTACTGCCACCTGCTGGACAGCAGCCACTGGGCAGAGATCTGTGAGACCTTTACCCGGGACGCCTGTTCCCTGCTGGGGCTTTCTGTGGAG 1138
M. musculus GAAGTCACCCTACTGCCACCTCTTAGACAACAGCCACTGGGCGGAGATCTGTGAGACCTTTACTCGGGATGCATGCTCCCTCCTGGGACTTTCAGTGGAG 1197
R. norvegicus GAAGTCACCCTACTGCCACCTCTTAGACAACAGCCACTGGGCAGAGATCTGTGAGACCTTTACTCGGGATGCATGCTCCCTCCTGGGGCTTTCAGTGGAG 1197
C. familiaris GAAGTCACCCTACTGCCATCTCCTGGACAATAGCCATTGGGCAGAGATCTGTGAGACCTTCACCCGGGACGCTTGCTCCCTGCTGGGGCTTTCTGTAGAG 1034


H. sapiens TCCCCCCTTAGCGTCAGCTTTGCCTCTGGCTGTGTGGCGCTGCCTGTGTTGATGAACATCAAGGCTGTGATTGAGCAGCGGCAGTGCACTGGGGTCTGGA 1123
P. troglodytes TCCCCCCTTAGCGTCAGCTTTGCCTCTGGCTGTGTGGCGCTGCCCGTGTTGATGAACATCAAGGCTGTGATTGAGCAGAGGCAGTGCACTGGGGTCTGGA 1238
M. musculus TCCCCACTTAGTGTCAGCTTCGCGTCTGGCTGTGTGGCGCTGCCCGTGCTGATGAACATTAAAGCTGTGATCGAACAGAGGCAGTGCACTGGGGTGTGGA 1297
R. norvegicus TCCCCACTCAGTGTCAGCTTTGCTTCTGGCTGTGTGGCACTGCCAGTGCTGATGAACATTAAAGCTGTGATCGAACAGAGGCAGTGCACTGGAGTGTGGA 1297
C. familiaris TCCCCCCTCAGCGTCAGCTTTGCCTCTGGCTGTGTGGCGCTGCCTGTGCTGATGAACATCAAAGCTGTGATTGAGCAGAGGCAGTGCACGGGGGTCTGGA 1134
ATCACAAGGACGAGTTACCGATTGAGATTGAACTAGGCATGAAGTGCTGGTACCACTCCGTGTTCGCTTGCCCCATCCTCCGCCAGCAGACGTCAGATTC 1223
P. troglodytes ATCACAAGGACGAGTTACCGATTGAGATTGAACTAGGCATGAAGTGCTGGTACCACTCCGTGTTCGCTTGCCCCATCCTCCGCCAGCAGACGTCAGATTC 1338
M. musculus GTCACAAGGATGAGTTGCCGATTGAGATAGAGCTGGGCATGAAGTGCTGGTACCACTCAGTGTTTGCATGCCCTATCCTGCGACAGCAGACCTCAGATTC 1397
R. norvegicus GTCACAAGGATGAGTTGCCGATTGAGATTGAGCTGGGCATGAAGTGCTGGTATCACTCTGTGTTTGCGTGCCCTATCCTGCGACAGCAGACCTCAGATTC 1397
C. familiaris GTCACAAGGACGAGTTACCGATTGAGATCGAACTCGGCATGAAGTGCTGGTACCACTCAGTGTTCGCATGCCCCATCCTCAGGCAGCAGACGTCAGATTC 1234
CAACCCTCCCATCAAGCTCATCTGTGGCCATGTTATCTCCCGAGATGCACTCAATAAGCTCATTAATGGAGGAAAGCTGAAGTGTCCCTACTGTCCCATG 1323
P. troglodytes CAACCCTCCCATCAAGCTCATCTGCGGCCATGTTATCTCCCGAGATGCACTCAATAAGCTCATTAATGGAGGAAAGCTGAAGTGTCCCTACTGTCCCATG 1438
M. musculus CAACCCCCCCATCAAGCTCATCTGTGGCCACGTCATCTCCAGAGATGCACTCAACAAACTCATCAATGGAGGAAAGCTAAAGTGTCCCTACTGTCCCATG 1497
R. norvegicus CAACCCCCCTATCAAGCTCATCTGTGGCCACGTCATCTCCAGAGATGCACTCAACAAGCTCATCAATGGAGGAAAGCTAAAGTGTCCCTATTGTCCCATG 1497
C. familiaris CAACCCTCCCATCAAGCTCATATGTGGCCACGTTATCTCGCGGGATGCACTCAACAAGCTCATTAATGGAGGAAAGCTGAAGTGTCCCTACTGTCCCATG 1334
GAGCAGAACCCGGCAGATGGGAAACGCATCATATTCTGATTCCTACCTGGAAGGAATTTTGTTGAAAGGGGTTTTCACCTGTGAGCCTTGGTCTGTCTCG 1423
P. troglodytes GAGCAGAACCCGGCAGATGGGAAACGCATCATATTCTGATTCCTACCTGGAAGGAATTTTGTTGAAAGGGGTTTTCACCTGTGAGCCTTGGTCTGTCTCG 1538
M. musculus GAACAGAATCCAGCAGATGGGAAACGCATCATATTCTGATTCC-------AAGGAACATTCTAGAAGGTGTAATCCACCCATGGGCCTTTGT-------- 1582
R. norvegicus GAGCAGAACCCAGCAGATGGGAAACGTATCATATTCTGATTCC-------AAGGAACATTTTAGAAGGTGTAATCCACCCATGGGCCTTTGT-------- 1582
C. familiaris GAGCAGAACCCAGCAGATGGGAAACGCATCATATTCTGATACCTGCTCGGGATGAACTTTGTCAGAGGGGTTTCCCACCTATGAGCTGTGGTCTGTCTTG 1434
GTAGG-GTGGTCAACTTCAGTGGACTGTGGTTGGTTTCAGAGCGCCTGGCTGAGGAGTTCCACTGAGGGGAGCACTGGAGCAGCCCTTTGGCAGAGGCTG 1522
P. troglodytes GTAGG-GTGGTCAACTTCAGTGGACTGTGGTTGGTTTCAGAGCGCCTGGCTGAGGAGTTCCACTGAGGGGAGCACTGGAGCAGCCCTTTGGCAGAGGCTG 1637
M. musculus --GGA-GGGACTGGCTTCAGCAGACTGTGATGCCTCTCAGACCAGCATTACCAAGAGACCCAACCTG----------CCTAGGCAGAGGCCA 1661
R. norvegicus --GGA-GGGACTGGCTTCAGCAGACTGTGATGCCTTTCAGACCAGCATTACCAAGAGACCCAACCTG----------CCCAGGCAGAGGCCA 1661
C. familiaris GTGGGCGTGGCTGACTTCAG---ATTGTGGTTTGCTTCAGAGCAA-ATGACTGAGTGCCACCATGGGTAGAGG----------CCAAGAAAGGAGACA 1518
AGGAGGGAGATGG--ACCAGCCCACGCCTGGCACCTGGCTCCATGGCATAAGGAAAGGGAGATGCTGGCCTCTGTGCTCCTGCTGTCTTTTCCTGTTTCT 1620
P. troglodytes AGGAGGGAGATGG--ACCAGCCCACGCCTGGCACCTGGCTCCATGGCATAAGGAAAGGGAGATGCTGGCCTCTGTGCTCCTGCTGTCTCTTCCTGTTTCT 1735
M. musculus GGGAAGGCTGTGA--ACCAGCAGCCTATGCTTCCTTACCTTCTAGGGGGACTGGCTACTCTGTTCCTGCA----TTCTGTTTACACTTGCCCCTGACGGA 1755
R. norvegicus GGGAAGGTCTTGA--ACCAG---CCTATGCCACTTTACCTGTGAGGGGGACTGGCTGTTCTGTTCCTGCTGCCTTTCTGTTTACACTTGCCCCTGACTGA 1756
C. familiaris AACCAGTCTGTGATGGGCAGCTGGCTCCTTGGCTGGAAGGGTGGGAGACATGGGCCTCTGCACTCCTGGTGTT-TCCTGTTTATACCTGCCAGTGACTTG 1617

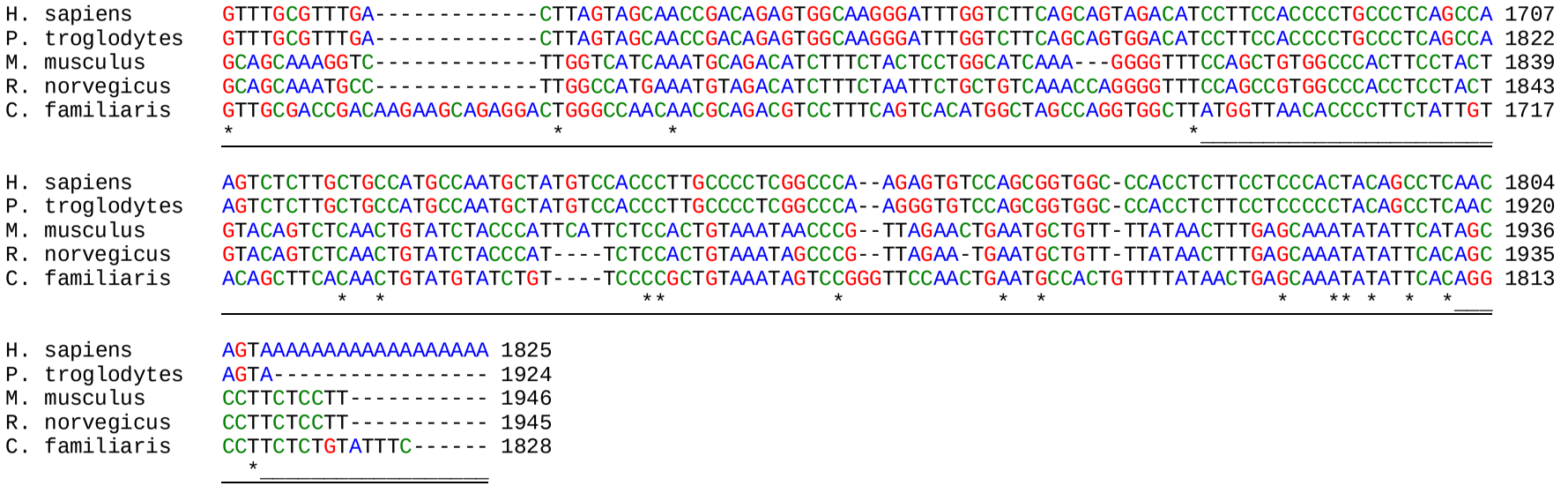

Figure 4.5 Sequence alignments of mammalian FLJ22318 mRNA. Alignment of mammalian FLJ22318 mRNA using CLUSTALW (Thompson et al., 1994) indicates a high degree of sequence conservation (star) between the different species within the coding exons (alternating black-red:coding-highlighted). All coding exons share more than 80% sequence homology with exons 2, 6, 8 sharing >85% and exon 9 >90% nucleotide conservation.

genome and the way this process changes from one site to the next (Siepel et al., 2005). Using this model it can be seen that there is conservation in the area immediately prior to the transcription start site (TSS) and within intronic regions of these genes, suggesting conservation of regulatory elements within these regions (Figure 4.6). In relation to the human gene, conserved regions can be observed in intron 2 prior to the translation start site as well as in introns 8, 9 and 10 and interestingly these conserved intronic regions correspond to the alternative splice variants as proposed in Figure 4.4. Furthermore, the alternative exon 1 proposed in splice variants e and j corresponds to conserved regions seen only in the human and chimpanzee genomes, suggesting that these transcripts may be specific for primates (Figure 4.6).

Comparison of the chromosomal locations of human *FLJ22318* with the homologous rat *LOC497900* and mouse *0610039K22Rik* genes demonstrates a high degree of chromosomal synteny including gene structure and transcript orientation (Figure 4.7). Both the rat and mouse genes are identical to one another in exon-intron structure and comprise 10 exons and 9 introns respectively. When compared to FLJ22318, the coding exons are completely conserved between all 3 genes and although mouse and rat exons 1 and 10 differ in length to human exons 1-3 and exon 11, these exons are conserved in size relative to the transcription start site and stop codon (Table 4.2). In addition to homology within FLJ22318, the syntenic regions of human, mouse and rat chromosomes that encompass the FLJ22318 orthologues also include Nedd4 binding protein 3 (N4BP3) proximally and nucleolar protein family A member 2 (NOLA2) and heterogenous nuclear ribonucleoprotein A/B (HNRPAB) distally (Figure 4.7).

4.2.1.2 Transcriptional Regulation of *FLJ22318* Expression

As the transcriptional regulation of *FLJ22318* is undetermined, and based on the previous analysis of genomic sequence homology (Figure 4.6), a 1366bp segment comprising 1000 bases upstream of the transcription start site (TSS) and the CpG island were examined for potential *cis*-regulatory factor binding sites using the programme MatInspector V6.0 (http://www.genomatix.de/matinspector) which contains 431 vertebrate matrices in 148 families and represents the largest publicly accessable library currently available (Cartharius et al., 2005). Forty three high quality ($\geq$0.90) potential transcription factor binding sites were identified, including 17 sites for genes belonging to the ANTP, PRD, TALE , SINE and POU homeobox classes. Of these 17 sites, 11

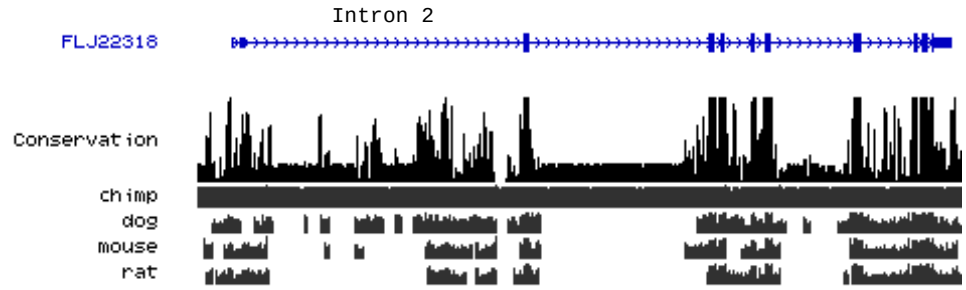

Figure 4.6 Comparison of genomic nucleotide conservation between mammalian homologues of FLJ22318. As well as the high degree of sequence homology observed within the exons, sequence homology can also be seen in genomic DNA immediately prior to the transcription start site and in intron 2 prior to the translation start site as well as in regions that correspond to alternative transcripts proposed for this gene (see Figure 4.4; Adapted from http://genome.ucsc.edu/cgi-bin/hgTracks).

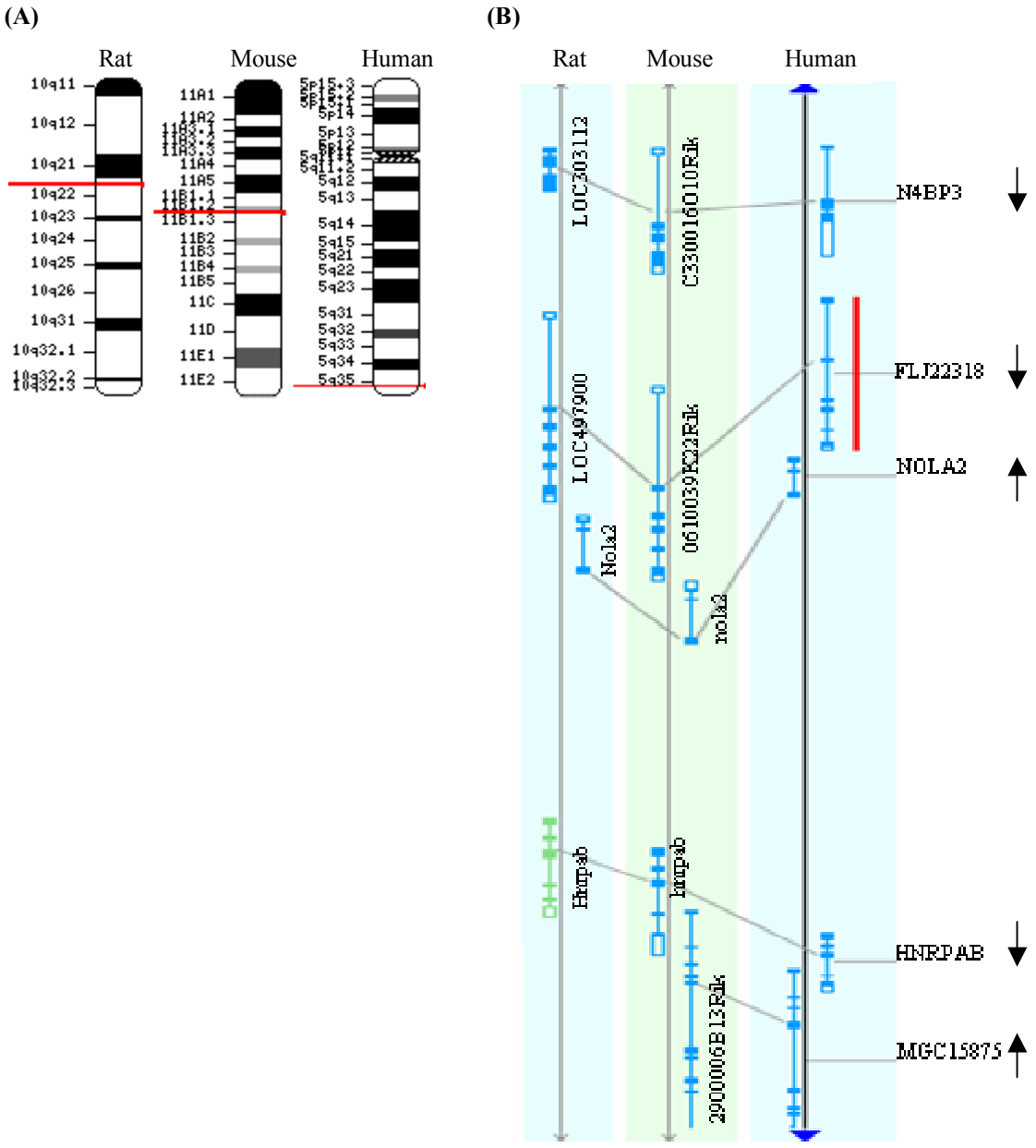

Figure 4.7 Analysis of the chromosomal localisation of FLJ22318 from the human, rat and mouse genomes. **(A)** Ideograms depicting the chromosomal localisation of human FLJ22318 to chromosome 5q35.3 and the rat and mouse homologues to chromosomes 10q21 and 11B1.2. **(B)** Schematic representation of the high degree of synteny demonstrated between human chromosome 5q35.3 to rat chromosome 10q21 and mouse chromosome 11B1.2 including the structure and orientation of transcripts for FLJ22318, N4BP3, NOLA2 and HNRPAB (Adapted from http://www.ncbi.nlm.nih.gov/mapview/maps.cgi).

Table 4.2 Comparison of gene structure between FLJ22318 and the rat and mouse homologues demonstrates that the coding exons are completely conserved between species.

Human FLJ22318			**Rat LOC497900**			**Mouse 0610039K22Rik**		
Exon	Length (bp)	Coding exon (bp)	Exon	Length (bp)	Coding exon (bp)	Exon	Length (bp)	Coding exon (bp)
1	28							
2	140		1	307		1	307	
3	151	139	2	186	139	2	186	139
4	146	146	3	146	146	3	146	146
5	141	141	4	141	141	4	141	141
6	101	101	5	101	101	5	101	101
7	167	167	6	167	167	6	167	167
8	166	166	7	166	166	7	166	166
9	103	103	8	103	103	8	103	103
10	155	155	9	155	155	9	155	155
11	509	64	10	473	64	10	473	64

were for the NK-related genes NKX2-1, NKX2-5, NKX3-2 and NKX5-1. Besides the potential homeobox gene binding sites that were identified, a number of potential binding sites were also identified for other transcriptional regulators involved in embryonic development and differentiation such as CP2, FOXN1, GATA1, MZF1, MYT1, TH1L and WT1 as well as 4 potential binding sites for the oncogenes N-Myc and MYB (Figure 4.8).

A transcription factor binding site that occurs at a similar relative position in promoters from genes that presumably have the same function would suggest evolutionary conservation and provide additional evidence that the site may be functional (Cartharius et al., 2005). Therefore, the 1000 bases upstream of the TSS from the human and mouse *FLJ22318* genes were compared identifying 9 binding sites (>0.83) that are common to both promoters including sites for CHREBP, HIC1, NKX5-1, SP1 and an additional MYB site that was not identified in the original promoter analysis (Figure 4.9).

4.2.1.3 *FLJ22318* Single Nucleotide Polymorphisms

As there is a high degree of nucleotide sequence homology between mammalian *FLJ22318* genes together with possible conservation of transcription factor binding sites within the promoter regions, a search of the dsSNP build 125 available from ftp.ncbi.nih.gov/snp was performed in order to identify sequence variants that may affect transcription or regulation of transcription of *FLJ22318*. This search revealed the presence of 44 single nucleotide polymorphisms (SNPs), five of which are located in the locus region within 2000 bases of the *FLJ22318* gene. Of these five SNPs, four fall within potential NKX3-2 (-922), WT1 (-884), FOXN1 (-396) and TH1L (-203) transcription binding sites as identified by the MatInspector V 6.0 programme. Interestingly, the remaining 39 SNPs are all located within untranslated or intronic regions of the *FLJ22318* gene with no SNPs having been identified within the coding region, suggesting that the invariant protein product from this gene has a function that is critical to the cell (Figure 4.10).

4.2.2 FLJ22318 Protein Structure and Homology

FLJ22318 transcribes a proposed protein comprised of 393 amino acids with a molecular weight of 44414 Daltons. Examination of this amino acid sequence identified three putative nuclear receptor boxes (NRBs) that are motifs found in nuclear proteins,

Figure 4.8 Transcription factor binding sites (red) as identified using the MatInspector Version 6.0 programme of a region encompassing 1000bp upstream of the *FLJ22318* gene TSS as well as the putative CpG island (boxed).

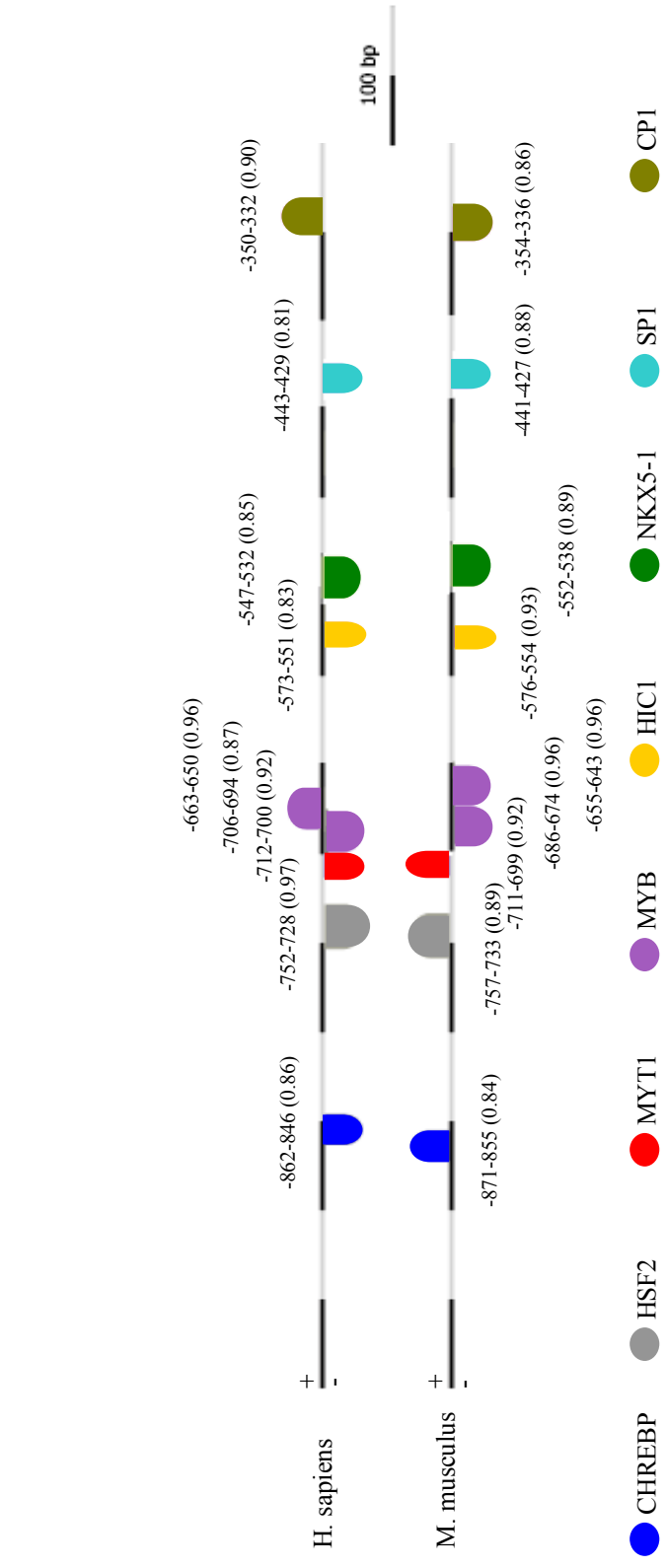

Figure 4.9 Comparative analysis of the promoters from the human and mouse FLJ22318 genes using MatInspector Version 6.0 identified 9 binding sites that are potentially evolutionarily conserved between species suggesting functionality (Adapted from www.genomatix.de).

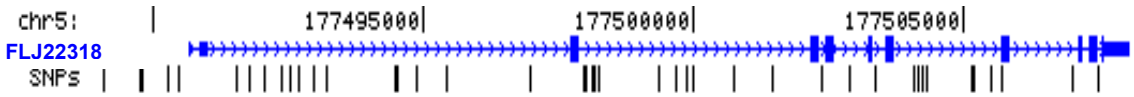

Figure 4.10 Position of single nucleotide polymorphisms (SNPs) associated with the FLJ22318 gene. Schematic representation showing that the SNPs associated with the FLJ22318 gene are located within the untranslated and intronic regions of the gene together with 4 SNPs that are within 2000 bases of the transcription start site.

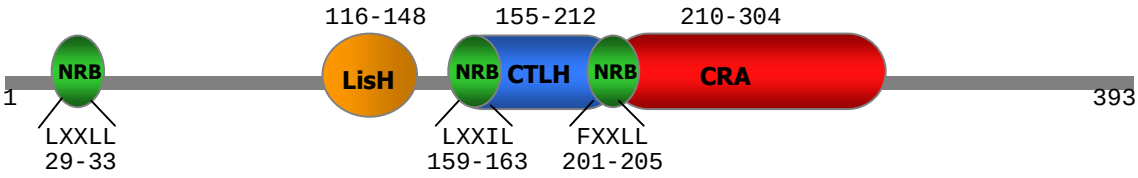

Figure 4.11 Domain structure of the FLJ22318 protein. Examination of the FLJ22318 amino acid sequence identified a lissencephaly type-1-like homology motif (LisH), a C-terminal to LisH motif (CTLH), a CT11-RanBPM (CRA) domain and three putative nuclear receptor boxes (NRB).

including nuclear receptor co-regulators (Huang et al., 1998; Li et al., 2001). A search of the simple modular architecture research tool (SMART) database (Schultz et al., 1998) also revealed three conserved protein motifs/domains, a lissencephaly type-1- like homology motif (LisH; SMART accession number SM00667), a C-terminal to LisH motif (CTLH; SMART accession number SM00668), and a CT11-RanBPM domain (CRA; SMART accession number SM00757; Figure 4.11). The proposed NRBs comprise amino acids LXXLL, LXXIL and FXXLL[3] and encompass residues 29-33, 159-163 and 201-205 respectively, with the LXXIL and FXXLL NRBs lying within the proposed CTLH motif. The LisH motif extends 33 residues from position 116 to 148, the CTLH motif 58 residues from position 155 to 212, and the CRA domain 95 residues from position 210 to 304.

Currently the SMART non-redundant database contains 108 eukaryotic proteins or protein fragments displaying the same protein organisation as FLJ22318. Of these proteins, only two, glucose-induced degradation protein 8 (GID8) from yeast and macrophage erythroblast attacher (MAEA) protein from mouse and human have been characterised. MAEA is involved in erythroblast–macrophage cell attachment, terminal maturation and enucleation of erythroid cells, erythroblast inhibition, apoptosis and in addition has recently been shown to contribute to nuclear architecture and cell division (Bala et al., 2006). Similarly, GID8 is also required for cell cycle progression where it interacts with the G_1/S phase cell cycle regulator *SWI4* to accelerate DNA replication (Pathak et al., 2004). In addition to its role in cell cycle progression, GID8 is also required for the ubiquitination and glucose-induced degradation of FBPase where it forms part of a large protein complex containing RMD5, the yeast orthologue of FLJ22318 (Regelmann et al., 2003).

Although FLJ22318 is a proposed orthologue of RMD5 they do not share the same protein domain organisation as RMD5 contains only a CTLH motif. Therefore, a search of the InParanoid orthology database (http://inparanoid.cgb.ki.se) was performed in order to identify other mammalian orthologues of RMD5 to ascertain whether their domain organisation was similar to that of FLJ22318. This search resulted in the identification of 10 orthologous proteins which could be divided into two paralogous

[3] F – phenylanine, I – isoleucine, L – leucine, X – any amino acid

groups with a representative from human, chimpanzee, dog, mouse and rat in each group, all of which comprised the same domain organisation to that of FLJ22318 (Table 4.3). To determine the level of sequence conservation between FLJ22318 and the four other mammalian orthologues comprising this group, a multiple sequence alignment was performed using the CLUSTALW programme (Thompson et al., 1994). All proteins demonstrated an exceptionally high degree of sequence conservation (>97%) which was as expected as there is more than 80% nucleotide homology within the coding region of these genes (section 4.2.1.1; Figure 4.12). Moreover, this sequence conservation extended to the entire length of the protein and was not confined to the identified protein motifs/domains. These findings indicate that the N- and C-terminal regions of these proteins, which comprise approximately 100 amino acids each, are also necessary for biological function.

The level of sequence conservation was also examined in the other orthologous group of RMD5 proteins (FLJ13910), and although sequence conservation was not as high within this group, as both the rat and chimpanzee proteins showed N-terminal diversification, the human, dog and mouse proteins displayed sequence conservation that also extended the entire length of the protein, providing further evidence that the N- and C-terminal regions of FLJ22318 are required for functionality (Table 4.3; Figure 4.13A). Comparison of human FLJ22318 and FLJ13910 indicated 70% amino acid identity with only 9% of amino acids non-conserved (Figure 4.13B).

4.3 Discussion

FLJ22318 is a novel hypothetical protein that was identified as a potential NKX3-1 interacting protein in prostate cancer cells. NKX3-1 binding proteins are poorly characterised in prostate cancer and regulation of NKX3-1 expression is not well understood, therefore characterisation of NKX3-1 binding proteins such as FLJ22318 is essential to our understanding of NKX3-1 regulation and function. As the *in vivo* function of FLJ22318 has not been determined, its activity in prostate cancer cells and the effects of its interaction with NKX3-1 are unknown. FLJ22318 has several features that make it an interesting gene and protein for further analysis including its chromosomal location and protein-protein interaction motifs which suggest involvement in multiple cellular functions.

Table 4.3 Proposed mammalian orthologues of *S. cerevisiae* RMD5

FLJ22318 Orthologues		
Species	NCBI Protein Accession Number	Amino Acids
H. sapiens	NP_073599	393
P. troglodytes	XP_518140	393
C. familiaris	XP_531873	393
M. musculus	XP_079622	393
R. norvegicus	XP_573086	393
FLJ13910 Orthologues		
Species	NCBI Protein Accession Number	Amino Acids
H. sapiens	NP_073617	391
P. troglodytes	XP_525806	400
C. familiaris	XP_532970	391
M. musculus	XP_077250	391
R. norvegicus	XP_232051	570

```
CLUSTAL W (1.83) multiple sequence alignment

H. sapiens      MEQCACVERELDKVLQKFLTYGQHCERSLEELLHYVGQLRAELASAALQGTPLSATLSLVMSQCCRKIKDTVQKLASDHKDIHSSVSRVGKAIDRNFDSE 100
P. troglodytes  MEQCACVERELDKVLQKFLTYGQHCEQSLEELLHYVGQLRAELASAALQGTPLSATLSLVMSQCCRKIKDTVQKLASDHKDIHSSVSRVGKAIDRNFDSE 100
M. musculus     MEQCACVERELDKVLHKFLTYGQHCEQSLEELLHSVGQLRAELASAALQGTPLSATLSLVMSQCCRKIRDTVQKLASDHKDIHSSVSRVGKAIDRNFDSE 100
R. norvegicus   MEQCACVERELDKVLHKFLTYGQHCEQSLEELLHYVGQLRAELASAALQGTPLSATLSLVMSQCCRKIKDTVQKLASDHKDIHSSVSRVGKAIDRNFDSE 100
C. familiaris   MEQCASVEREVDKVLQKFLTYGQHCEQSLEELLRYVGQLRAELAGTALQGTPLSATLSLVMSQCCRKIKDTVQKLASDHKDIHSSVSRVGKAIDRNFDSE 100
                *****.****:****:**********:****** :*********.:**********************:******************************

H. sapiens      ICGVVSDAVWDAREQQQQILQMAIVEHLYQQGMLSVAEELCQESTLNVDLDFKQPFLELNRILEALHEQDLGPALEWAVSHRQRLLELNSSLEFKLHRLH 200
P. troglodytes  ICGVVSDAVWDAREQQQQILQMAIVEHLYQQGMLSVAEELCQESTLNVDLDFKQPFLELNRILEALHEQDLGPALEWAVSHRQRLLELNSSLEFKLHRLH 200
M. musculus     ICGVVSDAVWDSREKQQQILQMAIVEHLYQQGMLSVAEELCQESTLNVDLDFKQPFLELNRILEALHEQDLGPALEWAVSHRQRLLELNSSLEFKLHRLH 200
R. norvegicus   ICGVVSDAVWDSREKQQQILQMAIVEHLYQQGMLSVAEELCQESTLNVDLDFKQPFLELNRILEALHEQDLGPALEWAVSHRQRLLELNSSLEFKLHRLH 200
C. familiaris   ICGVVSDAVWDSREKQQQILQMAIVEHLYQQGMLSVAEELCQESTLNVDLDFKQPFLELNRILEALHEQDLGPALEWAVSHRQRLLELNSSLEFKLHRLH 200
                ***********:**:************************************************************************************

H. sapiens      FIRLLAGGPAKQLEALSYARHFQPFARLHQREIQVMMGSLVYLRLGLEKSPYCHLLDSSHWAEICETFTRDACSLLGLSVESPLSVSFASGCVALPVLMN 300
P. troglodytes  FIRLLAGGPAKQLEALSYARHFQPFARLHQREIQVMMGSLVYLRLGLEKSPYCHLLDSSHWAEICETFTRDACSLLGLSVESPLSVSFASGCVALPVLMN 300
M. musculus     FIRLLAGGPEKQLEALSYARHFQPFARLHQREIQVMMGSLVYLRLGLEKSPYCHLLDNSHWAEICETFTRDACSLLGLSVESPLSVSFASGCVALPVLMN 300
R. norvegicus   FIRLLAGGPEKQLEALSYARHFQPFARLHQREIQVMMGSLVYLRLGLEKSPYCHLLDNSHWAEICETFTRDACSLLGLSVESPLSVSFASGCVALPVLMN 300
C. familiaris   FIRLLAGGPEKQLEALSYARHFQPFARLHQREIQVMMGSLVYLRLGLEKSPYCHLLDNSHWAEICETFTRDACSLLGLSVESPLSVSFASGCVALPVLMN 300
                ********* ********************************************.****************************************

H. sapiens      IKAVIEQRQCTGVWNHKDELPIEIELGMKCWYHSVFACPILRQQTSDSNPPIKLICGHVISRDALNKLINGGKLKCPYCPMEQNPADGKRIIF 393
P. troglodytes  IKAVIEQRQCTGVWNHKDELPIEIELGMKCWYHSVFACPILRQQTSDSNPPIKLICGHVISRDALNKLINGGKLKCPYCPMEQNPADGKRIIF 393
M. musculus     IKAVIEQRQCTGVWSHKDELPIEIELGMKCWYHSVFACPILRQQTSDSNPPIKLICGHVISRDALNKLINGGKLKCPYCPMEQNPADGKRIIF 393
R. norvegicus   IKAVIEQRQCTGVWSHKDELPIEIELGMKCWYHSVFACPILRQQTSDSNPPIKLICGHVISRDALNKLINGGKLKCPYCPMEQNPADGKRIIF 393
C. familiaris   IKAVIEQRQCTGVWSHKDELPIEIELGMKCWYHSVFACPILRQQTSDSNPPIKLICGHVISRDALNKLINGGKLKCPYCPMEQNPADGKRIIF 393
                **************.************************************************************************
```

Figure 4.12 Sequence alignments of mammalian FLJ22318 proteins. Alignment of FLJ22318 proteins using CLUSTALW (Thompson et al., 1994) indicates the high degree of sequence conservation (>97%) that has been maintained between mammalian species. Conservation indicators (star, colon and dot) represent identical, conserved and semi-conserved amino acids, respectively. Colouring indicates residue[vi] property (red - small + hydrophobic including aromatic Y, blue – acidic, magenta – basic, green – hydroxyl + amine + basic Q).

[vi] A – alanine, C – cysteine, D – aspartate, E – glutamate, F – phenylalanine, G – glycine, H – histidine, I – isoleucine, K – lysine, L – leucine, M – methionine, N – asparagine, P – proline, Q – glutamine, R – arginine, S – serine, T – threonine, V – valine, W – tryphtophan, Y – tyrosine.

(A)

```
H. sapiens      ----------------------------------------------------------------------------------------------------
P. troglodytes  ----------------------------------------------------------------------------------------------------
C. familiaris   ----------------------------------------------------------------------------------------------------
M. musculus     ----------------------------------------------------------------------------------------------------
R. norvegicus   MPCGDNTNCKQGEVLEKTALLIYPVSPRGFPVEDLSASLQVTPLQQREHWLDPLPGRGSWCRPGEPGHRPVPVKTKTIGGAAGGRPNAARQGARGETRRR 100

H. sapiens      ----------------------------------------------------------------------MDQCVTVERELEKVLHKFSGY 21
P. troglodytes  ----------------------------------------------------------MIPFDQEEDSGGDHLDCTEERLESN-HSLEFS 32
C. familiaris   ----------------------------------------------------------------------MDQCVTVERELEKVLHKFSGY 21
M. musculus     ----------------------------------------------------------------------MDQCVTVERELEKVLHKFSGY 21
R. norvegicus   VGRASERARAAGPGRHGAGGHGLRGALRVPRLARPPCLRLPRCPPAALGEEEQDAASVGPGPNHCGPLGAGEPSAAVSGMDQCVTVERELEKVLHKFSGY 200
                                                                                      *:   .*..**.  *.:.

H. sapiens      GQLCERGLEELIDYTGGLKHEILQSHGQDAELSGTLSLVLTQCCKRIKDTVQKLASDHKDIHSSVSRVGKAIDKNFDSDISSVGIDGCWQADSQRLLNEV 121
P. troglodytes  LASGEPRLDRASRNRKGRGLRKGE-IGQDAELSGTLSLVLTQCCKRIKDTVQKLASDHKDIHSSVSRVGKAIDKNFDSDISSVGIDGCWQADSQRLLNEV 130
C. familiaris   GQLCERGLEELIDYTGGLKHEILQSHGQDAELSGTLSLVLTQCCKRIKDTVQKLASDHKDIHSSVSRVGKAIDKNFDSDISSVGIDGCWQADSQRLLNEV 121
M. musculus     GQLCERGLEELIDYTGGLKHEILQSHGQDAELSGTLSLVLTQCCKRIKDTVQKLASDHKDIHSSVSRVGKAIDKNFDSDISSVGIDGCWQADSQRLLNEV 121
R. norvegicus   GQLCERGLEELIDYTGGLKHEILQSHGQDAELSGTLSLVLTQCCKRIKDTVQKLASDHKDIHSSVSRVGKAIDKNFDSDISSVGIDGCWQADSQRLLNEV 300
                      *:.     *   .  :  ************************************************************************

H. sapiens      MVEHFFRQGMLDVAEELCQESGLSVDPSQKEPFVELNRILEALKVRVLRPALEWAVSNREMLIAQNSSLEFKLHRLYFISLLMGGTTNQREALQYAKNFQ 221
P. troglodytes  MVEHFFRQGMLDVAEELCQESGLSVDPSQKEPFVELNRILEALKVRVLRPALEWAVSNREMLIAQNSSLEFKLHRLYFISLLMGGTTNQREALQYAKNFQ 230
C. familiaris   MVEHFFRQGMLDVAEELCQESGLSVDPSQKEPFVELNRILEALKVRVLRPALEWAVSNREMLIAQNSSLEFKLHRLYFISLLMGGTTNQREALQYAKNFQ 221
M. musculus     MVEHFFRQGMLDVAEELCQESGLSVDPSQKEPFVELNRILEALKVRVLRPALEWAVSNREMLIAQNSSLEFKLHRLYFISLLMGGTTNQREALQYAKNFQ 221
R. norvegicus   MVEHFFRQGMLDVAEELCQESGLSVDPSQKEPFVELNRILEALKVRVLRPALEWAVSNREMLIAQNSSLEFKLHRLYFISLLMGGTTNQREALQYAKNFQ 400
                ********************************************************************************************

H. sapiens      PFALNHQKDIQVLMGSLVYLRQGIENSPYVHLLDANQWADICDIFTRDACALLGLSVESPLSVSFSAGCVALPALINIKAVIEQRQCTGVWNQKDELPIE 321
P. troglodytes  PFALNHQKDIQVLMGSLVYLRQGIENSPYVHLLDANQWADICDIFTRDACALLGLSVESPLSVSFSAGCVALPALINIKAVIEQRQCTGVWNQKDELPIE 330
C. familiaris   PFALNHQKDIQVLMGSLVYLRQGIENSPYVHLLDANQWADICDIFTRDACALLGLSVESPLSVSFSAGCVALPALINIKAVIEQRQCTGVWNQKDELPIE 321
M. musculus     PFALNHQKDIQVLMGSLVYLRQGIENSPYVHLLDANQWADICDIFTRDACALLGLSVESPLSVSFSAGCVALPALINIKAVIEQRQCTGVWNQKDELPIE 321
R. norvegicus   PFALNHQKDIQVLMGSLVYLRQGIENSPYVHLLDANQWADICDIFTRDACALLGLSVESPLSVSFSAGCVALPALINIKAVIEQRQCTGVWNQKDELPIE 500
                ********************************************************************************************

H. sapiens      VDLGKKCWYHSIFACPILRQQTTDNNPPMKLVCGHIISRDALNKMFNGSKLKCPYCPMEQSPGDAKQIFF 391
P. troglodytes  VDLGKKCWYHSIFACPILRQQTTDNNPPMKLVCGHIISRDALNKMFNGSKLKCPYCPMEQSPGDAKQIFF 400
C. familiaris   VDLGKKCWYHSIFACPILRQQTTDNNPPMKLVCGHIISRDALNKMFNGSKLKCPYCPMEQSPGDAKQIFF 391
M. musculus     VDLGKKCWYHSIFACPILRQQTTDNNPPMKLVCGHIISRDALNKMFNGSKLKCPYCSMEQSPGDAKQIFF 391
R. norvegicus   VDLGKKCWYHSIFACPILRQQTTDNNPPMKLVCGHIISRDALNKMFNGSKLKCPYCPMEQSPGDAKQIFF 570
                ************************************************.*************
```

(B)

```
FLJ22318        MEQCACVERELDKVLQKFLTYGQHCERSLEELLHYVGQLRAELASAALQGTPLSATLSLVMSQCCRKIKDTVQKLASDHKDIHSSVSRVGKAIDRNFDSE 100
FLJ13910        MDQCVTVERELEKVLHKFSGYGQLCERGLEELIDYTGGLKHEILQSHGQDAELSGTLSLVLTQCCKRIKDTVQKLASDHKDIHSSVSRVGKAIDKNFDSD 100
                *:**. *****:***:**  *** ***.****:.*.* *: *: .:  *.: **.*****::***::*****************************:****:

FLJ22318        ICGVVSDAVWDAREQQQQILQMAIVEHLYQQGMLSVAEELCQESTLNVDLDFKQPFLELNRILEALHEQDLGPALEWAVSHRQRLLELNSSLEFKLHRLH 200
FLJ13910        ISSVGIDGCWQAD--SQRLLNEVMVEHFFRQGMLDVAEELCQESGLSVDPSQKEPFVELNRILEALKVRVLRPALEWAVSNREMLIAQNSSLEFKLHRLY 198
                *..*  *. *:*   .*::*: .:***:::****.******** *.** . *:**:*********: : * ********:*: *:  ***********:

FLJ22318        FIRLLAGGPAKQLEALSYARHFQPFARLHQREIQVMMGSLVYLRLGLEKSPYCHLLDSSHWAEICETFTRDACSLLGLSVESPLSVSFASGCVALPVLMN 300
FLJ13910        FISLLMGGTTNQREALQYAKNFQPFALNHQKDIQVLMGSLVYLRQGIENSPYVHLLDANQWADICDIFTRDACALLGLSVESPLSVSFSAGCVALPALIN 298
                ** ** **.::* ***.**::*****  **::***:******** *:*:*** ****:.:**:**: ******:**************::******.*:*

FLJ22318        IKAVIEQRQCTGVWNHKDELPIEIELGMKCWYHSVFACPILRQQTSDSNPPIKLICGHVISRDALNKLINGGKLKCPYCPMEQNPADGKRIIF 393
FLJ13910        IKAVIEQRQCTGVWNQKDELPIEVDLGKKCWYHSIFACPILRQQTTDNNPPMKLVCGHIISRDALNKMFNGSKLKCPYCPMEQSPGDAKQIFF 391
                ***************:*******::** ******:**********:*.***:**:***:********::**.**********.*.*.*:*:*
```

Figure 4.13 Sequence alignment of mammalian **(A)** FLJ13910 proteins using CLUSTALW (Thompson et al., 1994) indicating that sequence conservation has been maintained in the 100 amino acid N- and C-terminal regions between human, dog and mouse species and providing additional evidence that these regions are necessary for biological function. **(B)** Homology of particular amino acids between FLJ22318 and FLJ13910 may indicate regions that are required for similar biological activity whereas regions containing multiple amino acid changes between paralogues may reflect differences in function. Conservation indicators (star, colon and dot) represent identical, conserved and semi-conserved amino acids, respectively. Colouring indicates residue[vii] property (red - small + hydrophobic including aromatic Y, blue – acidic, magenta – basic, green – hydroxyl + amine + basic Q).

[vii] A – alanine, C – cysteine, D – aspartate, E – glutamate, F – phenylalanine, G – glycine, H – histidine, I – isoleucine, K – lysine, L – leucine, M – methionine, N – asparagine, P – proline, Q – glutamine, R – arginine, S – serine, T – threonine, V – valine, W – tryphtophan, Y – tyrosine.

Comparison of human chromosomal region 5q35.3 with syntenic regions on mouse chromosome 11b1.3 and rat chromosome 10q22 indicate that the relative positions of FLJ22318 orthologues are identical. The regions of these chromosomes encompassing the *FLJ22318* orthologues also show analogous gene organisation with regard to the adjacent genes *N4BP3*, *NOLA2* and *HNRPAB*. Recently it has been shown that there is remarkable conservation in gene organisation between species and that while gene expression evolves very quickly, particularly in mammals, gene order is both evolutionarily very stable and in specific circumstances may be related to gene expression (Hillier et al., 2004; Khaitovich et al., 2004).

Within this syntenic region, N4BP3 and HNRPAB are both transcribed in the same direction as FLJ22318 whereas the intervening gene NOLA2 is transcribed convergently to FLJ22318. Investigation of eukaryotic genomes has identified co-evolution of gene expression when neighbouring genes are transcribed in the same or divergent directions but not when the genes are transcribed in convergent directions (Sèmon and Duret, 2006). In addition, N4BP3 and HNRPAB are positioned within 4.9 and 56Kb respectively of FLJ22318 and co-expressed genes have been shown to cluster more closely than non co-expressed genes with the average distance between co-expressed genes in humans being 284kb (median 89kb) compared to 617kb (median 222kb) for neighbouring genes that are not co-expressed (Sèmon and Duret, 2006). These findings provide evidence for investigation of co-expression of FLJ22318 and its surrounding genes, N4BP3 and HNRPAB in human tissues.

According to the AceView and NCBI UniGene databases, FLJ22318 is ubiquitously expressed, N4BP3 (Hs. 101761) is found in cDNA libraries and ESTs from a variety of tissues and is expressed more than would be expected for the average gene, whilst HNRPAB (Hs. 591731) is ubiquitously expressed at 8.7 times the average gene (Thierry-Mieg et al., 2005). Clusters of co-expressed genes in mammals are typically located within a gene dense region, are highly expressed and generally contains 2 or 3 genes (Versteeg et al., 2003). Although FLJ22318, N4BP3 and HNRPAB are all highly expressed, the UniGene database does not contain cDNA libraries or ESTs from every human tissue at all stages of development therefore it is not known to what extent FLJ22318, N4BP3 and HNRPAB are expressed in the same tissues or at the same stages

of development. Clusters of co-expressed genes are proposed to be maintained by selective pressure as greater than expected conservation of gene linkage is evident between species during evolution. Functional relationships of co-expressed genes have also been hypothesised although the extent of this is unknown (Sèmon and Duret, 2006). As the biological activity of FLJ22318 has yet to be characterised, determination of FLJ22318 function and investigation of its distribution of expression and co-expression with N4BP3 and/or HNRPAB will be required to characterise this cluster of highly expressed genes.

Bioinformatic analysis of the promoter region of the FLJ22318 gene identified a putative CpG island of 843 bases surrounding the FLJ22318 transcription start site and the first two exons of the FLJ22318 gene. CpG islands are associated with the upstream region of many genes, generally cover all or part of the promoter and may extend into the first exon and beyond. All widely expressed (housekeeping) genes and up to 40% of tissue specific genes are associated with CpG islands, the majority of which are not methylated (Robinson et al., 2004). Hypermethylation of CpG islands is associated with both transcriptional silencing of gene expression such as tumour suppressor genes in cancer (Esteller, 2005) and constitutive gene expression. The presence of FLJ22318 mRNAs and ESTs in a wide range of different non-malignant and malignant tissues indicates widespread maintenance of expression of FLJ22318 and suggests that if hypermethylated, the FLJ22318 CpG island is not associated with transcriptional silencing. However, further investigation of the methylation status of the FLJ22318 CpG island and its relationship to FLJ22318 expression will be required in order to determine the contribution of the CpG island to regulation of FLJ22318 mRNA transcription and steady-state levels.

The cytogenetic location of FLJ22318 at 5q35.3 on chromosome 5 is important as chromosomal additions, deletions and translocations of the 5q35 region have been reported in a number of cancers including leukaemia, lymphoma, breast, ovarian and prostate cancer. Furthermore, deletions of 5q are the most frequent abnormality seen in breast cancers of BRCA1 mutation carriers (Johannsdottir et al., 2006). The 5q35.3 cytogenetic location is also associated with hereditary prostate cancer and early age at onset of breast cancer, especially in women with BRCA1 and BRCA2 mutations (Johannsdottir et al., 2006; Xu et al., 2005b). These findings suggest that genes

affecting cancer progression, such as genes involved in cell cycle progression or DNA repair may be located within this region. Mapping studies within the 5q35.2-5q35.3 region have shown that mutations and deletions at the *NSD1* locus are responsible for Sotos syndrome, which is characterised by accelerated growth and macrocephaly (Douglas et al., 2003). However as patients with Sotos syndrome are also at an increased risk of developing cancer it indicates the presence of genes within the 5q35.2-5q35.3 region that are required for growth regulation and whose deregulation may lead to uncontrolled cell cycle progression and cell transformation. Loss of heterozygosity at the *NPM1* locus at 5q35.3 is associated with leukaemia and lymphoma but the genes within this region that are associated with breast and prostate cancer have not been mapped (Berger et al., 2006). None of the studies performed to date have included the FLJ22318 locus therefore it remains unknown whether loss or gain of FLJ22318 expression could be involved in the cancers that are associated with this chromosomal region.

The yeast orthologue of FLJ22318, RMD5, which contains only a CTLH motif is required for protein ubiquitination, degradation and cell division (Enyenihi and Saunders, 2003; Regelmann et al., 2003). Examination of the FLJ22318 amino acid sequence revealed that it contains LisH, CTLH and CRA domains, a domain structure that is present in 108 eukaryotic proteins of divergent genomes. Acquisition of the LisH and CRA domains suggests that human FLJ22318 has evolved different or additional functions in comparison to yeast RMD5. Of the proteins containing a similar domain composition to human FLJ22318, only MAEA and GID8 have been characterised and both are involved in cell cycle progression (Bala et al., 2006; Pathak et al., 2004). However, their interacting proteins or the domains contributing to these interactions have not been reported. Previous studies have shown that all of the characterised 29 human proteins or protein fragments which contain a LisH motif either on its own or in combination with other domains, are involved in development, where they are also associated with the cell cycle (Schultz et al., 1998). In these proteins, the LisH motif has been shown to function as a protein-protein interaction domain, to affect protein stability and to direct protein localisation. The function of the CTLH domain has not been characterised whereas the CRA domain has also been described as a protein-protein interaction domain that can modulate RNA binding. Analysis of the PAFAH1B1 and RanBP9 proteins with these domains has determined that these proteins assume an

α-helical secondary structure composed of several highly conserved elements and has resulted in the identification of regions that are required for protein function (Kim et al., 2004b; Menon et al., 2004). Functional characterisation of FLJ22318 would also therefore investigate its secondary structure and the involvement of the LisH, CTLH and CRA domains in protein-protein interactions, protein localisation and the potential role of FLJ22318 in control of cell proliferation.

Recently it has been suggested that the CTLH motif may be necessary for an open or closed protein conformation which may depend on protein binding. Within the CTLH motif of FLJ22318 there are two putative nuclear receptor boxes (NRB's), one of which (LXXIL) is located at the N-terminus whilst the other (FXXLL) is located at the C-terminus of the CTLH domain. NRB's are short amino acid sequences which facilitate co-receptor binding to nuclear receptors. Nuclear receptors function as ligand-activated transcription factors where ligand binding to the receptor ligand binding domain causes a conformational change (Mangelsdorf and Evans, 1995). In the majority of nuclear receptors, co-regulator binding occurs through the activation function 2 (AF2) motif, an α-helical motif located in the C-terminus and also requires the NRB to adopt an α-helical conformation (Durand et al., 1994). The putative LXXIL and FXXLL NRBs in FLJ22318 lie within the proposed α-helical CTLH motif and these motifs have been shown in previous studies to bind thyroid receptor (TR), retinoid X receptor (RXR) and retinoid acid receptor (RAR) in the presence of their ligands, thyroid hormone and retinoids. FLJ22318 also contains a third putative NRB LXXLL located at amino acids 29-33 and previous studies have shown this motif can bind RAR in the absence of ligand and androgen receptor (AR) in the presence of ligand (Huang et al., 1998). The presence of these putative NRBs suggests that FLJ22318 may interact with members of the nuclear receptor superfamily and future studies would be necessary to determine whether FLJ22318 interacts with TR, RXR, RAR, AR or other nuclear receptors in the presence or absence of their respective ligands.

Comparison of the 16 proposed *FLJ22318* gene transcripts reveals that all but two of these transcripts encode proteins that comprise specific regions of the NCBI reference protein (NP_073599) with the remaining two transcripts, 'n' and 'p', proposed to encode completely different proteins. Transcript variants 'k' and 'l' encode proteins

comprising the N-terminal region prior to the LisH motif, the LisH motif and distinct portions of the CTLH motif. Transcript variant 'i' is similar to variant 'l' except that this variant encodes an extra exon which introduces another putative LXXLL NRB. In contrast, transcript variant 'j' encodes a protein comprising a truncated CTLH motif and CRA domain but is missing the LisH motif and highly conserved region prior to the LisH motif. Transcript variants 'a', 'e', 'g' and 'h' all encode proteins with intact LisH, CTLH and CRA domains, however variants 'a' and 'e' have different intron and exon structures prior to the LisH motif compared to the reference sequence, whilst variant 'g' is truncated prior to the LisH motif and following the CRA domain. The three variants, 'b', 'c' and 'd' all encode proteins identical to the reference sequence but contain distinct 3` and 5` UTRs indicating that if expressed, these variants may be under differential transcriptional and/or translational regulation.

The presence of ESTs in a wide range of normal and malignant tissues for the distinct variants 'n' and 'p' suggests expression of these transcripts as does the presence of ESTs for variant 'i' which encodes an extra distinct exon. Of interest is that these ESTs are detected in embryonic stem cells and normal brain and uterine tissue indicating that specific FLJ22318 transcripts may be expressed in different tissue and at distinct stages of development. As transcript variants are also proposed which encode only the highly conserved N and C-terminal regions of FLJ22318 prior to the LisH motif and following the CRA domain, functional elements may reside within these regions. A number of these transcript variants are also proposed to encode proteins comprising combinations or part of the putative LisH, CTLH and CRA protein-protein interaction domains although expression of all of these variants cannot be distinguished using EST expression data.

As the deduced subcellular location differs for proteins encoded by the proposed transcripts, it can be speculated that similar to other proteins including the previously described HNRPAB, FLJ22318 isoforms may perform different functions in distinct subcellular compartments. Northern blotting or library screening in future experiments will help to determine which FLJ22318 transcripts are expressed in specific tissues, however, generation of FLJ22318 antibodies will be required to examine expression of FLJ22318 isoforms in prostate, prostate cancer and in other tissues. This is further discussed in Chapter five.

Bioinformatic analysis of the *FLJ22318* promoter and CpG island identified several potential transcription factor binding sites for homeodomain proteins, which are important regulatory factors that are involved in diverse biological activities in embryonic and adult tissues including differentiation, proliferation and apoptosis (section 1.3.1). The majority of these proposed binding sites are for transcription factors that belong to the NK-related class of homeodomain proteins which generally have a tissue specific expression pattern. Previous studies have shown that the regulation of gene expression is governed by binding of different combinations of transcription factors in specific tissues and that subsets of binding sites may be relevant for specific tissues but not for others. Potential transcription factor binding sites in the mouse *FLJ22318* promoter were also identified as identification of binding sites common to promoters in multiple species provides supporting evidence that these motifs may be functional. This analysis confirmed the presence of 9 potential binding sites for transcription factors that are common to both promoters. Of these 9 binding sites, the putative SP1 binding site is particularly interesting as constitutive expression of some genes has been shown to be dependent on SP1 binding (Zhang et al., 2006). In addition, as the yeast orthologue of FLJ22318, RMD5 is involved in the degradation of proteins involved in gluconeogenesis, the identification of the putative CHREBP binding site in the human *FLJ22318* promoter region is of particular interest as CHREBP regulates gene transcription in a glucose dependent manner and previous studies have shown that RMD5 expression is repressed in response to glucose. Bioinformatic analysis of potential transcription factor binding sites in the *FLJ22318* promoter has provided a starting point for investigating the regulation of FLJ22318 expression and suggests that FLJ22318 may have a constitutive basal level of expression that is modulated by binding of additional factors. Deletion analysis of the *FLJ22318* promoter region to identify specific regions with promoter activity will be useful in determining the molecular mechanisms by which FLJ22318 expression is regulated.

To date, no single nucleotide polymorphisms (SNPs) have been identified that are located within the coding exons of the *FLJ22318* gene despite the identification of 44 other SNPs that are located in the 5` and 3` untranslated and intronic regions of the gene. Polymorphisms associated with the promoters of genes can introduce new regulatory elements or disrupt existing transcription factor binding sites, allowing differential gene expression. In addition, intronic regions of genes can harbour

enhancers and therefore polymorphisms located in these regions can also regulate levels of expression (Tsukada et al., 2006). Analysis of all 44 SNPs across species to assess phylogenetic conservation, which may provide clues to their functional importance, identified just two SNPs where the reference nucleotide is conserved across a number of species. The most conserved SNP position, Rs11956603 in intron 5, was located in a DNA stretch completely conserved from human, chimpanzee, rhesus macaque and cow. In addition, single nucleotide conservation was also observed at this position from mouse, rat, rabbit and elephant. The second SNP position, Rs10036388 located in intron 2, was located in a stretch of DNA that showed a high degree of conservation between human, chimpanzee, rhesus macaque, elephant and lesser hedgehog. Although the biological relevance of the SNPs in FLJ22318 are unknown, the regional conservation of these two sequences containing SNPs Rs11956603 and Rs10036388 warrants further study to determine whether these regions harbour regulatory elements that may be functionally important to *FLJ22318* transcription. More importantly, the exceptionally high degree of sequence conservation seen within the coding exons across species coupled with the absence of known mutations within this region suggests that the protein encoded by this gene may be critical for cell survival and/or function.

Since a significant conservation of nucleotide and amino acid sequences between human FLJ22318 and its orthologues in a diverse range of mammalian species provides strong evidence that FLJ22318 function is critical in the cell, the identification of protein-protein interaction domains in FLJ22318 that in other proteins are required for biological activity and which are associated with cell cycle regulation represents a significant finding. This may be especially relevant as the *FLJ22318* gene maps to 5q35.3, a region linked to hereditary prostate cancer that is thought to harbour genes whose deregulation leads to cell transformation and uncontrolled cell cycle progression. As such, characterisation of FLJ22318 and its interaction with NKX3-1 in prostate cancer cells will provide a better understanding of NKX3-1 function in human prostate cancers and the consequences of its loss in androgen dependent prostate cancers.

Chapter Five

Chapter Five – Characterisation of FLJ22318 Interaction with NKX3-1

5.1 Introduction

To determine how molecular pathways that operate within cells contribute to various biological functions, characterisation of protein-protein interactions is essential. Within the cell, proteins form rapid and transient complexes with other proteins and it is these complexes that control a large number of cellular processes such as proliferation, migration, basic or specialised metabolism and the activation and integration of signalling pathways. In addition, transient protein-protein interactions are involved in the assembly of transcriptional machinery at specific promoters, are required for protein transport and direct the formation and degradation of subcellular structures such as microtubules during the cell cycle (Phizicky and Fields, 1995). To understand the significance of protein-protein interactions within the cell, it is necessary to characterise the extent to which they occur and the functional consequences of the interactions. To elucidate the mechanisms involved in NKX3-1 regulation, this thesis investigated the interaction between NKX3-1 and FLJ22318.

Protein-protein interactions can be studied using a variety of molecular based methods including yeast two-hybrid analysis, affinity chromatography and immunoprecipitation, each of which has particular advantages and disadvantages. Numerous eukaryotic transcription factors have DNA-binding and transcriptional activation domains that are distinct from one another and this is utilised in yeast two-hybrid analysis where protein interactions are examined by fusing one of the proteins to the DNA-binding domain of the yeast GAL4 transcription factor and the other to the GAL4 DNA-activation domain (Phizicky and Fields, 1995). Plasmids encoding the two proteins are transfected into yeast and interactions detected by assaying for expression of a reporter gene construct containing a binding site for GAL4 (Fields and Song, 1989). One advantage of using yeast two-hybrid analysis to confirm a protein-protein interaction is that this method is independent of endogenous protein expression and is often more sensitive than *in vitro* methods, making it better suited to detect weak and/or transient interactions (Gietz and Woods, 2002).

The yeast two-hybrid system however, is known to produce a significant number of false positive protein-protein interactions which are classified as being either technical or biological in origin (Vidalain et al., 2004). Technical false positives include those false positives which arise as a result of spontaneous mutations that occur in the BD-fusion protein plasmid during the course of the library screen producing BD-fusion proteins which can auto-activate the reporter genes without interacting with an AD-fusion protein (Walhout and Vidal, 1999). Another more common type of false positive is AD-fusion proteins that activate the reporter genes without interacting with the BD-fusion protein (Vidalain et al., 2004). This type of false positive accounts for the high proportion of ribosomal subunits, heat shock proteins, proteasome subunits and cytoskeletal components that are commonly identified as interacting with numerous BD-fusion proteins in yeast two-hybrid library screens. The interactions are conjectured to occur as a result of the intrinsically sticky nature of these proteins, either because they have numerous binding partners or because of non specific coiled-coil domain interactions (Serebriiskii and Golemis, 2001).

The other main category of false positives detected in yeast two-hybrid screens is the biological false positive. These false positives are protein-protein interactions that occur in yeast cells in comparison to the proteins' native environment where the two proteins may not be expressed in the same tissue or cellular compartment, or at the same time (Gietz et al., 1997). Extensive knowledge of the functions of the two interacting proteins, their subcellular localisation and identification of additional binding partners is required in order to confirm this type of false positive.

Another commonly used method for detecting protein-protein interactions is the GST pull-down assay. This assay is based on the inducible, high-level expression of a protein in *Escherichia coli* that is fused with the *Schistosoma japonicum* GST tag at the amino terminus (Smith and Johnson, 1988). When expressed in *E. coli*, fusion proteins accumulate within the cytoplasm of the cell, can undergo dimerisation similar to that seen in nature and retain full enzymatic activity (Maru et al., 1996). The GST-fusion proteins can then be purified from the bacterial lysates by affinity chromatography using immobilised glutathione. The advantage of affinity chromatography to validate a protein-protein interaction is that this method is very sensitive and can detect interactions with a binding constant as weak as 10^{-5} M which is within the range that is

likely to be physiologically relevant (Formosa et al., 1991). In addition, this technique has a built-in specificity control as all proteins within a cell lysate are tested equally to see whether they interact with the GST-fusion protein (Phizicky and Fields, 1995).

A major consideration when using GST pull-down assays is that the protein-protein interactions are detected *in vitro* on the sepharose beads and therefore may not be functionally significant. In addition, cellular lysis leads to the disruption of subcellular structures thereby creating non physiological interactions amongst proteins that may normally reside in different cellular compartments (Monti et al., 2005).

Co-immunoprecipitation is another well characterised method for detecting protein-protein interactions whereby cell lysates are incubated with an antibody to the protein of interest, the antigen is precipitated then washed, and proteins bound to the antigen-antibody complexes are eluted and analysed by western blotting (Phizicky and Fields, 1995). Immunoprecipitating antibodies can be directed against the endogenous protein or alternatively, if antibodies to the protein of interest are not available, fusion proteins which carry an epitope for which antibodies are commercially available can be prepared. Once the fusion proteins have been constructed they can be utilised to test interactions with a number of different proteins. In addition, protein-protein interactions can be tested in the appropriate cell lines and the epitope tags are often small thereby minimising any effects they may have on protein function or localisation within the cell (Figeys, 2003). Nonetheless since transfection is required, examination of interacting proteins carrying epitopes can only be performed in cell lines and not in tissues (Droit et al., 2005).

The biological activity of the fusion protein may also be affected by the amino acid composition of the epitope and its location at the N- or C-terminal of the protein (Bucher et al., 2002). More importantly, since the tagged protein will be overexpressed, it will not be present in the cell in the stoichiometric ratio necessary for optimum interactions to occur and as a consequence may compete with the endogenous non-tagged protein in forming interactions with its partners (Droit et al., 2005). Another concern is that not all antibodies are suitable for immunoprecipitation, as these assays require antibodies with a high affinity for the correct antigen in order to avoid detecting non-specific protein interactions between closely related antigens (Monti et al., 2005). A

major advantage of immunoprecipitation assays, as with GST pull-down assays, is that these methods have negligible effects on the tertiary structure and therefore biological activity of the isolated proteins, which may be used subsequently in functional assays (Droit et al., 2005). Furthermore, all proteins within the cell are competing equally for binding indicating specificity when a protein-protein interaction occurs (Phizicky and Fields, 1995).

Confirmation of a protein-protein interaction by several different techniques, combined with demonstration of co-localisation of the proteins within the cell would then provide strong supporting evidence of an interaction between NKX3-1 and FLJ22318 that is biologically significant *in vivo*.

5.2 Results

5.2.1 Construction of FLJ22318 Expression Vectors

During this thesis, FLJ22318 cDNA corresponding to the coding region was ligated into the yeast expression vector pGBKT7 for yeast two-hybrid analyses (section 5.2.2), the pGEX2TK vector for GST pull-down assays (section 5.2.3) and the mammalian expression vectors, pcDNA3.1/V5-His-TOPO, pCMV-Myc, pCMV-HA and pEGFP-C2 for studies of FLJ22318 protein expression, intracellular localisation and co-immunoprecipitation assays (sections 5.2.4; 5.2.5 and 5.2.6).

5.2.1.1 Construction of the FLJ22318-pcDNA3.1/V5-His-TOPO Vector

5.2.1.1.1 PCR Optimisation with *Taq* Polymerase

Full-length FLJ22318 was cloned into the mammalian expression plasmid, pcDNA3.1/V5-His-TOPO to allow it to be expressed with C-terminal V5 and His tags following transfection into mammalian cell lines. The 1179bp coding region of FLJ22318 was PCR amplified from LNCaP cDNA using FLJTOPO sense and FLJTOPO antisense primers using an initial annealing temperature of 55°C with 35 cycles of PCR and increasing concentrations of $MgCl_2$ (1-2mM). However, only two bands of approximately 200bp and 400bp were amplified at all $MgCl_2$ concentrations tested (Figure 5.1A). When the annealing temperature was increased to 65°C to increase primer specificity and the number of cycles increased to 45, multiple bands were observed including a band at the correct molecular size of ~1200bp (Figure 5.1B). The

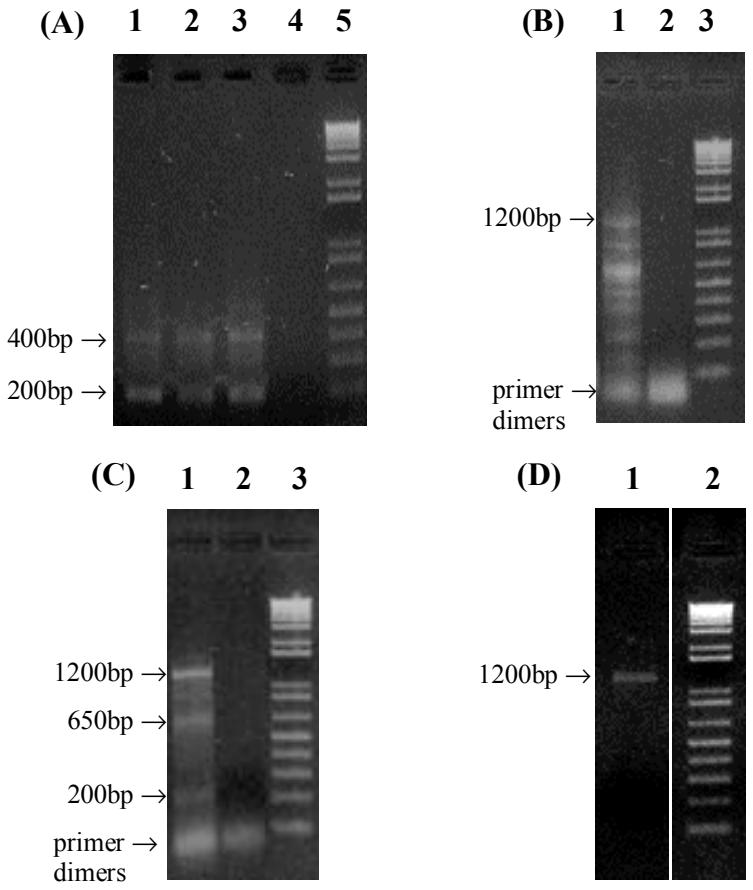

Figure 5.1 PCR amplification and ligation of FLJ22318 cDNA into pcDNA3.1/V5-His-TOPO. **(A)** PCR amplification of full length FLJ22318 using FLJTOPO sense and anti-sense primers and an initial annealing temperature of 55°C with 35 cycles amplified two bands of ~200bp and ~400bp at all $MgCl_2$ concentrations tested. **(B)** When the annealing temperature was increased to 65°C with 45 cycles, multiple bands were amplified including a band of the correct molecular size for FLJ22318 of ~1200bp. **(C)** Decreasing the number of PCR cycles to 40 resulted in amplification of the target band of ~1200bp and two additional bands of ~200bp and ~650bp. **(D)** The band corresponding to full-length FLJ22318 cDNA was excised and purified from the gel, a 5µL aliquot was electrophoresed in a 2% agarose gel and the concentration determined from the gel to be 10ng/µL.

(A)
1 1.0mM $MgCl_2$
2 1.5mM $MgCl_2$
3 2.0mM $MgCl_2$
4 -ve control (no cDNA)
5 1Kb Plus™ DNA Ladder

(B)
1 1.5mM $MgCl_2$
2 -ve control (no cDNA)
3 1Kb Plus™ DNA Ladder

(C)
1 1.5mM $MgCl_2$
2 -ve control (no cDNA)
3 1Kb Plus™ DNA Ladder

(D)
1 Extracted and purified FLJ22318 cDNA
2 1Kb Plus™ DNA Ladder

number of PCR cycles was then reduced to 40 to decrease the number of products amplified and this resulted in the amplification of a ~1200bp band and two additional bands of approximately 200bp and 650bp (Figure 5.1C). As the additional amplified products were significantly different in size to the target product, the target band was gel purified and 5µL visualised in a 2% agarose gel which indicated the presence of the desired ~1200bp product at an estimated concentration of 10ng/µL (sections 3.1.4; 3.1.6; Figure 5.1D).

5.2.1.1.2 Cloning of FLJ22318 into pcDNA3.1/V5-His-Topo

Following purification, 40ng (4µL) of the FLJ22318 fragment was ligated into 1µL (10ng) of the pcDNA3.1/V5-His-TOPO cloning vector and 2µL of the ligation reaction was transformed into competent TOP10 *E. coli* bacteria (sections 3.2.4; 3.2.6). Transformants were selected on LB agar/ampicillin plates from which 10 colonies were picked into small-scale cultures, the plasmid DNA isolated (section 3.3.1), RNase treated, then digested using *Hin*d III and *Not* I and 5µL visualised in agarose gels (sections 3.1.4; 3.2.2). The presence of an insert of approximately 1200bp in clones A1 to A7, A9 and A10 indicated that cloning of FLJ22318 into pcDNA3.1/V5-His-TOPO had been successful and glycerol stocks were prepared of these 9 clones (Figure 5.2).

To confirm that the cloned insert was FLJ22318 as published by NCBI (Accession No. NM_022762), plasmid DNA isolated from clones A1 to A4 was purified and sequenced using the BGHREV primer then analysed using BLAST™ (sections 3.1.5; 3.4). All sequences from clones A1 to A4 were found to encode ~600bp of the 1179bp ORF of FLJ22318 cloned in frame into pcDNA3.1/V5-His-TOPO, however only clones, A2 and A4, were found to encode the insert in the sense orientation and were sequenced further. To obtain the remaining 600bp of the ORF, the FLJREV and FLJREV2 antisense primers were used in additional sequencing reactions. Upon completion of sequencing, clone A2 was found to have a T > C mutation at position 586bp of the ORF which would encode a proline instead of leucine. Clone A4 however, contained the correct FLJ22318 sequence (Figure 5.3). Large-scale cultures of clone A4 were grown from the glycerol stock, the plasmid DNA was purified and used in subsequent experiments to characterise the expression and function of FLJ22318 (sections 3.1.5; 3.3.2).

Figure 5.2 Cloning of FLJ22318 into pcDNA3.1/V5-His-TOPO. 40ng of the purified FLJ22318 fragment was ligated into the pcDNA3.1/V5-His-Topo cloning vector and transformants selected on LB agar/ampicillin plates. Ten transformants were picked and grown into small scale cultures and the plasmid DNA isolated then digested using *Hind* III and *Not* I. Following digestion, a 5µL aliquot was visualised in a 2% agarose gel indicating the presence of digested pcDNA3.1/V5-His-TOPO (5437bp) and an insert of the correct molecular size of FLJ22318 (1265bp) in clones A1 to A7, A9 and A10.

1-10 Clones A1-A10 digested with *Hind* III and *Not* I
11 1Kb Plus™ DNA Ladder

(A)

gi|34147687|ref|NM_022762.3| Homo sapiens required for meiotic nuclear division 5 homolog B (S. cerevisiae)(RMND5B), mRNA Length=1825 Score = 1211 bits (611), Expect = 0.0 Identities = 611/611 (100%), Gaps = 0/611 (0%)
Strand=Plus/Minus

```
Query  1    AGGCGGATGAAGTGCAGTCGGTGCAGCTTGAACTCCAGGGAGCTGTTGAGTTCCAGCAGGCGCTGCCTGTGGGAGACGGCCCATTCCAACGCAGGACCCA
            ||||||||||||||||||||||||||||||||||||||||||||||||||||||||||||||||||||||||||||||||||||||||||||||||||||
Sbjct  791  AGGCGGATGAAGTGCAGTCGGTGCAGCTTGAACTCCAGGGAGCTGTTGAGTTCCAGCAGGCGCTGCCTGTGGGAGACGGCCCATTCCAACGCAGGACCCA

Query  101  GGTCTTGTTCGTGCAGGGCTTCCAGGATTCGATTCAACTCTAGGAAAGGCTGCTTGAAATCCAAGTCCACATTCAGCGTTGATTCCTGGCACAGCTCCTC
            ||||||||||||||||||||||||||||||||||||||||||||||||||||||||||||||||||||||||||||||||||||||||||||||||||||
Sbjct  691  GGTCTTGTTCGTGCAGGGCTTCCAGGATTCGATTCAACTCTAGGAAAGGCTGCTTGAAATCCAAGTCCACATTCAGCGTTGATTCCTGGCACAGCTCCTC

Query  201  GGCCACGCTGAGCATGCCCTGCTGATACAGGTGTTCCACGATGGCCATCTGCAGGATCTGCTGCTGCTGTTCCCGCGCGTCCCACACCGCATCTGACACA
            ||||||||||||||||||||||||||||||||||||||||||||||||||||||||||||||||||||||||||||||||||||||||||||||||||||
Sbjct  591  GGCCACGCTGAGCATGCCCTGCTGATACAGGTGTTCCACGATGGCCATCTGCAGGATCTGCTGCTGCTGTTCCCGCGCGTCCCACACCGCATCTGACACA

Query  301  ACACCACAGATCTCAGAGTCGAAGTTCCTGTCAATGGCTTTGCCCACTCGGGATACACTGCTGTGAATGTCCTTATGGTCCGAAGCCAGTTTCTGCACCG
            ||||||||||||||||||||||||||||||||||||||||||||||||||||||||||||||||||||||||||||||||||||||||||||||||||||
Sbjct  491  ACACCACAGATCTCAGAGTCGAAGTTCCTGTCAATGGCTTTGCCCACTCGGGATACACTGCTGTGAATGTCCTTATGGTCCGAAGCCAGTTTCTGCACCG

Query  401  TATCTTTGATCTTCCGGCAGCACTGTGACATCACCAGAGAGAGGGTGGCTGAGAGAGGGGTCCCCTGGAGGGCTGCGCTGGCCAGCTCAGCCCGCAGCTG
            ||||||||||||||||||||||||||||||||||||||||||||||||||||||||||||||||||||||||||||||||||||||||||||||||||||
Sbjct  391  TATCTTTGATCTTCCGGCAGCACTGTGACATCACCAGAGAGAGGGTGGCTGAGAGAGGGGTCCCCTGGAGGGCTGCGCTGGCCAGCTCAGCCCGCAGCTG

Query  501  GCCCACGTAGTGCAGCAGCTCCTCCAGGCTCCGCTCACAGTGCTGCCCGTAGGTCAGGAACTTCTGCAGGACCTTGTCCAGCTCTCTCTCCACGCACGCA
            ||||||||||||||||||||||||||||||||||||||||||||||||||||||||||||||||||||||||||||||||||||||||||||||||||||
Sbjct  291  GCCCACGTAGTGCAGCAGCTCCTCCAGGCTCCGCTCACAGTGCTGCCCGTAGGTCAGGAACTTCTGCAGGACCTTGTCCAGCTCTCTCTCCACGCACGCA

Query  601  CACTGCTCCAT  611
            ||||||||||
Sbjct  191  CACTGCTCCAT  181
```

(B)

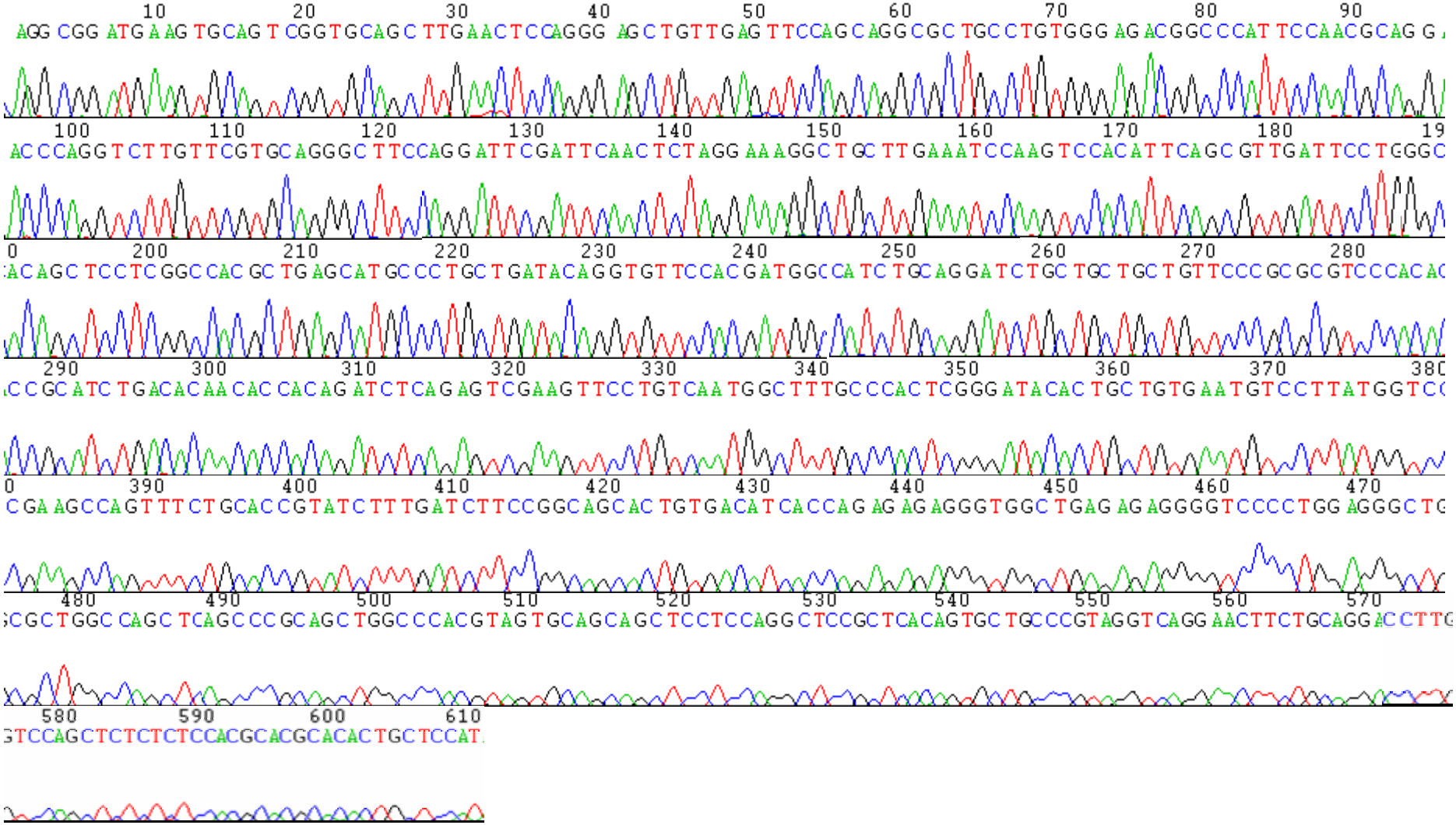

Figure 5.3 Representative sequence and chromatograph of FLJ22318. **(A)** FLJ22318-pcDNA3.1/V5-His-TOPO Clone A4 was sequenced using the FLJREV2 antisense primer and analysed using BLAST™ (http://www.ncbi.nlm.nih.gov/blast/Blast.cgi#34147687). **(B)** Corresponding chromatograph of FLJ22318-pcDNA3.1/V5-His-TOPO Clone A4 (http://www.technelysium.com.au/chromas.html).

5.2.1.2 Construction of the pGEX2TK-FLJ22318 Vector

5.2.1.2.1 PCR Optimisation with *Taq* Polymerase

In order to clone FLJ22318 into the pGEX2TK cloning vector, full-length FLJ22318 was amplified from the FLJ22318-pcDNA3.1/V5-His-TOPOA4 vector using FLJBamHI sense and FLJBamHI antisense primers (section 5.2.1.1.1). This PCR resulted in insertion of *BamH* I restriction sites at both ends of the coding region to enable ligation of FLJ22318 into *BamH* I digested pGEX2TK.

PCR conditions were similar to those initially used for amplification of FLJ22318 (section 5.2.1.1.1) however multiple bands were observed at all $MgCl_2$ concentrations tested including a band at the correct molecular size of ~1200bp (Figure 5.4A). The number of PCR cycles was reduced to 30 to decrease the number of products amplified and this resulted in the amplification of a fragment of the correct molecular size (~1200bp) using a $MgCl_2$ concentration of 1.0mM (Figure 5.4B). Following amplification, the FLJ22318 fragments were purified and the concentration determined from the gel to be 50ng/µL (section 3.1.5; results not shown).

5.2.1.2.2 Preparation of pGEX2TK Vector

To enable FLJ22318 to be ligated into pGEX2TK, the vector was linearised by digestion with *BamH* I (section 3.2.2). Following digestion, 20µL of linearised plasmid was treated with calf intestinal alkaline phosphatase (CIAP) to remove the 5' phosphate groups from the DNA, preventing vector self re-ligation. Following CIAP treatment, the plasmid was purified, 5µL was electrophoresed in a 2% agarose gel and the concentration estimated to be 10ng/µL (section 3.1.5; Figure 5.5C).

5.2.1.2.3 Cloning of FLJ22318 into pGEX2TK

Fifty ng (1.0µL) of the FLJ22318 fragment was initially ligated into 2µL (50ng) of the pCR®2.1 plasmid and 2µL of the ligation reaction was transformed into competent DH5α *E. coli* bacteria (sections 5.2.1.2.1; 3.2.4; 3.2.6). Transformants were selected on LB agar/ampicillin/X-Gal plates from which 23 white colonies were picked and grown in small-scale cultures (section 3.3.1). These colonies were screened by PCR for the presence of the FLJ22318 insert using the FLJBamHI sense and antisense primers (section 3.1.3; Figure 5.5A). Of the clones screened, plasmid DNA was isolated from

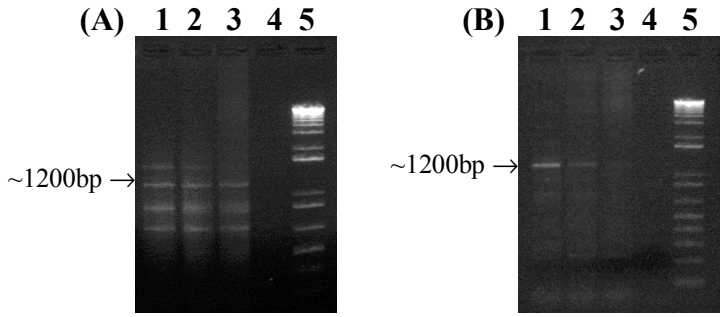

Figure 5.4 Optimisation of PCR conditions for FLJ22318 amplification using *Taq* polymerase. **(A)** Amplification of FLJ22318 from the FLJ22318-pcDNA3.1/V5/His TOPO vector with BamHI sense and anti-sense primers using an annealing temperature of 65°C, 40 PCR cycles and varying concentrations of $MgCl_2$ resulted in multiple bands including a band of the correct molecular size of ~1200bp **(B)** To decrease the products amplified the number of PCR cycles was reduced to 30 resulting in amplification of a single product at the correct size for FLJ22318 using 1.0mM $MgCl_2$.

(A)	1	1.0mM $MgCl_2$	**(B)**	1	1.0mM $MgCl_2$
	2	1.5mM $MgCl_2$		2	1.5mM $MgCl_2$
	3	2.0mM $MgCl_2$		3	2.0mM $MgCl_2$
	4	-ve control (no cDNA)		4	-ve control (no cDNA)
	5	1Kb Plus™ DNA Ladder		5	1Kb Plus™ DNA Ladder

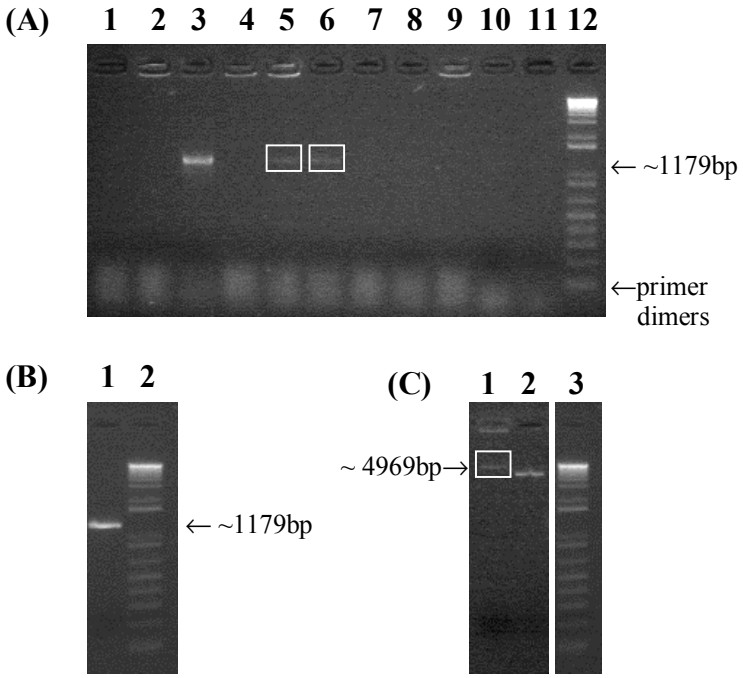

Figure 5.5 Construction of pGEX2TK-FLJ22318. To construct the pGEX2TK-FLJ22318 vector, **(A)** 50ng of purified FLJ22318 amplified from pcDNA3.1/V5-His-TOPO clone A4 with FLJBamHI sense and anti-sense primers was ligated into pCR2.1®. pCR®2.1-FLJ22318 transformants were blue/white selected on LB agar/ampicillin/X-Gal plates from which 23 colonies were grown in small-scale cultures and PCR screened identifying FLJ22318 inserts in clones F13, F15, and F16. **(B)** A 5µL aliquot of *BamH* I digested and purified pCR2.1®-FLJ22318 clone F13 was electrophoresed in a 2% agarose gel and its concentration was estimated from the gel to be 50ng/µL. **(C)** The pGEX2TK plasmid was *BamH* I digested, CIAP treated and purified. 5µL of the prepared plasmid was electrophoresed in a 2% agarose gel and its concentration was estimated from the gel to be 10ng/µL.

(A) 1-10 pCR®2.1-FLJ22318 transformants F11-F20
11 -ve control (no cDNA)
12 1Kb Plus™ DNA Ladder

(B) 1 Purified *BamH* I digested FLJ22318 fragment (50ng/µL)
2 1Kb Plus™ DNA Ladder

clones F13, F15 and F16 which contained FLJ22318 inserts and glycerol stocks were prepared of these bacteria. These 3 clones were *BamH* I digested from pCR®2.1 and an aliquot of the digest electrophoresed to confirm the presence of a ~1200bp fragment corresponding to FLJ22318 (results not shown). Multiple *BamH* I digests of the pCR2.1®2.1-FLJ22318F13 vector were performed (section 3.2.2), the digested plasmid was electrophoresed in a 2% agarose gel and the 1179bp fragment corresponding to FLJ22318 was gel extracted and purified (results not shown). Following purification, a 5µL aliquot was visualised in a 2% agarose gel and its concentration determined from the gel to be ~50ng/µL (Figure 5.5B).

Thity-five ng (0.7µL) of the FLJ22318 insert was ligated into 50ng (5.0µL) of the *BamH* I cut and CIAP treated pGEX2TK plasmid (section 5.2.1.2.2), and 2µL of the ligation reaction was transformed into competent DH5α *E. coli* (sections 3.2.5; 3.2.6). Transformants were selected on LB/agar/ampicillin plates from which 13 were picked into small-scale cultures and PCR screened for the presence of a FLJ22318 insert using the pGEX sense and antisense primers (section 3.1.3; Figure 5.6A). Of the clones PCR screened, plasmid DNA was isolated from clones H3, H6, H7, H10 and H12 which contained FLJ22318 inserts and glycerol stocks were prepared of these bacterial clones. Following *Rsa* I digestion of plasmids isolated from these 5 clones, fragments of the expected sizes of approximately 845bp, 916bp, 1985bp and 2132bp, which indicated ligation of the FLJ22318 insert in the sense orientation, were seen in clones H7, H10 and H12 (Figure 5.6B). *Rsa* I digestion of plasmid DNA isolated from clones H3 and H6 produced fragments of approximately 1455bp, 1985bp and 2132bp, which corresponded to the size of the pGEX2TK vector containing the FLJ22318 insert in the antisense orientation (Figure 5.6B).

To verify that the cloned insert was FLJ22318, plasmid DNA isolated from clone H10 was purified and sequenced using the pGEX sense primer then analysed using BLAST™ (sections 3.1.5; 3.4). The sequence from clone H10 was found to encode ~500bp of the 1179bp ORF of FLJ22318 cloned in frame into pGEX2TK in the sense orientation (results not shown). To obtain the remaining 679bp of the ORF, the FLJREV and pGEX antisense primers were used in additional sequencing reactions (results not shown). Upon completion of sequencing, clone H10 was found to contain the correct

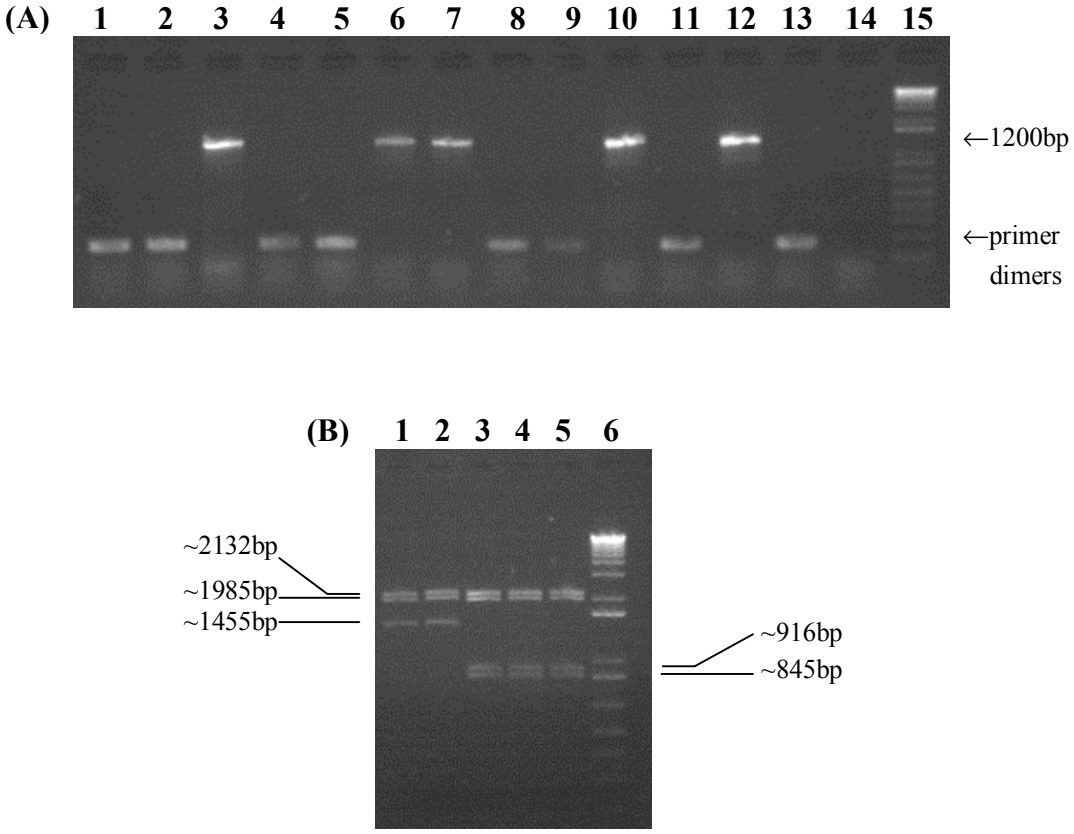

Figure 5.6 Screening of pGEX2TK-FLJ22318 transformants. **(A)** PCR screen of pGEX2TK-FLJ22318 transformants using pGEX sense and anti-sense primers identified ligation of the 1179bp FLJ22318 insert in clones H3, H6, H7, H10 and H12. **(B)** Rsa I digestion of plasmid DNA isolated from clones H3, H6, H7, H10 and H12 visualised in a 2% agarose gel. The presence of bands at 1455bp, 1985bp and 2132bp indicated ligation of the FLJ22318 insert in the anti-sense orientation (clones H3 and H6), while bands at 845bp, 916bp, 1985bp and 2132bp indicated that the FLJ22318 insert was in the sense orientation (clones H7, H10 and H12).

(A) 1-13 Clones E4-E9
14 -ve control (no cDNA)
15 1Kb Plus™ DNA Ladder

(B) 1-2 *Rsa* I digest of clones H3 and H6
3-5 *Rsa* I digest of clones H7, H10 and H12 respectively
6 1Kb Plus™ DNA Ladder

FLJ22318 sequence and large-scale cultures of this clone were grown from the glycerol stock and the plasmid DNA isolated for use in GST pull-down assays (sections 3.2.7; 3.3.2; 3.8).

5.2.1.3 Construction of the pGBKT7-FLJ22318 Bait Vector

5.2.1.3.1 PCR Optimisation with *Pfu* Polymerase

Full-length FLJ22318 was amplified from the FLJ22318-pcDNA3.1/V5-His-TOPOA4 vector using FLJSalI sense and FLJSalI antisense primers for cloning into the pGBKT7 vector (section 5.2.1.1.1). This amplification would insert *Sal* I restriction sites at both ends of the coding region enabling ligation of FLJ22318 into *Sal* I digested pGBKT7. To eliminate mutations, the FLJ22318 fragment was amplified using *Pfu* polymerase as this enzyme, unlike *Taq* polymerase, has 3' → 5' exonuclease (proof-reading) activity. Amplified PCR fragments were then ligated into the pCR®2.1 cloning vector and sub-cloned into pGBKT7.

PCR conditions were similar to those used for *Taq* polymerase cloning of FLJ22318 into pcDNA3.1/V5-His-TOPO (section 5.2.1.1.1), however the annealing time was reduced to 30 seconds and the extension time increased to 2.5 minutes according to the manufacturer's recommendations. When 35 PCR cycles were used, no fragments were amplified using these conditions (results not shown). Therefore the annealing time was increased to 1 minute and the extension time increased to 3 minutes and using these cycling conditions a fragment of the correct molecular size (1179bp) was amplified (Figure 5.7A). Following PCR amplification, the reaction was incubated with *Taq* polymerase to add 3' adenines to the FLJ22318 fragment, which is required for ligation into the pCR®2.1 plasmid (section 3.1.3). The amplified fragment was purified (section 3.1.5), a 5µL aliquot of the purified fragment was electrophoresed in a 2% agarose gel and its concentration was estimated from the gel to be 50µg/µL (Figure 5.7B).

5.2.1.3.2 Preparation of pGBKT7 Vector

To enable FLJ22318 to be ligated into pGBKT7, the pGBKT7 cloning vector was linearised by digestion with *Sal* I (section 3.2.2). Following digestion, 20µL of the linearised plasmid was treated with CIAP as previously described (section 3.2.3),

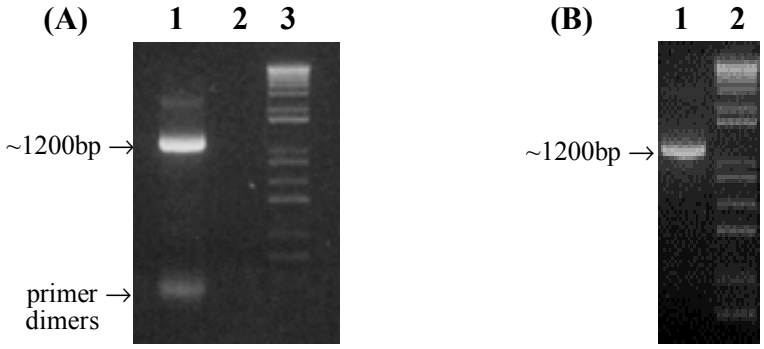

Figure 5.7 PCR Optimisation of FLJ22318 amplification using *Pfu* polymerase and FLJSalI sense and anti-sense primers. **(A)** Full length FLJ22318 was amplified from the FLJ22318-pcDNA3.1/V5/His TOPO vector using an annealing temperature of 65°C, annealing time of 1 minute, extension time of 3 minutes and 35 PCR cycles. **(B)** 50µL of amplified FLJ22318 product was incubated with *Taq* polymerase to add 3' adenines to the FLJ22318 fragment for ligation into the pCR®2.1 vector then purified. 5µL of the purified PCR product was electrophoresed in a 2% agarose gel and its concentration was estimated from the gel to be 50ng/µL.

(A)	1	*Pfu* polymerase amplified FLJ22318
	2	-ve control (no cDNA)
	3	1Kb Plus™ DNA Ladder
(B)	1	Purified FLJ22318 PCR fragment (50ng/µL)
	2	1Kb Plus™ DNA Ladder

purified and 5µL was electrophoresed in a 2% agarose gel (section 3.1.5). The plasmid concentration was estimated from the gel to be 45ng/µL (Figure 5.8A).

5.2.1.3.3 Cloning of FLJ22318 into pGBKT7

Fifteen ng (0.3µL) of the FLJ22318 fragment was ligated into 1µL (50ng) of the pCR®2.1 plasmid and 2µL of the ligation reaction was transformed into competent TOP10 *E. coli* bacteria (sections 5.2.1.3.1; 3.2.4; 3.2.6). Transformants were selected on LB agar/ampicillin/X-Gal plates from which 10 white colonies were picked and grown in small-scale cultures then PCR screened for the presence of the FLJ22318 insert using the FLJSalI sense and FLJSalI antisense primers (sections 3.1.3; 3.3.1). Of the 10 clones PCR screened, plasmid DNA was isolated from clones C1, C6, C8 and C9 which contained FLJ22318 inserts and glycerol stocks of these bacteria were prepared (Figure 5.8B). The clones were *Sal* I digested from pCR®2.1 and an aliquot of the digest electrophoresed to confirm the presence of a ~1200bp fragment corresponding to FLJ22318 (results not shown). In order to clone FLJ22318 into the pGBKT7 vector, multiple *Sal* I digests of the pCR2.1®2.1-FLJ22318C9 vector were performed and the digested plasmid was electrophoresed in a 2% agarose gel (section 3.2.2; results not shown). The 1179bp fragment corresponding to FLJ22318 was excised from the gel, purified and its concentration determined from the gel to be 30ng/µL (Figure 5.8C).

Forty-eight ng (1.6µL) of the FLJ22318 insert was ligated into 100ng (2.2µL) of the *Sal* I cut and CIAP treated pGBKT7 (section 5.2.1.3.2; Figure 5.8A), and 6µL of the ligation reaction was transformed into competent DH5α *E. coli* (section 3.2.5; 3.2.6). Transformants were selected on LB/agar/kanamycin plates producing 9 colonies of which 3 were picked into small-scale cultures and the plasmid DNA isolated (section 3.3.1), RNase treated, then *Hin*d III digested to screen for the presence of a FLJ22318 insert (section 3.2.2). Following *Hin*d III digestion of plasmids isolated from these 3 clones, fragments of the expected sizes of approximately 1498bp, 2368bp and 4938bp, which corresponded to the size of the pGBKT7 vector containing FLJ22318 insert, were seen in clone E3 (Figure 5.9A). *Hin*d III digestion of plasmid DNA isolated from clones E1 and E2 produced 3 fragments of approximately 868bp, 1498bp and 4938bp, which corresponded to the size of the pGBKT7 vector without insert (Figure 5.9A).

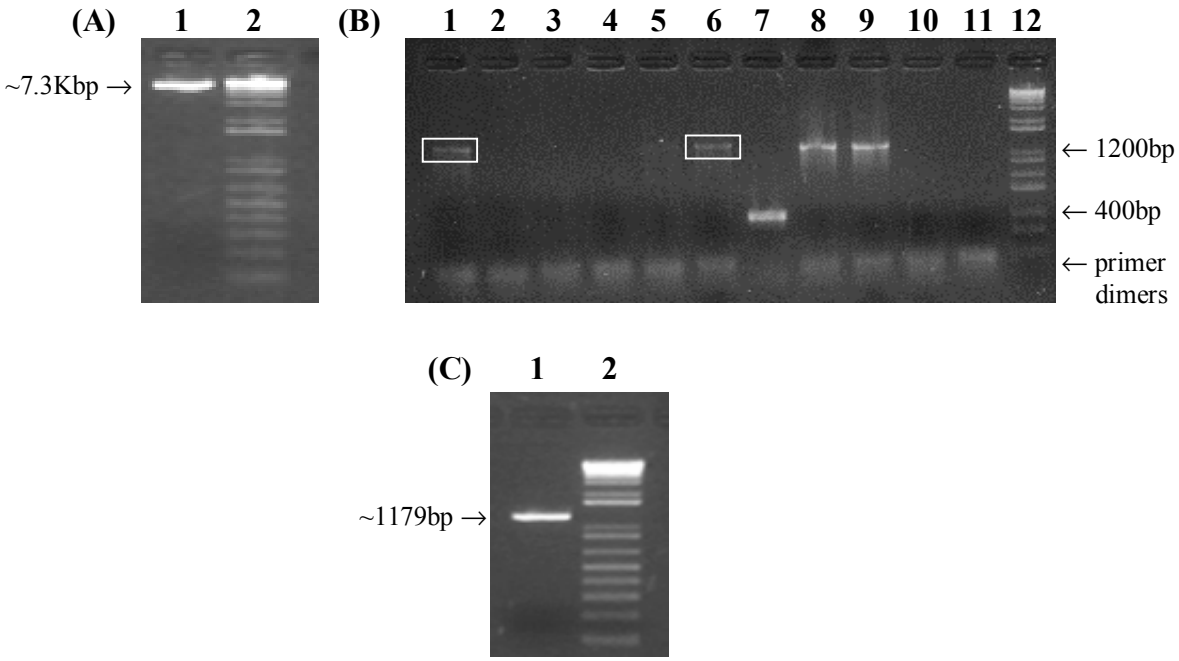

Figure 5.8 Construction of the pGBKT7-FLJ22318 bait vector. To construct the pGBKT7-FLJ22318 vector, **(A)** the pGBKT7 plasmid was *Sal* I digested, CIAP treated and purified. 5µL of the prepared plasmid was electrophoresed in a 2% agarose gel and its concentration was estimated from the gel to be 45ng/µL. **(B)** 10 pCR®2.1-FLJ22318 transformants were picked and grown in small scale cultures and 1µL of the bacterial culture PCR amplified using FLJSalI sense and anti-sense primers identifying FLJ22318 inserts of ~1200bp in clones C1, C6, C8 and C9. **(C)** 80µL of *Sal* I digested pCR2.1®-FLJ22318 was electrophoresed in a 2% agarose gel and the 1179bp fragment corresponding to FLJ22318 excised and purified. 5µL of the purified plasmid was electrophoresed in a 2% agarose gel and its concentration was estimated from the gel to be 30ng/µL.

(A) 1 Purified *Sal* I digested and CIAP treated pGBKT7 (45ng/µL)
2 1Kb Plus™ DNA Ladder

(B) 1-10 pCR®2.1-FLJ22318 transformants C1-C10
11 -ve control (no cDNA)
12 1Kb Plus™ DNA Ladder

(C) 1 Purified *Sal* I digested FLJ22318 fragment (30ng/µL)
2 1Kb Plus™ DNA Ladder

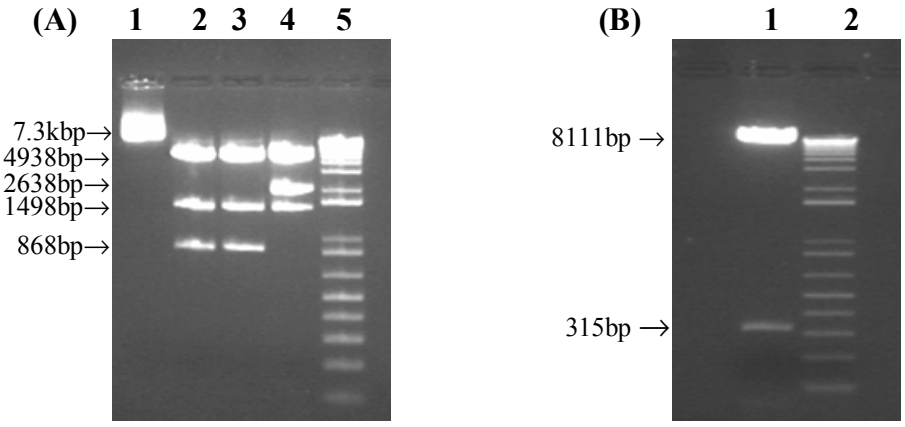

Figure 5.9 Screening of pGBKT7-FLJ22318 clones. **(A)** Undigested pGBKT7 (7.3kbp) and *Hin*dIII digested clones E1, E2 and E3 were electrophoresed in a 2% agarose gel. The presence of bands at 868bp, 1498bp and 4938bp indicated pGBKT7 vector without insert (clones E1 and E2) whereas bands at 1498bp, 2368bp and 4938bp indicated presence of a FLJ22318 insert in the pGBKT7 vector (clone E3). (B) To determine the orientation of the FLJ22318 insert, clone E3 was digested with *Pst* I and electrophoresed in a 2% agarose gel. The presence of bands at 315bp and 8111bp indicated ligation of the FLJ22318 insert in the anti-sense orientation.

(A) 1 Undigested pGBKT7 control
2 *Hin*dIII digested clone E1
3 *Hin*dIII digested clone E2
4 *Hin*dIII digested clone E3
5 1Kb Plus™ DNA Ladder

(B) 1 *Pst* I digested clone E3
2 1Kb Plus™ DNA Ladder

Clone E3 containing the FLJ22318 insert was then digested with *Pst* I to determine the orientation of FLJ22318 in the pGBKT7 vector. Electrophoresis of the *Pst* I digested E3 plasmid produced fragments of 315bp and 8111bp, which indicated that the insert was ligated in the antisense orientation (Figure 5.9B). The remaining 6 colonies were then picked into small-scale cultures and PCR screened for the presence of FLJ22318 using FLJSalI sense and antisense primers (section 3.3.1; 3.1.3). Of these clones, only clone E5 contained a FLJ22318 insert (Figure 5.10A). Plasmid DNA was isolated from this clone, RNase treated, and *Pst* I digested to determine the orientation of the FLJ22318 insert. The presence of bands at 315bp, 827bp and 7341bp confirmed ligation of the FLJ22318 insert in the sense orientation (Figure 5.10B).

To confirm the identity of this insert, clone E5 was purified (section 3.1.5), sequenced using the DNA-BD sense primer (section 3.4) and analysed using BLAST™ which confirmed 818bp of the ORF sequence of FLJ22318 that was in frame and contained no mutations (results not shown). To obtain the remaining 361bp of the ORF, the FLJ789 sense primer was used in additional sequencing reactions (section 3.4). Upon completion of sequencing, it was confirmed that clone E5 contained the correct FLJ22318 sequence, therefore glycerol stocks were prepared of this clone (section 3.2.7; sequencing not shown). Large-scale cultures of clone E5 were grown from the glycerol stock to be used for small-scale yeast transformations (section 3.5.4).

5.2.1.4 Construction of the pCMV-Myc-FLJ22318 Vector

5.2.1.4.1 PCR Optimisation with *Pfu* Polymerase

In order to clone FLJ22318 into the pCMV-Myc cloning vector, full-length FLJ22318 was amplified from the FLJ22318-pcDNA3.1/V5-His-TOPOA4 cloning vector using pCMV sense and FLJSalI antisense primers (section 5.2.1.1.1. These primers inserted *Sal* I restriction sites at both ends of the coding region enabling ligation of FLJ22318 into the (*Sal* I digested) pCMV-Myc mammalian expression plasmid, which encodes an N-terminal c-Myc epitope. Amplified PCR fragments were ligated into the pCR®2.1 cloning vector prior to sub-cloning into pCMV-Myc.

PCR conditions were optimised as previously described with a band of the correct molecular weight of ~1200bp amplified using a DNA extension time of 3 minutes, an

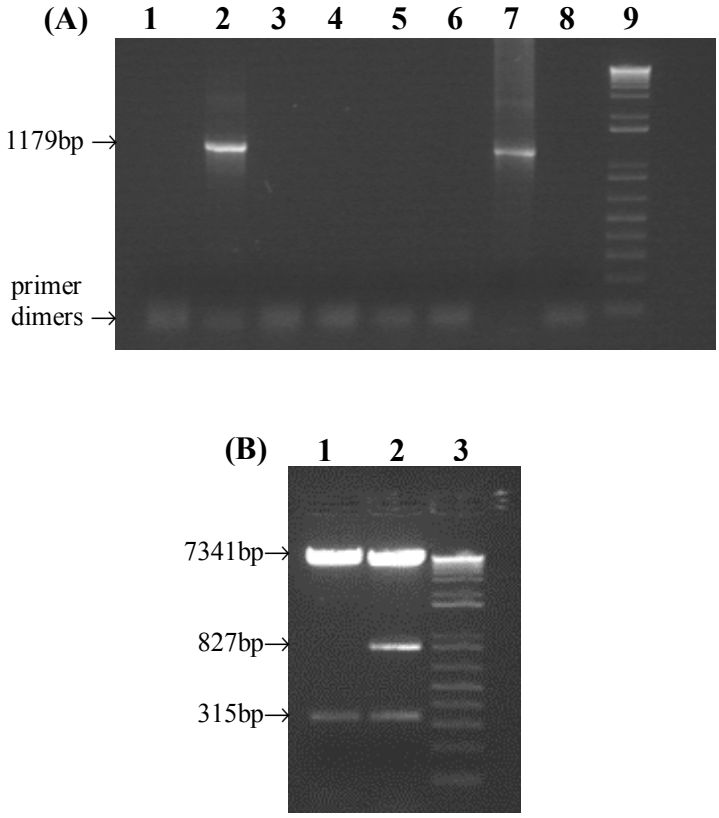

Figure 5.10 Identification of pGBKT7 containing a FLJ22318 insert. **(A)** Six pGBKT7-FLJ22318 transformed colonies were screened directly by PCR for the presence of a FLJ22318 insert using 1μL of bacterial culture as target DNA. Amplification of a 1179bp product indicated that FLJ22318 had been ligated into pGBKT7 (clone E5). **(B)** To determine the orientation of the FLJ22318 insert, clone E5 was digested with *Pst* I. The presence of bands at 315bp, 827bp and 7341bp indicated ligation of the FLJ22318 insert in the sense orientation (clone E5), while bands at 315bp and 8111bp indicated that the FLJ22318 insert was in the anti-sense orientation (clone E3).

(A) 1-6 Clones E4-E9
7 Positive control (clone E3)
8 -ve control (no cDNA)
9 1Kb Plus™ DNA Ladder

(B) 1 *Pst* I digested clone E3
2 *Pst* I digested clone E5
3 1Kb Plus™ DNA Ladder

annealing temperature of 65°C and 35 cycles of PCR (section 5.2.1.3.1; results not shown). Following amplification and incubation with *Taq* polymerase (section 3.1.3), the FLJ22318 fragments were purified (section 3.1.5), a 5µL aliquot was electrophoresed in a 2% agarose gel and the DNA concentration was determined from the gel to be 50ng/µL (results not shown).

5.2.1.4.2 Preparation of the pCMV-Myc Vector

To enable FLJ22318 to be ligated into pCMV-Myc, the pCMV-Myc cloning vector was linearised by digestion with *Sal*I (section 3.2.2). Following digestion, 20µL of linearised plasmid was CIAP treated, purified and 5µL electrophoresed in a 2% agarose gel and the concentration estimated from the gel to be 10ng/µL (section 3.1.4; results not shown).

5.2.1.4.3 Cloning of FLJ22318 into pCMV-Myc

Following purification, 15ng (0.3µL) of the FLJ22318 fragment (section 5.2.1.4.1) was ligated into 1µL (50ng) of the pCR®2.1 cloning vector and 2µL of the ligation reaction was transformed into competent TOP10 *E. coli* bacteria (sections 3.2.4; 3.2.6). Transformants were selected on LB agar/ampicillin/X-Gal plates from which 20 white colonies were picked and grown in small-scale cultures then PCR screened for the presence of the FLJ22318 insert using the pCMV sense and FLJSalI antisense primers (sections 3.1.3; 3.3.1; Figure 5.11). Of the 20 colonies PCR screened, glycerol stocks were prepared for clones B13-B15 and B17-B19 which contained FLJ22318 inserts. Plasmid DNA was isolated from these 6 clones (section 3.3.1), RNase treated, multiple *Sal* I digests of clone B14 were electrophoresed in a 2% agarose gel and the 1179bp fragment representing FLJ22318 was gel extracted and purified (section 3.1.6). Following purification, a 5µL aliquot of the FLJ22318 fragment was visualised in a 2% agarose gel and its concentration determined from the gel to be 25ng/µL (section 3.1.4; results not shown).

Forty ng (1.6µL) of the FLJ22318 insert was ligated into 50ng (5µL) of the *Sal* I cut and CIAP treated pCMV-Myc plasmid (section 5.2.1.4.2), and 2µL of the ligation reaction was transformed into competent TOP10 *E. coli* (sections 3.2.5; 3.2.6). Transformants were selected on LB/agar/ampicillin plates producing 40 colonies of which 30 were

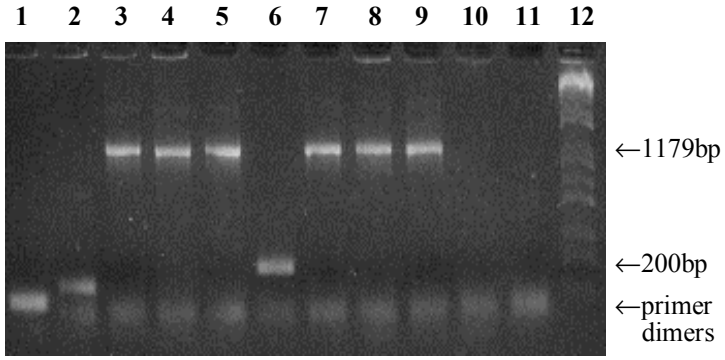

Figure 5.11 PCR screen for FLJ22318 in pCR®2.1. Twenty pCR®2.1-FLJ22318 transformants were picked and grown in small scale cultures. 1µL of each bacterial culture was PCR amplified using pCMV sense and FLJSalI antisense primers identifying FLJ22318 inserts of 1179bp in clones B13, B14, B15, B17, B18 and B19.

1-10 pCR®2.1-FLJ22318 transformants B11-B20
13 -ve control (no cDNA)
14 1Kb Plus™ DNA Ladder

picked into small-scale cultures and screened by PCR for the presence of the FLJ22318 insert as previously described (section 3.1.3; Figure 5.12A). Of the 30 colonies screened, only 2 clones, D31 and D37, contained FLJ22318 inserts. Plasmid DNA was isolated from these 2 clones, RNase treated, then *Pst I* digested to confirm the presence and orientation of the FLJ22318 insert (sections 3.2.2; 3.3.1). Electrophoresis of the *Pst* I digested plasmids identified fragments of the expected sizes of approximately 315bp, 918bp, 1071bp and 2665bp from clone D37, which corresponded to the size of the pCMV-Myc plasmid containing FLJ22318 insert in the sense orientation (Figure 5.12B). *Pst* I digestion of plasmid DNA isolated from clone D31 produced 2 fragments of approximately 1126bp and 2665bp, which corresponded to the size of the pCMV-Myc vector without insert (Figure 5.12B).

To confirm the identity of this insert, clone D37 was purified and sequenced using the pCMV sense primer (sections 3.1.5; 3.4) then analysed using BLAST™ which confirmed the presence of 775bp of the ORF sequence of FLJ22318 inserted in frame into pCMV-Myc (results not shown). To obtain the remaining 404bp of the ORF, the FLJREV and FLJ789 sense primers were used in additional sequencing reactions (section 3.4). Results of sequencing indicated that the pCMV-Myc-FLJ22318 insert did not contain any mutations and glycerol stocks were prepared (section 3.2.7; sequencing results not shown). An aliquot of glycerol stock from clone D37 was grown in a large-scale culture, the plasmid DNA isolated and the concentration determined spectrophotometrically to be 185ng/µL (sections 3.3.2; 3.3.3).

5.2.1.5 Construction of the pCMV-HA-FLJ22318 Vector

5.2.1.5.1 Preparation of the pCMV-HA Vector

To enable FLJ22318 to be ligated into pCMV-HA, the pCMV-HA vector was prepared by digestion with *Sal* I and 20µL of the linearised plasmid was CIAP treated (section 3.2.3). Following purification, a 5µL aliquot of the prepared vector was electrophoresed in a 2% agarose gel and the concentration estimated from the gel to be 10ng/µL (section 3.1.4; results not shown).

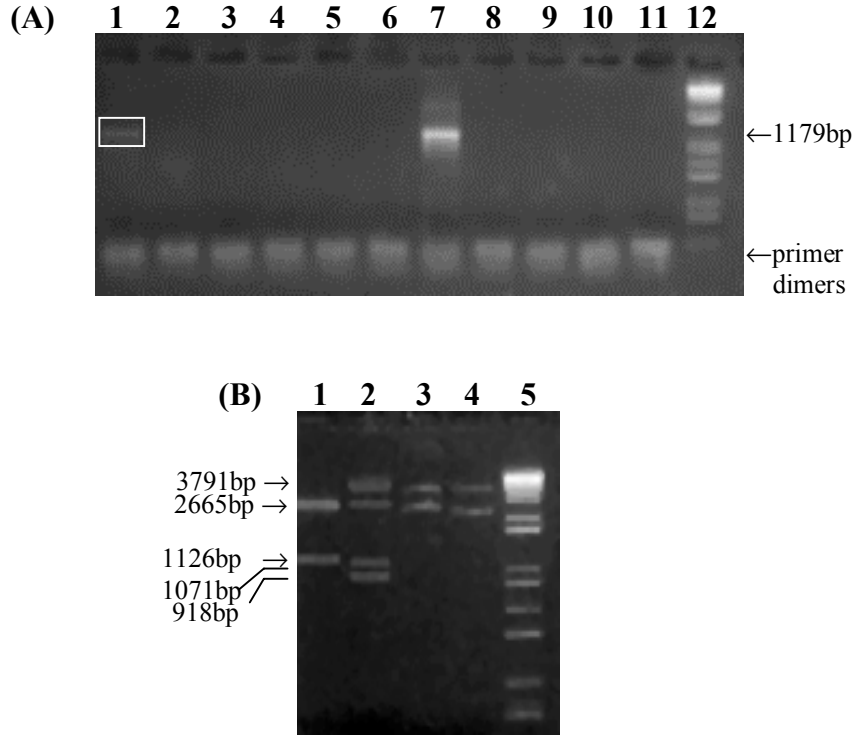

Figure 5.12 Screening of pCMV-Myc-FLJ22318 clones. **(A)** Thirty pCMV-Myc-FLJ22318 transformants were picked and grown in small scale cultures. 1µL of each bacterial culture was PCR amplified using pCMV sense and FLJSalI anti-sense primers, identifying FLJ22318 inserts of 1179bp in clones D31 and D37. **(B)** To determine the orientation of the insert, clones D31 and D37 were digested with *Pst* I. The presence of bands at 1126bp and 2665bp indicated pCMV-Myc vector without insert (clone D31), whereas bands at 918bp, 1071bp and 2665bp indicated the presence of the FLJ22318 insert in pCMV-Myc in the sense orientation (clone D37).

(A)	1-10	pCMV-Myc-FLJ22318 transformants D31-D40
	11	-ve control (no cDNA)
	12	1Kb Plus™ DNA Ladder
(B)	1	*Pst* I digested clone D31
	2	*Pst* I digested clone D37
	3	Undigested pCMV-Myc-FLJ22318 control
	4	Undigested pCMV-Myc-FLJ22318 control
	5	1Kb Plus™ DNA Ladder

5.2.1.5.2 Cloning of FLJ22318 into pCMV-HA

In order to clone FLJ22318 into the pCMV-HA vector, multiple *Sal*I digests of the pCR2.1®2.1-FLJ22318B14 vector were performed and the digested plasmid was electrophoresed in a 2% agarose gel (section 5.2.1.4.3; results not shown). The 1179bp fragment corresponding to FLJ22318 was excised from the gel, purified and its concentration determined from the gel to be 25ng/µL (results not shown). Fifteen ng (0.6µL) of the FLJ22318 insert was ligated into 100ng (5.0µL) of the *Sal* I cut and CIAP treated pCMV-HA vector (section 5.2.1.5.1), and 2µL of the ligation reaction transformed into competent DH5α *E. coli* (sections 3.2.5; 3.2.6). Transformants were selected on LB/agar/ampicillin plates producing 29 colonies of which 13 were picked into small-scale cultures and screened by PCR for the presence of an FLJ22318 insert using the pCMV sense and FLJSalI antisense primers (section 5.2.1.4.3; Figure 5.13A). Following PCR screening, plasmid DNA was isolated from clone G7 (the only clone containing an insert) and *Pst* I digested (sections 3.3.1; 3.2.2) producing fragments of approximately 315bp, 909bp, 1071bp and 2665bp, which corresponded to the size of the pCMV-HA vector containing an FLJ22318 insert in the sense orientation (Figure 5.13B).

To confirm the identity of this insert, clone G7 was purified, sequenced using the pCMV sense primer (sections 3.1.5; 3.4) and analysed using BLAST™ which confirmed 530bp of the ORF sequence of FLJ22318 that was in frame and contained no mutations (results not shown). To obtain the remaining 649bp of the ORF, the FLJ789S sense and FLJREV antisense primers were used in additional sequencing reactions (section 3.4). Upon completion of sequencing, it was confirmed that clone G7 contained the correct FLJ22318 sequence, therefore glycerol stocks of this clone were prepared, large-scale cultures were grown from the glycerol stock and the plasmid DNA isolated (sections 3.2.7; 3.3.2).

5.2.1.6 Construction of the pEGFP-C2-FLJ22318 Vector

5.2.1.6.1 Preparation of pEGFP-C2 Vector

To enable FLJ22318 to be ligated into the pEGFP-C2 vector, pEGFP-C2 was *Sal* I digested and CIAP treated and a 5µL aliquot was visualised in a 2% agarose gel where the concentration was estimated to be 10ng/µL (sections 3.2.2; 3.2.3; Figure 5.14A).

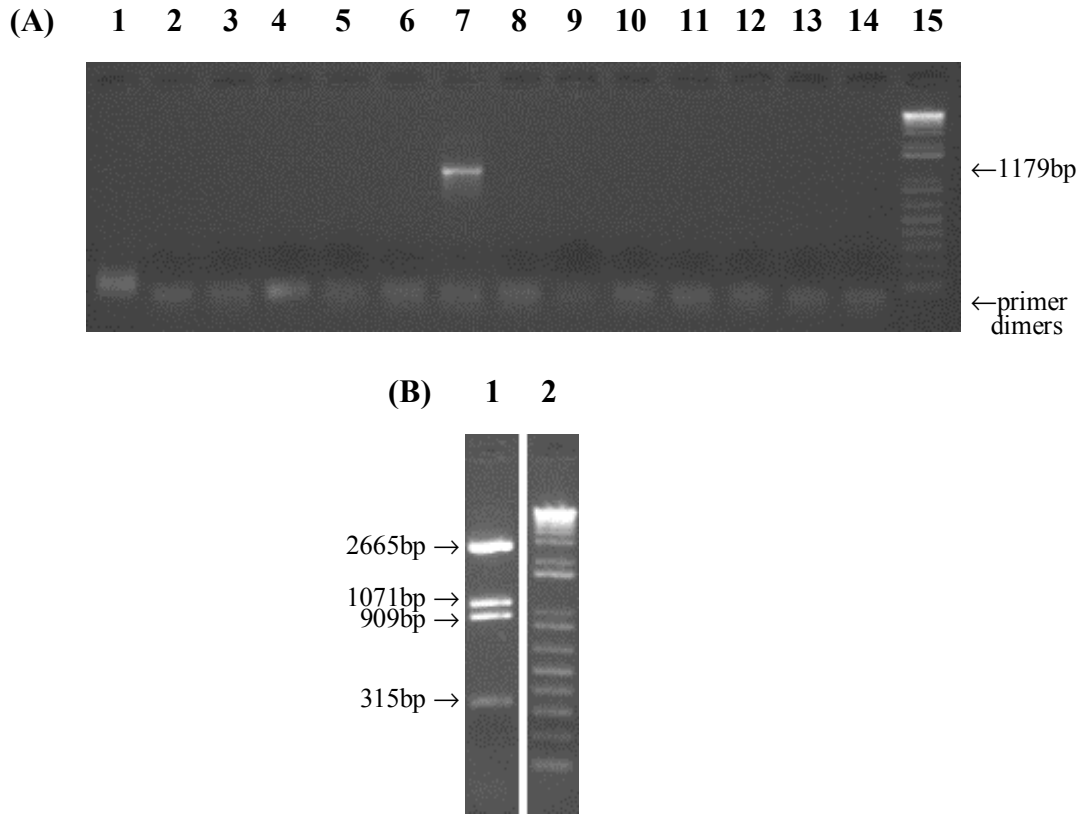

Figure 5.13 Screening of pCMV-HA-FLJ22318 clones. To screen for the presence of FLJ22318, 13 pCMV-HA-FLJ22318 transformants were picked and grown in small scale cultures. 1µL of the bacterial culture was amplified by PCR using the pCMV sense and FLJSalI anti-sense primers which identified an FLJ22318 insert in clone G7. **(B)** *Pst* I digested clone G7 was electrophoresed in a 2% agarose gel. The presence of bands at 315bp, 909bp, 1071bp and 2665bp indicated the presence of an FLJ22318 insert in the pCMV-HA vector in the sense orientation.

(A)	1-13	pCMV-HA-FLJ22318 transformants G1-G13
	14	-ve control (no cDNA)
	15	1Kb Plus™ DNA Ladder
(B)	1	*Pst* I digested clone G7
	2	1Kb Plus™ DNA Ladder

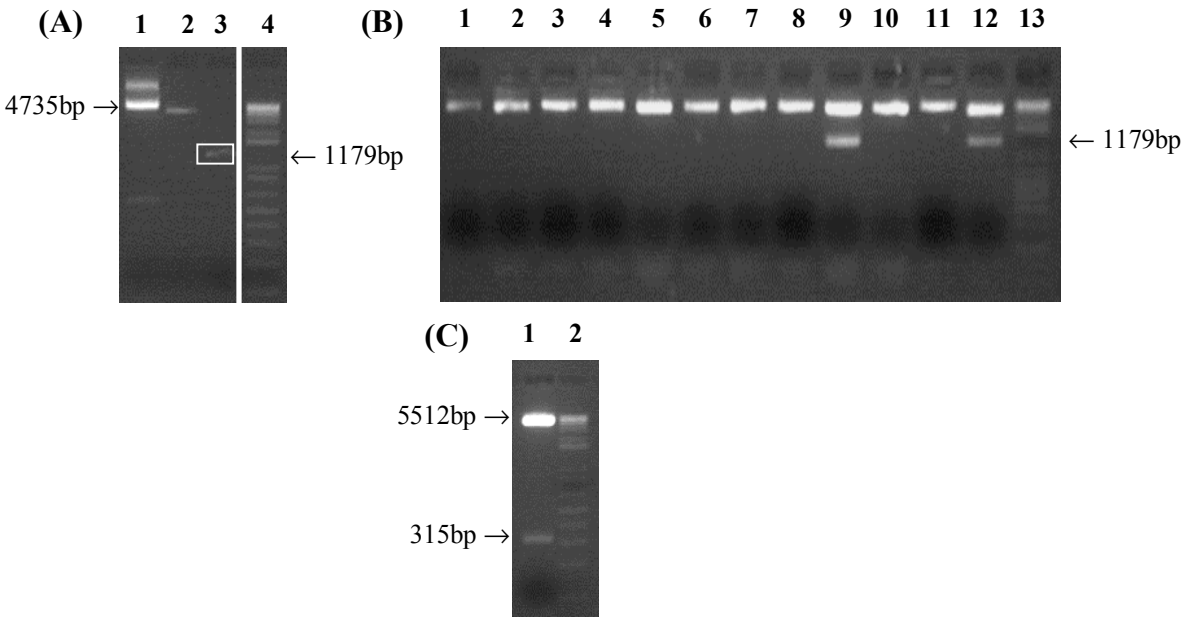

Figure 5.14 Construction of the pEGFP-C2-FLJ22318 vector. To construct the pEGFP-C2-FLJ22318 vector, **(A)** 1µg of the pEGFP-C2 plasmid was *Sal* I digested, CIAP treated and purified and 5µL of the prepared plasmid was electrophoresed in a 2% agarose gel. The concentration from the gel was estimated to be 10ng/µL. 20µL of *Sal* I digested pCR2.1®-FLJ22318 was electrophoresed in a 2% agarose gel and the 1179bp fragment corresponding to FLJ22318 excised and purified. 5µL of the purified plasmid was electrophoresed in a 2% agarose gel and its concentration was estimated from the gel to be 5ng/µL. **(B)** Twenty pEGFP-C2-FLJ22318 transformed colonies were grown from bacterial culture and the plasmid DNA isolated then *Sal* I digested to screen for the presence of a FLJ22318 insert. A band of the expected size for FLJ22318 (1179bp) indicated ligation of FLJ22318 into pEGFP-C2 clone I19. **(C)** To determine the orientation of the FLJ22318 insert, clone I19 was digested with *Pst* I. The presence of bands at 315bp and 5512bp indicated ligation of the FLJ22318 insert in the sense orientation.

(A) 1 Undigested pEGFP-C2 vector
2 Purified *Sal* I digested and CIAP treated pEGFP-C2 (10ng/µL)
3 Purified *Sal* I digested FLJ22318 fragment (5ng/µL)
4 1Kb Plus™ DNA Ladder

B) 1-10 Clones I11-I20
11 Negative control (clone I10)
12 Positive control (pCMV-HA-FLJ22318)
13 1Kb Plus™ DNA Ladder

(C) 1 *Pst* I digested clone I19
2 1Kb Plus™ DNA Ladder

5.2.1.6.2 Cloning of FLJ22318 into pEGFP-C2

In order to clone FLJ22318 into pEGFP-C2, multiple *Sal* I digests of the pCR2.1®-FLJ22318C8 vector were performed and the digested plasmid was electrophoresed in a 2% agarose gel (section 5.2.1.3.3; results not shown). The 1179bp fragment corresponding to FLJ22318 was excised from the gel, purified and its concentration determined from the gel to be 5ng/μL (Figure 5.14A). Fifteen ng (3.0μL) of the FLJ22318 insert was ligated into 50ng (5.0μL) of the prepared pEGFP-C2 vector and 5μL of the ligation reaction was transformed into competent DH5α *E. coli* (sections 5.2.1.6.1; 3.2.5; 3.2.6). Transformants were selected on LB/agar/kanamycin plates and 20 colonies were picked and grown into small-scale cultures. Plasmid DNA was isolated from these cultures and *Sal* I digested to screen for the presence of an FLJ22318 insert (sections 3.2.2; 3.3.1). Of the 20 clones screened, only one clone, I19 contained an insert of the correct size of ~1179bp (Figure 5.14B) and was further digested with *Pst* I to determine the orientation of FLJ22318 in the pEGFP-C2 vector. Electrophoresis of the *Pst* I digested I19 plasmid produced fragments of 315bp and 5512bp, indicating that the insert was ligated in the sense orientation (Figure 5.14C).

To confirm the identity of this insert, clone I19 was purified and sequenced using the EGFP 1266 sense primer and glycerol stocks were prepared (sections 3.1.5; 3.2.7; 3.4). Following sequencing, analysis using BLAST™ confirmed 893bp of the ORF sequence of FLJ22318 in frame with no mutations (results not shown). Therefore to obtain the remaining 286bp of the ORF, the FLJ789S sense primer was used in additional sequencing reactions (section 3.4). Upon completion of sequencing, it was confirmed that clone I19 contained the published FLJ22318 sequence, therefore large-scale cultures were grown from the glycerol stock and the plasmid DNA was isolated (section 3.3.2; sequencing results not shown).

5.2.2 Reverse Yeast Two-Hybrid Analysis

In order to confirm the results of the original yeast two-hybrid analysis that identified an interaction between NKX3-1 and FLJ22318, yeast two-hybrid analysis was repeated with NKX3-1 and FLJ22318 ligated into plasmids in the reverse order to that used in the original screen. As such, interaction of FLJ22318 in the pGBKT7 plasmid (section

5.2.1.3) and NKX3-1 in the pGADT7-Rec plasmid (available in the laboratory) was investigated in AH109 yeast.

5.2.2.1 pGBKT7-FLJ22318 Protein Expression

To verify FLJ22318 protein expression prior to the reverse yeast-two hybrid analysis, AH109 yeast cells were transformed with the pGBKT7-FLJ22318 construct using a small-scale yeast transformation which should result in expression of FLJ22318 as a fusion protein containing a c-Myc epitope tag (section 5.2.1.3; 3.5.4). Proteins were extracted 16 hours post transformation and analysed by anti-Myc western blotting (sections 3.7.1-3.7.4). Untransformed AH109 yeast cells did not exhibit immunoreactivity with the Myc epitope, while pGBKT7-FLJ22318 transformed AH109 cells exhibited Myc immunoreactivity with a protein band of ~45.6kDa, the expected size for Myc-FLJ22318 protein (Figure 5.15).

5.2.2.2 Transcriptional Activation of pGBKT7-FLJ22318

Prior to using pGBKT7-FLJ22318 to confirm an interaction with NKX3-1 in a reverse yeast two-hybrid analysis, it was also necessary to confirm that the construct did not have autonomous reporter gene activity in AH109 yeast cells. AH109 can only grow on SD/-Trp agar plates if a functional *TRP1* gene carried by pGBKT7-FLJ22318 is induced (positive transformation control) and should not grow on SD/-Ade/-His agar plates unless the *ADE2* and *HIS3* GAL4-responsive nutritional reporter genes carried by AH109 are activated (when the DNA-BD of the pGBKT7-FLJ22318 construct interacts with the AD of the pGADT7-Rec-NKX3-1 construct). Therefore to test the pGBKT7-FLJ22318 DNA-BD fusion for intrinsic transcriptional activation, AH109 yeast cells were made competent and transformed with pGBKT7-FLJ22318 or pGBKT7 empty vector using a small-scale yeast transformation (sections 3.5.3; 3.5.4). As AH109 also carries the endogenous *MEL1* reporter gene, whose gene product α-galactosidase is secreted into the culture medium where it catalyses the hydrolysis of X-α-Gal to yield a blue end product, transformants were selected on SD/-Trp, SD/-His/-Trp and SD/-Ade/-Trp dropout media plates to which X-α-Gal was added (section 3.5.9). As MEL1 should not be expressed without activation by GAL4, growth of white colonies only on the SD/-Trp media plate (Figure 5.16) and no growth on the SD/-His/-Trp and SD/-Ade/-Trp media plates (results not shown) confirmed that the pGBKT7-FLJ22318 bait protein

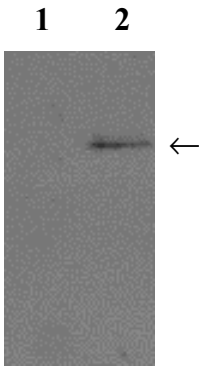

Figure 5.15 Expression of Myc-FLJ22318 in yeast. AH109 cells were transformed with pGBKT7-FLJ22318, which should result in expression of Myc-tagged FLJ22318. Anti-Myc western blotting of proteins extracted from pGBKT7-FLJ22318 transformed cells identified expression of a protein of the expected size of ~45.6kDa.

1 Untransfected AH109 yeast cells (negative control)

2 pGBKT7-FLJ22318 transformed AH109 yeast cells

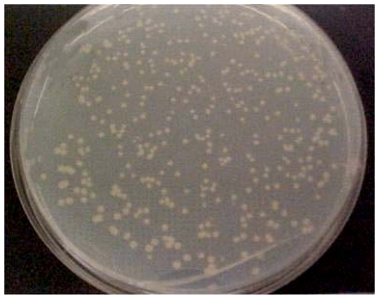

Figure 5.16 AH109 *S. cerevisiae* yeast transformed with pGBKT7-FLJ22318. Transformants were able to grow as white colonies only on SD/-Trp/X-α-Gal indicating a successful transformation with no autonomous activation of the endogenous yeast *MEL1* reporter gene.

was inactive and therefore suitable to use in a reverse yeast two-hybrid analysis. Similar results were obtained for AH109 cells transformed with pGBKT7 empty vector (results not shown). Following confirmation that the pGBKT7-FLJ22318 construct was inactive, glycerol stocks were prepared from a single white colony growing on the SD/-Trp media plate (section 3.5.7; Figure 5.16).

5.2.2.3 Toxicity of pGBKT7-FLJ22318

In addition to confirming that the bait protein was inactive, it was also important to examine whether the pGBKT7-FLJ22318 plasmid was toxic to yeast cells. Therefore, pGBKT7-FLJ22318 transformed AH109 yeast cells were grown from frozen stocks for 4 days at 30°C on SD/-Trp agar plates. From these cells a single large colony of approximately 2-3mm was cultured in SD/-Trp/Kan media (section 3.5.10) and the OD_{600} measured, an OD_{600} much less than 0.8 indicating the DNA-BD fusion may be toxic to the yeast cells. Following 20 hours of incubation, the OD_{600} of the pGBKT7-FLJ22318 transformed yeast was 1.08, suggesting that expression of FLJ22318 did not impede yeast growth.

5.2.2.4 Reverse Yeast Two-Hybrid Analysis

In the original yeast two-hybrid screen (section 1.3.3.7), an interaction between full length FLJ22318 and NKX3-1 was demonstrated by growth of yeast that were shown to contain the pGADT7-Rec-FLJ22318 and pGBKT7-NKX3-1 plasmids. In order to confirm the interaction between the two proteins, full length FLJ22318 and NKX3-1 were cloned into the pGBKT7 and pGADT7-Rec plasmids respectively, the reverse to that used in the original screen and used in a yeast two-hybrid assay.

For this screen, pGBKT7-FLJ22318 (section 5.2.1.3), pGADT7-Rec-NKX3-1 (prepared previously in this laboratory) and competent AH109 yeast were used in a small scale yeast co-transformation (sections 3.5.3; 3.5.4). To confirm that the pGBKT7-FLJ22318 and pGBKT7-FLJ22318/pGADT7-Rec-NKX3-1 plasmids had been successfully transformed, the transformation mixture was spread on SD/-Trp and SD/-Leu/-Trp Double Dropout (DDO) medium, whereas to select for co-transformants expressing interacting proteins the transformation mixture was spread on SD/-His/-Leu/-Trp Triple Dropout (TDO) and SD/-Ade/-His/-Leu/-Trp Quadruple Dropout (QDO) medium.

Following 4 days of incubation at 30°C, growth of white colonies was observed on the SD/-Trp media plates for the pGBKT7-FLJ22318 plasmid, whereas no growth was observed on the pGBKT7-FLJ22318/pGADT7-Rec-NKX3-1 DDO, TDO and QDO media plates (results not shown). Therefore, although transformation of pGBKT7-FLJ22318 had been successful, no growth on the DDO medium indicated that co-transformation of pGBKT7-FLJ22318 and pGADT7-Rec-NKX3-1 had been unsuccessful or that FLJ22318 and NKX3-1 did not interact in this assay.

As the pGBKT7-FLJ22318 construct was not toxic to yeast growth (section 5.2.2.3) it was decided to examine the interaction between FLJ22318 and NKX3-1 using sequential transformation of AH109 yeast. For the sequential transformation, AH109/pGBKT7-FLJ22318 yeast were made competent and a small scale transformation performed with the pGADT7-Rec-NKX3-1 construct (sections 5.2.2.4; 3.5.3; 3.5.4). To select for transformation of the pGADT7-Rec-NKX3-1 plasmid, the transformation mixture was spread on DDO media plates, whereas to select for pGBKT7-FLJ22318/pGADT7-Rec-NKX3-1 transformants expressing interacting proteins the transformation mixture was spread on TDO and QDO medium. Following 4 days of incubation at 30°C growth of colonies could be observed on the DDO media plates indicating that yeast colonies contained both the pGBKT7-FLJ22318 and pGADT7-Rec-NKX3-1 plasmids (Figure 5.17A). In addition, growth of colonies on the TDO media plates indicated the *HIS3* gene had been activated showing an interaction had occurred between FLJ22318 and NKX3-1 (Figure 5.17B). The presence of colonies on the QDO media plate indicated the *ADE2* gene had also been activated demonstrating a strong interaction between the two proteins (Figure 5.17C).

Following 4 days of growth, single colonies from each of these plates were replica plated together with yeast cultures containing transformed pGADT7-Rec-FLJ22318, pGBKT7-NKX3-1 and co-transformed pGADT7-Rec-FLJ22318/pGBKT7-NKX3-1, from the original two-hybrid screen that were grown from frozen stocks, onto DDO, TDO and QDO medium to verify that correct phenotypes were maintained (Figure 5.18).

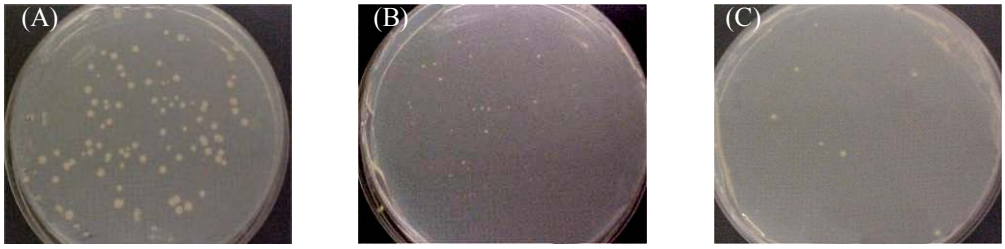

Figure 5.17 Investigation of FLJ22318 interaction with NKX3-1 using (reverse) yeast two-hybrid analysis. **(A)** Growth of yeast colonies on media lacking Leu and Trp (DDO) indicates the successful transformation of the pGADT7-Rec-NKX3-1 construct into AH109/pGBKT7-FLJ22318 yeast whereas **(B)** growth of colonies on media lacking His, Leu and Trp (TDO) indicates activation of the *HIS3* reporter gene demonstrating an interaction between FLJ22318 and NKX3-1. **(C)** The presence of colonies on media lacking Ade, His, Leu and Trp (QDO) demonstrates a strong interaction between FLJ22318 and NKX3-1 as the *ADE2* reporter gene has also been activated.

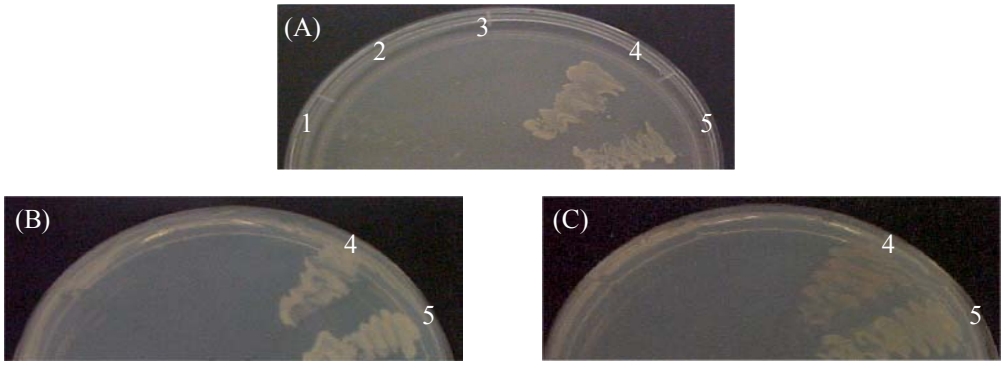

Figure 5.18 Confirmation of an interaction between FLJ22318 and NKX3-1 in the original and reverse yeast-two hybrid screen. Yeast strain AH109 transformed with pGBKT7-FLJ22318/pGADT7-NKX3-1 (4) and pGADT7-FLJ22318/pGBKT7-NKX3-1 (5) were replica plated on **(A)** media lacking Leu and Trp (DDO), **(B)** on media lacking His, Leu and Trp (TDO) and **(C)** on media lacking Ade, His, Leu and Trp (QDO), demonstrating that correct phenotypes had been maintained. As negative controls, untransformed AH109 yeast (1) and AH109 transformed with pGBKT7-FLJ22318 (2) and pGADT7-NKX3-1 (3) constructs were also plated on media lacking Leu and Trp.

5.2.3 GST Pull-Down Analysis

5.2.3.1 pGEX2TK-FLJ22318 Protein Expression

In order to verify and optimise expression of glutathione S-transferase (GST)-FLJ22318 fusion proteins in bacteria, screening of pGEX2TK-FLJ22318 recombinant clones was performed. For these expression studies, competent BL21 bacterial cells were transformed with the pGEX2TK-FLJ22318H10 construct and transformants were selected on LB/ agar/ampicillin plates (sections 3.2.5; 3.2.6; 5.2.1.2). The 4 colonies produced were individually picked into small-scale cultures together with 2 individual pGEX2TK transformed colonies (controls) that had been grown from glycerol stocks. Expression of GST and FLJ22318 as a C-terminal fusion to GST was induced by addition of isopropyl-β-D-thiogalactoside (IPTG) to the culture medium and the proteins were extracted 2 hours post IPTG induction (section 3.8.1). Extracted proteins were analysed by SDS-PAGE with Coomassie blue staining of protein gels (section 3.8.2) revealing the presence of cellular proteins only in lane 2 (negative control, no IPTG induction), cellular proteins with a prominent protein band of approximately 29kDa in lane 3 (positive control, GST alone), while proteins extracted from the 4 pGEX2TK-FLJ22318 clones (lanes 4-7) exhibited cellular proteins with prominent protein bands of approximately 73kDa, the expected size for GST-FLJ22318 (Figure 5.19A). As expression of the GST-FLJ22318 fusion protein was highest from clone 1, this clone was selected for further studies.

5.2.3.2 Production and Purification of GST-FLJ22318 Fusion Protein

Following GST-FLJ22318 fusion protein production, large scale production and purification of GST and GST-FLJ22318 fusion proteins was performed from 100mL bacterial cultures (section 3.8.3). Fusion proteins were purified from bacterial lysates using glutathione immobilised to sepharose and detected using SDS-PAGE with Coomassie blue staining of gels to verify size and purity of the proteins (section 3.8.2). Fusion protein concentration was estimated by comparing GST and GST-FLJ22318 protein bands to a BSA protein standard (Figure 5.19B), with the concentration of GST protein estimated at 1.5µg/µL, whilst the concentration of GST-FLJ22318 protein was much lower than expected at 125ng/µL (Figure 5.19B).

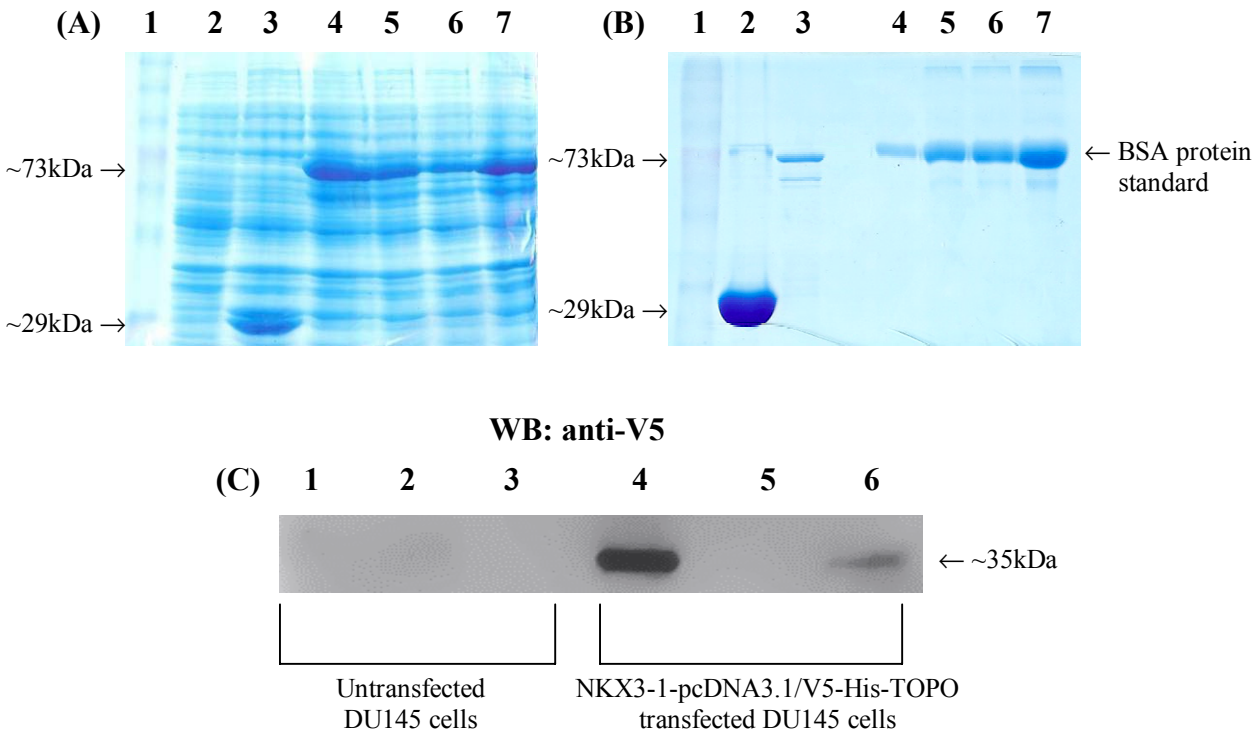

Figure 5.19 GST-FLJ22318 pull-down Assay. **(A)** The presence of protein bands of ~73kDa indicates expression of the GST-FLJ22318 fusion protein (Lanes 4-7) from IPTG induced pGEX2TK-FLJ22318H10. **(B)** Purified GST-FLJ22318 protein of ~73kDa with a protein concentration estimated from the gel to be 125ng/µL. **(C)** GST-FLJ22318 immobilised to glutathione was incubated with lysates from untransfected and from NKX3-1-pcDNA3.1/V5-His-TOPO transfected DU145 cells. The interaction between FLJ22318 and NKX3-1 was detected by anti V5 western blotting in protein precipitates incubated with GST-FLJ22318, but not in protein precipitates that had been incubated with GST alone.

(A)	1	Benchmark™ Prestained Protein Ladder
	2	No IPTG induction (negative control)
	3	IPTG induced GST expression (positive control; ~29kDa)
	4-7	IPTG induced GST-FLJ22318 expression (~73kDa)
(B)	1	Benchmark™ Prestained Protein Ladder
	2	IPTG induced GST expression ~29kDa (positive control)
	3	IPTG induced GST-FLJ22318 expression ~73kDa (125ng/µL)
	4-7	BSA standard (0.5µg, 1.0µg, 2.0µg, 5.0µg)
(C)	1,4	Whole cell lysates
	2,5	GST protein precipitates
	3,6	GST-FLJ22318 protein precipitates

5.2.3.3 GST Pull-Down Assay

GST pull-down assays were performed using large scale preparations of the purified GST and GST-FLJ22318 fusion proteins (sections 5.2.3.2; 3.8.3). For these assays, DU145 prostate cancer cells, chosen as they do not express endogenous NKX3-1, were transiently transfected with NKX3-1-pcDNA3.1/V5-His-TOPO plasmids encoding NKX3-1 as a N-terminal fusion to a V5 epitope (sections 3.6.2; 5.2.1.1). Twenty-four hours post transfection, cells were lysed and 300µL aliquots of the lysate incubated with 7.5µg GST alone or GST-FLJ22318 immobilised to glutathione. Following 18 hours of incubation, the protein complexes were precipitated and proteins separated by SDS-PAGE then transferred onto nitrocellulose filters (sections 3.7.2; 3.7.3). To detect the interaction between FLJ22318 and NKX3-1, western blotting was performed using antibodies directed against the V5 epitope of the NKX3-1-pcDNA3.1/V5-His-TOPO fusion protein (section 3.7.4). In untransfected DU145 cells (controls), NKX3-1 was not detectable, whereas in NKX3-1-pcDNA3.1/V5-His-TOPO transfected cells NKX3-1 could be detected in whole cell lysates and in protein precipitates incubated with GST-FLJ22318, but not in protein precipitates that had been incubated with GST alone (Figure 5.19C). These results support the reverse yeast two-hybrid analysis results (section 5.2.2) and provide further evidence of an interaction between FLJ22318 and NKX3-1 *in vitro*.

5.2.4 Co-immunoprecipitation of FLJ22318 and NKX3-1

5.2.4.1 Co-immunoprecipitation of FLJ22318-pcDNA3.1/V5 and NKX3-1

To verify FLJ22318-V5 protein expression prior to co-immunoprecipitation assays, DU145 prostate cancer cells were transiently transfected with the FLJ22318-pcDNA3.1/V5-His-TOPO construct, the proteins extracted 24 hours post transfection and analysed by anti-V5 western blotting (sections 5.2.1.1; 3.6.2; 3.7.1-3.7.4). Untransfected DU145 cells did not exhibit immunoreactivity with the V5 epitope, while FLJ22318-pcDNA3.1/V5-His-TOPO transfected DU145 cells exhibited V5 immunoreactivity with a protein band of 49.4kDa, the expected size for FLJ22318-V5 protein (results not shown).

As commercially available NKX3-1 antibodies are not precipitating antibodies, immunoprecipitation could not be performed using NKX3-1 antibody. Therefore,

FLJ22318-pcDNA3.1/V5-His-TOPO constructs were transiently transfected into LNCaP prostate cancer cells which express endogenous NKX3-1, and FLJ22318-V5 complexes were immunoprecipitated using antibodies directed against the V5 epitope (sections 5.2.1.1; 3.10; Figure 5.20). Following immunoprecipitation however, the NKX3-1 antibody failed to detect endogenous NKX3-1 or NKX3-1 in controls (results not shown), suggesting that the NKX3-1 antibody available at the time was not sensitive enough for these experiments.

5.2.4.2 Co-immunoprecipitation of pCMV-Myc-FLJ22318 and NKX3-1

Co-immunoprecipitation assays were also carried out using Myc-tagged FLJ22318. For these experiments pCMV-Myc-FLJ22318 constructs were transiently transfected into LNCaP prostate cancer cells and western blotting was performed on extracted proteins using an anti c-Myc antibody, which confirmed expression of a Myc-FLJ22318 fusion protein of the correct size of 45.6kDa (sections 5.2.1.4.3; 3.7.1-.3.7.4; Figure 5.21). pCMV-Myc-FLJ22318 constructs were then transiently transfected into LNCaP cells together with NKX3-1-pcDNA3.1/V5-His-TOPO and NKX3-1-V5 complexes immunoprecipitated using antibodies directed against the V5 epitope as previously described (Figure 5.21B). Western blotting using a polyclonal anti-Myc antibody however, failed to detect FLJ22318 as part of a NKX3-1 complex or in controls, although when a monoclonal Myc antibody was used, FLJ22318 was detected in controls but not as part of a NKX3-1 complex (results not shown). As endogenous NKX3-1, which is present in LNCaP cells, was thought to be sequestering the transfected FLJ22318, the assays were repeated using the DU145 prostate cancer cell line, which has undetectable expression of endogenous NKX3-1 protein.

For these assays, pCMV-Myc-FLJ22318 and NKX3-1-pcDNA3.1/V5-His-TOPO constructs were transiently transfected into the DU145 prostate cancer cell line and NKX3-1-V5 complexes were immunoprecipitated as previously described. However following immunoprecipitation, western blotting with monoclonal c-Myc antibodies detected non specific bands in both the untransfected DU145 cells (negative controls) and pCMV-Myc-FLJ22318 transfected cells suggesting that the c-Myc antibody was not specific enough for these experiments (section 3.7; Figure 5.21C).

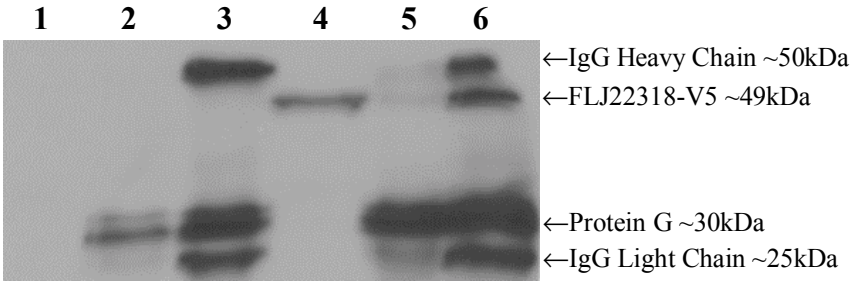

Figure 5.20 Immunoprecipitation of FLJ22318-pcDNA3.1/V5-His-TOPO. Plasmids expressing FLJ22318-V5 were transiently transfected into LNCaP prostate cancer cells and 24 hours post transfection proteins were immunoprecipitated with anti-V5 antibodies. Protein complexes were collected with protein G sepharose and resolved by SDS-PAGE prior to western blotting with antibodies directed against the V5 epitope. In transfected cells, FLJ22318 can be detected in the whole cell lysate and in protein complexes immunoprecipitated with V5 antibody but not in protein complexes collected using protein G alone. In untransfected cells (controls) FLJ22318-V5 is not detectable.

1 Untransfected LNCaP cells – whole cell lysate
2 Untransfected LNCaP cells – protein G
3 Untransfected LNCaP cells – protein G/anti-V5 antibody
4 FLJ22318-V5 transfected LNCaP cells – whole cell lysate
5 FLJ22318-V5 transfected LNCaP cells – protein G
6 FLJ22318-V5 transfected LNCaP cells – protein G/anti-V5 antibody

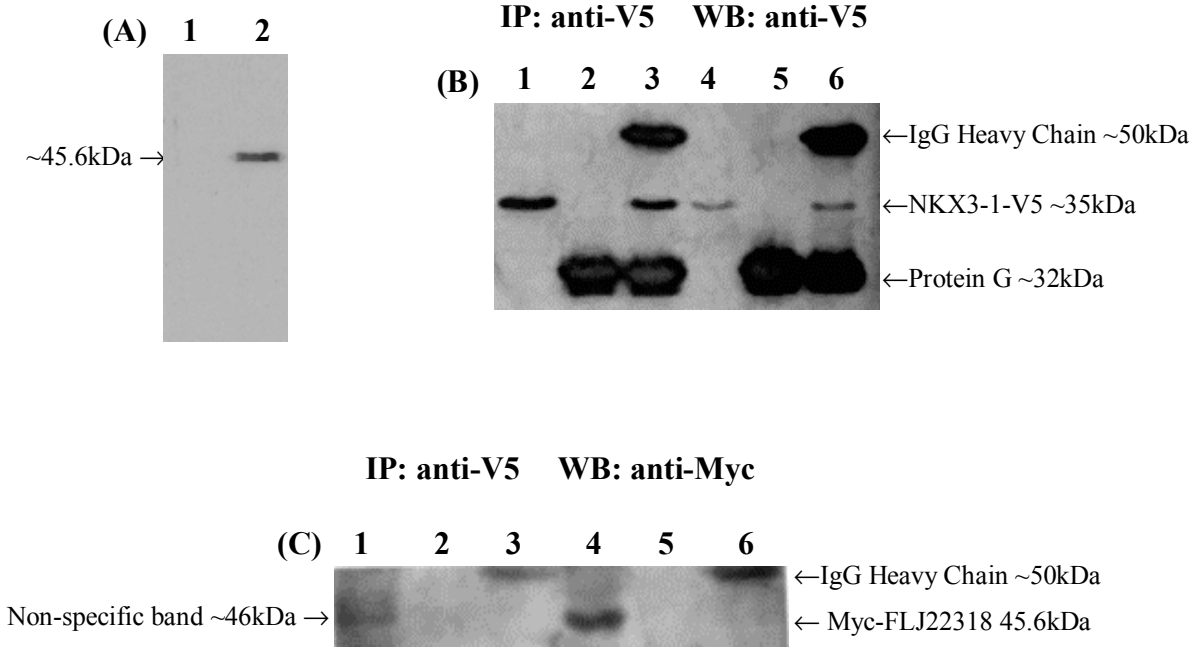

Figure 5.21 Co-immunoprecipitation of NKX3-1-V5 and Myc-FLJ22318 **(A)** Anti-Myc western blotting detected expression of Myc-FLJ22318 in pCMV-Myc-FLJ22318 transfected LNCaP cells but not in untransfected cells. **(B)** LNCaP, and **(C)** DU145 cells were transfected with either NKX3-1-pcDNA3.1/V5-His-TOPO or co-transfected with NKX3-1-pcDNA3.1/V5-His-TOPO and pCMV-Myc-FLJ22318. Proteins were harvested 24 hours post-transfection and immunoprecipitated with anti-V5 antibodies. **(B)** Anti-V5 western blotting indicated successful immunoprecipitation of NKX3-1-V5 from LNCaP cells. **(C)** Anti-Myc western blotting did not identify co-immunoprecipitation of Myc-FLJ22318 with NKX3-1-V5 but detected a nonspecific band of similar size to Myc-FLJ22318 in whole cell lysates.

(A) 1 Untransfected LNCaP cells
2 pCMV-Myc-FLJ22318 transfected LNCaP cells

(B,C) 1 NKX3-1-V5 transfected cells – whole cell lysate
2 NKX3-1-V5 transfected cells – protein G
3 NKX3-1-V5 transfected cells – protein G/ anti-V5
4 NKX3-1-V5/Myc-FLJ22318 transfected cells – whole cell lysate
5 NKX3-1-V5/Myc-FLJ22318 transfected cells – protein G
6 NKX3-1-V5/Myc-FLJ22318 transfected cells – protein G/anti-V5

5.2.4.3 Co-immunoprecipitation of pCMV-HA-FLJ22318 and NKX3-1

Due to difficulties with the immunoprecipitation experiments, LNCaP cells were transiently co-transfected with NKX3-1-pcDNA3.1/V5-His-TOPO and FLJ22318-pCMV-HA constructs encoding V5-tagged NKX3-1 and HA-tagged FLJ22318 and protein complexes were immunoprecipitated using V5 antibodies (section 5.2.1.5.2). Proteins were separated by SDS-PAGE, and transferred to nitrocellulose membranes. Western blotting with HA antibodies detected FLJ22318 in whole cell lysates, however FLJ22318 could not be confirmed as part of immunoprecipitated NKX3-1 complexes as the IgG heavy chain of the immunoprecipitating antibodies was of a similar size to HA-FLJ22318 (results not shown).

5.2.4.4 Co-immunoprecipitation of pEGFP-C2-FLJ22318 and NKX3-1

Prior to using the pEGFP-C2-FLJ22318 construct in immunoprecipitation assays, anti-GFP western blotting of transiently transfected LNCaP cells was performed to confirm the expression of a GFP-FLJ22318 fusion protein of the expected size of approximately 70kDa (sections 5.2.1.6.2; 3.6.2; 3.7.2-3.7.4; results not shown). Following verification of GFP-FLJ22318 protein expression, LNCaP cells were transiently co-transfected with NKX3-1-pcDNA3.1/V5-His-TOPO and pEGFP-C2-FLJ22318 vectors encoding NKX3-1-V5 and GFP-FLJ22318 fusion proteins and protein complexes were immunoprecipitated with V5 antibodies (or no antibody controls) 24 hours later. Western blotting using anti GFP antibodies detected FLJ22318 in whole cell lysates and in immunoprecipitated complexes with NKX3-1 but not in untransfected controls (section 3.7; Figure 5.22). These findings confirmed that FLJ22318 and NKX3-1 interacted *in vivo* and supported the *in vitro* assay results.

5.2.5 Characterisation of *FLJ22318* Expression

5.2.5.1 Preparation of cDNA Probes

5.2.5.1.1 Preparation of the FLJ22318 cDNA Probe

To prepare the FLJ22318 cDNA probe, 5µg of the pCMV-HA-FLJ22318 vector was digested using *Sal* I and *Pst* I and the digested plasmid electrophoresed in a 2% agarose gel (sections 5.2.1.5.2; 3.1.4; 3.2.2; results not shown). The 315bp fragment corresponding to the last 92bp of exon 3, exon 4 and the first 77bp of exon 5 of

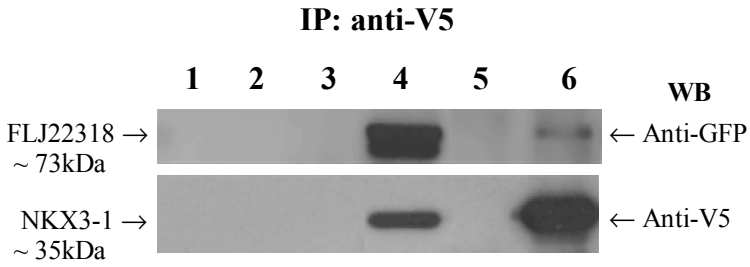

Figure 5.22 FLJ22318 interacts with NKX3-1 *in vivo*. Plasmids expressing GFP-FLJ22318 and NKX3-1-V5 fusion proteins were transfected into LNCaP cells and proteins immunoprecipitated with V5 antibodies. In the FLJ22318/NKX3-1 transfected cells, western blotting using anti-V5 and anti-GFP antibodies detected both proteins in the whole cell lysate and in protein complexes immunoprecipitated with V5 antibodies but not in protein complexes precipitated using protein G alone. GFP-FLJ22318 and NKX3-1-V5 were not detected in untransfected cells.

1 Untransfected cells – LNCaP whole cell lysate
2 Untransfected cells – Protein G
3 Untransfected cells – Protein G/Anti-V5
4 FLJ22318-NKX3-1 transfected cells – LNCaP whole cell lysate
5 FLJ22318-NKX3-1 transfected cells – Protein G
6 FLJ22318-NKX3-1 transfected cells – Protein G/Anti-V5

FLJ22318 was excised from the gel, purified and its concentration determined from the gel to be 10ng/μL (section; 3.1.6; Figure 5.23).

5.2.5.1.2 Preparation of the GAPDH cDNA Probe

To prepare the GAPDH cDNA probe, multiple *Pst* I digests of 1μg of the pHc-GAPDH vector were performed and the digested plasmid purified then digested with *Xba* I and electrophoresed in a 2% agarose gel (sections 2.1.3; 3.1.6; 3.2.2; results not shown). The 1283bp fragment corresponding to GAPDH was excised from the gel, purified and its concentration determined spectrophotometrically to be 21ng/μL (section 3.1.6).

5.2.5.2 *FLJ22318* Expression in Prostate and Breast Cancer Cells

Expression of *FLJ22318* mRNA was examined by Northern blotting in human LNCaP, DU145 and PC-3 prostate cancer cells, and MCF-7 breast cancer cells. Total cellular RNA was extracted from the cell lines, RNA concentration was determined spectrophotometrically and 10μg of each sample was separated in 1% MOPS/formaldehyde gels then transferred overnight onto nylon membranes (sections 3.3.3; 3.6.1; 3.13.1-3.13.3).

FLJ22318 mRNA levels were determined by Northern blotting with ^{32}P labelled FLJ22318 cDNA probes followed by exposure to autoradiographic film (sections 5.2.5.1; 3.13.4-3.13.5). Unexpectedly, Northern blotting identified two transcripts of ~1.8kbp and ~4kbp in all samples examined by plotting the mobility versus the log of the molecular weight in base pairs of the 18S and 28S rRNAs (Figure 5.24). The more abundant 1.8kbp transcript corresponds in size to the published RNA sequence that is proposed to encode a protein of 44.4kDa (NCBI Accession No. NP_073599). However, the FLJ22318 cDNA probe would have detected all but variant 'm' of the alternative transcripts as proposed by AceView, therefore this transcript may represent variant 'a', which also has a transcript size of approximately 1.8kbp (section 4.2.1; Table 4.1). The proposed protein encoded by this variant has a variant N-terminal to the published sequence that contains a clathrin box motif which is found on cargo adaptor proteins. The other transcript of ~4kbp detected by the FLJ22318 probe corresponds in size to transcript variant 'd'. This variant is also proposed to encode the 44.4kDa protein as

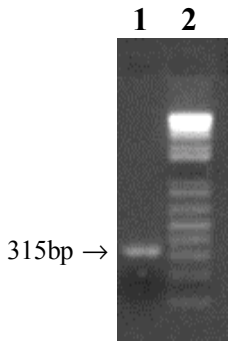

Figure 5.23 Construction of the cDNA probes. To construct the FLJ22318 cDNA probe, 10µg the pCMV-HA-FLJ22318 vector was digested with *Sal* I and *Pst* I, and electrophoresed in a 2% agarose gel. The 315bp fragment corresponding to exons 3, 4 and 5 of FLJ22318 was excised, purified and 5µL electrophoresed in a 2% agarose gel. The concentration was estimated from the gel to be 10ng/µL.

1 Purified *Sal* I/*Pst* I digested FLJ22318 cDNA probe (10ng/µL)
2 1Kb Plus™ DNA Ladder

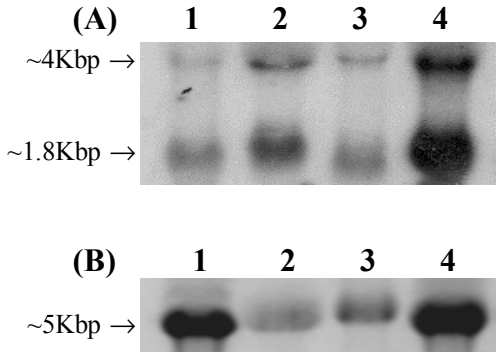

Figure 5.24 Expression of *FLJ22318* in prostate and breast cancer cell lines. To examine expression of *FLJ22318*, **(A)** 10µg of total cellular RNA from LNCaP, DU145, and PC-3 prostate cancer cell lines and MCF-7 breast cancer cells was transferred onto nylon membranes. Northern blotting with ^{32}P labelled FLJ22318 cDNA probes identified two *FLJ22318* transcripts of approximately 4Kbp and 1.8Kbp in all cell lines tested. **(B)** Ethidium bromide stained RNA gel showing the 28S (~5Kbp) rRNA.

1 LNCaP prostate cancer cell line
2 DU145 prostate cancer cell line
3 PC-3 prostate cancer cell line
4 MCF-7 breast cancer cell line

published by NCBI, and differs in transcript size to the published NCBI mRNA sequence (Accession No. NM_022762) only in its 3' and 5'-UTRs.

5.2.5.3 Androgen Regulation of *FLJ22318* Expression

To examine the regulation of *FLJ22318* expression, mRNA levels of *FLJ22318* were studied in LNCaP cells cultured in 5% CS-FCS medium containing 1 nM DHT for 0, 3, 6, 12, 24, 48 and 72 hours (section 3.6.4). Following treatment, the *FLJ22318* RNA was extracted and RNA concentration was determined spectrophotometrically as previously described (section 3.3.3). Ten µg of total cellular RNA from each sample was separated in 1% MOPS/formaldehyde gels and transferred overnight onto nylon membranes. *FLJ22318* mRNA levels were determined by Northern blotting with ^{32}P labelled FLJ22318 cDNA probes and exposed to autoradiographic film (sections 5.2.5.1.1; 3.13.4-3.13.5). Developed films were then analysed using Quantity One V4.5.2 software. To determine *FLJ22318* expression, membranes were re-probed with ^{32}P labelled GAPDH cDNA probes and for each sample, *FLJ22318* expression determined as a proportion of *GAPDH* expression and represented as a proportion of *FLJ22318* mRNA levels detected in untreated controls (section 5.2.5.1.2).

Following DHT treatment, *FLJ22318* mRNA levels remained similar to that observed in the untreated cells at all time points tested suggesting that *FLJ22318* expression is not regulated by androgens (Figure 5.25).

5.2.6 Cellular Localisation and Co-localisation of FLJ22318 and NKX3-1

To confirm that FLJ22318 and NKX3-1 are present within the same cellular compartment, DU145 and LNCaP cells were transiently transfected with 1µg of pCMV-Myc-FLJ22318 and NKX3-1-pcDNA3.1/V5-His-TOPO vectors encoding Myc-FLJ22318 and NKX3-1-V5 fusion proteins and the localisation and co-localisation of Myc-FLJ22318 and NKX3-1-V5 was determined by confocal microscopy using antibodies directed against the Myc and V5 epitopes (sections 5.2.1.4.3; 3.6.2; 3.11). Untransfected control cells displayed no immunoreactivity with the c-Myc or V5 antibodies (results not shown).

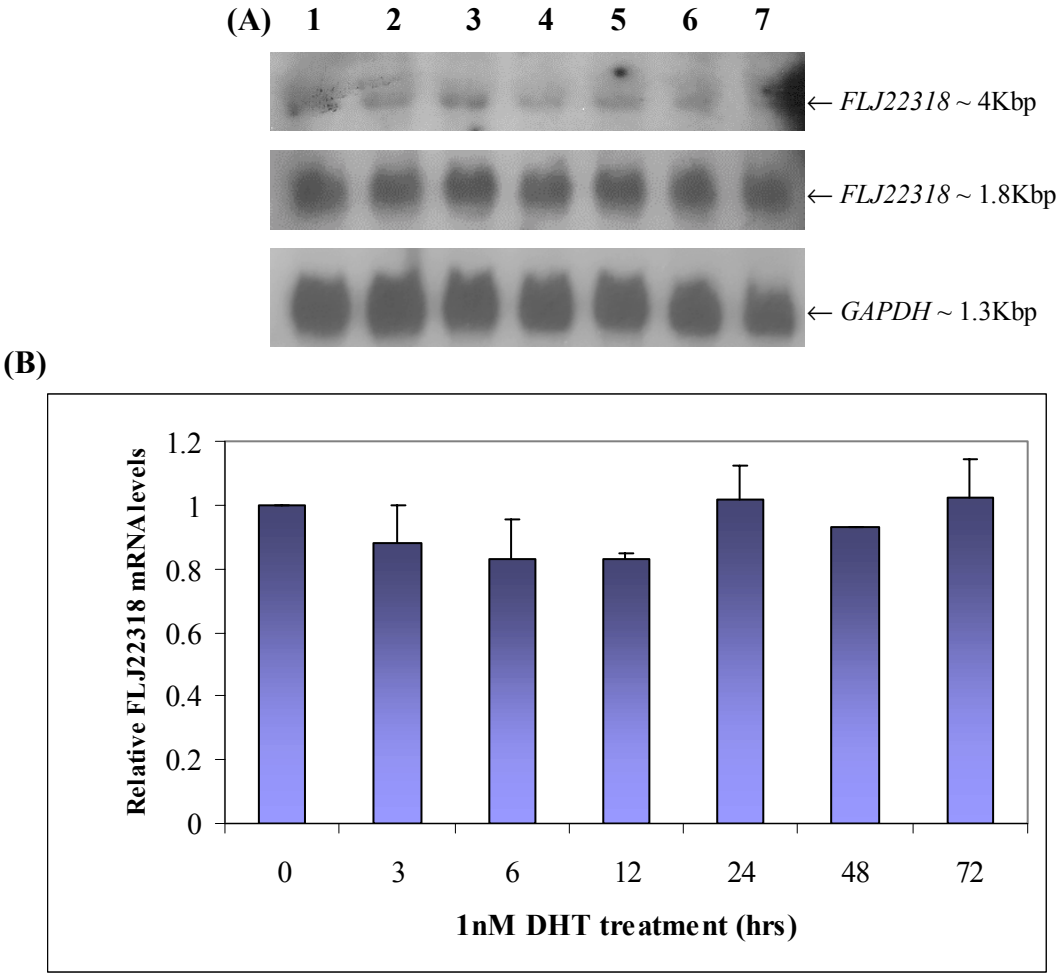

Figure 5.25 Androgen regulation of *FLJ22318* mRNA in LNCaP cells. **(A)** LNCaP cells were cultured with 10^{-8}M DHT for 0-72 hours prior to RNA extraction and Northern blotting for *FLJ22318* and *GAPDH* (loading control). **(B)** *FLJ22318* mRNA levels were calculated as proportion of *GAPDH* mRNA and presented as mean ± SEM of *FLJ22318* mRNA levels relative to time 0.

(A) DHT Treatment (hr)
Lane 1 0
Lane 2 3
Lane 3 6
Lane 4 12
Lane 5 24
Lane 6 48
Lane 7 72

In the DU145 prostate cancer cell line, FLJ22318 displayed a diffuse nuclear and perinuclear localisation. NKX3-1 was also localised to the perinuclear and nuclear regions of the cells but displayed a more punctate pattern of fluorescence compared to that of FLJ22318 (Figure 5.26). In the cells where NKX3-1 was predominantly localised to the perinuclear region of the cells with little nuclear localisation, very little co-localisation with FLJ22318 was observed (Figure 5.26A). However, in cells where NKX3-1 was localised in both the perinuclear and nuclear regions, more extensive co-localisation of FLJ22318 and NKX3-1 was observed in these areas (Figure 5.26B)

The finding that NKX3-1 localised to the perinuclear region of the cells was unexpected as previous studies have shown NKX3-1 to be a nuclear protein as would be expected for a transcription factor (Korkmaz et al., 2004). Previous studies were performed using the androgen responsive LNCaP cell line and as NKX3-1 expression has been shown to be altered or lost in advanced androgen independent prostate cancer and the DU145 cell line was derived from an androgen independent metastatic prostate cancer cell, it is possible that the cellular localisation of NKX3-1 in this cell line may be altered.

Consequently, the localisation and co-localisation of FLJ22318 and NKX3-1 was re-characterised in the LNCaP cell line as NKX3-1 is endogenously expressed in this cell line and as such other factors that may affect protein localisation would also be present. pCMV-Myc-FLJ22318 and NKX3-1-pcDNA3.1/V5-His-TOPO were transiently transfected into LNCaP cells and the cellular localisation determined by confocal microscopy using antibodies directed against the Myc or V5 epitopes as described previously (sections 5.2.1.4.3; 3.11). Similar to results using the DU145 cell line, FLJ22318 showed a diffuse localisation throughout the perinuclear and nuclear region of the cells, however NKX3-1 showed a mainly perinuclear localisation with very little nuclear localisation or co-localisation with FLJ22318 (Figure 5.27A).

As NKX3-1 is an androgen regulated gene and the LNCaP cell line is androgen responsive, confocal microscopy was also performed in LNCaP cells transfected as described above and treated with 1nM DHT. In DHT-treated cells, FLJ22318 displayed a similar perinuclear and nuclear localisation to that observed in untreated cultures. However, NKX3-1 was localised to both the perinuclear and nuclear regions of the

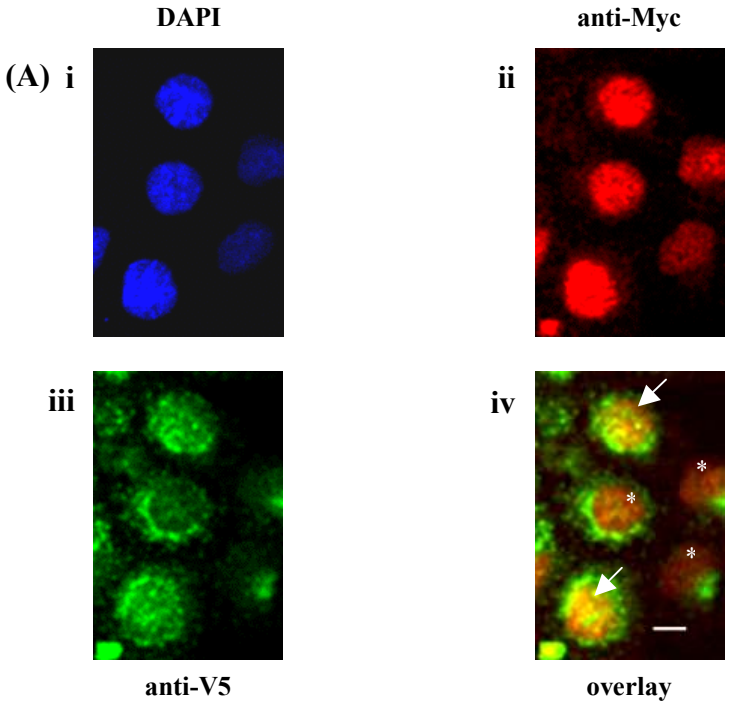
DAPI
anti-Myc
(A) i
ii
iii
iv
anti-V5
overlay

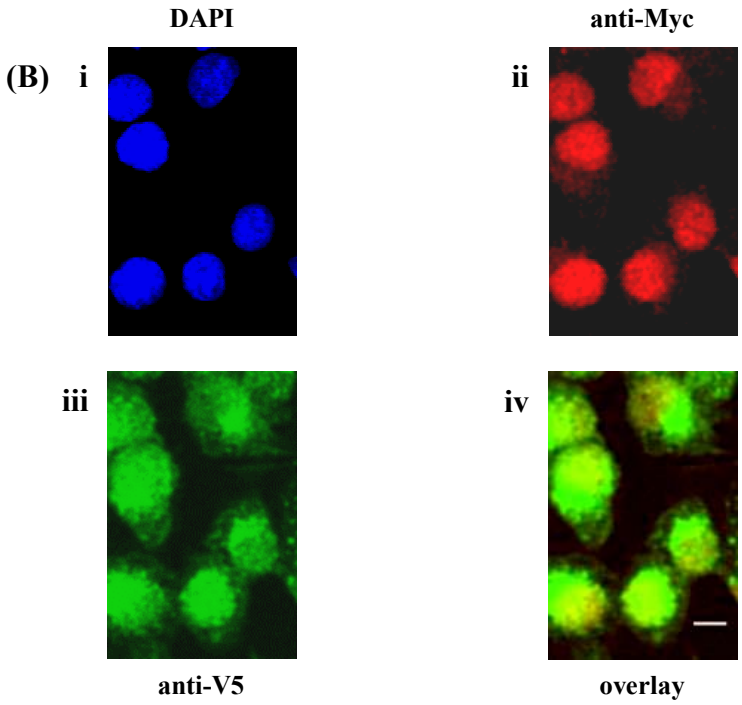
DAPI
anti-Myc
(B) i
ii
iii
iv
anti-V5
overlay

Figure 5.26 FLJ22318 and NKX3-1 localisation and co-localisation in DU145 prostate cancer cells. DU145 cells were co-transfected with pCMV-Myc-FLJ22318 and pcDNA3.1-NKX3-1-V5 vectors and incubated for 24 hours to allow expression of recombinant proteins. **(i)** Cell nuclei were visualised using DAPI, and immunostained with **(ii)**, anti-Myc and **(iii)** and anti-V5 antibodies prior to confocal microscopy. Myc-FLJ22318 exhibited diffuse nuclear and perinuclear localisation while NKX3-1-V5 exhibited either predominantly perinuclear **(A iii)** or both nuclear and perinuclear fluorescence **(B iii)**. When images were overlayed, co-localisation (yellow) of FLJ22318 and NKX3-1 was detected in cells where localisation of NKX3-1 was both perinuclear and nuclear **(A iv (arrow) and B iv)** whereas in cells where localisation of NKX3-1 was predominantly perinuclear, very little co-localisation of both proteins was observed **(A iv *)**. Bar = 10μm.

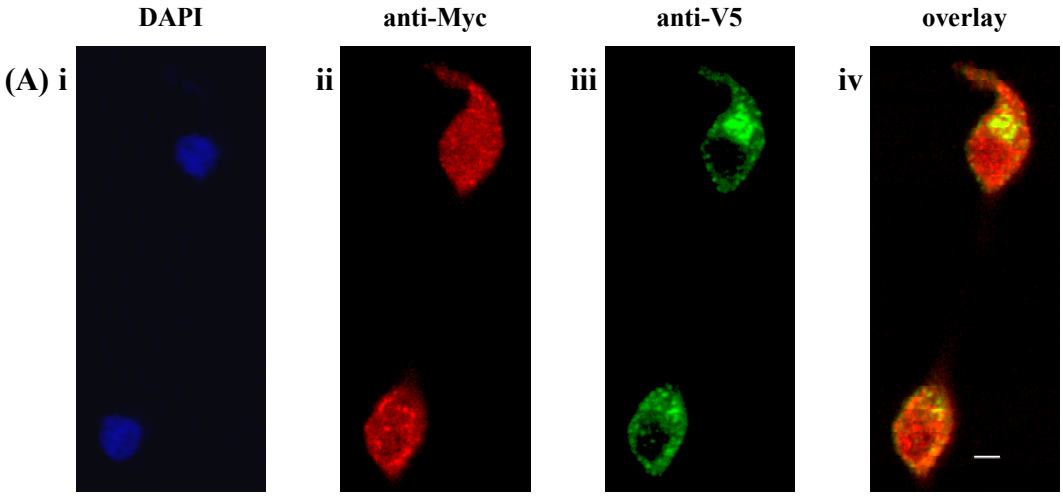
DAPI
anti-Myc
anti-V5
overlay
(A) i
ii
iii
iv

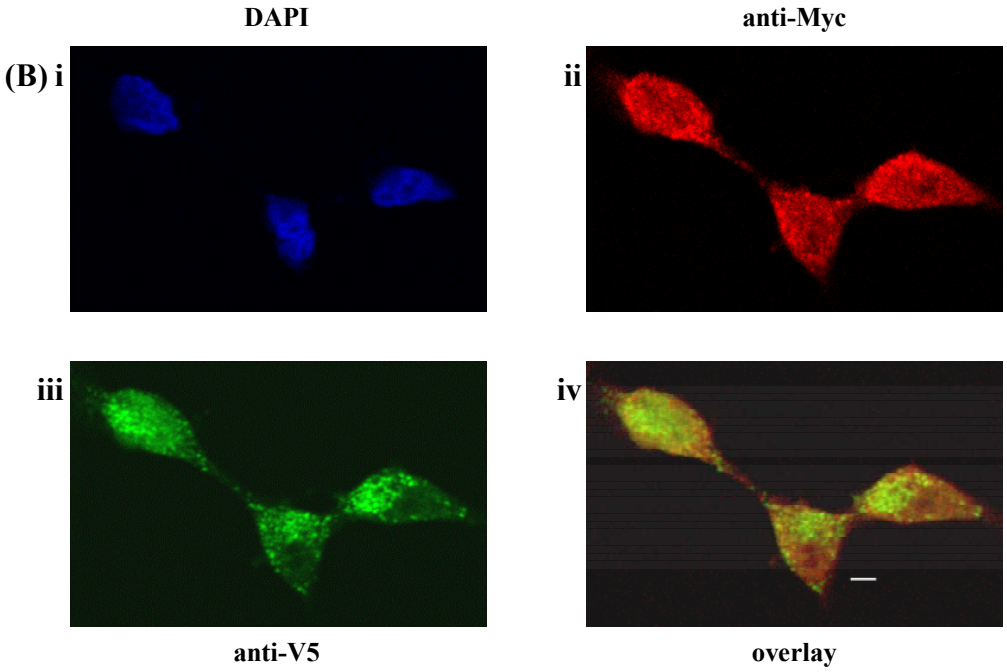
DAPI
anti-Myc
(B) i
ii
iii
iv
anti-V5
overlay

Figure 5.27 FLJ22318 and NKX3-1 localisation and co-localisation in LNCaP prostate cancer cells. LNCaP cells were transfected with 1µg of pCMV-Myc-FLJ22318 and pcDNA3.1-NKX3-1-V5 vectors and incubated for 24 hours in the absence **(A)** or presence **(B)** of 1nM DHT. Cell nuclei were visualised using **(i)** DAPI and cells were immunostained with **(ii)** anti-Myc and **(iii)** anti-V5 prior to confocal microscopy. FLJ22318 exhibited diffuse nuclear and perinuclear localisation in untreated **(A ii)** and DHT-treated **(B ii)** cultures, while NKX3-1 exhibited either **(A iii)** mainly perinuclear fluorescence in untreated cells or **(B iii)** both nuclear and perinuclear fluorescence in the DHT-treated cells. When images were overlayed, **(A iv)** limited perinuclear co-localisation of Myc-FLJ22318 and NKX3-1-V5/His was detected in untreated cells. **(B iv)** In DHT treated cells, extensive nuclear and perinuclear co-localisation of Myc-FLJ22318 and NKX3-1-V5/His was detected. Bar = 10µm.

DHT-treated LNCaP cells and extensive nuclear and perinuclear co-localisation of FLJ22318 and NKX3-1 was detected in these cultures (Figure 5.27B).

5.2.7 Transcriptional Activity of FLJ22318

The transcriptional activity of FLJ22318 and the regulation of NKX3-1 transcriptional activity by FLJ22318 were investigated in transiently transfected DU145 prostate cancer cells (section 3.6.2). Transcriptional activity was assessed by luciferase activity (section 3.12), induced from a herpes simplex virus thymidine kinase (TK) promoter upstream of a firefly luciferase gene (Luc). The DU145 cells were transfected with the reporter plasmids TK-Luc (control) or NKX-TK-Luc which contained three copies of a 'TCGATATTAAGTATAGGATTAAGTATAGGGATTAAGTAT' NKX3-1 response element (underlined) and various expression plasmids as listed in Figure 5.28. Cells were lysed 24 hours post-transfection and induced luciferase activity determined (section 3.12). An appropriate amount of pcDNA3.1/V5-His-TOPO/*lac*Z (Figure 3.9) was included in all transfections so that each well was transfected with an equal amount of DNA and the pRL/SV40 *Renilla* plasmid (Figure 3.10) was also included in all transfections to control for variations in transfection efficiency. In addition, DU145 cells were transiently transfected with either FLJ22318-pcDNA3.1/V5-His-TOPO or FLJ22318-pCMV-Myc to compare the effects on transcription of C-terminal V5 tagged FLJ22318 with N-terminal Myc tagged FLJ22318 protein. The data represents the average of two separate experiments normalised by *Renilla* luciferase activity.

In both sets of experiments DU145 cells transfected with *Renilla* plasmid exhibited negligible background luciferase activity of 0.2% as did DU145 cells transfected with the TK-Luc luciferase reporter plasmid (2-3%), which represented the background activity of the TK promoter (Figure 5.28B,C). DU145 cells transfected with the NKX-TK-Luc luciferase reporter plasmid exhibited a 32-fold and 49-fold increase in luciferase activity respectively when compared to controls (Figure 5.28B,C) which was then reduced by 83-88% when NKX-TK-Luc transfected DU145 cells were co-transfected with NKX3-1-pcDNA3.1/V5-His-TOPO (Figure 5.28B,C). These results are in accordance with previous findings that NKX3-1 acts as a transcriptional repressor on this response element (Steadman et al., 2000). When compared to DU145 cells transfected with NKX-TK-Luc alone, cells co-transfected with NKX-TK-Luc and FLJ22318-pcDNA3.1/V5-His-TOPO, displayed a 44% reduction in luciferase activity

(Figure 5.28B). Consistent with these results, DU145 cells co-transfected with NKX-TK-Luc and pCMV-Myc-FLJ22318, displayed a 47% reduction in luciferase activity when compared to DU145 cells co-transfected with NKX-TK-Luc alone (Figure 5.28C). These results suggest that FLJ22318 may have transcriptional repressor activity on this NKX3-1 response element.

Compared to DU145 cells co-transfected with NKX-TK-Luc and NKX3-1-pcDNA3.1/V5-His-TOPO, DU145 cells transfected with NKX-TK-Luc, NKX3-1-pcDNA3.1/V5-His-TOPO and FLJ22318-pcDNA3.1/V5-His-TOPO exhibited a further 42% decrease in luciferase activity (Figure 5.28B). Similarly, a further decrease in luciferase activity of 55% was observed in those cells transfected with NKX-TK-Luc, NKX3-1-pcDNA3.1/V5-His-TOPO and pCMV-Myc-FLJ22318 (Figure 5.28C). These findings suggest that FLJ22318 may act as a transcriptional co-repressor with NKX3-1 and indicate that neither the C-terminal V5 epitope of the FLJ22318-V5 fusion protein or the N-terminal Myc epitope of the FLJ22318-Myc fusion protein affected the transcriptional repressor or co-repressor activity of FLJ22318.

5.2.8 Effect of FLJ22318 on NKX3-1 Protein Levels

To assess whether the increase in NKX3-1 transcriptional repressor activity (section 5.2.7) was a consequence of increased NKX3-1 protein levels following exogenous expression of FLJ22318, NKX3-1 protein levels were assessed by western blotting (section 3.7). For these experiments, LNCaP cells were transiently transfected with increasing amounts of vectors encoding FLJ22318-V5, GFP-FLJ22318 and HA-FLJ22318 to compare the effects of C-terminal V5-tagged FLJ22318 or N-terminal GFP- and HA-tagged FLJ22318 on NKX3-1 protein levels (section 3.6.2; Figure 5.29). An appropriate amount of pcDNA3.1/V5-His-TOPO/*lac*Z (Figure 3.9) was included in all transfections so that each well was transfected with an equal amount of DNA. NKX3-1 proteins were detected using anti-NKX3-1 antibodies (section 2.1.6; Figure 5.29A), and protein levels in samples standardised to β-actin. Results are presented as mean ± SEM of NKX3-1 protein levels relative to untransfected LNCaP cells.

Following exogenous expression of FLJ22318 in LNCaP cells, NKX3-1 protein levels remained similar to that observed in the untransfected and solely pcDNA3.1/V5-His-

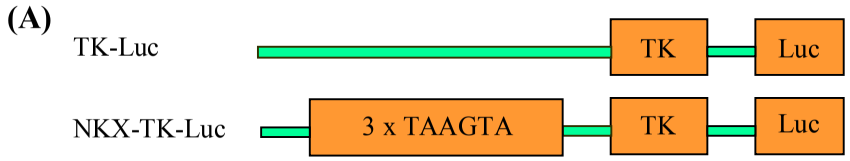

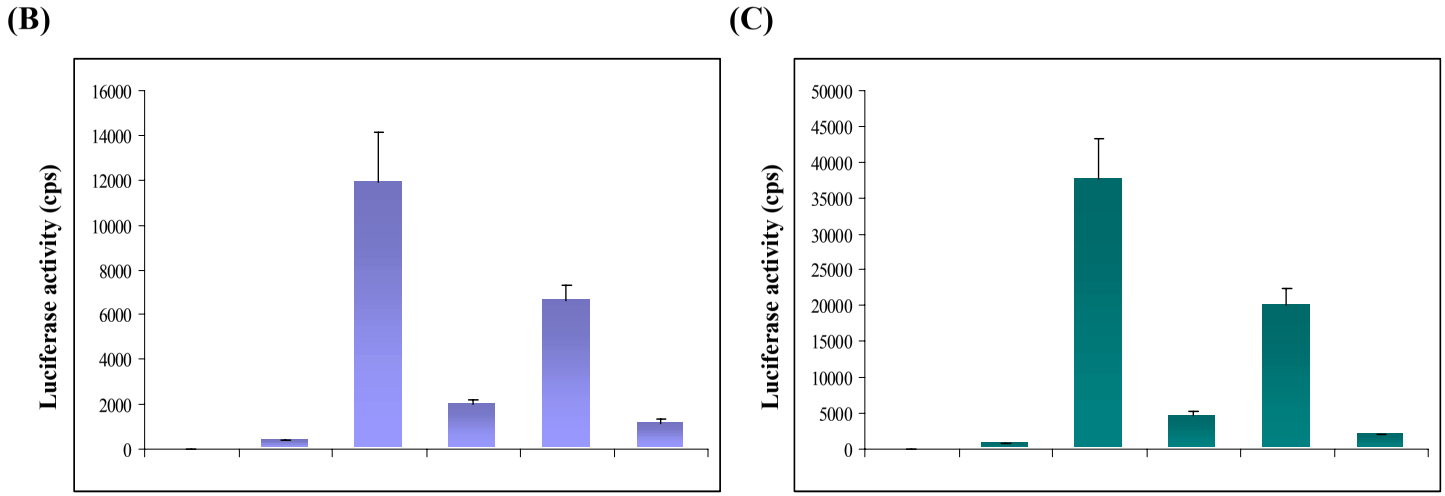

pRLSV40 *Renilla*	10ng	10ng	10ng	10ng	10ng	10ng	10ng	10ng	10ng	10ng	10ng	10ng
***lacZ*-pcDNA3.1-/V5-His-TOPO**	3µg	2µg	2µg	1µg	1µg	-	3µg	2µg	2µg	1µg	1µg	-
TK-Luc	-	1µg	-	-	-	-	-	1µg	-	-	-	-
NKX-TK-Luc	-	-	1µg	1µg	1µg	1µg	-	-	1µg	1µg	1µg	1µg
NKX3-1- pcDNA3.1-/V5-His-TOPO	-	-	-	1µg	-	1µg	-	-	-	1µg	-	1µg
FLJ22318- pcDNA3.1-/V5-His-TOPO	-	-	-	-	1µg	1µg	-	-	-	-	-	-
pCMV-Myc-FLJ22318	-	-	-	-	-	-	-	-	-	-	1µg	1µg

Figure 5.28 Transcriptional repressor activity of FLJ22318. **(A)** Luciferase reporter plasmids transiently transfected into DU145 cells. **(B,C)** Normalised induced luciferase activity following transfection of the indicated plasmids. Results are presented as mean ± SEM of luciferase activity induced from the NKX-TK-Luc plasmid.

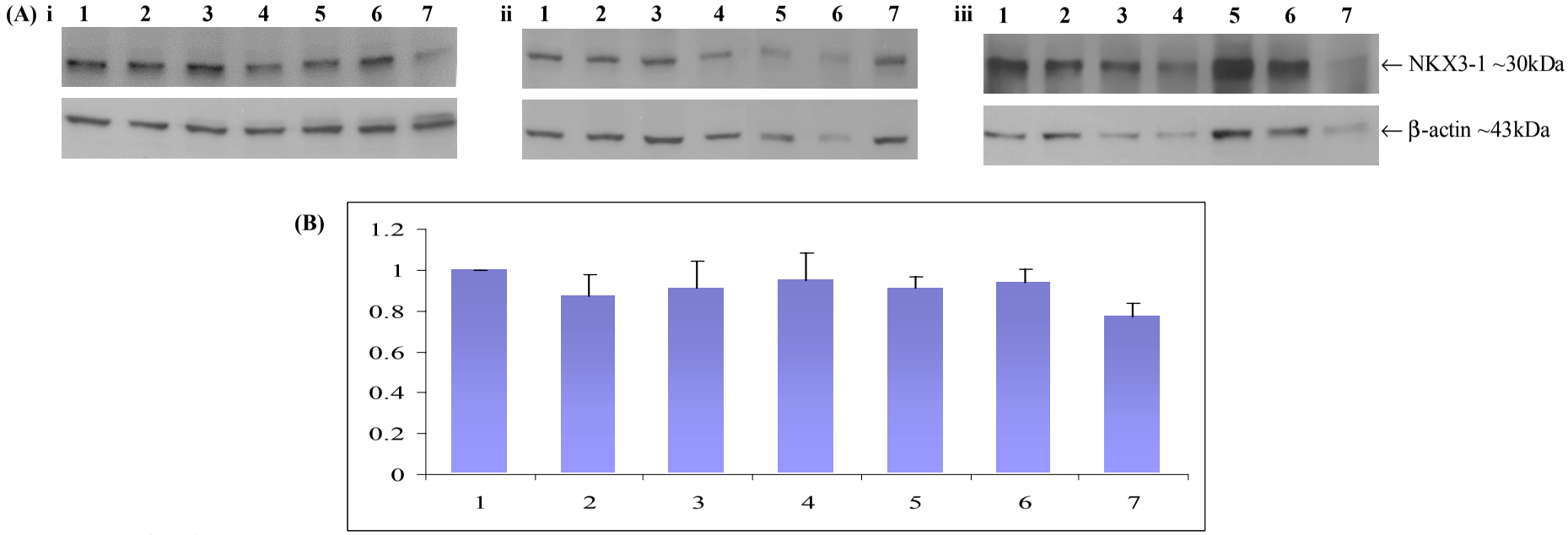

Untransfected	+	-	-	-	-	-	-
*Lac*Z-pcDNA3.1/V5-His-TOPO	-	3µg	2.75µg	2.5µg	2µg	1µg	-
FLJ22318- pcDNA3.1/V5-His-TOPO **or**	-	-	0.25µg	0.5µg	1µg	2µg	3µg
pEGFP-C2-FLJ22318 **or**	-	-	0.25µg	0.5µg	1µg	2µg	3µg
pCMV-HA-FLJ22318 **or**	-	-	0.25µg	0.5µg	1µg	2µg	3µg

Figure 5.29 Exogenous expression of FLJ22318 does not regulate NKX3-1 protein levels in LNCaP cells. **(A)** LNCaP cells transiently transfected with increasing amounts of **(i)** FLJ22318-pcDNA3.1/V5-His-TOPO, **(ii)** pEGFP-C2-FLJ22318 or **(iii)** pCMV-HA-FLJ22318 were harvested 24 hours post transfection and NKX3-1 and β-actin levels were determined by western blotting. **(B)** Relative NKX3-1 protein levels following transfection of the indicated plasmids standardised to β-actin protein levels and presented as mean ± SEM of NKX3-1 protein levels in untransfected cells.

TOPO/*lac*Z transfected cells at all concentrations tested (Figure 5.29B). These results indicated that FLJ22318 does not regulate NKX3-1 protein levels in LNCaP prostate cancer cells.

5.3 Discussion

FLJ22318 was originally identified as a putative interacting partner of NKX3-1 by yeast two-hybrid analysis. To provide supporting evidence that the interaction between NKX3-1 and FLJ22318 was not a result of the intrinsic technical limitations of this method, full length FLJ22318 and NKX3-1 were cloned into yeast expression plasmids, the reverse to that used in the original screen and the yeast two-hybrid screen was repeated.

In the initial reverse yeast two-hybrid screen, although transformation of FLJ22318 into yeast was successful, co-transformation of both FLJ22318 and NKX3-1 into the yeast cells was not. Therefore in the subsequent screen, FLJ22318 transformed yeast cells were used in a sequential transformation with NKX3-1 to confirm the interaction between FLJ22318 and NKX3-1. Co-transformation of FLJ22318 and NKX3-1 was unsuccessful most likely as the result of low transformation efficiency especially as efficiencies of transformations with single plasmids were lower than expected. The low transformation efficiencies may have resulted from suboptimal yeast competent cells, carrier DNA or plasmid DNA. The plasmid DNA was purified prior to transformation using the Wizard® SV Gel and PCR Clean-Up System (section 2.2). However before transformation, additional ethanol precipitation of the plasmid DNA is recommended (Sambrook and Russell, 2001) therefore the low transformation efficiencies seen in these studies may have been due to residual guanidine isothiocyanate contamination of the plasmid DNA from the Wizard® SV Gel and PCR Clean-Up System membrane binding solution.

The interaction between NKX3-1 and FLJ22318 detected using GST pull-down and immunoprecipitation assays in these studies also proved to be technically difficult. This may have been due to an insufficient concentration of NKX3-1 and FLJ22318 able to be used to readily detect an interaction. The cellular concentration of an expressed protein can be influenced by a number of factors including the local molecular environment,

protein turnover and expression. For the GST-FLJ22318 pull-down assays, NKX3-1 was exogenously expressed with a C-terminal V5 epitope in transiently transfected DU145 cells. Similarly for the immunoprecipitation assays, LNCaP prostate cancer cells were transiently transfected with plasmids encoding NKX-3-1/V5 and plasmids expressing FLJ22318 as a fusion protein with either a C-terminal V5 or N-terminal Myc, HA or GFP epitopes. Although it is possible that these epitopes may have interfered with the NKX3-1/FLJ22318 protein-protein interaction the epitopes have all been well characterised. Whereas one epitope may have caused a conformational change which inhibited or reduced protein binding it is less likely that all epitope tags at the C- and N-terminals used in these studies would have affected protein binding. It is possible however, that the level of protein expression affected the concentration of protein available for an interaction to occur. In transiently transfected cells, gene expression can be detected for between one and four days but expression is required for approximately one day following transfection before sufficient protein has accumulated in the cell to enable detection. As both NKX3-1 and FLJ22318 are predicted to be unstable *in vivo* (http://au.expasy.org/tools/protparam) and the mechanisms that regulate their turnover are unknown, it is possible that the rate of protein turnover exceeded the rate of protein synthesis leaving insufficient concentrations of one or both proteins for an interaction to be readily detected. A recent study in this laboratory has identified the half-life of endogenous NKX3-1 to be ~25 minutes (Thomas et al., 2006), however the half lives of exogenously expressed tagged NKX3-1 and FLJ22318 are unknown.

The affinity of one protein for another can also be altered by the presence or absence of an effector molecule such as ATP. In addition, a change in physiological conditions such as temperature, pH or covalent modification including phosphorylation can all affect protein binding (Nooren and Thornton, 2003). In PAFAH1B1 the region containing the LisH motif followed by a coiled-coiled region switches between an open or closed conformation dependent on the salt concentration. In very low salt concentrations (<50mM NaCl) an open conformation is adopted whereas at concentrations above 50mM NaCl both open and closed conformations are found to be present (Mateja et al., 2006). Equilibrium between both conformations is reached at 150mM NaCl with higher salt concentrations favouring a closed conformation. When the coiled-coiled region assumes the closed conformation a hydrophobic pocket in the LisH motif is obscured, which is proposed to have functional implications as this region

is required for protein-protein interactions (Mateja et al., 2006). As CTLH motifs are proposed to have a similar function to coiled-coiled regions, FLJ22318 may also adopt an open or closed conformation that is dependent on the salt concentration. If this is the case, the salt concentrations of 150mM NaCl used in the immunoprecipitation assays in comparison to 50mM NaCl used in GST pull-down assays may have resulted in different proportions of alternative FLJ22318 conformations present in the two assays. As such, the salt concentrations used in GST pull-down and co-immunoprecipitation assays may account for the difficulties in detecting NKX3-1 and FLJ22318 interactions.

Another possible explanation is that the interaction between NKX3-1 and FLJ22318 may be weak and/or transient. Transient protein-protein interactions are regulated by physiological conditions that have the ability to change the affinity between partners thereby allowing for the effective control of dynamic protein complexes (Nooren and Thornton, 2003). In addition, protein-protein interactions can also be classified as obligate and non-obligate with obligate protein-protein complexes being formed by proteins that are not stable on their own *in vivo*. Proteins that are involved in strong obligate interactions are also generally expressed at the same time and are co-localised on synthesis (Nooren and Thornton, 2003). As co-localisation of NKX3-1 and FLJ22318 appears to be affected by androgens in LNCaP prostate cancer cells and both proteins are predicted to be unstable *in vivo*, NKX3-1 and FLJ22318 may be part of a weak obligate protein-protein complex. The exceptionally high degree of amino acid sequence conservation between mammalian FLJ22318 orthologues suggesting that FLJ22318 function is critical in the cell (section 4.2.2) is consistent with previous analyses which have indicated that complexes formed by obligate protein-protein interactions are also involved in essential functions in the cell.

GST pull-down and co-immunoprecipitation assays were also limited by the ability to perform the techniques only in one direction. For GST pull-down assays, only GST-FLJ22318 was able to be used to pull down NKX3-1/V5-His and for co-immunoprecipitation assays, only NKX3-1/V5-His was able to be used to immunoprecipitate GFP-FLJ22318. Extensive previous studies in this laboratory have not been able to induce expression of GST-NKX3-1 in bacterial cells (Hooper & Bentel, unpublished). The reasons for this are unknown, however the use of rare codons by human NKX3-1, which would limit its expression in bacteria, and the reported

(bacterial) transcription repressor activity of the C-terminal region of NKX3-1 cDNA may contribute to the inability to express GST-NKX3-1 in bacteria. The N-terminal region of NKX3-1 including the homeodomain has been able to be expressed in bacterial cells and it may be feasible in future studies to test this type of construct in GST pull-down assays with FLJ22318 (Steadman et al., 2000).

Co-immunoprecipitation of FLJ22318 and NKX3-1 was also technically extremely difficult and several expression plasmids were tested before a suitable combination of NKX3-1-pcDNA3.1/V5-His and pEGFP-C2-FLJ22318 were identified. The anti-V5 antibody used in these studies worked very well for immunoprecipitation and was eventually successful in co-precipitating NKX3-1/V5-His and GFP-FLJ22318. However, other technical difficulties including detection of nonspecific immunoreactivity from the anti-Myc antibodies, inefficient co-expression of combinations of tagged NKX3-1 and FLJ22318, interference by IgG heavy chain of detection of the similarly sized HA-tagged FLJ22318 as well as evidence from results obtained that NKX3-1 and FLJ22318 are not major binding partners of each other, each limited successful completion of the experiments. Future studies using NKX3-1 and FLJ22318 antibodies rather than antibodies to tagged exogenously expressed proteins will facilitate characterisation of additional NKX3-1 and FLJ22318 interacting proteins in *in vitro* and *in vivo* assays.

Northern blotting of *FLJ22318* mRNA extracted from human LNCaP, DU145 and PC-3 prostate cancer cells, and MCF-7 breast cancer cells demonstrated that FLJ22318 is expressed in these cell lines with the detection of two transcripts of approximately 1.8Kbp and 4Kbp. The 1.8Kbp transcript corresponds with theoretical data published by NCBI relating to the reference sequence as well as a proposed alternative transcript identified using AceView (section 4.2.1). As the expression of FLJ22318 has not been characterised previously, sequencing would be necessary to determine the identity of these transcripts. In addition, it remains unknown whether these transcripts are present in normal breast and prostate tissue as the tissue distribution of FLJ22318 mRNA in malignant compared to normal tissue has also not been reported. As antibodies to FLJ22318 are currently unavailable, translation of these transcripts into functional proteins and the molecular size(s) of the FLJ22318 proteins in relation to the proposed (hypothetical) proteins of 44.4 and 49.4kDa are also unknown. Due to the high amino

acid conservation in mammalian FLJ22318 proteins, raising antibodies to human FLJ22318 may represent a challenge as it would be important to avoid self-recognition of the peptide by the host animal. To overcome cross species reactivity, antibodies are generally raised in the chicken for highly conserved mammalian proteins (Angeletti et al., 1997), however at present the chicken orthologue of FLJ22318 has not been identified so it is unknown how homologous these proteins may be. The chicken orthologue of human FLJ13910 has been identified and shares 95% homology with the human protein suggesting that chicken and human FLJ22318 may also share a high degree of amino acid conservation. In addition, care would need to be taken to ensure specificity to FLJ22318 as human FLJ22318 shares 70% amino acid identity with its (human) paralogue FLJ13910.

As *NKX3-1* expression is up-regulated by androgens and NKX3-1 and androgens have been shown to act synergistically to regulate gene expression in the prostate (Magee et al., 2003), regulation of *FLJ22318* expression by androgens was investigated in this study. However, following treatment with the androgen DHT for up to 72 hours in LNCaP prostate cancer cells, *FLJ22318* mRNA levels were found to be unaltered. Although these results would suggest that *FLJ22318* expression is not androgen-regulated in LNCaP prostate cancer cells, a recent study has shown that overexpression of NKX3-1 can down-regulate the expression of AR thereby modulating AR mediated signalling in the prostate (Lei et al., 2006). Since genes such as *angiopoietin 2*, have been identified that are regulated by androgens only in the absence of NKX3-1 expression, it has been proposed that NKX3-1 may regulate expression of potential androgen target genes (Magee et al., 2003). Therefore, further studies will be necessary to determine whether *FLJ22318* expression is modulated by androgens in prostate cancers that do not express high levels of NKX3-1.

In this study, the cellular localisation of FLJ22318 and its co-localisation with NKX3-1 was investigated by confocal microscopy. In DU145 and LNCaP prostate cancer cells, FLJ22318 was seen to have a diffuse localisation in both the perinuclear and nuclear regions of the cells and co-localised with NKX3-1 in these areas in both androgen treated LNCaP prostate cancer cells and in a proportion of untreated LNCaP and DU145 prostate cancer cells. As NKX3-1 is a homeodomain protein and as such a transcription factor that localises to the nucleus (Korkmaz et al., 2004) it was expected that for

FLJ22318 to interact with NKX3-1, FLJ22318 would also be predominately localised to the nucleus. Although FLJ22318 does not contain a recognised nuclear localisation signal (NLS), at position 190 of the FLJ22318 amino acid sequence there is a putative casein kinase 2 (CK2) phosphorylation site. Previous studies have shown that proteins with a NLS can also contain putative CK2 sites at a distance of approximately 10-30 amino acid residues from the NLS (Rihs et al., 1991). At position 195 of the FLJ22318 amino acid sequence there is a stretch of positively charged amino acids (KXHRXH), reported to be a hallmark of NLS (Dingwall and Laskey, 1991) and although this stretch of amino acids is not continuous as is the case of the classical NLS it may nevertheless represent a novel NLS, which targets FLJ22318 to the nucleus. The transcription factor FOXO1 is one such protein that is targeted to the cell nucleus when a serine residue three amino acids from one of two non classical NLS is dephosphorylated (Zhao et al., 2004).

Although NKX3-1 was also seen to have a perinuclear and nuclear localisation, immunofluorescence was punctate in appearance suggesting the sequestering of NKX3-1 within subcellular structures. Cytoplasmic accumulation of NKX3-1 has been observed in prostate cancers and the abnormal cellular localisation of NKX3-1 has been suggested as one of the mechanisms by which NKX3-1 is inactivated (Kim et al., 2002b). Mechanisms that regulate the subcellular localisation and turnover of NKX3-1 have not been defined. Of particular interest in this study is the previously unreported finding that androgens are required to facilitate accumulation of NKX3-1 in the nucleus in androgen responsive prostate cancer cells. This observation indicates that as well as regulating *NKX3-1* expression at the transcriptional level, androgens may also be involved in mediating NKX3-1 activation at the protein level. Previous studies have shown that androgens are required for the phosphorylation and subsequent nuclear translocation of other proteins such as Erk-1 (Peterziel et al., 1999), and homeodomain proteins are known to be posttranslationally modified by phosphorylation which in turn can affect their subcellular localisation and DNA binding affinity. The pancreatic duodenal homeobox-1 protein shuttles between the perinuclear and nuclear region of cells depending on its phosphorylation status whilst phosphorylation of the *Drosophila* homeobox protein engrailed has been shown to increase its DNA binding ability (Bourbon et al., 1995; Elrick and Docherty, 2001). Phosphorylation of NKX3-1 by protein kinase C (PKC) was also shown to affect NKX3-1 DNA binding affinity

whereas phosphorylation by CK2 stabilised NKX3-1 protein levels protecting it from degradation via the ubiquitin-proteasomal pathway (Ju et al., 2006; Li et al., 2006b). At present, it is unknown whether phosphorylation by PKC or CK2 affects NKX3-1 localisation, although previous studies have shown CK2 phosphorylation of testis specific protein, Y-linked (TSPY) is a prerequisite for its nuclear localisation whilst PKC phosphorylation of lim-kinase 2 (LIMK2) was shown to inhibit LIMK2 nuclear import (Goyal et al., 2006; Krick et al., 2006). As both PKC and CK2 activity are modulated by androgens (Maddali et al., 2005; Tawfic and Ahmed, 1994), future studies will be required to determine whether the androgen-mediated nuclear translocation of NKX3-1 observed in these studies is associated with NKX3-1 phosphorylation.

Results from this study indicate that FLJ22318 acts as a transcriptional repressor on the TAAGTA NKX3-1 consensus response element and in addition, FLJ22318 increases the transcriptional repressor function of NKX3-1 on this element. As FLJ22318 exhibited significant repressor activity on the TAAGTA response element in the absence of NKX3-1, it is possible that FLJ22318 can bind DNA directly and this will need to be examined in future studies. In addition, it will be necessary to determine whether FLJ22318 exhibits transcriptional repressor activity and increases the transcriptional repressor activity of NKX3-1 in androgen responsive LNCaP cells and whether these effects are dependent or independent on the level of FLJ22318 expression. Furthermore as the TAAGTA DNA-binding sequence has not been reported for any other NK class homeodomain protein and NKX3-1 expression is largely prostate specific, another possibility is that FLJ22318 may exhibit broad spectrum co-repressor activity involving more than one transcription factor.

As the NKX3-1 consensus response element used in this study was determined experimentally (target genes for NKX3-1 were unknown at the time) an examination of the DNA sequence comprising the NKE response element was undertaken to identify other potential transcription factor binding sites. Using the MatInspector V6.0 programme this examination indicated the presence of putative ARID3A binding sites which partially overlap the NKX3-1 binding sites. ARID3A is a member of the ARID family of proteins which have various roles in embryonic development, cell cycle control and transcriptional regulation and is a homologue of the *Drosophila* ‘dead

ringer' protein (Wilsker et al., 2002). During development, the sea urchin orthologue of 'dead ringer' SpDri regulates expression of the NK2 class homeodomain protein SpNK2.1 during gastrulation and human ARID3A is expressed in all tissues examined thus far, including prostate cDNA libraries (Ma et al., 2003; Takacs et al., 2004). Therefore ARID3A may bind to the NKE in the pT109-NKX-TK-Luc plasmid in DU145 cells which do not express endogenous NKX3-1 and potentially competes with NKX3-1 for binding to these sequences. A previous study has shown that ARID3A is necessary for E2F1 transcriptional activation in mouse fibroblasts and promotes G1/S transition through the cell cycle (Ma et al., 2003). ARID3A has also been shown to exhibit growth suppressive effects in the presence of p53 (Peeper et al., 2002). As p53 is non-functional in DU145 cells, ARID3A expression may be one possible explanation for the induced luciferase activity seen in this cell line upon transfection with the NKE reporter plasmid. To investigate this further, future studies could determine the identity of transcription factors that induce luciferase expression from the NKX-TK-Luc reporter vector in NKX3-1 expressing (LNCaP) and nonexpressing (DU145) cells and how FLJ22318 interacts with NKX3-1, other transcription factors and the NKE DNA sequences to repress transcription. It will also be necessary to repeat these studies using a biologically relevant NKX3-1 responsive promoter such as the *SMGA* or *PSA* promoters (section 1. 3.3.6) to more fully investigate FLJ22318 effects on NKX3-1 mediated transcriptional regulation.

Exogenous expression of FLJ22318 in this study was shown not to effect endogenous levels of NKX3-1 protein in LNCaP prostate cancer cells. This would indicate the increase in transcriptional repressor activity of NKX3-1 upon co-transfection of FLJ22318 was not as a result of an increase in NKX3-1 protein levels. However, the effect of FLJ22318 expression on NKX3-1 protein levels in normal prostate tissues is unknown and this would have to be investigated in future studies.

To date, apart from FLJ22318, no other proteins containing LisH, CTLH and CRA domains are known to interact with homeodomain proteins, however NPAT which contains only a LisH domain is part of a large multi-protein complex containing the homeodomain protein OCT1 and OCA-S (Zheng et al., 2003), and mice lacking expression of Ofd1, which also contains only a LisH domain, have altered expression of *Hoxa* and *Hoxd* genes (Ferrante et al., 2006). Unlike FLJ22318, not all proteins

containing either LisH, CTLH, CRA or combinations of these domains localise to the cytoplasm and nucleus of cells, PAFAH1B is cytoplasmic whilst OFD1 localises to centrioles (Gerlitz et al., 2005; Keller et al., 2005). Intriguingly, RANBP9 which does contain all three domains also localises to both the cytoplasm and nucleus of cells and in addition associates with the plasma membrane once phosphorylated (Denti et al., 2004; Nishitani et al., 2001). Therefore it would be interesting to see in future studies whether FLJ22318 can be phosphorylated, especially as FLJ22318 contains a putative CK2 phosphorylation site, and whether phosphorylation affects FLJ22318 cellular localisation.

In summary, results from this chapter have demonstrated that FLJ22318 interacts with NKX3-1 both *in vitro* and *in vivo* and co-localises with NKX3-1 in the perinuclear and nuclear region of androgen dependent and androgen independent prostate cancer cells. In addition, FLJ22318 exhibited transcriptional repressor activity on an NKX3-1 response element and increased NKX3-1 transcriptional repressor activity on this element. As the yeast orthologue of FLJ22318, RMD5, is found in the cell as part of multi-protein complexes it is possible that FLJ22318 also exists within the cell as part of larger protein complexes. As such identification of other FLJ22318 binding proteins may indicate a biological function for FLJ22318 and help to clarify its interaction with NKX3-1 in prostate cancer cells.

Chapter Six

Chapter Six – Isolation of FLJ22318 Binding Partners

6.1 Introduction

6.1.1 Isolation of FLJ22318 Binding Partners

As discussed in chapter four, FLJ22318 is a ubiquitously expressed protein that is highly conserved in mammalian species, suggesting that it has important biological functions. In addition, FLJ22318 contains LisH, CTLH and CRA protein-protein binding motifs which are well conserved in higher eukaryotes. Although the overall function of proteins with this domain structure remains unknown, it is likely that a ubiquitously expressed protein that has multiple protein-protein interaction domains has numerous binding partners. It was shown in chapter five that FLJ22318 interacts with the homeodomain protein NKX3-1 and increases the transcriptional repressor activity of NKX3-1 on the NKX3-1 TAAGTA consensus binding sequence. Interestingly, FLJ22318 also showed transcriptional repressor activity on this sequence in the absence of NKX3-1 and as discussed in chapter five this may have been as a result of FLJ22318 acting as part of a co-repressor complex in conjunction with other unidentified factors present in prostate cancer cells. In the cell, proteins may stably or rapidly and transiently associate with larger protein complexes and the biological function of a protein in a particular cell type may therefore be characterised following the identification of its interacting partners. As the cellular function of FLJ22318 is unknown and cannot be deduced from proteins with similar domain structures in human cells or in cells of other species, FLJ22318 binding proteins in LNCaP prostate cancer cells were isolated using a yeast two-hybrid screen.

In recent years several strategies have been described to identify protein-protein interactions including protein mass spectrometry (MS) and yeast two-hybrid analysis. Other than its high cost, the main limitation of MS analysis of protein-protein interactions is that the protein complexes first need to be isolated. Using this approach a tagged bait protein and its interactors are selectively purified from a cell lysate and the isolated proteins digested into peptides using a protease such as trypsin. These peptide mixtures are then separated by two-dimensional gel analysis and analysed by MS, and the protein interactors identified by database searching (Droit et al., 2005). However many proteins will not be detected because they are too rare, large, small, acidic or alkaline to be studied by two-dimensional gel analysis (Mendelsohn and Brent, 1999).

Also, the biological activity of the fusion protein depends on the location and the amino acid composition of the tag. As the tagged protein is overexpressed, its stoichiometry is altered in comparison to that of its partners in the complex and it must compete for complex assembly with the non tagged version of the protein. Moreover, the increased level of expression of the bait protein may increase the occurrence of non-specific interactions. In addition, some interactions may be missed altogether as a result of the tag disturbing complex formation or transient and loosely associated proteins being washed off during purification. Use of this approach thereby predisposes to identification of protein complexes which are abundant within the cell and which form stable, high affinity interactions (Droit et al., 2005).

Yeast two-hybrid analysis is a technique for identifying cDNAs that encode proteins which interact with a protein of known coding sequence. The system utilises the transcription of yeast reporter genes to detect protein-protein interactions and provides a sensitive method for detecting weak and transient protein interactions. As the assay is performed *in vivo*, proteins are more likely to be in their native conformations, potentially increasing the accuracy of detection of *bona fide* binding partners of the protein of interest.

The yeast two-hybrid method takes advantage of the domain structure of eukaryotic transcription factors which have functionally distinct DNA-binding (DNA-BD) and transcription activating domains (AD). Its principle was demonstrated by Fields and Song, (1989) who showed that yeast transcription could be used to identify protein-protein interactions when one protein was fused to a DNA-BD and proteins encoded by the target or 'prey' cDNA library were fused to an AD. Several yeast two-hybrid systems have since have been developed and consist of (i) yeast plasmids for expression of the known protein fused to a DNA-BD, (ii) yeast plasmids for expression of proteins encoded by cDNA fused to a transcription AD and (iii) yeast reporter genes that contain binding sites for the DNA-BD. These systems typically use the DNA-BD from either Gal4 or LexA acting upon a yeast promoter from either the *GAL1* or *CYC1* gene fused to *lacZ*. The *lacZ* gene encodes β-galactosidase, a secreted enzyme which cleaves the X-Gal substrate to form a blue product (Yocum et al., 1984). Yeast two-hybrid systems use additional reporter genes and a yeast strain which requires expression of these genes

to grow on specific media. To express the AD fused cDNA proteins, B42, an AD derived from bacteria, a very strong AD from the Herpes simplex virus protein VP16 or the strong AD from Gal4 can be used in conjunction with either a constitutive promoter, or a conditional promoter such as *GAL1* which is induced by galactose (Yocum et al., 1984).

Although this system is a powerful method, it too has several limitations. In some cases, the DNA-BD or AD fusions themselves may obstruct the normal site of protein interaction, or impair protein folding resulting in the inability of the two proteins to interact (van Aelst et al., 1993). Also, it cannot detect interactions requiring three or more proteins or those depending on post-translational modifications such as glycosylation (Ito et al., 2002) and the detection of an interaction in the yeast two-hybrid system does not necessarily mean that there is a corresponding interaction in the native environment of the proteins (Fields and Sternglanz, 1994). Some protein interactions may not be detectable in a GAL4 based two-hybrid system but may be detectable using a LexA based system (Mendelsohn and Brent, 1994) and finally, a significant number of interactions that are not of biological origin (false positives) can arise (Uetz, 2002).

To isolate FLJ22318 binding partners in this study, the BD Matchmaker™ Library Construction and Screening Kit was used (Clontech). This system utilises four reporter genes to assay for protein-protein interactions which should significantly reduce the number of false positives that could arise using yeast two-hybrid systems.

6.1.2 Yeast Two-Hybrid Analysis

The BD Matchmaker™ Library Construction and Screening Kit is comprised of three components, (i) a plasmid for expression of the protein of interest, the 'bait' protein, fused to a Gal4 DNA-BD, (ii) the AH109 yeast strain and (iii) a cDNA library. A Gal4 based system was chosen in preference to a LexA system as LexA does not have a yeast nuclear localisation signal and although most LexA fusion proteins will enter the yeast nucleus this is not always the case. Also LexA requires a minimum level of expression before it will efficiently bind its BD sequence (Silver et al., 1986). On the other hand, the yeast GAL4 protein has an inherent nuclear localisation sequence (Fields and Song,

1989) that in this system is located at the amino terminus of the BD sequence. This DNA-BD sequence comprises the first 146 amino acids of the GAL4 protein and binds as a dimer to the galactose upstream activating sequence (UAS_G) located upstream of the yeast reporter genes (Bram and Kornberg, 1985).

The yeast strain AH109 used in this study has four reporter genes *ADE2*, *HIS3* and *MEL1/lacZ*. The *ADE2* and *HIS3* reporter genes are under the control of distinct GAL4 UAS's enabling transcription of the *ADE2* and *HIS3* genes to be measured by the ability of the yeast to grow in the absence of adenine or histidine (James et al., 1996). The third reporter *MEL1* is an endogenous GAL4 responsive gene (Liljestrom, 1985) whilst the *lacZ* reporter gene was introduced into the PJ69-2A yeast strain to create strain AH109 and is also under the control of a distinct GAL4 UAS (Holtz and Zhu, 1995). *MEL1* and *lacZ* encode α-galactosidase and β-galactosidase respectively. α-galactosidase is a secreted enzyme which catalyses the hydrolysis of X-α-Gal yielding a blue end product and so providing an additional assay of activation by the 'bait' and AD fused proteins that interact with it, together with some quantitative information about the strength of the interaction (Aho et al., 1997).

The final component is a library plasmid which directs the expression of cDNA encoded proteins fused at their amino termini to a SV40 T-antigen nuclear localisation signal, a transcription AD comprised of amino acids 768-881 of the GAL4 protein and a haemagglutinin epitope tag. The AD fused cDNA encoded protein is constitutively expressed in yeast at a high level from the ADH1 promoter (Chien et al., 1991).

The BD Matchmaker™ yeast two-hybrid system is illustrated in Figure 6.1A. The constitutively expressed 'bait' protein binds the GAL4 responsive UAS upstream of the reporter genes *ADE2*, *HIS3*, *MEL1/lacZ* but does not activate their transcription. When a (constitutively expressed) AD fused cDNA encoded protein interacts with the 'bait', transcription of the reporter genes occurs enabling yeast cells containing the interacting proteins to grow on medium lacking adenine and histidine and to form blue colonies on X-α-Gal indicator plates.

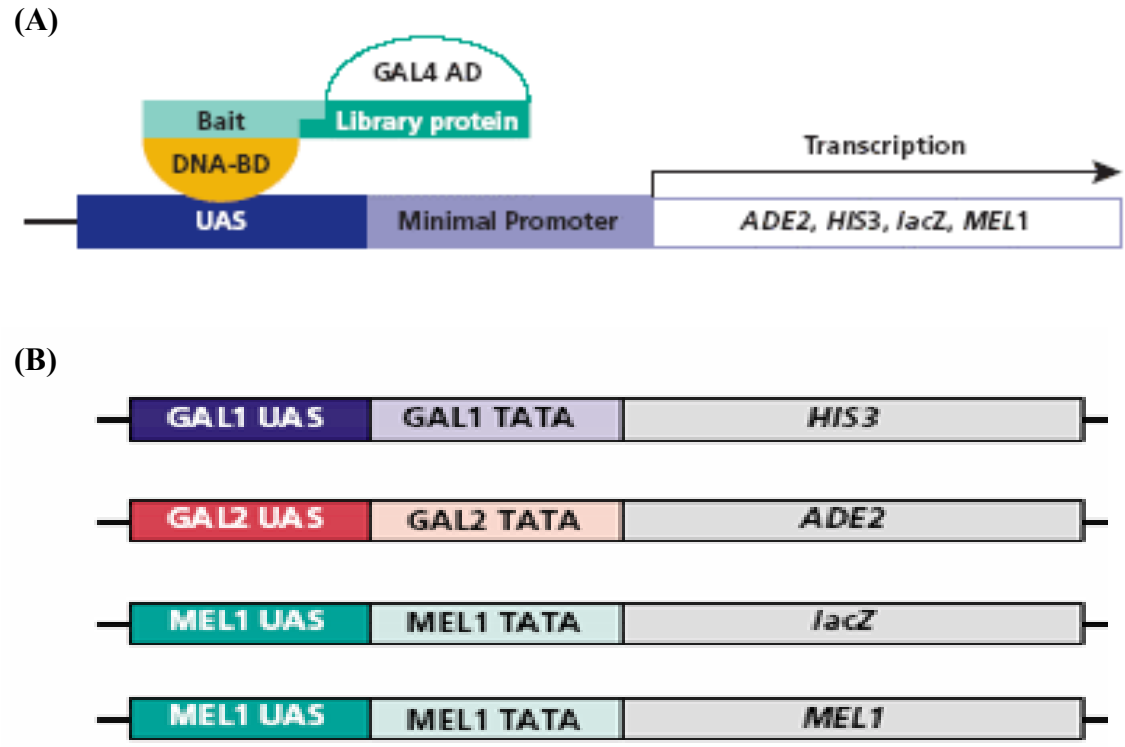

Figure 6.1 The BD Matchmaker™ yeast two-hybrid system. **(A)** A bait gene is expressed as a fusion to the GAL4 DNA-BD while cDNA encoded proteins are expressed as a fusion to the GAL4 AD. When bait and library fusion proteins interact the DNA-BD and AD are brought into close proximity activating transcription of the four reporter genes. **(B)** Reporter constructs in the AH109 yeast strain. Strain AH109 is a derivative of strain PJ69-2A and includes an introduced *lacZ* reporter, *ADE2* and *HIS3* markers and the endogenous *MEL1* gene. The *HIS3*, *ADE2* and *MEL1*/*lacZ* reporter genes are controlled by three distinct GAL4 responsive UAS and promoter elements, namely GAL1, GAL2 and MEL1.

6.1.3 The pGBKT7 GAL4 DNA-BD Expression Plasmid

pGBKT7 is a multi-copy yeast plasmid containing a yeast 2 μ origin of replication and yeast selectable marker gene *TRP1*, as well as a GAL4 DNA-BD flanked by the yeast ADH1 promoter and transcription terminator. Bait proteins are constitutively expressed at high levels from this plasmid and can be introduced and maintained in a $trp1^-$ yeast strain by selecting transformants on media lacking tryptophan. Moreover, yeast strains transformed with pGBKT7 have been shown to exhibit higher transformation efficiencies than strains transformed with other DNA-BD plasmids, which assists in the introduction of AD fusion libraries into yeast. The higher transformation efficiency also helps to maintain library complexity thereby increasing the possibility of detecting novel two-hybrid protein interactions (Louret et al., 1997).

6.1.4 AH109 Yeast Strain

The selection of cDNAs encoding interacting proteins depends on the yeast strain. AH109 are $gal4^-$ and $gal80^-$ to prevent interference of native regulatory proteins with the two-hybrid system and employs four reporter genes which are under the control of three distinct GAL4 UAS's and TATA boxes (Figure 6.1B). This greatly reduces the probability of false positives, as those false positives that interact directly with sequences flanking the GAL4 binding site and with transcription factors bound to specific TATA boxes are eliminated (James et al., 1996). Furthermore, the stringency of screening can be varied by selecting for the *ADE2* or *HIS3* reporter genes or both, further reducing the incidence of false positives (James et al., 1996). In addition to the nutritional selection, the use of the *MEL1* reporter provides further stringency to the system as false positives that may arise through activation of the *ADE2* or *HIS3* genes can be identified as they will fail to activate the *MEL1* reporter. Also the *MEL1* reporter provides a measure of the amount of transcription between a bait protein and a library protein allowing for the comparison of interaction strengths between the bait and different library proteins. Finally, in addition to the reporter genes, AH109 yeast carry mutations in the trp1 and leu2 marker genes allowing for selection of the plasmids used in the two-hybrid screen. The trp1 mutation is complemented by the *TRP1* gene in the pGBKT7 bait expression vector whilst the leu2 mutation is complemented by the *LEU2* gene in the pGADT7Rec library expression plasmid (James et al., 1996).

6.1.5 Construction of the cDNA Library

The cDNA library is constructed using BD SMART (**S**witching **M**echanism **a**t 5` end of **R**NA **T**ranscript) technology (Zhu et al., 2001). For first-strand cDNA synthesis, MMLV (Moloney Murine Leukaemia Virus) Reverse Transcriptase (RT) is used to transcribe poly A^+ RNA into DNA using a modified oligo(dT) primer, the BD Matchmaker™ CDS III Primer (Appendix 2). When MMLV RT reaches the 5` end of the mRNA, the enzyme's terminal transferase activity adds a few deoxycytidine (dC) nucleotides. The 3` end of the BD SMART III™ oligonucleotide (Appendix 2) anneals with this dC stretch forming an extended template. RT then switches templates and replicates the oligonucleotide, resulting in a single stranded (ss) cDNA containing the complete 5` end of the mRNA template as well as the sequence complementary to the BD SMART III™ oligonucleotide, the anchor. This anchor, together with the modified oligo(dT) then serve as priming sites for long distance (LD) PCR (Chenchik et al., 1998), where only the ss cDNAs with a SMART anchor at their 5` ends are amplified, eliminating amplification of incomplete cDNA thereby generating a higher percentage of full-length double stranded (ds) cDNA (Figure 6.2).

To produce the ds cDNA library, the ss cDNA is amplified by LD PCR using the BD Advantage 2 Polymerase Mix. This polymerase mix consists of a nuclease deficient N-terminal deletion of Taq DNA polymerase, BD TITANIUM™ Taq DNA Polymerase, together with BD TaqStart™ Antibody which provides an automatic hot-start PCR (Kellogg et al., 1994). Proofreading polymerase is also included in the polymerase mix to increase the fidelity of amplified DNA (of up to 20Kb) (Barnes, 1994).

6.1.6 pGADT7-Rec GAL4 AD Expression Plasmid and Library Screening

The library plasmid used for the expression of the AD fused cDNA proteins is pGADT7-Rec (Figure 3.7). This plasmid is a high copy plasmid containing the *LEU2* marker and has been engineered with the BD SMART III™ and CDS III sequences (Zhu et al., 2001) to utilise the homologous recombination system in yeast (Figure 6.3A). With recombination mediated cloning the yeast are co-transformed with *Sma*I linearised pGADT7-Rec and the ds library cDNA, which then recombine *in vivo* to form a closed circular expression plasmid that expresses the cDNA insert as a GAL4 AD fusion protein that can be selected for by plating transformants on media lacking leucine.

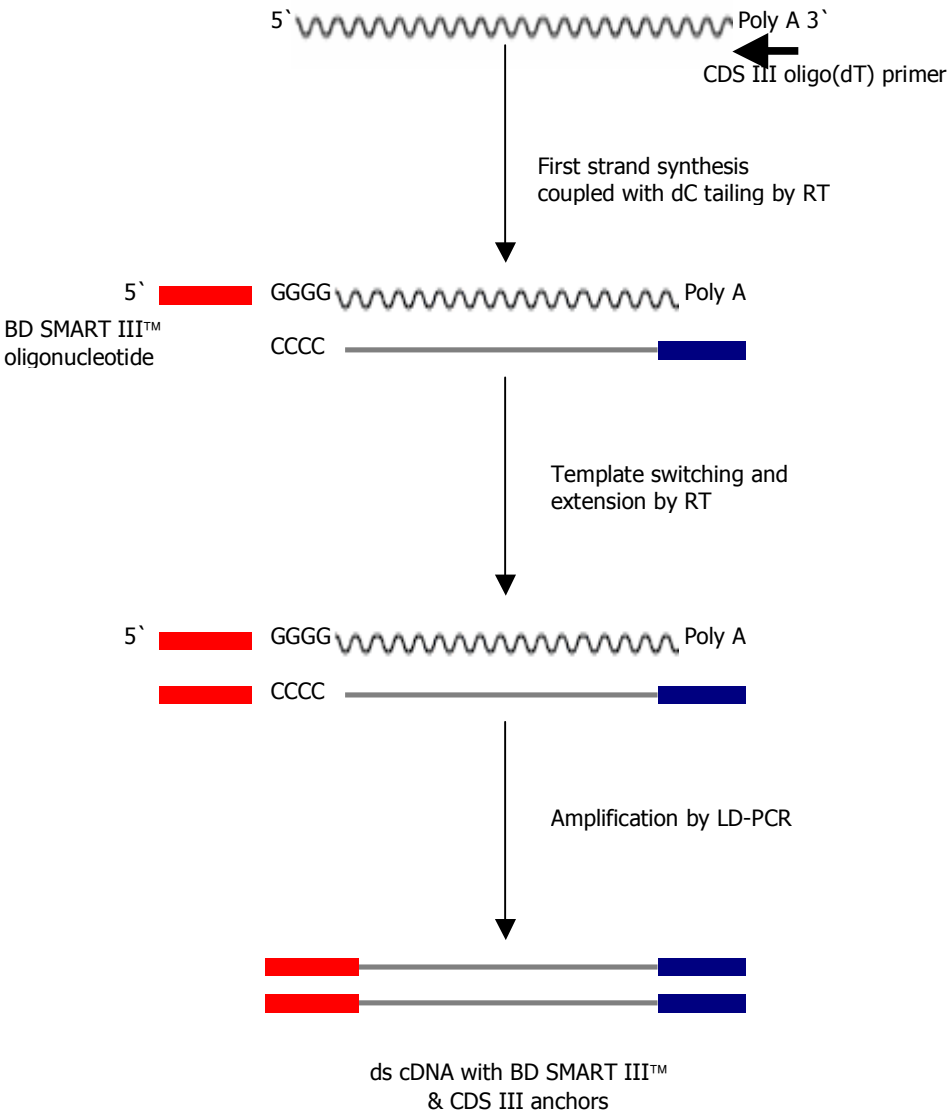

Figure 6.2 cDNA library construction. An oligo(dT) CDS III primer is used for first-strand synthesis from poly A^+ mRNA. When reverse transcriptase (RT) reaches the 5` end of the mRNA, the enzyme adds a few deoxycytidines (dC). The 3` end of the SMART III™ oligonucleotide anneals with the dC stretch forming a template for RT. The resultant single stranded cDNA is complementary to the mRNA template as well as the CDS III and SMART III™ oligos that serve as priming sites for LD-PCR. LD-PCRs result in double stranded cDNA products that have BD SMART III™ and CDS III anchors enabling ligation into the pGADT7-Rec library expression vector.

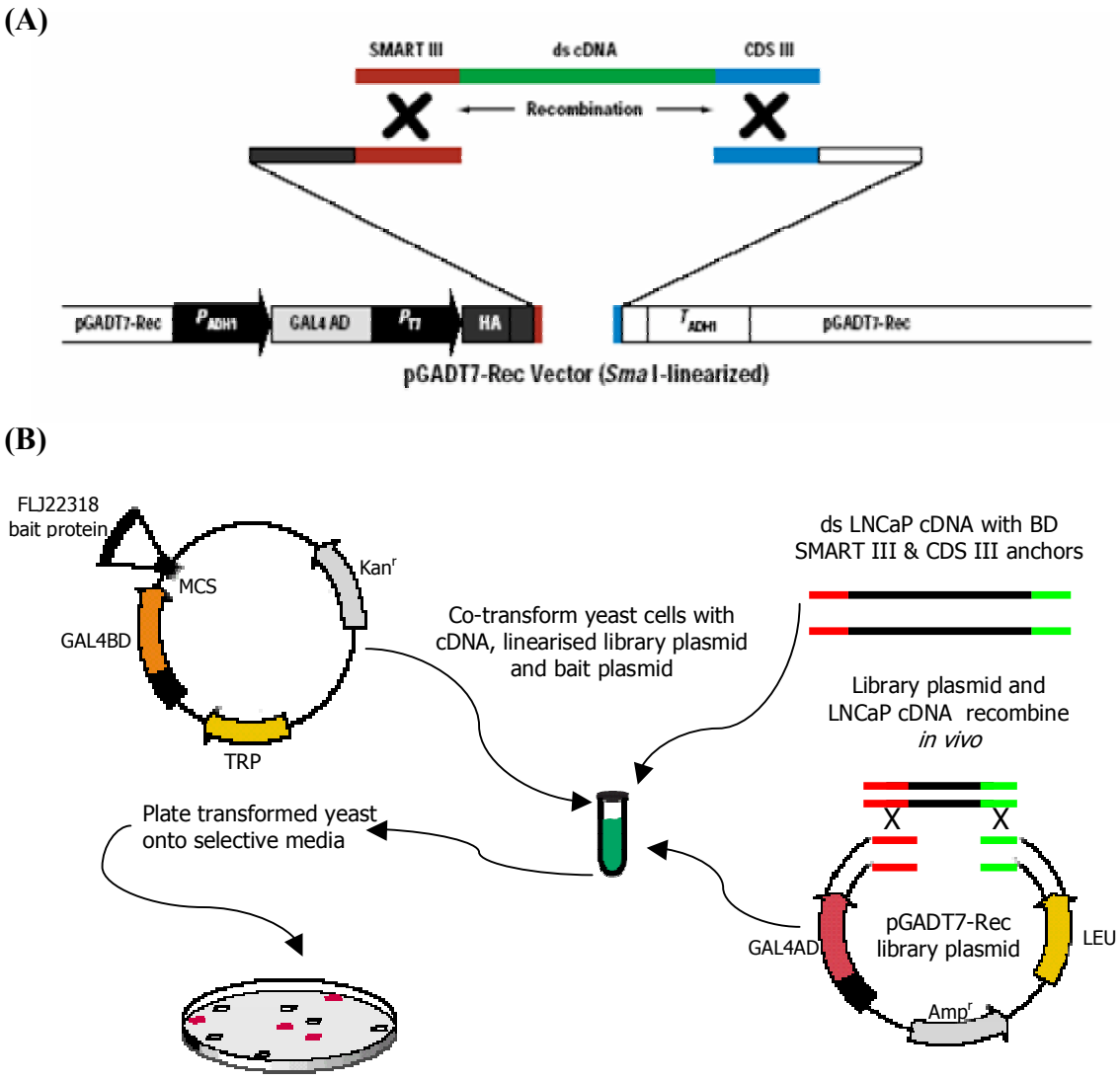

Figure 6.3 Yeast two-hybrid library screen. **(A)** When co-transformed into yeast the pGADT7-Rec plasmid is restored to its circular form by yeast enzymes using the homologous sequences at the cDNA ends to produce a GAL4 AD fused with a cDNA encoded protein expression plasmid. **(B)** Double stranded cDNA, the linearised GAL4 AD plasmid pGADT7-Rec and the GAL4 DNA-BD bait plasmid pGBKT7 are co-transformed into the AH109 yeast reporter strain where the cDNA recombines with homologous sequences in pGADT7-Rec. Transformants are then screened for two-hybrid interactions by plating on selective medium lacking adenine, histidine, leucine and tryptophan.

To perform the library screen, the cDNA library is introduced into the AH109 yeast in a large co-transformation with the bait protein to obtain many transformed cells. Those cells that contain library plasmids encoding proteins that interact with the bait protein are then selected by plating on minimal media lacking adenine, histidine, leucine and tryptophan (Figure 6.3B). Plasmid DNA is isolated from these cells, the cDNA inserts PCR amplified, sequenced and the insert sequences identified using Basic Local Alignment Search Tool (BLAST) analysis (Altschul et al., 1990).

6.2 Results

6.2.1 Yeast Two-Hybrid Analysis (I)

6.2.1.1 RNA Isolation and cDNA Synthesis

In order to generate a LNCaP cDNA library, poly A^+ RNA was isolated from 2 x 10^8 LNCaP prostate cancer cells using an Ambion Poly(A) Pure™ mRNA purification kit and 240ng poly A^+ RNA was used in first-strand cDNA synthesis using an oligo d(T) primer (sections 3.5.1.1-3.5.1.2). Following first-strand synthesis, duplicate 2µL aliquots of the reaction were amplified by long distance-PCR using an annealing temperature of 68°C and 24 PCR cycles, however no product was amplified (section 3.5.2.1; Figure 6.4A). This may have been due to PCR under cycling, therefore the number of PCR cycles was increased to 26 then 29 cycles, however no amplified products were detected (results not shown).

Since parallel reactions using human placenta poly A^+ RNA (positive control) were performed, producing ds cDNA of the expected size of 0.2kb to 2kb, the failure of LNCaP ds cDNA amplification may have been due to a low yield of first-strand cDNA synthesis (Figure 6.4A). These results indicated that the LNCaP poly A^+ RNA may have partially degraded prior to first-strand synthesis, therefore, new poly A^+ RNA was isolated from another 2 x 10^8 freshly cultured LNCaP cells and 152ng was used for first-strand cDNA synthesis (sections 3.5.1.1; 3.5.1.2). Following first-strand synthesis, a 2µL aliquot of ss cDNA was PCR amplified as described above, and a 2µL aliquot of the cDNA's was electrophoresed in a 1% agarose gel, resulting in identification of LNCaP cDNA products of ~0.2kb to 2kb (Figure 6.4B). To select for cDNA's in excess of 200bp, the amplified LNCaP cDNA was purified through a CHROMA SPIN+TE-400 column and 5µL of the purified cDNA's were electrophoresed in a 1% agarose gel

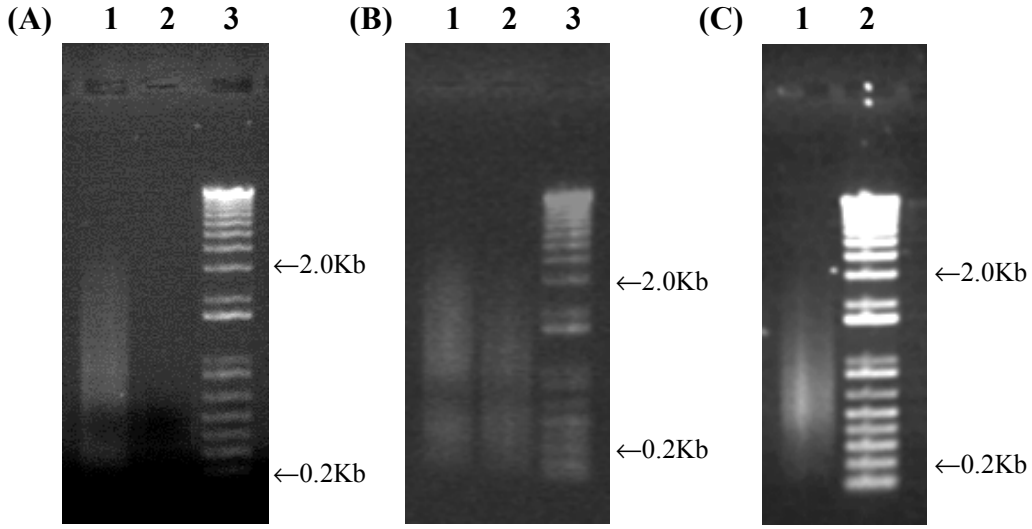

Figure 6.4 cDNA synthesis from LNCaP poly A^+ mRNA. **(A)** Initial PCR using an annealing temperature of 68°C and 24 PCR cycles failed to amplify LNCaP cDNA. **(B)** Using freshly isolated LNCaP poly A^+ RNA a smear of cDNA 0.2kb to 2kb was observed. **(C)** Electrophoresis of the purified LNCaP cDNA in preparation for cloning into pGADT7-Rec confirmed presence of products of ~0.2-2.0Kb.

(A) 1 Human placenta cDNA (positive control)
2 PCR amplified LNCaP cDNA
3 1Kb Plus™ DNA Ladder

(B) 1 Human placenta cDNA (positive control)
2 PCR amplified LNCaP cDNA
3 1Kb Plus™ DNA Ladder

(C) 1 Purified LNCaP cDNA
2 1Kb Plus™ DNA Ladder

resulting in identification of LNCaP cDNA products of ~0.2kb to 2kb (section 3.5.2.2; Figure 6.4C). Following purification, the LNCaP cDNA was stored at -20°C.

6.2.1.2 Yeast Two-Hybrid Analysis

For the initial yeast two-hybrid screen, AH109/pGBKT7-FLJ22318 yeast were made competent and a library scale transformation performed (sections 3.5.3; 3.5.6). To select for interacting proteins the transformation mixture was spread on SD/-His/-Leu/-Trp Triple Dropout Medium (TDO) and SD/-Ade/-His/-Leu/-Trp/X-α-Gal Quadruple Dropout Medium (QDO). SD/-Leu and SD/-Leu/-Trp media plates were included as controls for transformation efficiency. Following 4 days of incubation at 30°C the number of colonies growing on the SD/-Leu medium was ~1.2 x 10^4 which represented the number of transformants/3µg pGADT7-Rec. This was well below the number of expected transformants of ≥1 x 10^6/3µg pGADT7-Rec. The 1.65 x 10^4 colonies growing on the SD/-Leu/-Trp medium were also below the expected ≥5 x 10^5 clones screened/library and there was no growth observed on the QDO media. However, small colonies could be seen on the TDO media and these plates were incubated a further 3 days to confirm that the colonies were true Ade^+ as Ade^+ colonies are robust, can grow to >2mm in diameter and are white in colour, whereas Ade^- colonies never grow more than 1mm in diameter and turn red on adenine limited medium.

Following a total of 7 days of incubation, 77 true Ade^+ colonies were observed on the TDO media. In addition, growth of these colonies on the TDO media indicated the *HIS3* and *ADE2* genes had been activated suggesting an interaction between FLJ22318 and a protein in the LNCaP library in each transformant. The 77 colonies were replica plated onto the more stringent QDO media to eliminate the most common class of false positives and glycerol stocks were prepared (section 3.5.7). Of the 77 colonies, all grew on the QDO medium demonstrating that all 3 reporter genes *ADE2*, *HIS3* and *MEL1* had been activated. Plasmid DNA was isolated from these colonies and the AD/library inserts were PCR amplified using the ADLD primers (sections 3.1.3; 3.5.8; Appendix 2). Amplified products were then visualised in 1% agarose gels to screen for multiple AD/library plasmids or inserts and to determine insert sizes (Figure 6.5).

(A) **1 2 3 4 5 6 7 8 + - M**

(B) **1 2 3 4 5 6 7 8 + - M**

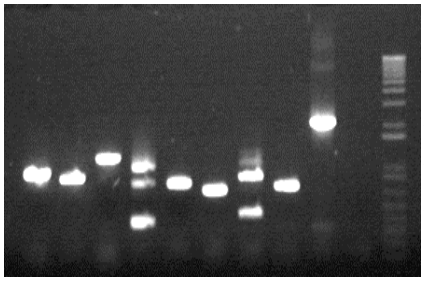

(C) **1 2 3 4 5 6 7 8 + - M**

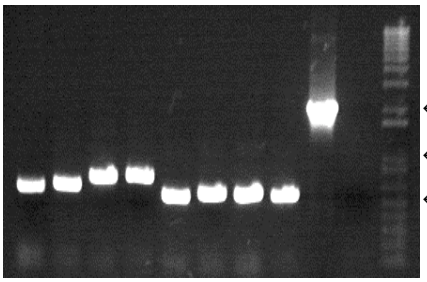

(D) **1 2 3 4 5 6 7 8 + - M**

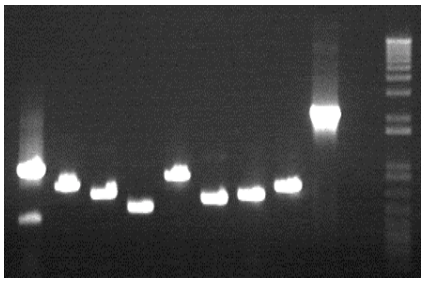

(E) **1 2 3 4 5 6 7 8 + - M**

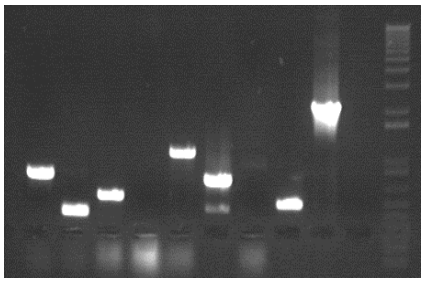

(F) **1 2 3 4 5 6 7 8 + - M**

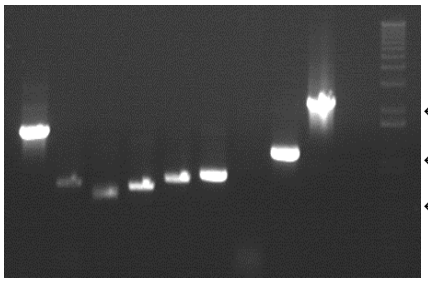

(G) **1 2 3 4 5 6 7 8 9 10 11 12 + - M**

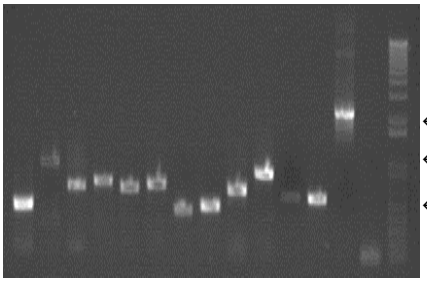

(H) **1 2 3 4 5 6 7 8 9 10 11 12 + - M**

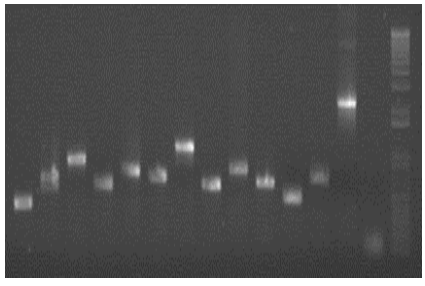

Figure 6.5 PCR screen of AD/library inserts from pGADT7-Rec to ascertain insert size and to check for multiple AD/library plasmids in colonies. Plasmid DNA was isolated from individual colonies, PCR amplified using ADLD primers and the amplified products electrophoresed in 1% agarose gels.

(+) AD-large T antigen (positive control)

(–) ddH_2O (negative control)

(M) 1Kb Plus™DNA Ladder

(A) 1-8 AD/library insert clones 1-8

(B) 1-8 AD/library insert clones 9-16

(C) 1-8 AD/library insert clones 17-24

(D) 1-8 AD/library insert clones 25-32

(E) 1-8 AD/library insert clones 33-40

(F) 1-8 AD/library insert clones 41-48

(G) 1-12 AD/library insert clones 50-55, 57-59, 61, 63-64

(H) 1-12 AD/library insert clones 65-76

AD/library inserts 2, 3, 8, 9, 11, 13, 48, 53, 63 and 65 were selected for initial analysis as these represented larger products or products of a size that was common to multiple clones. The PCR products for these inserts were purified and sequenced using the ADLD sense primer (sections 3.1.5; 3.4), then analysed using BLAST™. Of the 10 sequences analysed (Table 6.1), 9 were found to encode for proteins that are commonly recorded as false positives in yeast two-hybrid screens whilst the remaining sequence was found to encode a portion of the 3` UTR of C6orf48, a protein of unknown function. Due to the high rate of detection of false positive clones and the initial poor growth of colonies in the yeast two-hybrid analysis it was decided to repeat the library screen.

6.2.2 Yeast Two-Hybrid Analysis (II)

6.2.2.1 RNA Isolation and cDNA Synthesis

For the second yeast two-hybrid screen, poly A^+ RNA was isolated from 1.2 x 10^8 freshly cultured LNCaP cells using a Ambion Poly(A) Pure™ mRNA purification kit and 312ng poly A^+ RNA was used in first-strand cDNA synthesis (sections 3.5.1.1-3.5.1.2). Following first-strand synthesis, 4 x 1µL aliquots of ss cDNA were LD-PCR amplified using an annealing temperature of 68°C and 20 PCR cycles resulting in LNCaP cDNA products of ~0.1kb to 2kb (section 3.5.2.1; results not shown). Amplified LNCaP cDNA was then purified through a CHROMA SPIN+TE-400 column and a 5µL aliquot visualised in a 1% agarose gel producing a smear of approximately 0.2kb to 2kb (section 3.5.2.2; Figure 6.6). The purified LNCaP cDNA was then stored at -20°C until the repeat yeast two-hybrid screen was performed.

6.2.2.2 Yeast Two-Hybrid Analysis

For the repeat yeast two-hybrid screen, AH109/pGBKT7-FLJ22318 yeast were made competent, a library scale transformation performed and interacting proteins selected as previously described (sections 6.2.1.2; 3.5.3; 3.5.6). Following 6 days of incubation at 30°C, the number of transformants/3µg pGADT7-Rec was ~0.54 x 10^6 which was again below the number of expected transformants of $\geq$1 x 10^6/3µg pGADT7-Rec as was the total of 4.2 x 10^5 clones screened/library which was expected to be >5.0 x 10^5 clones screened/library. However, there was growth of 6 colonies on the QDO media and growth of 73 colonies on the TDO media, all of which were replica plated onto QDO

Table 6.1 mRNA transcripts identified in the initial yeast two-hybrid screen

Clone	Genbank Accession No.	Gene Name	CDS	Matching	Matching CDS (%)
2	NM_001009	Ribosomal protein S5	73-687	476-740	34
3	NM_022551	Ribosomal protein S18	46-504	213-531	64
8	NM_001003	Ribosomal protein large P1 transcript variant 1	130-474	84-507	100
9	NM_003295	Tumor protein, translationally-controlled 1	95-613	191-813	81
11	NM_053275	Ribosomal protein large P0 transcript variant 2	238-1191	443-558	13
13	NM_001009	Ribosomal protein S5	73-687	327-731	59
48	NM_053275	Ribosomal protein large P0 transcript variant 2	238-1191	487-1093	64
53	NM_001014	Ribosomal protein S10	69-566	236-604	66
63	NM_016947	Chromosome 6 open reading frame 48	42-422	466-708	3`UTR
65	NM_001004	Ribosomal protein large P2	106-453	414-484	11

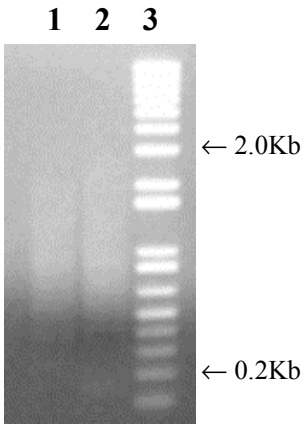

Figure 6.6 PCR amplification of LNCaP cDNA using poly A^+ RNA for the repeat yeast two-hybrid screen. LNCaP cDNA was amplified using an annealing temperature of 68°C and 20 PCR cycles then purified producing a product of approximately 0.2Kb to 2Kb.

1 Human placenta cDNA (positive control)
2 Purified LNCaP cDNA
3 1Kb Plus™ DNA Ladder

media and incubated for a further 6 days. Following 6 days of incubation, Q6, T8, T13, T22 and T36 failed to re-grow and no further analysis was performed for these clones. Of the remaining 5 QDO and 69 TDO colonies, all re-grew on the QDO media and glycerol stocks of the yeast clones were prepared (section 3.5.7). Plasmid DNA was isolated from the 74 colonies and the AD/library inserts were PCR amplified as previously described (section 3.1.3; Figure 6.7). Insert sizes of less than 1000bp predominated with the majority of inserts ranging in size from 650bp to 950bp (Figure 6.7).

No further analysis was carried out for clones T18, T57 and T79 as they were found to contain multiple AD/library inserts. The PCR amplified AD/library inserts for the remaining clones were purified (section 3.1.5), sequenced using the ADLD sense primer (section 3.4) and analysed using BLAST™. Of these 71 sequences, BLAST™ analysis identified 21 clones with inserts that had homology to either genomic DNA or in the case of 10 of these, homology to intronic regions of known genes. These inserts may represent false positives, as yet unidentified genes or alternatively spliced variants of known genes. Another 14 clones had inserts with homology to the 3`UTR's of 10 different proteins. This relatively high percentage (19%) may have been due to the use of an oligo(dT) primer when preparing the library cDNA instead of a random primer which would have resulted in a cDNA library with a greater representation of all portions of the gene, including amino-terminal and internal domains regardless of the mRNA secondary structure (Clontech, 2003). Analysis of the remaining 36 colonies identified inserts with homology to 33 different proteins with CKB, ATP5I and RPS15A each being identified twice. Four inserts (B2M, ATP5I, GEMIN7 and ARPC3) were found to contain complete ORF's with the remainder including between 10-91% of the ORF (Table 6.2).

Of the 33 proteins identified, 5 were found to be ribosomal proteins which have been identified as common false positives in yeast two-hybrid analysis (Gietz et al., 1997). One protein, ATAD3B was found to be out of frame and was also considered to be a false positive and excluded from further analysis. Of the remaining, 6 proteins STOML2, Loc401396, YIPF3, RWDD2, THAP4 and GAGE4 had unknown functions, whilst the remaining 21 proteins could be organised into 6 functional groups using Gene

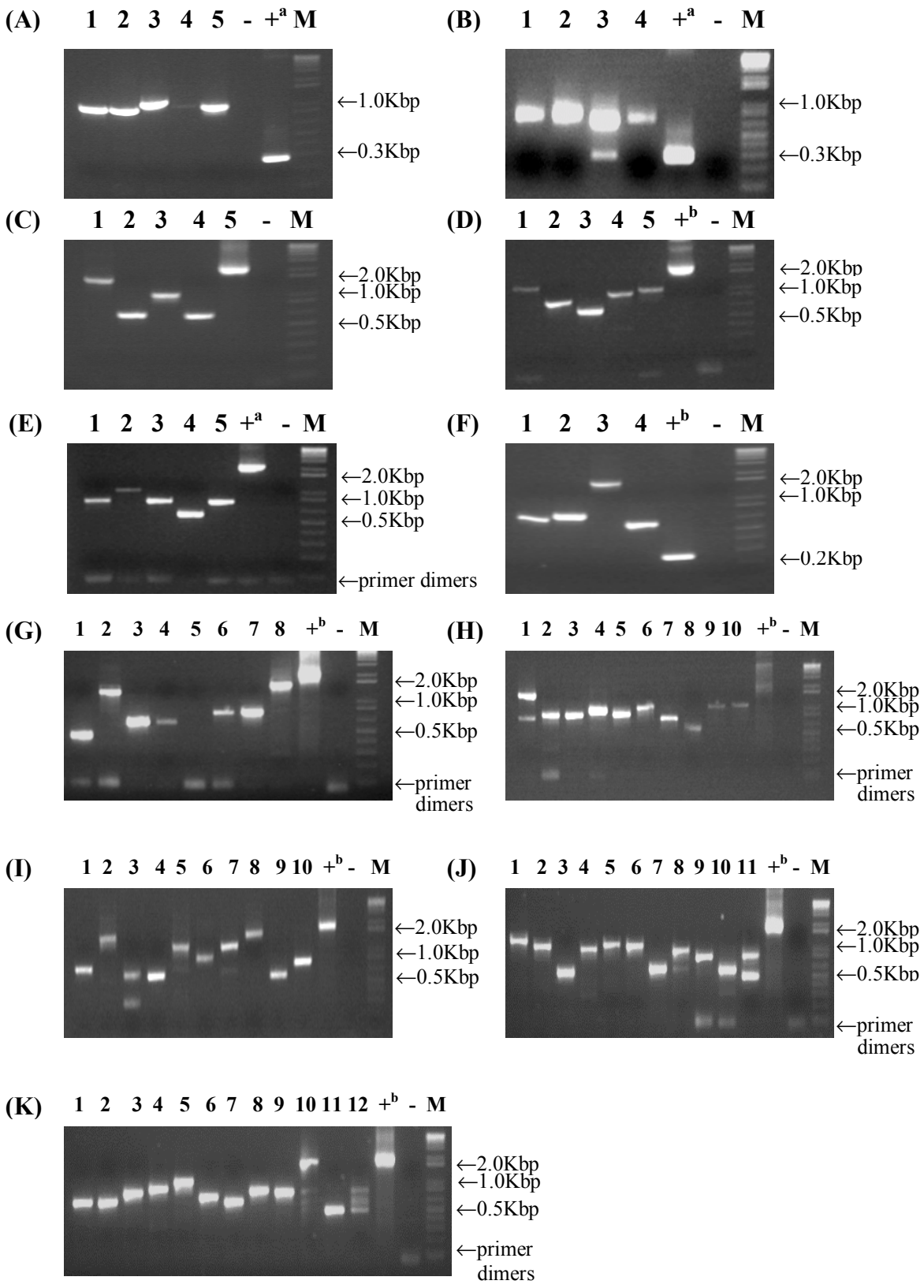
(A)
1 2 3 4 5 - +a M
←1.0Kbp
←0.3Kbp
(B)
1 2 3 4 +a - M
←1.0Kbp
←0.3Kbp
(C)
1 2 3 4 5 - M
←2.0Kbp
←1.0Kbp
←0.5Kbp
(D)
1 2 3 4 5 +b - M
←2.0Kbp
←1.0Kbp
←0.5Kbp
(E)
1 2 3 4 5 +a - M
←2.0Kbp
←1.0Kbp
←0.5Kbp
←primer dimers
(F)
1 2 3 4 +b - M
←2.0Kbp
←1.0Kbp
←0.2Kbp
(G)
1 2 3 4 5 6 7 8 +b - M
←2.0Kbp
←1.0Kbp
←0.5Kbp
←primer dimers
(H)
1 2 3 4 5 6 7 8 9 10 +b - M
←2.0Kbp
←1.0Kbp
←0.5Kbp
←primer dimers
(I)
1 2 3 4 5 6 7 8 9 10 +b - M
←2.0Kbp
←1.0Kbp
←0.5Kbp
(J)
1 2 3 4 5 6 7 8 9 10 11 +b - M
←2.0Kbp
←1.0Kbp
←0.5Kbp
←primer dimers
(K)
1 2 3 4 5 6 7 8 9 10 11 12 +b - M
←2.0Kbp
←1.0Kbp
←0.5Kbp
←primer dimers

Figure 6.7 PCR screen of AD/library inserts from pGADT7-Rec. Plasmid DNA was isolated from individual colonies, PCR amplified using ADLD primers and the amplified products electrophoresed in 1% agarose gels to ascertain the insert size and to check for multiple AD/library plasmids. pGADT7-Rec (200bp) or pGADT7-RecT containing an AD-large T antigen fusion (2Kbp) were included as positive controls. (Q = clones isolated on quadruple dropout medium, T = clones isolated on double dropout medium)

(+[a]) AD-no insert (positive control)

(+[b]) AD-large T antigen (positive control)

(–) ddH_2O (negative control)

(M) 1Kb Plus™ DNA Ladder

(A) 1-5 AD/library insert clone Q1-Q5

(B) 1-4 pGADT7-Rec AD/library insert clone T69-T72

(C) 1-4 AD/library insert clone Q4, T35, T40, T54

(D) 1-5 AD/library insert clone T11, T14, T25, T41, T68

(E) 1-5 AD/library insert clone T45, T56, T59, T63, T76

(F) 1-4 AD/library insert clone T10, T17, T33, T51

(G) 1-8 AD/library insert clone T27, T32, T38, T47, T52-T53, T61, T67

(H) 1-10 AD/library insert clone T7, T19, T12, T15, T29, T31, T34, T37, T60, T62

(I) 1-10 AD/library insert clone T9, T16, T18, T20-T21, T23-T24, T26, T28, T30

(J) 1-10 AD/library insert clone T39, T42-T44, T46, T48-T50, T52, T55, T57

(K) 1-10 AD/library insert clone T58, T63-T66, T73-T79

Table 6.2 mRNA transcripts identified in the second yeast two-hybrid screen

Clone	Genbank Accession No.	Gene	CDS	Matching	Matching CDS (%)
Q3	NM_004048	Beta-2-microglobulin (B2M)	61-420	27-657	100
Q4	NM_031921	ATPase family, AAA domain containing 3B (ATAD3B)	57-2003	1394-2121	31
T7	NM_017572	MAP kinase interacting serine/threonine kinase 2 (MKNK2)	236-1633	290-1011	50
T9	NM_002415	Macrophage migration inhibitory factor (glycosylation-inhibiting factor) (MIF)	98-445	177-561	77
T11	NM_001823	Creatine kinase brain (CKB)	81-1226	560-1366	58
T12	NM_053275	Ribosomal protein, large, P0 (RPLP0), transcript variant 2	238-1191	723-1255	42
T14	NM_001474	G antigen 4 (GAGE4)	83-436	1-487	
T17	NM_134440	Regulatory factor X-associated ankyrin-containing protein (RFXANK), transcript variant 2	506-1219	925-1337	41
T19	NM_014380	Nerve growth factor receptor (TNFRSF16) associated protein 1 (NGFRAP1), transcript variant 3	312-647	341-879	91
T24	NM_001007270	Gem (nuclear organelle) associated protein 7 (GEMIN7), transcript variant 3	152-547	1-899	100
T25	NM_013442	Stomatin (EPB72)-like 2 (STOML2)	64-1134	897-1212	22
T28	NM_007100	ATP synthase (ATP5I)	87-296	66-355	100
T30	NM_000972	Ribosomal protein L7a (RPL7A)	31-831	400-867	54
T31	NM_016129	COP9 constitutive photomorphogenic homolog subunit 4 (Arabidopsis) (COPS4)	140-1360	892-1141 & 1227-1708	31
T32	NM_001823	Creatine kinase brain (CKB)	81-1226	426-998	50
T34	NM_002512	Non-metastatic cells 2, protein (NM23B) expressed in (NME2)	73-531	219-665	68
T37	XM_379513	Hypothetical LOC401396 (LOC401396)	1-663	246-312	10
T43	NM_001019	Ribosomal protein S15a (RPS15A)	97-489	270-527	56

Table 6.2 mRNA transcripts identified in the second yeast two-hybrid screen

Clone	Genbank Accession No.	Gene	CDS	Matching	Matching CDS (%)
T45	NM_181493	Inosine triphosphatase (nucleoside triphosphate pyrophosphatase) (ITPA), transcript variant 2	143-676	598-1065	15
T46	NM_002046	Glyceraldehyde-3-phosphate dehydrogenase (GAPDH)	76-1083	424-1285	65
T48	NM_003690	Protein kinase, interferon-inducible double stranded RNA dependent activator (PRKRA)	108-1049	522-1368	56
T49	NM_001019	Ribosomal protein S15a (RPS15A)	97-489	212-522	71
T51	NM_000993	Ribosomal protein L31 (RPL31)	28-405	126-442	74
T52	NM_198216	Small nuclear ribonucleoprotein polypeptides B and B1 (SNRPB), transcript variant 1	164-886	472-1000	54
T55	NM_007100	ATP synthase (ATP5I)	87-296	66-357	100
T56	NM_145864	Kallikrein 3, (prostate specific antigen) (KLK3), transcript variant 2	42-356	279-805	25
T59	NM_015388	Yip1 domain family, member 3 (YIPF3)	158-1210	1078-1540	13
T60	NM_001402	Eukaryotic translation elongation factor 1 alpha 1 (EEF1A1)	63-1451	959-1707	35
T64	NM_033411	RWD domain containing 2 (RWDD2)	141-1019	842-1279	20
T66	NM_000126	Electron-transfer-flavoprotein, alpha polypeptide (glutaric aciduria II) (ETFA)	1-1002	593-1266	41
T68	NM_005719	Actin related protein 2/3 complex subunit 3, 21kDA (ARPC3)	94-630	81-864	100
T70	NM_015963	THAP domain containing 4 (THAP4)	224-1957	1657-2133	17
T73	NM_004152	Ornithine decarboxylase antizyme 1 (OAZ1)	79-282 & 284-761	529-894	34
T74	NM_001016	Ribosomal protein S12 (RPS12)	83-481	211-502	68
T75	NM_002168	Isocitrate dehydrogenase 2 (NADP+), mitochondrial (IDH2)	87-1445	1236-1732	15
T77	NM_198830	ATP citrate lyase (ACLY), transcript variant 2	164-3469	2198-2964	38

Ontology (GO) terms assigned from the GO database (www.geneontology.org). These functional groups comprised 3 translational regulation and pre mRNA splicing proteins EEF1A1, MKNK2 and SNRPB, 3 cellular energy and transport proteins ATP5I, ETFA and IDH2, 2 cellular motility proteins ARPC3 and GEMIN7, 2 degradation proteins COPS4 and KLK3, 5 proteins involved in cellular metabolism CKB, ITPA, GAPDH, OAZ1 and ACLY and 6 transcriptional regulators B2M, MIF, RFXANK, NGFRAP1, NME2 and PRKRA. Of these proteins, a number have important functions involved in providing energy to the cell such as GAPDH which is an important enzyme in glycolysis, being the only oxidisable molecule in the glycolytic pathway. IDH2 and ACLY are both required for the tricarboxylic acid (TCA) cycle and ETFA is involved in electron transport. ITPA is involved in the metabolism of amino acids and OAZ1 the biosynthesis of polyamines and these are all cellular functions in which mitochondria have been shown to play an important role (Becker et al., 1996). As IDH2 and ETFA are known mitochondrial proteins, a search of the mitochondrial proteome database (MITOP) which covers mitochondrial encoded proteins from *Saccharomyces cerevisiae*, *Mus musculus*, *Caenorhabditis elegans*, *Neurospora crassa* and *Homo sapiens* (http://www.mips.biochem.mpg.de/proj/medgen/mitop) was undertaken to see whether any of the other proteins isolated in the in the yeast two-hybrid screen also had associations with mitochondria.

Interestingly, this search identified 9 additional proteins as being associated with mitochondria. Of these, the nucleoside diphosphate kinase NME2 has been isolated from both human and mouse mitochondrial proteomes as has the glycolytic protein GAPDH and STOML2, one of the proteins of unknown function (Mootha et al., 2003; Taylor et al., 2003). Although GAPDH is regarded as a cytoplasmic glycolytic enzyme, the isolation of this protein from both mouse and human mitochondrial proteomes would suggest that this protein could be dual-targeted, reflecting its presence in multiple compartments. This is the case with Arabidopsis glycolytic enzymes which are found both in the cytoplasm and are functionally associated with the outer membrane of plant mitochondria (Giegĕ et al., 2003). A study showing that GAPDH may electrostatically associate with the mitochondrial outer membrane due its basic pI value lends support to this theory (Hartmann et al., 1993). Also, since glycolysis produces pyruvate which feeds into the TCA cycle in the mitochondrial matrix it would be biologically relevant for glycolytic enzymes to be in close proximity to the mitochondrion. Other proteins

that were isolated from mouse liver, brain, heart and kidney mitochondria were creatine kinase brain, ATP5I and OAZ1 (Mootha et al., 2003), and from human heart mitochondria the translation factor EEF1A1 (Taylor et al., 2003). In addition, OAZ1 has recently been shown to be involved in substrate delivery to the proteasome (Palanimurugan et al., 2004). Also of note, was the isolation from mouse mitochondria of subunits 2 and 6 of the COP9 signalosome, a multi-protein complex of the ubiquitin-proteasome pathway that shares structural similarity with the 26S proteasome lid complex. Both of these sub units, COPS2 and COPS6 have been shown to interact with the COPS4 sub unit (Schwechheimer, 2004) although the functional significance of this has yet to be determined. Literature based searches of the remaining proteins revealed a mitochondrial association with 4 more proteins, RFXANK which is part of a complex containing the mitochondrial pro-apoptotic proteins caspase-9 and procaspase-3 (Patriotis et al., 2001), NGFRAP1 which interacts with Smac, a protein released from the mitochondria during apoptosis and which promotes caspase activation (Yoon et al., 2004), PRKRA which associates with replicating mitochondria (Kim et al., 2004a) and ARPC3 whose yeast orthologue arc18p associates with mitochondria in budding yeast (Fehrenbacher et al., 2005). Although the remaining 7 proteins along with FLJ22318 were not identified as being associated with the mitochondria it has been estimated that there are 1500 human mitochondrial genes and proteins of which only 615 have been identified to date (Taylor et al., 2003).

6.2.2.3 Yeast Two-Hybrid Analysis Controls

Small scale yeast control co-transformation procedures were also performed in parallel to the library screens using pGADT7-RecT (Figure 6.8A), which encodes a fusion between the GAL4 AD and SV40 large T-antigen, and the positive control vector pGBKT7-53 which encodes a fusion between the GAL4 DNA-BD and murine p53 (Figure 6.8C) and the negative control vector pGBKT7-Lam (Figure 6.8B). In the AH109 yeast, pGBKT7-53 interacts with SV40 large T-antigen whereas pGBKT7-Lam which encodes a fusion of the DNA-BD with human lamin C does not interact with either SV40 large T-antigen or most other proteins and therefore controls for false interactions between either the pGADT7-RecT control or an AD/library plasmid. For both the initial and repeat yeast two-hybrid screens, AH109 yeast cells were made competent and a small-scale yeast transformation performed (sections 3.5.3-3.5.4). To confirm that the pGBKT7-53/pGADT7-RecT and pGBKT7-Lam/pGADT7-RecT

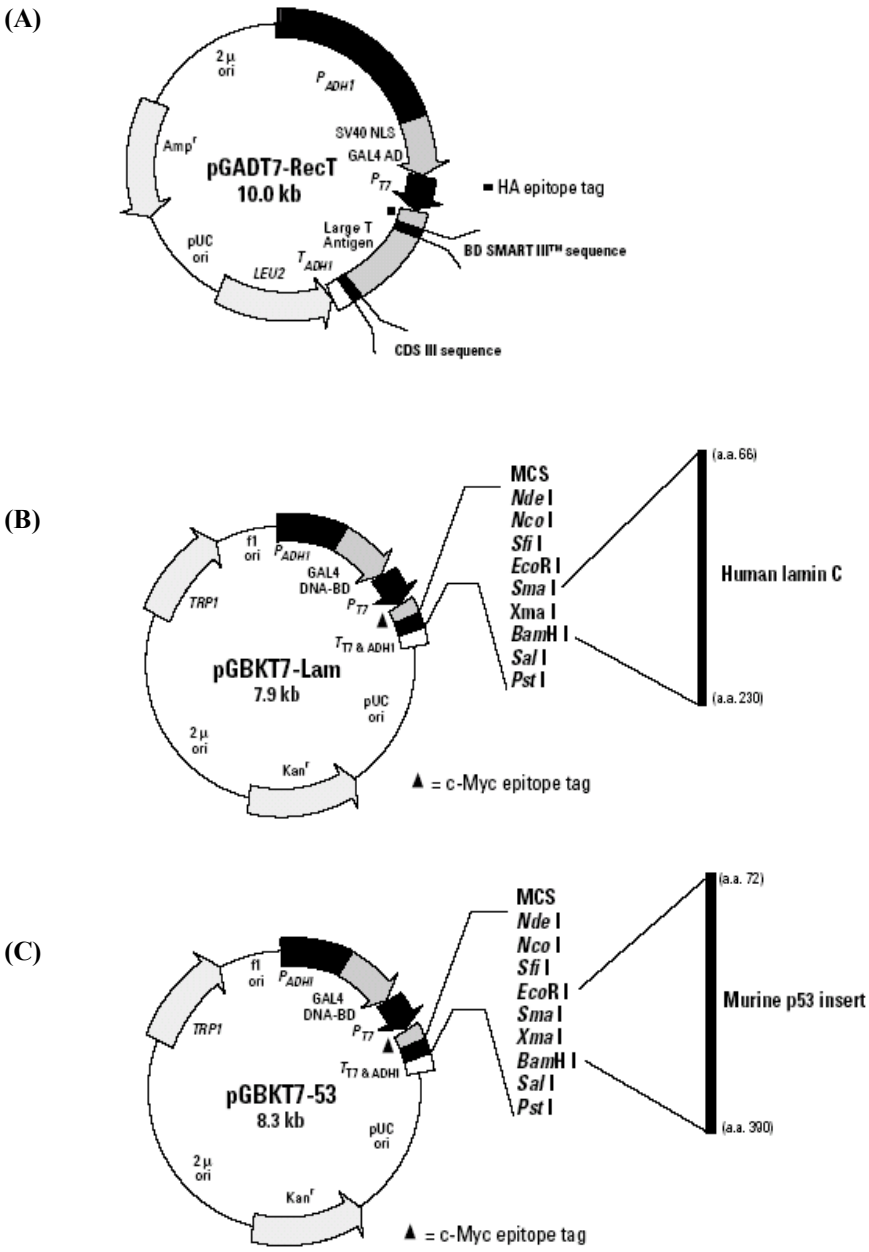

Figure 6.8 Vector maps of the Yeast-2 Hybrid control vectors **(A)** pGADT7-RecT is a product of recombination that encodes a fusion of the SV40 large T antigen and the GAL4 AD. **(B)** pGBKT7-lam is a negative control plasmid that encodes a fusion protein of the human lamin C protein and the GAL DNA-BD. Yeast co-transformed with pGADT7-RecT and pGBKT7-lam provide a measure of the background that is due to false positive two-hybrid interactions as Lamin C does not interact with most proteins including pGADT7-RecT. **(C)** pGBKT7-53 is a positive control plasmid that encodes a fusion protein of the murine p53 protein and the GAL4 DNA-BD (www.clontech.com).

plasmids had been successfully transformed, the transformation mixture was spread on SD/-Leu/-Trp Double Dropout Medium (DDO), whereas to select for co-transformants expressing interacting proteins the transformation mixture was spread on QDO media plates. Following 6 days of incubation at 30°C, growth of white colonies were seen on the DDO media plates for both the pGBKT7-53/pGADT7-RecT and pGBKT7-Lam/pGADT7-RecT plasmids, whereas growth of blue colonies was only observed on the pGBKT7-53/pGADT7-RecT QDO media plates (results not shown). This indicated that both the positive and negative control plasmids had been successfully transformed and that only the proteins encoded by the positive control plasmids pGBKT7-53 and pGADT7-RecT had interacted as expected.

6.3 Discussion

In this study a GAL4 based yeast two-hybrid system was used to identify proteins which interacted with the novel hypothetical protein FLJ22318. This *in vivo* method was chosen as it is often more sensitive and may therefore be more suited for detecting weak or transient and unstable interactions that may not be biochemically detectable, but which nonetheless are critical for the proper functioning of complex biological systems (Estojak et al., 1995).

Lower than expected transformation efficiencies were seen in both the initial and repeat yeast two-hybrid screens and this may have occurred as a result of FLJ22318 interacting weakly or transiently with the other proteins. In these instances the time taken for the *HIS3* reporter to be expressed as a result of a two-hybrid interaction and for the gene product to accumulate may not have allowed enough of the gene product to accumulate in the cells to permit survival of co-transformants plated directly onto TDO medium lacking His. Therefore, a *HIS3* "jumpstart" may have resulted in a greater number of positive transformants. Plating the transformation mixture onto DDO and selecting for the FLJ22318 and the AD/library plasmids first may have been a better strategy as this would have allowed higher levels of the fusion protein and the HIS3 gene product to be expressed before replating on the TDO and QDO medium. Also the lower than expected transformation efficiencies may have been due to a recovery step performed in YPD medium following library transformation. Later changes recommended by the

manufacturer on their website (www.clontech.com/clontech/techinfo/faqs/MMTechTip.shtml#GAL4) suggest elimination of this recovery step and plating of the transformation mixture on DDO medium to avoid loss of the DNA/bait vector in some of the cells which would reduce transformation efficiencies resulting in fewer colonies being isolated.

Only 3 proteins were identified more than once as interacting with FLJ22318 and although a known partner, NKX3-1, was not identified, with a 2.5Kb 3'UTR, it is unlikely that generation of the LNCaP cDNA library using oligo dT primers would have resulted in amplification of the NKX3-1 coding region and therefore detection in this assay. Data from 64 successful yeast two-hybrid screens has shown that although partners were known for 30 bait proteins prior to screening, only 11 of the screens identified previously known partners whereas 19 yeast two-hybrid analyses identified only novel partners (www.fccc.edu/research/labs/golemis/InteractionTrap/InWork.html). A number of studies have also reported that interactions which were originally identified only once in a yeast two-hybrid screen were true interactors as confirmed by subsequent methods. A recent example is HOXB2 which was one of 10 individual clones isolated in a yeast two-hybrid screen as binding to the cell proliferation regulator p205 (Asefa et al., 2006). A relatively high number of the proteins identified in the present screen have associations with mitochondria, and mitochondria-associated proteins along with ribosomal proteins have been reported to occur as false positives in yeast two-hybrid screens, although with a lesser frequency. However, the interacting proteins identified in this study are also involved in cellular metabolism and energy production as well as protein ubiquitination, degradation and programmed cell death, pathways (and proteins) which can function both in association with and independently of the mitochondria (Kim and Dang, 2005; Yang and Yu, 2003). These results are consistent with the reported functions of proteins that have a similar domain structure to that of FLJ22318 including the yeast homologue of FLJ22318, RMD5.

Two of the proteins involved in cellular metabolism isolated in this study are the enzymes ACYL and IDH2, which are required for the oxidation of citrate in the tricarboxylic acid (TCA) cycle. As citrate metabolism in both normal prostate cells and prostate cancer cells differs from other cells, the isolation of these proteins maybe

significant. Normal prostate peripheral zone secretory epithelial cells produce an approximate 40 fold increase in citrate production compared to other cells in the body. However, the majority of this citrate is not oxidised and instead is secreted from the cells (Costello et al., 2005). In addition, unlike other cells, the high levels of citrate would be expected to inhibit glycolysis through the regulation of phosphofructokinase (PFK) however this is not the case and prostate cells exhibit a high level of aerobic glycolysis, suggesting that the regulation of PFK in these cells and its effect on glycolysis are unique (Costello and Franklin, 1997). The accelerated utilisation of glucose in these cells also results in the synthesis of citrate through the production of acetyl-coA. The high level of aerobic glycolysis combined with a truncated TCA cycle should result in a ~65% decrease in ATP production in these cells. However, prostate cells exhibit the same levels of ATP as other cells suggesting the existence of alternative metabolic pathways (Costello and Franklin, 1997). At present, these pathways and the proteins involved remain unknown. In addition to the high levels of citrate seen in prostate cells, zinc levels are also high and in these cells prevents the oxidation of citrate by inhibiting aconitase. Furthermore, the cellular accumulation of zinc has been shown to inhibit cellular proliferation by apoptosis through a zinc-mitochondrial interaction, which has only been documented in citrate producing prostate cells and does not occur elsewhere in the body (Costello et al., 2005).

In contrast to normal cells, malignant prostate cells exhibit a decrease in aerobic glycolysis, have low levels of citrate and transform from citrate producing to citrate oxidising cells with a fully functional TCA cycle (Costello and Franklin, 1997). This is in contrast to other mammalian cancer cells which generally transform from energy-efficient, citrate oxidising cells to energy-inefficient citrate producing cells with a truncated TCA cycle, and in these cells the citrate is then transported to the cytoplasm for metabolism to acetyl-coA for lipogenesis, a process essential for cancer cell proliferation (Costello and Franklin, 1997). In addition to the low levels of citrate seen in malignant prostate cells, the level of zinc also falls, which in turn has been shown to inhibit apoptosis (Costello et al., 2005).

As malignant prostate cells exhibit a decrease in aerobic glycolysis, the isolation of GAPDH in conjunction with ACLY and IDH2 suggest that FLJ22318 is involved in the regulation of cellular metabolism. On the other hand, GAPDH has recently been shown

to function as part of a co-activator complex responsible for the S-phase dependent trans-activation of the histone *H2B* gene where it was proposed that GAPDH integrated energy metabolism with cell cycle regulation (Zheng et al., 2003). The role of GAPDH in regulating cellular proliferation has been suggested by several other studies, which reported it to be a target for an anti-proliferative bacterial agent, anti-cancer nucleoside analogues and when over-expressed in COS-7 cells, GAPDH has also been shown to induce apoptosis (Kim and Dang, 2005).

Integration between cellular metabolism and cellular proliferation is also well-characterised and is supported in this study by the isolation of proteins involved in both pathways. One of these proteins, ETFA is involved in generating mitochondrial membrane potential and disruptions to this mitochondrial membrane potential can result in the induction of programmed cell death through the release of pro-apoptotic proteins into the cytoplasm (Bras et al., 2005). Therefore the isolation of RFXANK and NGFRAP1, which have been shown to interact with these pro-apoptotic proteins (Patriotis et al., 2001; Yoon et al., 2004), maybe significant as may the isolation of PRKRA which has also been implicated in apoptotic cell death (Gupta and Patel, 2002).

It is now understood that programmed cell death pathways, classified as type I (apoptosis), type II (autophagic) or type III (necrosis-like) are most likely all linked through shared signalling pathways, with the mitochondria having a major role in integrating these cell death signals (Bras et al., 2005). At present however, there is little information on the proteins or pathways involved in the communication of mitochondria with the cytoplasm and nucleus.

As cancer develops when molecular pathways that control cellular proliferation and/or programmed cell death are deregulated, with a reduction in autophagic activity and resistance to apoptosis being common occurrences, the identification of proteins involved in these processes is of particular importance, especially as it is the acquisition of apoptosis resistance that leads to treatment resistance seen in advanced prostate cancer. In androgen responsive prostate cancer cells, androgens down regulate the expression of the pro-apoptotic protein Bax whilst the increased expression of the anti-apoptotic protein Bcl-2 is linked to the survival of prostate cancer cells following androgen ablation therapy (McKenzie and Kyprianou, 2006). Both Bax and Bcl-2 have

been identified as targets for ubiquitination and it is now known that the ubiquitination and proteasomal degradation pathway regulates numerous apoptosis associated proteins, a process that can contribute to the apoptosis resistance seen in cancer (Zhang et al., 2004).

For protein degradation to occur, activated ubiquitin is transferred to a target protein by a ubiquitin E3 ligase which can function as a single protein or as part of a multi-protein complex (Lee and Peter, 2003). Currently there are 2 known types of E3 ligases defined as either 'homologous to E6-AP carboxyl terminus' (HECT) or 'really interesting new gene' (RING) domains of which the RING domain family comprise the majority. However, of the ~200 RING domain family proteins in mammalian cells the majority remain uncharacterised (Yang and Yu, 2003). Once ubiquitinated, the target protein is degraded by the proteasome and although the mechanism of target protein delivery to the proteasome remains unknown, it is thought to require chaperone molecules which facilitate proteasome degradation (Yang and Yu, 2003).

As well as degradation by the proteasome, the regulation of cullin containing ubiquitin E3 ligases has recently been attributed to the COP9 signalosome. Cullin proteins act as scaffold proteins for E3 ligases and in this degradation pathway deneddylation of cullins is required for protein degradation to occur (Richardson and Zundel, 2005). As several of these cullin-mediated E3 ligases are implicated in cell cycle control and apoptosis (Willems et al., 2004) the identification of a component of the COP9 signalosome together with potential components of the 26S proteasome lends support to FLJ22318 being involved in ubiquitin mediated protein degradation.

Further support that FLJ22318 functions as a component of ubiquitin mediated protein degradation is provided by the *S. cerevisiae* protein RMD5. FLJ22318 is 1 of 2 orthologues of RMD5 and as such may be predicted to have a similar function. In yeast, RMD5 has been shown to be part of a large protein complex with a molecular mass of at least 600kDa. This complex consists of 8 proteins, 7 of which are required for the catabolite degradation of fructose-1,6-bisphosphatase (FBPase). Within this complex, RMD5 was specifically required for the ubiquitination of FBPase and is required for the proteasome dependent degradation of FBPase (Regelmann et al., 2003). More importantly as FBPase is degraded when the cell switches from anaerobic respiration to

aerobic respiration, if FLJ22318 has a similar role in mammalian cells, results from this study may provide a link between glycolytic PFK and gluconeogenic FBPase regulation in prostate cancer cells. Finally, other proteins containing a LisH domain, such as TBL1X, have been shown to recruit the ubiquitin-proteasome complex to nuclear receptor-regulated transcription factors. Therefore FLJ22318 may have a role in recruiting the ubiquitin-proteasome complex to transcription factors including NKX3-1 which is positively regulated by androgen receptor and whose degradation has recently been shown to be mediated by the ubiquitin-proteasome pathway (Lei et al., 2006).

As the yeast two-hybrid screen identified 6 candidate FLJ22318 interacting proteins that can act as transcriptional regulators, and FLJ22318 exhibited transcriptional regulatory activity on an NKX3-1 responsive element in the absence and presence of NKX3-1, it was decided to further investigate one of these proteins. The 6 transcriptional regulators isolated in the yeast two-hybrid screen were B2M, MIF, RFXANK, NGFRAP1, NME2 and PRKRA (Table 6.2). As PRKRA is a multifunctional protein with widespread expression and is involved in apoptosis and cellular proliferation, the interaction between PRKRA and FLJ22318 was examined in several preliminary studies carried out at the end of this thesis project.

Chapter Seven

Chapter Seven – Analysis of PRKRA: A Candidate FLJ22318 Binding Partner

7.1 Introduction

Protein kinase, interferon-inducible double stranded RNA dependent activator (PRKRA; PACT) was one of six transcriptional regulators isolated as a putative FLJ22318 binding partner using yeast two-hybrid analysis. Several features of PRKRA make it an interesting candidate for further study. PRKRA comprises 313 amino acids and contains three proposed protein-protein interaction domains, the first two resemble dsRNA binding motifs (dsRBM) whilst the 3rd domain comprising 66 amino acids remains largely uncharacterised (Li et al., 2006a). The PRKRA protein fragment isolated in this study encoded the C-terminal 175 amino acids which encompasses 73% of the 2nd dsRBM and the entire 3rd protein-protein interaction domain. Like NKX3-1, PRKRA is also involved in regulating cellular proliferation and apoptosis and to date is the only known protein activator of eukaryotic translation initiation factor 2-alpha kinase 2 (EIF2AK2; PKR; Li et al., 2006a). Activation of EIF2AK2 requires the 3rd domain of PRKRA which upon binding to the kinase domain of EIF2AK2 causes a change from a closed/inactive to an open/active conformation. Binding of either of the remaining domains to EIF2AK2 was also required in addition to the 3rd domain although the function of these domains was not clear (Li et al., 2006a).

EIF2AK2 is a ribosomal protein which is activated by phosphorylation, it is thought after release from the ribosome, and is involved in regulating a variety of cellular functions including host anti-viral defences, differentiation, cellular proliferation and apoptosis (Ruvolo et al., 2001). PRKRA has been shown to activate EIF2AK2 in the absence of dsRNA produced by viral infection and in uninfected cells activates EIF2AK2 in response to a number of cell stresses including serum starvation, growth factor withdrawal or ceramide treatment (Ruvolo et al., 2001; Yang et al., 2003).

Studies using RAX, the mouse homologue of PRKRA, indicated that under cellular stress PRKRA is phosphorylated which precedes EIF2AK2 activation and induction of apoptosis (Ito et al., 1999). In the presence of growth factors such as IL3 however, the pro-apoptotic function of PRKRA is inhibited as in normal proliferating cells PRKRA is

unphosphorylated and expression of both PRKRA and EIF2AK2 is very low (Ito et al., 1999). These findings are in agreement with other studies which show that PRKRA is expressed at very high levels in mouse epithelial cells of the colon as they exit the cell cycle and enter the apoptotic pathway. Expression of phosphorylated PRKRA was found to coincide with differentiating cells and was increased as cells moved towards the luminal surface and underwent apoptosis (Gupta and Patel, 2002). Exogenous expression of unphosphorylated PRKRA in proliferating cells was also found to be insufficient to activate EIF2AK2 and induce apoptosis (Ito et al., 1999). More recently, expression of an inactive unphosphorylated PRKRA mutant was shown to increase cell growth and promote cellular transformation (Bennett et al., 2006).

PRKRA has also been shown to enhance SV40 T-Ag dependent DNA replication, independent of EIF2AK2 binding, as well as enhancing Newcastle Disease Virus (NDV) activation (Iwamura et al., 2001; Yang et al., 2003). Expression of NDV together with PRKRA resulted in increased activation of the IFN-β gene enhancer, which was mediated by NF-κB activation and required binding of PRKRA to dsRNA although it is unknown which domain(s) of PRKRA were involved in this interaction (Iwamura et al., 2001). PRKRA was not shown to bind SV40 directly but was believed to regulate the interaction of AP1 with the SV40 enhancer (Yang et al., 2003). Due to the similarities between viral and mammalian DNA replication it was thought that PRKRA may also be involved in regulating mammalian DNA replication.

PRKRA is associated with pre-micro RNA (miRNA) processing and is required for the accumulation of mature miRNAs (Lee et al., 2006). miRNAs are small RNAs that function in a variety of regulatory pathways including induction of mRNA degradation and translational repression which is commonly referred to as RNA silencing (Baulcombe, 2005). miRNA are transcribed from endogenous genes and then transported to the cytoplasm for processing into mature miRNAs by Dicer (Hutvagner et al., 2001; Kim, 2005; Lund et al., 2004). These small RNAs are then assembled into the RNA-induced silencing complex (RISC) by a variety of factors including Dicer, hAgo2 and TRBP. TRBP has a similar domain structure to PRKRA and binds to EIF2AK2 through its 3rd domain, however, unlike PRKRA, TRBP has been shown to inhibit EIF2AK2 activation (Lee et al., 2006). PRKRA is also associated with RISC

where it is thought to contribute to the stabilisation of Dicer (Lee et al., 2006). Interestingly PRKRA binding to Dicer also required the 3rd domain of PRKRA, although this domain was not required for PRKRA binding to hAgo2. As both TRBP and PRKRA are required for binding and inactivation/activation of EIF2AK2 it was thought that crosstalk may exist between the EIF2AK2 pathway and the RNA silencing pathway (Lee et al., 2006). As PRKRA promotes growth or induces apoptosis in other tissues/cells dependent on its phosphorylation status, the nature of FLJ22318 interaction with PRKRA will provide additional information regarding the function of FLJ22318 in prostate cancer cells.

7.2 Results

7.2.1 PRKRA Protein Expression in LNCaP Prostate Cancer Cells

To investigate endogenous PRKRA expression in LNCaP prostate cancer cells, proteins were extracted from LNCaP cells, resolved by polyacrylamide gel electrophoresis then transferred to nitrocellulose membranes (sections 3.7.1-3.7.3). Following transfer, immunoreactive bands were detected by western blotting using rabbit or goat polyclonal anti-human PACT (PRKRA) antibodies of various concentrations (section 3.7.4). Benchmark™ pre-stained protein markers were run concurrently and used to generate standard curves. Molecular weight was plotted against mobility, from which the molecular weights of immunoreactive bands were determined.

Use of the goat anti-PRKRA antibody at 1:200 and 1:500 dilutions in western blotting produced immunoreactive bands of ~34kDa with a less intense band detected at ~68kDa (Figure 7.1A,B). This (commercial) antibody also produced a very high background on the filters. Western blots using the rabbit anti-PRKRA antibody at 1:200 and 1:500 dilutions also detected protein bands of ~34kDa and ~68kDa at a concentration of 1:200 and 1:500 as well as two additional bands of ~41kDa and ~115kDa (Figure 7.1C,D). Based on these results, additional western blotting experiments utilised the rabbit anti-PRKRA antibody while immunocytochemical analyses utilised the goat anti-PRKRA antibody as the antibody has been used previously for this application (Chen et al., 2006).

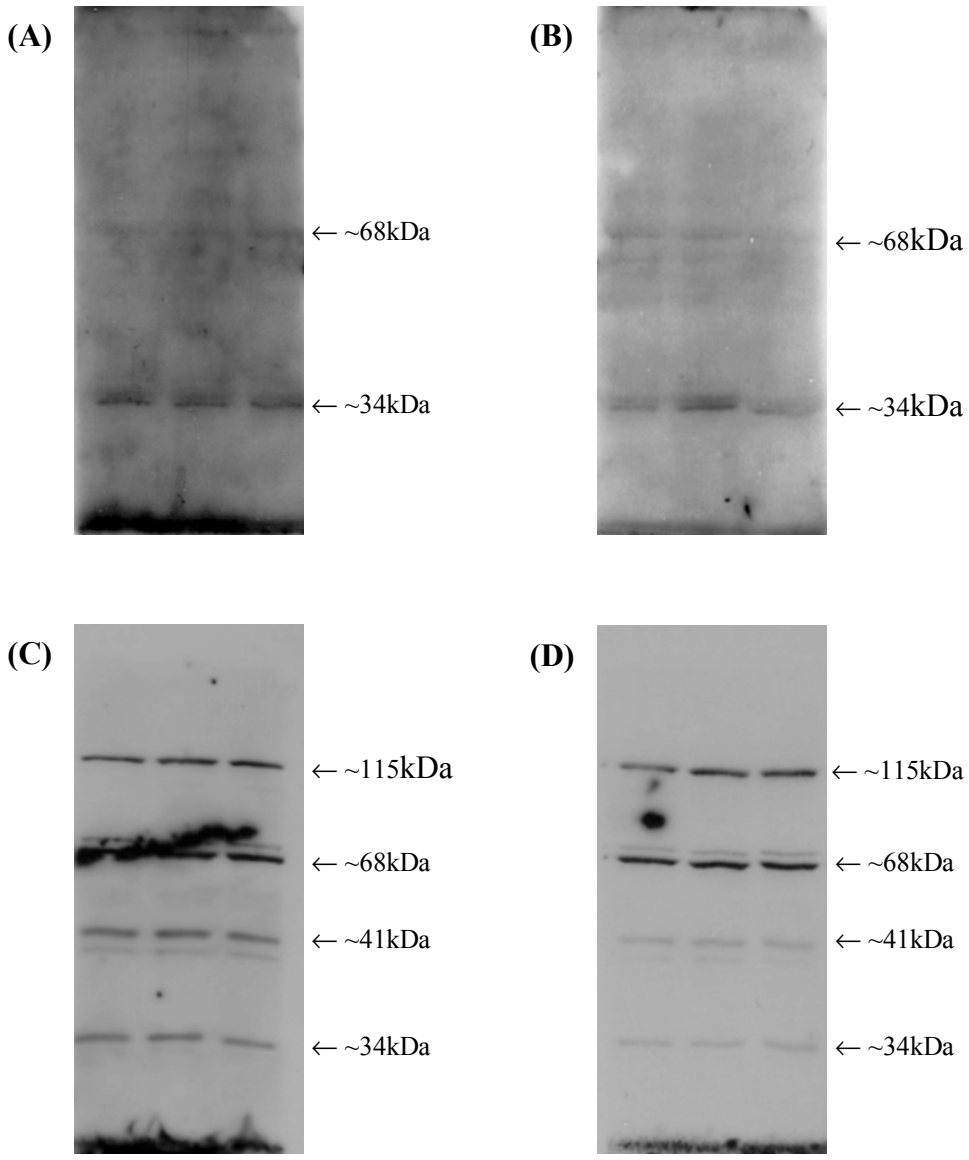

Figure 7.1 Western blot analysis of representative LNCaP prostate cancer cell lysates with anti-PRKRA antibodies to detect expression of endogenous PRKRA. **(A,B)** Goat anti-PRKRA antibodies detected protein bands of ~34kDa, the predicted molecular weight of PRKRA, and another band of ~68kDa. **(C,D)** Rabbit anti-PRKRA antibodies also detected immunoreactive bands of ~34kDa and ~68kDa as well as two additional bands of ~41kDa and ~115kDa. (A,C antibody dilution = 1:200; B,D antibody dilution = 1:500)

7.2.2 Cellular Localisation and Co-Localisation of PRKRA and FLJ22318

As the cellular localisation of PRKRA has not been reported previously in prostate cancer cell lines, immunocytochemistry was performed in initial studies using antibodies directed against endogenously expressed PRKRA protein in LNCaP prostate cancer cells to optimise experimental conditions and to determine PRKRA cellular localisation (section 3.9.2). Control cells (no primary antibody) displayed background immunoreactivity (Figure 7.2A) whereas LNCaP cells immunostained with goat anti-PRKRA antibodies displayed immunoreactivity at all antibody concentrations tested (Figures 7.2B-D).

These results demonstrated that PRKRA was distributed throughout the cytoplasm of the cell, which is consistent with previous studies using HeLa human cervical carcinoma and HT1080 human fibrosarcoma cell lines that reported PRKRA to be a mostly cytoplasmic protein (Iwamura et al., 2001; Peters et al., 2001). In a proportion of cells, increased perinuclear accumulation of PRKRA was also detected in addition to the PRKRA cytoplasmic staining (Figure 7.2C). To further investigate PRKRA cellular localisation and its co-localisation with FLJ22318, confocal microscopy was undertaken using a 1:1000 dilution of the goat anti-PRKRA antibody.

For the confocal microscopy studies, LNCaP cells were transiently transfected with 1μg of FLJ22318-pcDNA3.1/V5-His-TOPO vector (section 5.2.1.1.3) encoding FLJ22318-V5 fusion proteins and the localisation and co-localisation of PRKRA and FLJ22318-V5 were determined by confocal microscopy using antibodies directed against endogenous PRKRA and the V5 epitopes of the FLJ22318-V5 fusion proteins (sections 3.6.2; 3.11). As the LNCaP cell line is androgen responsive, confocal microscopy was also performed in transfected LNCaP cells that had been treated with 1nM DHT to determine whether androgens affected the cellular distribution of PRKRA or its co-localisation with FLJ22318.

Control cells (no primary antibody) displayed no immunoreactivity (data not shown). In the untreated and DHT treated cells FLJ22318 was distributed throughout the perinuclear and nuclear region of most cells consistent with previous results (section 5.2.6; Figure 7.3A). In a proportion of cells, FLJ22318 was localised to the cytoplasm

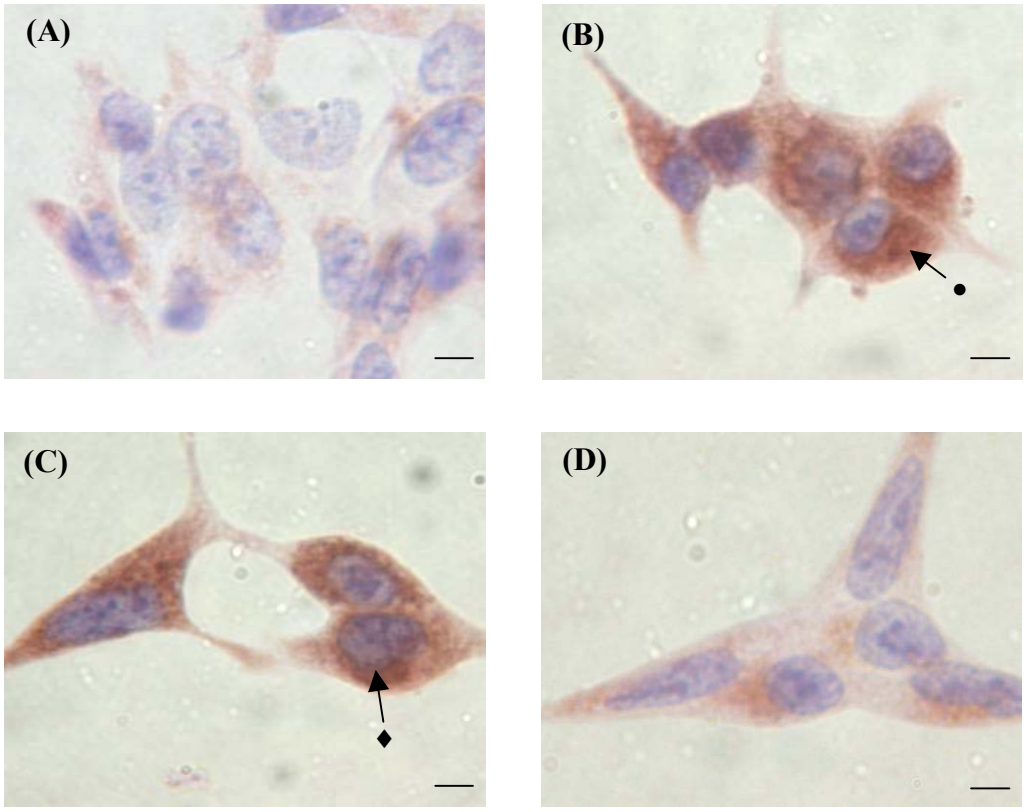

Figure 7.2 Localisation of PRKRA in LNCaP prostate cancer cells. **(A)** LNCaP cells treated with no primary antibody (negative control) exhibited background immunoreactivity whereas cells treated with goat anti-PRKRA antibody at concentrations of 1:750 **(B)** 1:1000 **(C)** and 1:1500 **(D)** demonstrated cytoplasmic (●) and perinuclear (♦) immunoreactivity. (Bar = 10µm).

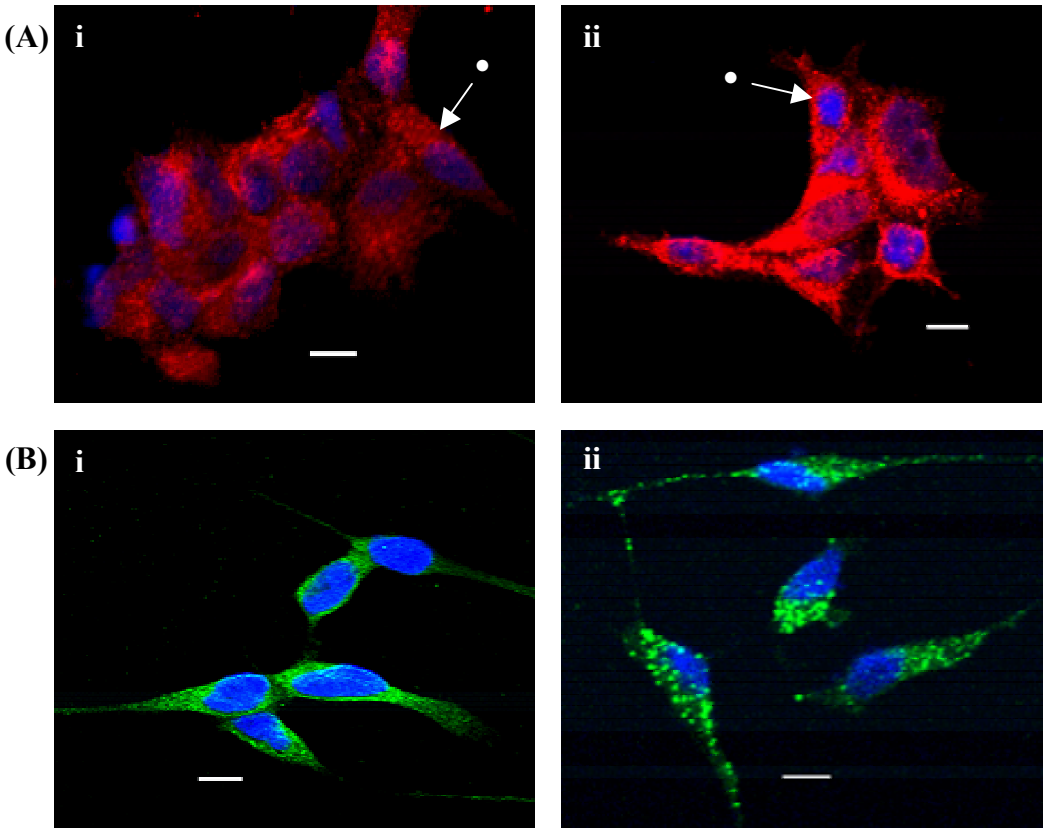

Figure 7.3 Cellular localisation of FLJ22318 and PRKRA in LNCaP prostate cancer cells. LNCaP cells either untreated **(i)** or treated with 1nM DHT **(ii)** were transfected with 1µg of pcDNA3.1-FLJ22318-V5 vectors and incubated for 24 hours to allow expression of recombinant proteins. Cell nuclei were stained with DAPI **(blue)**, anti-V5 **(red)** and anti-PRKRA **(green)** antibodies then examined using confocal microscopy. FLJ22318 exhibited a mainly nuclear and perinuclear localisation although in a few cells FLJ22318 is localised to the cytoplasm **(•)** and in these cells very little FLJ22318 nuclear localisation is evident **(A i; A ii).** PRKRA exhibited a predominantly cytoplasmic fluorescence **(B i; B ii)**. (Bar =10µm).

and perinuclear regions of the cell with very little nuclear localisation evident and was punctate in appearance (Figures 7.3A; 7.4A). Comparable to the immunocytochemistry results, PRKRA localised within the cytoplasm in both the untreated and DHT treated cells, however the immunoreactivity was punctate, rather than diffuse in appearance (Figures 7.3B; 7.4B). Results from these studies indicated that the localisation of both PRKRA and FLJ22318 was not altered in DHT-treated LNCaP cells.

Extensive co-localisation of FLJ22318 and PRKRA was observed in those cells where FLJ22318 was localised to the cytoplasm and the perinuclear regions of the cell and in these cells co-localisation of FLJ22318 and PRKRA appeared to be predominantly cytoplasmic (Figure 7.4). To further investigate the localisation and co-localisation of FLJ22318 and PRKRA, a more detailed examination of a single cell was undertaken. For these studies, images of FLJ22318-V5 and PRKRA were taken at 1μM intervals through the cell and combined to produce a 3-D image. From the data collected, it was evident that FLJ22318-V5 and PRKRA are distributed throughout the cytoplasm and have a punctate pattern of fluorescence (Figure 7.5A, B). A proportion of FLJ22318 and PRKRA co-localise, predominantly in the perinuclear region of the cell in what appears to be discrete vesicles (Figure 7.5C). Data obtained from overlaying images in which the cell nuclei were coloured red determined that co-localisation of FLJ22318 and PRKRA does not occur in the nucleus (results not shown).

7.2.3 GST Pull-Down Analysis

Interaction between FLJ22318 and PRKRA was also investigated by GST pull-down assays using purified GST-FLJ22318 fusion proteins (section 3.8.3). Large scale production and purification of GST and GST-FLJ22318 fusion proteins was performed from 100mL bacterial cultures (section 3.8.3) and the proteins were purified from bacterial lysates using glutathione immobilised to sepharose. SDS-PAGE with Coomassie blue staining of gels was carried out to verify size and purity of the proteins (section 3.8.2) and fusion protein concentration was estimated by comparing GST and GST-FLJ22318 protein bands to BSA protein standards (Figure 7.6A). The concentration of GST protein was estimated to be 750ng/μL, whilst the concentration of GST-FLJ22318 protein was much lower at 150ng/μL (Figure 7.6A).

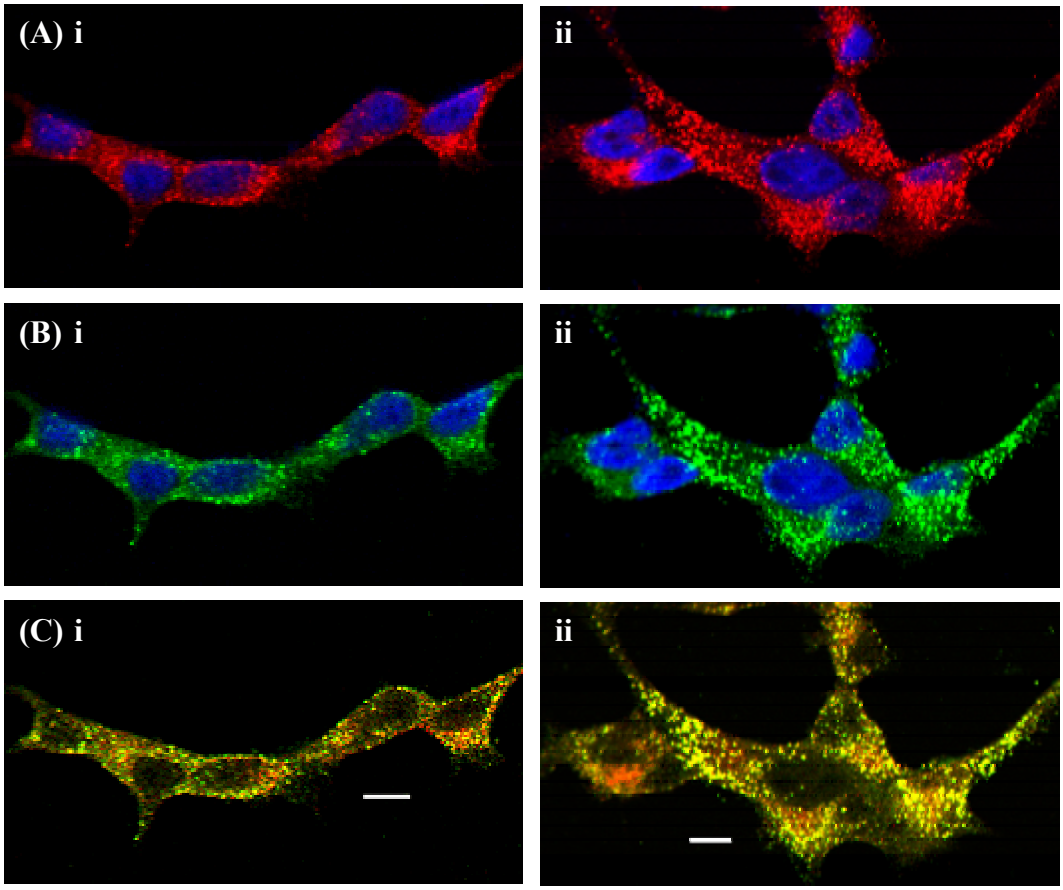

Figure 7.4 Co-localisation of FLJ22318 and PRKRA in LNCaP prostate cancer cells. LNCaP cells either untreated **(i)** or treated with 1nM DHT **(ii)** were transfected with 1µg of pcDNA3.1-FLJ22318-V5 vector and the co-localisation of FLJ22318 and PRKRA was detected by confocal microscopy using antibodies directed against the V5 epitope **(red)** and endogenous PRKRA protein **(green)**. FLJ22318 **(A i; A ii)** and PRKRA **(B i; B ii)** displayed a cytoplasmic and perinuclear localisation, and when the images were overlayed **(C i; C ii),** co-localisation (yellow) of FLJ22318 and PRKRA was predominantly cytoplasmic. (Bar =10µm).

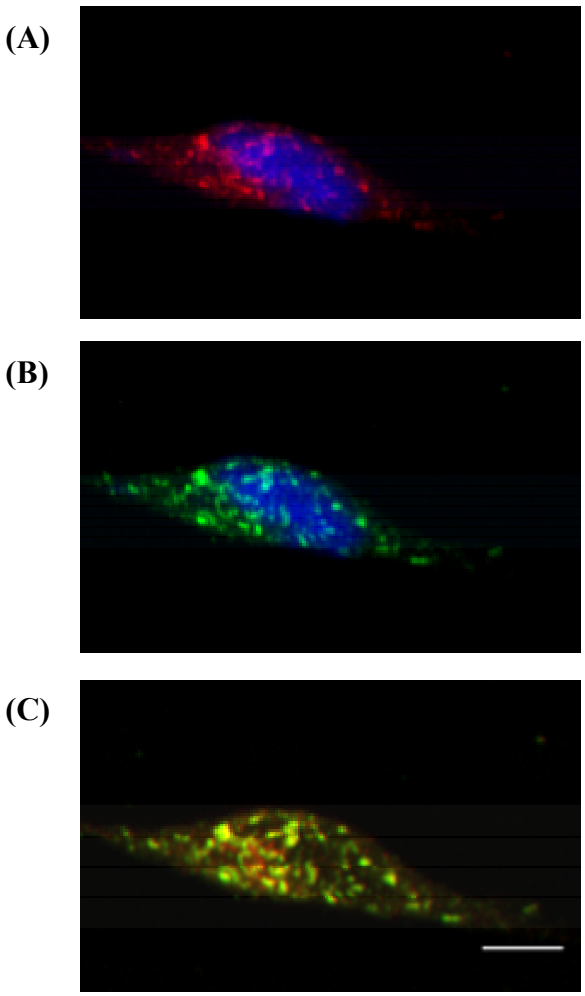

Figure 7.5 Analysis of FLJ22318 and PRKRA co-localisation in LNCaP prostate cancer cells. LNCaP cells were transfected with 1µg of pcDNA3.1-FLJ22318-V5 vectors and incubated for 24 hours to allow expression of recombinant proteins. Cell nuclei were stained with DAPI **(blue)**, anti-V5 **(A, red)** and anti-PRKRA **(B, green)** antibodies, then examined using confocal microscopy. FLJ22318 and PRKRA exhibited a cytoplasmic fluorescence that was punctate in appearance **(A; B)**. When images were overlayed, co-localisation **(yellow)** of FLJ22318 and PRKRA was seen within discrete vesicles in the perinuclear region of the cell **(C)**. (Bar =10µm).

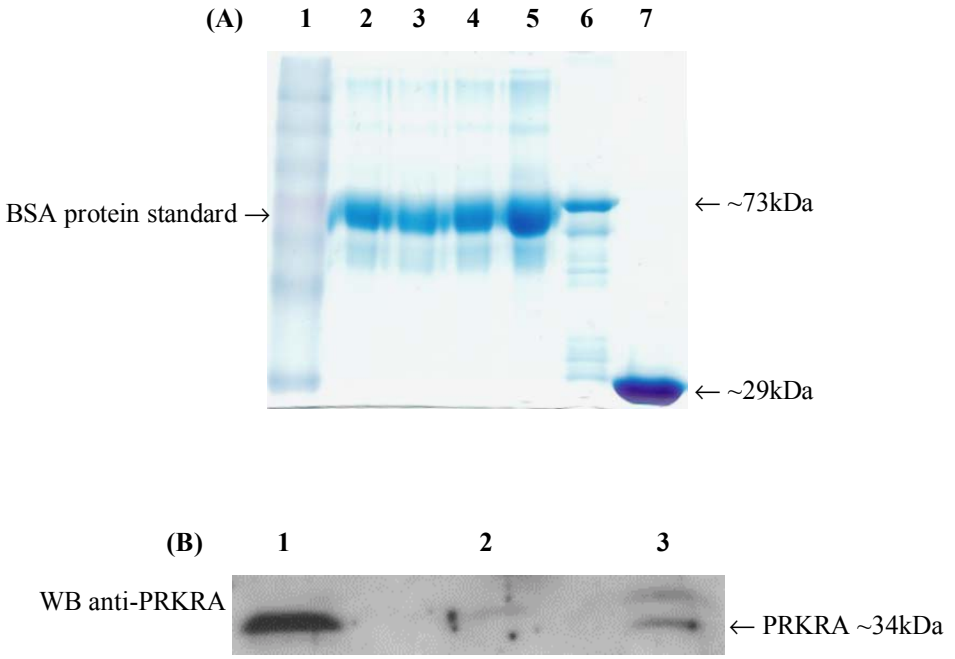

Figure 7.6 GST-FLJ22318 pull-down assay. **(A)** Electrophoresis of purified GST-FLJ22318 protein (~73kDa) and GST (~29kDa). Protein concentrations were estimated in comparison to the BSA standards to be 150ng/µL (GST-FLJ22318) and 750ng/µL (GST). **(B)** GST-FLJ22318 immobilised to glutathione was incubated with lysates from LNCaP cells which express endogenous PRKRA. The interaction between FLJ22318 and PRKRA was detected by anti PRKRA western blotting in protein precipitates incubated with GST-FLJ22318, but not in protein precipitates that had been incubated with GST alone.

(A) 1 Benchmark™ Prestained Protein Ladder
2-5 BSA standard (0.5µg, 1.0µg, 2.0µg, 5.0µg)
6 IPTG induced GST-FLJ22318 expression ~73kDa (150ng/µL)
7 IPTG induced GST expression ~29kDa (positive control)

(B) 1 Whole cell lysates
2 GST protein precipitates
3 GST-FLJ22318 protein precipitates

For the GST pull-down assays, 300µL aliquots of LNCaP prostate cancer cell lysates, chosen as LNCaP cells express endogenous PRKRA (section 7.2.1), were incubated with 15µg GST alone or GST-FLJ22318 immobilised to glutathione and protein complexes were precipitated following 18 hours of incubation (section 3.8.4). Proteins were separated by SDS-PAGE then transferred onto nitrocellulose filters and the interaction between FLJ22318 and PRKRA detected by western blotting using antibodies directed against PRKRA (section 3.7.4). PRKRA (34kDa) was detected in whole cell lysates and in protein precipitates incubated with GST-FLJ22318 (Figure 7.6B), but was not detected in precipitates that had been incubated with GST alone (Figure 7.6B). These findings supported an interaction between FLJ22318 and PRKRA although the weak intensity of the precipitated PRKRA protein band suggested that the interaction between FLJ22318 and PRKRA was of low affinity, that PRKRA was not a major FLJ22318 binding partner or that the experimental conditions required further optimisation.

7.2.4 Co-immunoprecipitation of FLJ22318-pcDNA3.1/V5 and PRKRA

To investigate the *in vivo* interaction of FLJ22318-V5 and PRKRA, FLJ22318-pcDNA3.1/V5-His-TOPO constructs were transiently transfected into LNCaP prostate cancer cells which express endogenous PRKRA and FLJ22318-V5 complexes were immunoprecipitated 24 hours later using V5 antibodies and protein G (sections 5.2.1.1.3; 3.10). Following immunoprecipitation western blotting with PRKRA antibodies detected PRKRA in whole cell lysates, however PRKRA could not be confirmed as part of immunoprecipitated FLJ22318 complexes as protein G was of a similar size to PRKRA (results not shown). Therefore FLJ22318-pcDNA3.1/V5-His-TOPO constructs were transiently transfected into LNCaP cells and FLJ22318-V5 complexes were immunoprecipitated 24 hours later using V5 antibodies and protein A. Western blotting using V5 antibodies indicated very weak affinity for the FLJ22318-V5 complexes for protein A (results not shown), which is consistent with the manufacturer's datasheets indicating that protein A binding to mouse antibodies is less than its binding to rabbit antibodies.

Due to difficulties performing the experiments using the V5 antibody, FLJ22318-pcDNA3.1/V5-His-TOPO constructs were transiently transfected into LNCaP cells and

complexes were immunoprecipitated 24 hours later using rabbit anti-PRKRA antibodies. Following immunoprecipitation, western blotting using rabbit anti-PRKRA antibodies was performed, which detected PRKRA in whole cell lysates and in the lane containing immunoprecipitated proteins but not in control lysates 'immunoprecipitated' without antibody (section 3.7; Figure 7.7A).

Western blotting using anti V5 antibodies detected FLJ22318-V5 in whole cell lysates and in complexes immunoprecipitated with anti-PRKRA antibodies, findings which support an *in vivo* interaction between FLJ22318-V5 and PRKRA (section 3.7; Figure 7.7B,C). However, nonspecific bands were also detected in control lanes of the the V5 western blots which were of similar size to FLJ22318-V5 (~49-50kDa). While the bands can be distinguished on western blots, the quality of the results is insufficient to provide definitive evidence of PRKRA-FLJ22318-V5 co-immunoprecipitation. Further experiments using different PRKRA antibodies and alternatively tagged FLJ22318, or ideally, antibodies to endogenous FLJ22318 will be required to confirm these results.

7.3 Discussion

Of the six cDNA's classified as transcriptional regulators isolated in the yeast two-hybrid screen as interacting with FLJ22318, PRKRA is unique in that it can bind dsRNA and is the only known protein activator of EIF2AK2, a serine/threonine kinase that is induced by interferons (IFN) or viral infection. PRKRA activation of EIF2AK2 *in vivo* results in activation of the apoptotic pathway.

In this study, antibodies to detect the expression of endogenous PRKRA protein in LNCaP prostate cancer cells reacted with distinct protein bands of approximately 34kDa, 41kDa, 68kDa and 115kDa. Only one protein of 34kDa is published in the National Center for Biotechnology Information (NCBI) database (Accession NP003681). According to AceView (www.ncbi.nlm.nih.gov/IEBResearch/Acembly/av) however the *PRKRA* gene may produce 10 different protein isoforms by alternative splicing. Of these, isoform 'a' has a predicted molecular weight of ~42kDa whereas isoform 'b' has a predicted molecular weight of ~39kDa. As PRKRA expression is unknown in prostate cancer cells it is possible that the ~41kDa band observed in this

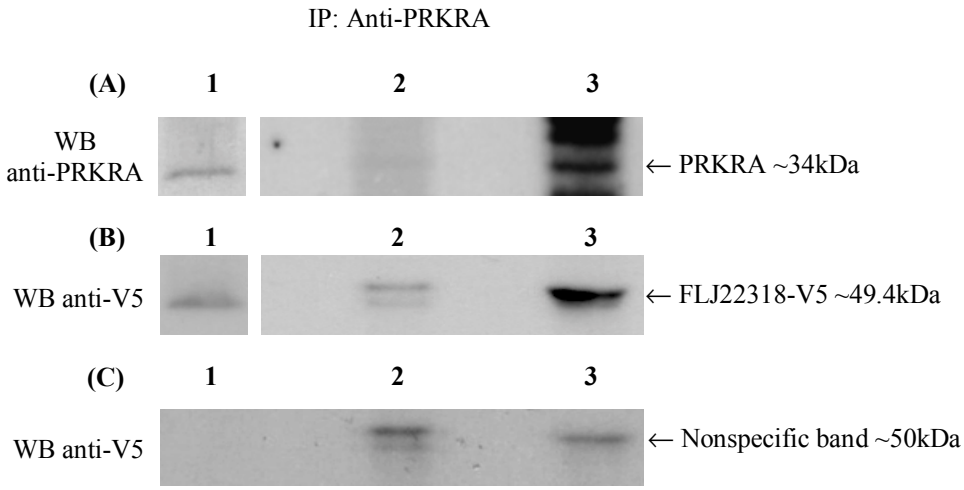

Figure 7.7 Co-immunoprecipitation of FLJ22318-V5 and PRKRA. FLJ22318-V5 expression plasmids were transfected into LNCaP cells and cellular proteins were immunoprecipitated with PRKRA antibodies using protein A sepharose. **(A, B)** In the FLJ22318-V5 transfected cells, western blotting using anti-PRKRA and anti-V5 antibodies detected PRKRA and FLJ22318 in the whole cell lysates and in protein complexes immunoprecipitated with PRKRA antibody but not in protein complexes precipitated using protein A sepharose alone. **(C)** FLJ22318-V5 was not detected in untransfected (control) cells. (A,B Lane 1 – film has been exposed for a longer period of time compared to Lanes 2 and 3).

1 LNCaP whole cell lysate
2 IP: No antibody/Protein A
3 IP: Anti-PRKRA/Protein A

study represents one of the protein isoforms as predicted by AceView and the higher molecular weight bands may be multimers (dimers or trimers) of one of these isoforms.

Comparison of the two predicted *PRKRA* mRNA's indicates that they encode proteins with an additional N-terminal exon to that of the reference protein (www.ncbi.nlm.nih.gov/IEB Research/Acembly/av.). Isoform 'a' is predicted to localise to mitochondria and isoform 'b' to the nucleus, suggesting that PRKRA isoforms if present may function in distinct subcellular compartments. The punctate appearance of PRKRA detected using confocal microscopy is consistent with a mitochondrial localisation, however further confocal microscopy studies using mitochondrial markers such as MitoTracker® (Molecular Probes) would be required to determine whether PRKRA (or FLJ22318) co-localise with the mitochondria. In the case of isoform 'a', the additional exon introduces several new putative phosphorylation sites including two for AKT (http://elm.eu.org).

Reports of PRKRA ESTs in both normal and malignant tissues suggests expression of these transcripts, however the presence of alternative transcripts and potentially variant proteins have not been explored. Further investigation of PRKRA expression, including expression of tissue- or disease-specific isoforms will be required to determine whether the higher molecular weight proteins detected by western blotting of LNCaP cell lysates represent PRKRA isoforms. Use of PRKRA monoclonal antibodies rather than the polyclonal antisera used in the present study may also clarify results. Results using the commercially available goat anti-PRKRA antibodies have been reported in the literature for immunoblotting and immunohistochemistry studies however the immunoblot data was not shown (Chen et al., 2006). It is also noted that most *in vitro* studies of PRKRA have used transfected tagged PRKRA cDNA's with detection of the protein products performed using anti-tag antibodies (Lee et al., 2006; Ruvolo et al., 2001)

Existence of PRKRA dimers has not been reported previously, however previous studies have shown that the 3rd protein-protein interaction domain of PRKRA is able to oligomerise *in vitro* (Hitti et al., 2004). Whether PRKRA forms dimers or complexes with other proteins resistant to the weakly denaturing conditions used in the present studies will require further investigation. However, as the *Xenopus laevis* homologue of

PRKRA, Xlrbpa, predominantly forms dimers *in vitro* and is thought to exist as a dimer/multimer *in vivo* (Hitti et al., 2004), it is feasible that the multiple immunoreactive bands detected by western blotting represent PRKRA dimers or PRKRA-containing complexes.

In this study localisation of PRKRA and co-localisation of PRKRA with FLJ22318 was predominantly cytoplasmic. This finding is consistent with previous studies that have reported the cellular localisation of PRKRA to be predominantly cytoplasmic, however in those studies endogenous and transfected PRKRA displayed a diffuse immunofluorescence throughout the cytoplasm (Iwamura et al., 2001; Lee et al., 2006). In the present study, PRKRA immunoreactivity appeared diffuse using immunocytochemical staining with DAB detection and had a punctate appearance using confocal microscopy in cells that were untransfected or co-transfected to express FLJ22318-V5. As previous studies have all used immunofluorescence and not confocal microscopy, it is feasible that differences in the appearance of cytoplasmic PRKRA staining were due in part to the increased resolution afforded by 3-D confocal microscopy imaging.

In virally infected cells treatment with TNF-α, which is known to induce phosphorylation and subsequent activation of PRKRA, was shown to induce cytoplasmic aggregation of PRKRA, in that case with viral replication complexes (Iwamura et al., 2001). It is possible that inactive PRKRA exhibits a predominantly diffuse cytoplasmic localisation whereas activated PRKRA localises to discrete vesicles within the cytoplasm. Serum deprivation is known to activate PRKRA (Bennett et al., 2006) and the cells used for confocal microscopic analysis in this study were cultured in steroid-depleted media, which is growth inhibitory, prior to DHT treatments. Therefore the punctate immunofluorescence pattern observed for PRKRA may be associated with its activation due to the cell culture conditions. In future studies comparison of the cytoplasmic distribution of PRKRA in cells growing under normal culture conditions and under growth-restricting culture conditions will be useful in elucidating PRKRA localisation and co-localisation with FLJ22318.

As PRKRA was initially isolated as an interacting partner of FLJ22318 by yeast two-hybrid analyses, GST pull-down and immunoprecipitation assays were performed to provide supporting evidence of an interaction between PRKRA and FLJ22318 *in vitro* and *in vivo*. Although there were technical problems associated with both of these assays, PRKRA was identified in GST pull-down assays using GST-FLJ22318, supporting yeast two-hybrid analysis results that had indicated interaction of FLJ22318 and PRKRA. In addition, preliminary co-immunoprecipitation studies indicate that FLJ22318 and PRKRA interact *in vivo*.

Technical difficulties associated with the GST pull-down and co-immunoprecipitation assays involved both the antibodies and interference by protein A and protein G which dissociated from the sepharose bead during the immunoprecipitation procedure. Although recommended by the manufacturer for use in western blotting, the commercially prepared goat anti-PRKRA antibody used in this study was not sensitive enough to detect endogenous PRKRA and in addition produced very high levels of background. Interference due to the similar size of protein A and protein G bands with bands of interest also hindered interpretation of results and several alternative strategies could be used in future experiments to improve the GST pull-down and co-immunoprecipitation experiments. For GST pull-down assays these include alteration of buffer salt concentrations and/or pH to facilitate FLJ22318-PRKRA interactions, transfection of LNCaP cells to overexpress PRKRA to increase detection of complexes and development of GST-PRKRA so that the assays could also be carried out in reverse. For co-immunoprecipitation assays, transfection of cells to overexpress PRKRA would also potentially increase the amount of FLJ22318-PRKRA complexes able to be formed and therefore immunoprecipitated. The use of PRKRA monoclonal antibodies may also facilitate detection of proteins and use of different tagged proteins whose molecular weights do not coincide with that of protein A/G bands would also assist in completion of experiments confirming the interaction of FLJ22318 and PRKRA.

As PRKRA expression has been reported to be low in proliferating cells in other tissues (Gupta and Patel, 2002), the interaction between FLJ22318 and PRKRA may also have been difficult to detect due to low expression of PRKRA in LNCaP cells. In addition as previous studies have reported PRKRA to be unphosphorylated and inactive in proliferating cells unless cellular stress occurs (Bennett et al., 2006; Peters et al., 2006),

it is feasible that FLJ22318 and PRKRA are minor binding partners when PRKRA is in either an active or an inactive form. Treatment of cells with ethanol was recently shown to enhance co-immunoprecipitation of the phosphorylated mouse homologue of PRKRA, RAX with EIF2AK2 although an unphosphorylatable PRKRA mutant was still able to co-immunoprecipitate EIF2AK2 but at a greatly reduced concentration (Chen et al., 2006). Although extensive co-localisation was observed in this study in cells that had been growth-restricted as part of DHT treatment protocols future studies are needed to determine whether co-immunoprecipitation of PRKRA and FLJ22318 is altered depending on the phosphorylation status of PRKRA, treatment of the cells with various stress inducing or growth factors and the phosphorylation or activation status of PRKRA.

Phosphorylation of specific residues within the 3rd protein-protein interaction domain of PRKRA has recently been shown to be required for PRKRA activation, binding to EIF2AK2 and initiation of apoptosis (Peters et al., 2006). As the protein fragment isolated in the yeast two-hybrid screen encompassed this domain, a series of GAL4-PRKRA and GAL4-FLJ22318 deletion mutants could also be created in future studies and screened by yeast two-hybrid analysis to determine the protein-protein interaction domains of PRKRA and FLJ22318. Finally, co-immunoprecipitation and kinase assays would determine the affect of FLJ22318 interaction with PRKRA on PRKRA function, including binding to and activation of EIF2AK2 and regulation of miRNA processing.

In summary, the data presented in this chapter provides preliminary evidence of an *in vitro* and *in vivo* interaction between FLJ22318 and PRKRA supporting results from the yeast two-hybrid analysis. Future studies continuing characterisation of the interaction between FLJ22318 and PRKRA as well as interactions and functional consequences of the interactions between FLJ22318 and other candidate binding partners identified in the yeast two-hybrid analysis will help to determine the biological activity of FLJ22318. These results will be critical in describing the role of FLJ22318 in malignant cells, especially those with abnormalities in the 5q35 locus harbouring the *FLJ22318* gene.

Chapter Eight

Chapter Eight – General Discussion

8.1 Discussion

FLJ22318 is a novel hypothetical protein that was identified by yeast two-hybrid analysis to interact with the prostatic homeodomain protein, NKX3-1. An androgen-regulated gene, *NKX3-1* is expressed in secretory epithelial cells of the adult prostate where it is involved in maintaining the differentiated state of the prostatic epithelium (Bhatia-Gaur et al., 1999). Expression of NKX3-1 is reduced or lost in prostate tumours, leading to its classification as a prostate-specific tumour suppressor (Bowen et al., 2000). As a homeodomain protein NKX3-1 is a transcriptional regulator, acting in multiprotein complexes to regulate transcription of its target genes. In this thesis, the structure and biological activity of the candidate NKX3-1 interactor, FLJ22318 was investigated.

Yeast two-hybrid analysis performed to isolate NKX3-1 binding proteins had identified cDNA's encoding a variety of characterised and uncharacterised (hypothetical) proteins. As NKX3-1 is a homeodomain protein and therefore active in the nucleus where it functions as a transcription factor (Abdulkadir, 2005), it would be expected that NKX3-1 binding proteins would include proteins regulating intracellular transport including nuclear import and export proteins, factors involved in modification (eg phosphorylation) of target proteins and transcriptional co-regulators including coactivators, corepressors and scaffolding proteins that may anchor NKX3-1 in complexes, including transcriptional regulatory complexes. Although an uncharacterised protein, the isolation of FLJ22318 in multiple clones from the yeast two-hybrid screen and its unusual domain structure indicated it to be a novel and potentially interesting modifier of NKX3-1 activity.

Bioinformatic analysis suggested that the FLJ22318 protein contains three strong protein-protein interaction domains, a Lissencephaly type-1-like homology (LisH), a C-terminal to LisH (CTLH) and a CT11-RanBPM (CRA) domain (http://smart.embl-heidelberg.de/), motifs which are found in a diverse range of proteins, several of which function as transcriptional co-regulators or are involved in cell cycle progression. Although individually, LisH, CTLH and CRA domains have been identified and

characterised in a variety of proteins, the number of proteins with similar domain composition and organisation to FLJ22318 is limited.

Currently there are seven human proteins with this domain composition including FLJ22318 and its orthologue FLJ13910. The remaining five proteins are C20orf11, MAEA isoform 1, MAEA isoform 2, RANBP9 and RANBP10. Interestingly, all seven of these proteins have the same domain organisation, an N-terminal LisH motif followed by the CTLH domain and then the C-terminal CRA domain, although both RANBP9 and RANBP10 also contain an additional SPRY domain N-terminal to the LisH domain. These findings suggest that the domain organisation as well as the domain composition of this group of proteins may be functionally significant. At present however, studies of proteins with this domain organisation are limited to RANBP9, containing the additional SPRY domain, and MAEA and although MAEA is involved in erythroid cell differentiation, apoptosis and contributes to cell division it is unknown which domain(s) are associated with or contribute to a particular function (Bala et al., 2006; Hanspal et al., 1998; Soni et al., 2006). RANBP9 is also associated with apoptosis and has been shown to function as a transcriptional coactivator or corepressor. The SPRY domain in combination with the LisH domain was required for RANBP9 corepressor activity whereas the C-terminal region of RANBP9 encompassing the CTLH and CRA domains was found to be necessary for its coactivator activity (Poirier et al., 2006; Zou et al., 2003).

In this study FLJ22318 was shown to exhibit transcriptional repressor activity on an NKX3-1 response element although the regions of FLJ22318 involved in this activity were not determined. Of interest was the finding that FLJ22318 exhibited repressor activity on the NKE in both the absence and presence of NKX3-1. The functioning of this response element is unusual as luciferase activity is induced from the element in the absence of NKX3-1 by as yet unidentified transcription factors (Steadman et al., 2000), with overexpression of NKX3-1 repressing the induced luciferase activity. FLJ22318 does not contain recognised DNA binding domains and it is likely that its repressor activity is mediated by binding to transcription factors or transcriptional regulatory complexes including those involving NKX3-1. The repressor activity of FLJ22318 on the NKE in the absence of NKX3-1 indicated that FLJ22318 can target transcription factors other than NKX3-1, a finding consistent with the widespread expression of

FLJ22318 in all tissues of the body in comparison to the prostate restricted expression of NKX3-1 (Bieberich et al., 1996). While the SPRY and LisH domains of RANBP9 have been shown to be required for its corepressor activity (Zou et al., 2003), FLJ22318 does not contain a SPRY domain and the function of the highly conserved N-terminal of FLJ22318 has not been investigated previously. As such, the contribution of the domains identified in FLJ22318 to its function as a corepressor will need to be addressed in future studies.

The LisH and/or CTLH domains can be found in >40 human proteins which have a diverse range of functions, however the CRA domain is found in only nine proteins (http://smart.embl-heidelberg.de/). Interestingly, these are the seven previously mentioned proteins plus two additional hypothetical proteins FLJ43512 and FLJ46442 where the CRA domain is located at the N-terminal and is the only recognised domain within the predicted coding regions of these genes. The CRA domain has been described as a protein-protein interaction domain that can inhibit RNA binding (Menon et al., 2004). In RANBP9, the CRA domain is required for its interaction with FMR1 and was shown to inhibit FMR1 binding to RNA although RANBP9 did not bind RNA directly (Menon et al., 2004). As inhibition of RNA binding was more specific for RNAs that bound to RGG boxes of RNA binding proteins it was thought the CRA domain may interact with RGG boxes thereby directly competing for binding with RNAs (Menon et al., 2004).

This study has shown that FLJ22318 localises to the nucleus and perinucleus of DU145 cells and in addition, localises to the cytoplasm as well as the perinuclear and nuclear regions of LNCaP cells. MAEA and RANBP9 are widely distributed throughout the cell localising to the plasma membrane, cytoplasm, perinucleus and nucleus of cells (Bala et al., 2006; Hanspal et al., 1998; Kramer et al., 2005; Rao et al., 2002; Wang et al., 2002). As such, it has been suggested that these proteins have specific and distinct functions in the nucleus as compared to the cytoplasm. Cytoplasmic MAEA is required for the attachment of erythroblasts to macrophages and in the absence of attachment, apoptosis of erythroblasts occurs suggesting that MAEA is an inhibitor of apoptosis (Hanspal et al., 1998). In the nucleus, MAEA functions in cell division and has a recognised nuclear localisation signal (NLS) although it is unknown whether this signal actually mediates import of MAEA into the nucleus (Bala et al., 2006). A function for cytoplasmic

RANBP9 has not been elucidated, however it has been reported that a decrease in cytoplasmic RANBP9 coincides with an increase in nuclear RANBP9, following RANBP9 interaction with p73 (Kramer et al., 2005). In the presence of their respective ligands nuclear RANBP9 has been shown to activate glucocorticoid receptor, androgen receptor and thyroid receptor enhancing their transcriptional activation (Poirier et al., 2006; Rao et al., 2002).

A NLS has not been reported for RANBP9 however, RANBP9 was originally isolated as a binding partner of Ran which is involved in the nucleocytoplasmic transport of proteins through the nuclear pore complex (NPC) (Nakamura et al., 1998). Like RANBP9, FLJ22318 does not contain a recognised NLS however FLJ22318 does contain a putative non classical NLS and nuclear export signal (NES) that fits the consensus sequence that is commonly bound by the export receptor CRM1 and is found in other proteins that depend on the Ran GTP/GDP axis (Heger et al., 2001; Pemberton and Paschal, 2005). The presence of two mRNA transcripts identified in these studies suggests that more than one isoform of FLJ22318 may be present in prostate and breast cancer cells, possibly with different cellular localisations. Although additional studies will be necessary to investigate this, the use of C-terminal V5 and N-terminal Myc tagged fusion proteins and the detection by western blotting of only a single protein of the predicted size encoded by these expression plasmids provides evidence that the cellular distribution of FLJ22318 observed in this study relates to the same protein. Therefore it appears that FLJ22318 is localised and may also shuttle between the cytoplasm and nucleus of the cell although whether FLJ22318 has specific and distinct functions in the nucleus and in the cytoplasm will require further investigation. Recent reports have provided strong evidence that the shuttling of proteins between the nucleus and cytoplasm plays a key role in regulating the cell cycle, proliferation and apoptosis and as such, intracellular localisation and movement of FLJ22318 will be important to address in future studies (Fahrenkrog, 2006; Wang and Hung, 2005).

A number of homeodomain proteins including the paired-like homeodomain proteins Vsx1 and Chx10 are known to actively shuttle between the cytoplasm and nucleus (Knauer et al., 2005). Nuclear export of Vsx1 and Cx10 is mediated by CRM1 and facilitates their degradation via the ubiquitin/proteasome pathway whereas preventing the nuclear export of both proteins was shown to increase protein stability and increase

their transcriptional activation activity (Knauer et al., 2005). Although not yet explored, modulation of the nuclear import/export of NKX3-1 may be an important regulatory mechanism governing NKX3-1 function as a transcriptional repressor, in particular in the presence of androgens. As FLJ22318 was detected in both the nucleus and cytoplasm in this study, one possible explanation for the observed nuclear localisation and co-localisation of FLJ22318 with NKX3-1 is that their repressor activities are mediated in part, by nucleocytoplasmic shuttling (ie. their localisation). It is feasible that in the nucleus FLJ22318 either binds DNA directly or more likely interacts with regulatory complexes which bind DNA. This may account for the increase in NKX3-1 transcriptional repressor activity that was seen in these studies upon co-transfection of FLJ22318. As the nuclear export of proteins has been shown to promote their degradation via the ubiquitin/proteasome pathway (Xu and Massague, 2004), it will also be interesting in future studies to investigate whether the cytoplasmic localisation of NKX3-1 observed in these studies represents newly synthesised NKX3-1 being retained in the cytoplasm or is due to the increased nuclear export of NKX3-1.

During 2006, FLJ22318 and its orthologue FLJ13910 were renamed by the HUGO Gene Nomenclature Committee. FLJ13910 was renamed "required for meiotic nuclear division 5 homologue A (*S. cerevisiae)* (RMND5A)" whilst FLJ22318 was renamed RMND5B. A comparison of FLJ22318 and FLJ13910 with the yeast protein RMD5 revealed 21.8% sequence homology between FLJ22318 and RMD5 and 23.2% sequence homology between FLJ13910 and RMD5. In addition, RMD5 was found to contain only a CTLH motif as compared to FLJ22318 and FLJ13910 which contain LisH, CTLH and CRA domains. It has been predicted that during vertebrate evolution whole genome duplication events occurred twice which have been followed by loss of some of the duplicated genes in particular in frog, chicken and fish genomes, with comparatively fewer duplicate genes lost in mammalian genomes (Blomme et al., 2006). This finding may account for the observation that to date RMND5A (FLJ13910) and RMND5B (FLJ22318) paralogues only appear in mammalian genomes. Following gene duplication, one gene may retain the ancestral function, in this case that of RMD5, and the second duplicated gene can diverge in sequence and function. Alternatively, mutations may occur in both duplicated genes resulting in either the retention of different aspects of the original function or the evolution of new functions or expression patterns (Hancock, 2005). It would appear from sequence comparisons between

FLJ22318 and FLJ13910 and their domain organisation that both paralogues have diverged markedly in sequence and therefore have probably acquired additional functions in comparison to the ancestral RMD5 gene.

Bioinformatic analysis in this study has identified an exceptionally high degree of sequence conservation between FLJ22318 protein homologues in mammalian species (>97%) with significant but lesser homology between FLJ22318 and its orthologue FLJ13910 (>70%), suggesting microfunctionalisation. The lack of reported sequence variations (polymorphisms) within the FLJ22318 protein coding region provides strong evidence that FLJ22318 is essential and/or critical to cell function or survival. Although the determination of FLJ22318 transcriptional repressor activity and intracellular localisation, along with the isolation and preliminary categorisation of candidate FLJ22318 interacting factors have provided a basic characterisation of FLJ22318 and a foundation for future research, the function of FLJ22318 remains enigmatic.

8.2 Future Directions

This thesis has generated important information that has begun to characterise the structure of the FLJ22318 gene and protein, the interaction between FLJ22318 and NKX3-1 and the potential biological functions of FLJ22318 in eukaryotic cells.

Initial bioinformatic analysis of the amino acid sequence of FLJ22318 indicated the presence of LisH and CTLH motifs which are proposed to form α-helices in other proteins including PAFAH1B1. Further analyses using programmes such as PSA (http://bmerc-www.bu.edu/psa/request.htm) would be required to indicate whether the proposed LisH and CTLH motifs in FLJ22318 are able to adopt an α-helical conformation, which has been shown for other proteins containing these motifs to direct cellular localisation and biological activity. Crystallography studies could also be used to determine full-length FLJ22318 structure *in vitro* and in particular whether FLJ22318 can adopt an open and closed conformation as is the case with the PAFAH1B1 protein which has a LisH motif followed by a coiled-coiled region. As 11 of the 14 deduced FLJ22318 isoforms are proposed to encode proteins that are truncated within the highly conserved N-terminal (CTLH domain) and C-terminal (CRA domain), similar studies could also be used to determine whether these alternative FLJ22318 proteins form α-

helices *in vitro*. Crystallography could also provide additional information regarding the putative nuclear receptor boxes of FLJ22318 as previous crystal structure studies have indicated that nuclear receptor binding occurs as a result of these motifs adopting an α-helical conformation.

Several readily available bioinformatic programmes were used in this thesis to identify and confirm the presence of protein motifs and to examine FLJ22318 homologues in other species. Use of additional and more comprehensive programmes including PSI-BLAST and PHI-BLAST could be used in additional studies to identify other protein-protein interaction domains and to more fully characterise the motifs identified in the present work. These programmes may be particularly useful in identifying proteins that are distantly related to FLJ22318 and could provide additional information regarding FLJ22318 function or cellular localisation.

In this study, FLJ22318 was shown to interact with NKX3-1 although this proved very difficult due in part to technical limitations associated with the lack of FLJ22318 antibodies available at the time that the experiments were performed. In addition, it appeared that FLJ22318 and NKX3-1 were not major binding partners of each other, a finding consistent with bioinformatic evidence of multiple protein-protein interaction domains in FLJ22318. As discussed in Chapter 5, development of FLJ22318 antibodies that can be used for western blotting, immunoprecipitation and immunohistochemistry will be essential for future functional and translational studies. FLJ22318 has not been characterised previously therefore it is unknown which domain(s) of FLJ22318 directly interact with NKX3-1. Future studies using GAL4-FLJ22318 deletion mutants, in particular, constructs with deletions of the LisH, CTLH and CRA domains could be employed in yeast two-hybrid analyses with NKX3-1 to identify FLJ22318 interaction domains. A similar series of deletion mutants could also be constructed to identify the regions of NKX3-1 that are required for binding to FLJ22318. The use of FLJ22318 deletion constructs in mammalian expression vectors may also assist in determining which regions of FLJ22318 direct its cellular location and are required for FLJ22318 transcriptional repressor activity.

Preliminary studies performed in this thesis identified transcriptional repressor activity of FLJ22318 on an NKX3-1 response element in both the absence and presence of NKX3-1. At present it is unknown whether FLJ22318 can bind DNA directly or whether it forms complexes either with NKX3-1 or with other as yet unidentified transcription factors that are able to bind DNA. Electromobility shift assays (EMSAs) and supershift assays could be used to determine whether FLJ22318 is present in protein complexes bound to the target DNA sequence (NKE). Until FLJ22318 antibodies are generated, these experiments would have to be carried out by transfection of cells to overexpress tagged FLJ22318 protein, with antibodies to the tag (eg. V5, GFP) used in supershift assays. Technical difficulties with such experiments would include competition between transfected and endogenous FLJ22318 for inclusion in the DNA-binding complexes and the potential for the tagged FLJ22318 to destabilise the protein complexes (due to the tag). FLJ22318-deletion constructs could then be used to assess the formation of DNA binding complexes in similar EMSAs. To isolate other proteins in DNA binding complexes (in the presence and absence of NKX3-1), antibodies to FLJ22318 could be used to precipitate the complexes followed by mass spectrophotometry to identify the bound proteins.

Northern blotting in this study identified two FLJ22318 transcripts in LNCaP, DU145 and PC-3 prostate cancer cell lines. Bioinformatic analysis suggests that these transcripts correspond to the reference sequence as published by NCBI and alternative proposed transcripts ‘a’ and ‘d’. To confirm the identity of these mRNA’s further studies would require sequencing of the transcripts from cDNA libraries of the cell lines. Following their identification, it would then be possible to screen other cell lines and human tissue specimens (including non-malignant and malignant prostate) using more routine methods such as RT-PCR or real-time RT-PCR to determine both the presence and the levels of FLJ22318 transcripts. Real-time RT-PCR would also identify whether the relative levels of FLJ22318 transcripts are altered between normal and malignant prostate, during progression of prostate cancers to androgen independence or in prostate cancer metastases. *In situ* hybridisation using probes specific for the identified transcripts would determine the cellular distribution of these transcripts in normal and malignant prostate and in particular prostate tumours that have progressed from androgen dependence to androgen independence. Transcript variant ‘d’ is proposed to encode the same protein as the reference sequence transcript with the

difference in size due to alternative 5` and 3`-UTR sequences. It is possible that these transcripts are differentially regulated and further bioinformatic analyses of these regions in comparison to the UTRs of the reference sequence transcript may suggest regulatory elements specific to each transcript that could then be functionally tested in cell culture studies.

Following the development of antibodies to FLJ22318, western blotting could be performed to investigate FLJ22318 proteins expressed in prostate cancer and other cell lines as well as in normal and malignant prostate tissues. The presence of alternative FLJ22318 protein isoforms indicates the potential for differential function and/or cellular localisation of the proteins, especially if one of the isoforms includes a clathrin box. It may be necessary to develop further FLJ22318 antibodies that are specific for the different isoforms and use these to compare the localisation of the isoforms using confocal microscopy. Availability of isoform-specific FLJ22318 antibodies would also permit identification of which isoforms(s) were able to interact with NKX3-1 and whether they exhibited transcriptional repressor activity (in the absence or presence of NKX3-1).

Bioinformatic analysis indicated that the FLJ22318 promoter contains a putative CpG island. As CpG islands can be associated with either transcriptional silencing or constitutive expression (housekeeping genes), the function, if any, of this sequence and its methylation status cannot be deduced. Bisulphite genomic sequencing and methylation-specific PCR targeted to the area surrounding the transcription start site and encompassing the proposed CpG island could be used to determine the methylation status of this region in cell lines and potentially in human tissues. As *FLJ22318* expression has been noted in cDNA libraries from both normal and malignant tissues, the methylation status of the FLJ22318 promoter would need to be established for both normal and malignant tissues. If the FLJ22318 promoter is hypermethylated, changes in FLJ22318 mRNA levels in cell lines following treatment with a DNA demethylating agent such as 5-aza-2`-deoxycytidine could be carried out to investigate the functional consequences of methylation of the CpG island and would provide a useful adjunct to other promoter analyses (discussed in Chapter 4).

Two proteins containing only LisH, CTLH and CRA domains, MAEA and GID8, have been characterised to date, both of which are involved in cell cycle progression, however proteins with a wide variety of functions contain individual or two of these domains. Studies performed in this thesis have not identified the cellular function(s) of FLJ22318 and further experiments will be required to characterise the biological activity of this ubiquitously expressed gene. These could include siRNA knock-down of identified FLJ22318 transcripts both individually and in combination, with real-time RT-PCR enabling identification of the reduction in FLJ22318 mRNA.

Following FLJ22318 knockdown, changes in cell morphology including cytoskeletal and nuclear features could be examined using light, confocal and electron microscopy. Cell proliferation could be examined in both monolayer cultures and by anchorage independent growth and cell cycle distribution and progression could be examined using propidium iodide staining and flow cytometry. The effects of FLJ22318 knockdown on NKX3-1 levels and transcriptional repressor activity could also be investigated to determine whether FLJ22318 is required, either directly or indirectly, for NKX3-1 function.

The yeast two-hybrid analysis carried out during this thesis to identify FLJ22318 interacting proteins, resulted in the isolation of a number of candidate proteins and protein fragments. Although these candidate proteins could be divided into several functional groups, which will assist in the characterisation of the biological activity of FLJ22318, it will be essential in future studies to confirm the interaction of key proteins. These studies would involve techniques used in this thesis including reverse yeast two-hybrid analyses, GST pull-down and co-immunoprecipitation assays, evidence of co-localisation of FLJ22318 and candidate interacting proteins by confocal microscopy and determination of the effects of FLJ22318 overexpression (by transfection) or knockdown on the cellular levels, localisation and function of the interacting protein(s).

Finally, as disruption of 5q35.3 including the *FLJ22318* gene locus is associated with prostate, breast and other cancer types, generation of *FLJ22318* knockout mice may also assist in the elucidation of both the normal cellular function of FLJ22318 as well as its role in carcinogenesis. Due to the ubiquitous expression of FLJ22318 and its reported

detection in cDNA libraries derived from early embryonic tissues, it is acknowledged that *FLJ22318* knockout may be embryonic lethal. As such targeted *FLJ22318* knockout could be used (eg. to prostate tissues) for these studies.

8.3 Concluding Remarks

Data presented in this thesis has demonstrated that the FLJ22318 gene and protein are highly conserved in mammalian species and contain a unique domain composition that is shared by only six other known proteins in the human genome. FLJ22318 was shown to interact with NKX3-1 in prostate cancer cells and exhibited transcriptional repressor function on an NKX3-1 responsive element in the presence and absence of NKX3-1, results that are consistent with the reported widespread expression of FLJ22318 and which are suggestive of FLJ22318 interaction with transcriptional regulators other than NKX3-1. With further functional studies, the normal biological activity of FLJ22318 will be determined, leading to identification of alterations in its function and expression that contribute to prostate carcinogenesis and to development of other tumour types.

References

References

Abate-Shen, C. and Shen, M.M. (2000) Molecular genetics of prostate cancer. *Genes Dev*, **14**, 2410-2434.

Abdulkadir, S.A. (2005) Mechanisms of Prostate Tumorigenesis: Roles for Transcription Factors Nkx3.1 and Egr1. *Ann N Y Acad Sci*, **1059**, 33-40.

Aho, S., Arffman, A., Pummi, T. and Uitto, J. (1997) A novel reporter gene *MEL1* for the yeast two-hybrid system. *Anal Biochem*, **253**, 270-272.

AIHW and AACR. (2004) *Cancer in Australia 2001*. AIHW cat no. CAN 23, Canberra: AIHW (Cancer Series no. 28).

AIHW, AACR and NCSG: Ian McDermid. (2005) *Cancer incidence projections, Australia 2002 to 2011*. Canberra: Australian Institute of Health and Welfare (AIHW), Australian Association of Cancer Registries (AACR) and the National Cancer Strategies Group (NCSG).

Alcaraz, A., Takahashi, S., Brown, J.A., Herath, J.F., Bergstralh, E.J., Larson-Keller, J.J., Lieber, M.M. and Jenkins, R.B. (1994) Aneuploidy and aneusomy of chromosome 7 detected by fluorescence in situ hybridization are markers of poor prognosis in prostate cancer. *Cancer Res*, **54**, 3998-4002.

Altschul, S.F., Gish, W., Miller, W., Meyers, E.W. and Lipman, D.J. (1990) Basic Local Alignment Search Tool. *J Mol Biol*, **215**, 403-410.

American Urological Association. (2000) Prostate-specific antigen (PSA) best practice policy. *Oncology (Williston Park)*, **14**, 267-272, 277-268, 280 passim.

Angeletti, R.H., Bonewald, L.F. and Fields, G.B. (1997) Six-year study of peptide synthesis. *Methods Enzymol*, **289**, 607-717.

Asatiani, E., Huang, W.X., Wang, A., Rodriguez Ortner, E., Cavalli, L.R., Haddad, B.R. and Gelmann, E.P. (2005) Deletion, methylation, and expression of the NKX3.1 suppressor gene in primary human prostate cancer. *Cancer Res*, **65**, 1164-1173.

Asefa, B., Dermott, J.M., Kaldis, P., Stefanisko, K., Garfinkel, D.J. and Keller, J.R. (2006) p205, a potential tumor suppressor, inhibits cell proliferation via multiple pathways of cell cycle regulation. *FEBS Lett*, **580**, 1205-1214.

Aumuller, G., Leonhardt, M., Janssen, M., Konrad, L., Bjartell, A. and Abrahamsson, P.A. (1999) Neurogenic origin of human prostate endocrine cells. *Urology*, **53**, 1041-1048.

Azpiazu, N. and Frasch, M. (1993) *tinman* and *bagpipe*: two homeobox genes that determine cell fates in the dorsal mesoderm of *Drosophila*. *Genes Dev*, **7**, 1325-1340.

Bala, S., Kumar, A., Soni, S., Sinha, S. and Hanspal, M. (2006) Emp is a component of the nuclear matrix of mammalian cells and undergoes dynamic rearrangments during cell division. *Biochem Biophys Res Commun*, **342**, 1040-1048.

Bandyk, M.G., Zhao, L., Troncoso, P., Pisters, L.L., Palmer, J.L., von Eschenbach, A.C., Chung, L.W. and Liang, J.C. (1994) Trisomy 7: a potential cytogenetic marker of human prostate cancer progression. *Genes Chromosomes Cancer*, **9**, 19-27.

Banerjee-Basu, S. and Baxevanis, A.D. (2001) Molecular evolution of the homeodomain family of transcription factors. *Nucleic Acids Res*, **29**, 3258-3269.

Barnes, W.M. (1994) PCR amplification of up to 35-kb DNA with high fidelity and high yield from I bacteriophage templates. *Proc Natl Acad Sci U S A*, **91**, 2216-2220.

Bassi, M.T., Ramesar, R.S., Caciotti, B., Winship, I.M., De Grandi, A., Riboni, M., Townes, P.L., Beighton, P., Ballabio, A. and Borsani, G. (1999) X-linked late-onset sensorineural deafness caused by a deletion involving OA1 and a novel gene containing WD-40 repeats. *Am J Hum Genet*, **64**, 1604-1616.

Bast, R., Kufe, D., Pollock, R., Weichselbaum, R., Holland, J. and Frei, E. (eds.). (2000) *Cancer Medicine*. BC Decker Inc., Canada.

Bauer, J., Srivastava, S., Connelly, R., Sesterhenn, I., Preston, D., McLeod, D. and Moul, J. (1998) Significance of familial history of prostate cancer to traditional prognostic variables, genetic biomarkers, and recurrence after radical prostatectomy. *Urology*, **51**, 970-976.

Baulcombe, D. (2005) RNA silencing. *Trends Biochem Sci*, **30**, 290-293.

Becker, W.M., Reece, J.B. and Poenie, M.F. (1996) *The World of the Cell*. Benjamin Cummings, New York.

Bennett, R.L., Blalock, W.L., Abtahi, D.M., Pan, Y., Moyer, S.A. and May, W.S. (2006) RAX, the PKR activator, sensitizes cells to inflammatory cytokines, serum withdrawal, chemotherapy, and viral infection. *Blood*, **108**, 821-829.

Berger, R., Busson, M., Baranger, L., Helias, C., Lessard, M., Dastugue, N. and Speleman, F. (2006) Loss of the NPM1 gene in myeloid disorders with chromosome 5 rearrangements. *Leukemia*, **20**, 319-321.

Bhatia-Gaur, R., Donjacour, A.A., Sciavolino, P.J., Kim, M., Desai, N., Young, P., Norton, C.R., Gridley, T., Cardiff, R.D., Cunha, G.R., Abate-Shen, C. and Shen, M.M. (1999) Roles for Nkx3.1 in prostate development and cancer. *Genes Dev*, **13**, 966-977.

Bidoli, E., Talamini, R., Bosetti, C., Negri, E., Maruzzi, D., Montella, M., Franceschi, S. and La Vecchia, C. (2005) Macronutrients, fatty acids, cholesterol and prostate cancer risk. *Ann Oncol*, **16**, 152-157.

Bieberich, C.J., Fujita, K., He, W.W. and Jay, G. (1996) Prostate-specific and androgen-dependent expression of a novel homeobox gene. *J Biol Chem*, **271**, 31779-31782.

Blomme, T., Vandepoele, K., De Bodt, S., Simillion, C., Maere, S. and Van de Peer, Y. (2006) The gain and loss of genes during 600 million years of vertebrate evolution. *Genome Biology*, **7**, R43.

Bonkhoff, H., Stein, U. and Remberger, K. (1994) Multidirectional differentiation in the normal, hyperplastic, and neoplastic human prostate: simultaneous demonstration of cell-specific epithelial markers. *Hum Pathol*, **25**, 42-46.

Bonkhoff, H., Stein, U. and Remberger, K. (1995) Endocrine-paracrine cell types in the prostate and prostatic adenocarcinoma are postmitotic cells. *Hum Pathol*, **26**, 167-170.

Bostwick, D. (1999) Prostatic intraepithelial neoplasia is a risk factor for cancer. *Urol Oncol*, **17**, 187-198.

Bostwick, D., Amin, M., Dundore, P., Marsh, W. and Schultz, D. (1993) Architectural patterns of high-grade prostatic intraepithelial neoplasia. *Human Pathol*, **24**, 298-310.

Bostwick, D.G., Burke, H.B., Djakiew, D., Euling, S., Ho, S.-m., Landolph, J., Morrison, H., Sonawane, B., Shifflett, T., Waters, D.J. and Timms, B. (2004) Human Prostate Cancer Risk Factors. *Cancer*, **101**, 2371-2490.

Bostwick, D.G., Shan, A., Qian, J., Darson, M., Maihle, N.J., Jenkins, R.B. and Cheng, L. (1998) Independent origin of multiple foci of prostatic intraepithelial neoplasia: comparison with matched foci of prostate carcinoma. *Cancer*, **83**, 1995-2002.

Bourbon, H.M., Martin-Blanco, E., Rosen, D. and Kornberg, T.B. (1995) Phosphorylation of the *Drosophila* engrailed protein at a site outside its homeodomain enhances DNA binding. *J Biol Chem*, **270**, 11130-11139.

Bowen, C., Bubendorf, L., Voeller, H.J., Slack, R., Willi, N., Sauter, G., Gasser, T.C., Koivisto, P., Lack, E.E., Kononen, J., Kallioniemi, O.P. and Gelmann, E.P. (2000) Loss of NKX3.1 expression in human prostate cancers correlates with tumor progression. *Cancer Res*, **60**, 6111-6115.

Bram, R. and Kornberg, R. (1985) Specific protein binding to far upstream activating sequences in polymerase II promoters. *Proc Natl Acad Sci U S A*, **82**, 43-47.

Bras, M., Queenan, B. and Susin, S.A. (2005) Programmed Cell Death via Mitochondria: Different Modes of Dying. *Biochemistry (Moscow)*, **70**, 231--239.

Brawley, O., Giovannucci, E. and Kramer, B. (2000) Epidemiology of prostate cancer. In Vogelzang, N., Scardino, P., Shippley, P., Shippley, W. and Coffey, D. (eds.), *Comprehensive Textbook of Genitourinary Oncology. 2nd Ed*. Lippincott, Philadelphia, p. 533–544.

Brothman, A.R. (2002) Cytogenetics and Molecular Genetics of Cancer of the Prostate. *Am J Med Gen*, **115**, 150-156.

Bucher, M.H., Evdokimov, A.G. and Waugh, D.S. (2002) Differential effects of short affinity tags on the crystallization of *Pyrococcus furiosus* maltodextrin-binding protein. *Acta Crystallographica Section D Biological Crystallography*, **58**, 392-397.

Bussemakers, M.J.G., van Bokhoven, A., Verhaegh, G.W., Smit, F.P., Karthaus, H.F.M., Schalken, J.A., Debruyne, F.M.J., Ru, N. and Isaacs, W.B. (1999) DD3: a new prostate-specific gene, highly overexpressed in prostate cancer. *Cancer Res*, **59**, 5975-5979.

Bussiere, J.R., Beer, T.M., Neiss, M.B. and Janowsky, J.S. (2005) Androgen deprivation impairs memory in older men. *Behav Neurosci*, **119**, 1429-1437.

Cahana, A., Escamez, T., Nowakowski, R.S., Hayes, N.L., Giacobini, M., von Holst, A., Shmueli, O., Sapir, T., McConnell, S.K., Wurst, W., Martinez, S. and Reiner, O. (2001) Targeted mutagenesis of Lis1 disrupts cortical development and LIS1 homodimerization. *Proc Natl Acad Sci U S A*, **98**, 6429-6434.

Cancel-Tassin, G. and Cussenot, O. (2005) Genetic susceptibility to prostate cancer. *BJU Int*, **96**, 1380-1385.

Carson, J.A., Fillmore, R.A., Schwartz, R.J. and Zimmer, W.E. (2000) The smooth muscle gamma-actin gene promoter is a molecular target for the mouse bagpipe homologue, mNkx3-1, and serum response factor. *J Biol Chem*, **275**, 39061-39072.

Carter, B.S., Ewing, C.M., Ward, W.S., Treiger, B.F., Aalders, T.W., Schalken, J.A., Epstein, J.I. and Isaacs, W.B. (1990) Allelic loss of chromosomes 16q and 10q in human prostate cancer. *Proc Natl Acad Sci U S A*, **87**, 8751-8755.

Cartharius, K., Frech, K., Grote, K., Klocke, B., Haltmeier, M., Klingenhoff, A., Frisch, M., Bayerlein, M. and Werner, T. (2005) MatInspector and beyond: promoter analysis based on transcription factor binding sites. *Bioinformatics*, **21**, 2933-2942.

Caspi, M., Atlas, R., Kantor, A., Sapir, T. and Reiner, O. (2000) Interaction between LIS1 and doublecortin, two lissencephaly gene products. *Hum Mol Genet*, **9**, 2205-2213.

Castren, M., Tervonen, T., Karkkainen, V., Heinonen, S., Castren, E., Larsson, K., Bakker, C.E., Oostra, B.A. and Akerman, K. (2005) Altered differentiation of neural stem cells in fragile X syndrome. *Proc Natl Acad Sci U S A*, **102**, 17834-17839.

Chan, J.M., Gann, P.H. and Giovannucci, E.L. (2005) Role of Diet in Prostate Cancer Development and Progression. *J Clin Oncol*, **23**, 8152-8160.

Chang, B.L., Zheng, S.L., Hawkins, G.A., Isaacs, S.D., Wiley, K.E., Turner, A., Carpten, J.D., Bleecker, E.R., Walsh, P.C., Trent, J.M., Meyers, D.A., Isaacs, W.B. and Xu, J. (2002) Polymorphic GGC repeats in the androgen receptor gene are associated with hereditary and sporadic prostate cancer risk. *Hum Genet*, **110**, 122-129.

Chen, G., Ma, C., Bower, K.A., Ke, Z. and Luo, J. (2006) Interaction between RAX and PKR modulates the effect of ethanol on protein synthesis and survival of neurons. *J Biol Chem*, **281**, 15909-15915.

Chen, H. and Bieberich, C.J. (2005) Structural and functional analysis of domains mediating interaction between NKX-3.1 and PDEF. *J Cell Biochem*, **94**, 168-177.

Chen, H., Mutton, L.N., Prins, G.S. and Bieberich, C.J. (2005) Distinct regulatory elements mediate the dynamic expression pattern of Nkx3.1. *Dev Dyn*, **234**, 961-973.

Chen, H., Nandi, A.K., Li, X. and Bieberich, C.J. (2002) NKX-3.1 interacts with prostate-derived Ets factor and regulates the activity of the PSA promoter. *Cancer Res*, **62**, 338-340.

Chenchik, A., Zhu, Y.Y., Diatchenko, L., Li, R., Hill, J. and Siebert, P.D. (1998) Generation and use of high-quality cDNA from small amounts of total RNA by SMART PCR. In *Gene Cloning and Analysis by RT-PCR*. BioTechniques Books, MA, pp. 305-319.

Cher, M.L., Bova, G.S., Moore, D.H., Small, E.J., Carroll, P.R., Pin, S.S., Epstein, J.I., Isaacs, W.B. and Jensen, R.H. (1996) Genetic alterations in untreated metastases and androgen-independent prostate cancer detected by comparative genomic hybridization and allelotyping. *Cancer Res*, **56**, 3091-3102.

Chien, C.T., Bartel, P.L., Sternglanz, R. and Fields, S. (1991) The two-hybrid system: A method to identify and clone genes for proteins that interact with a protein of interest. *Proc Natl Acad Sci U S A*, **88**, 9578-9582.

Clontech. (2003) User Manual PT3529-1. *BD Matchmaker™ Library Construction & Screening Kits*.

Costello, L.C. and Franklin, R.B. (1997) Citrate Metabolism of Normal and Malignant Prostate Epithelial Cells. *Urology*, **50**, 3-12.

Costello, L.C., Franklin, R.B. and Feng, P. (2005) Mitochondrial function, zinc, and intermediary metabolism relationships in normal prostate and prostate cancer. *Mitochondrion*, **5**, 143-153.

Courey, A. (2001) Cooperativity in transcriptional control. *Curr Biol*, **10**, R250-R252.

Cunha, G.R., Donjacour, A.A., Cooke, P.S., Mee, S., Bigsby, R.M., Higgins, S.J. and Sugimura, Y. (1987) The endocrinology and developmental biology of the prostate. *Endocr. Rev.*, **8**, 338-362.

Cunningham, J.M., Shan, A., Wick, M.J., McDonnell, S.K., Schaid, D.J., Tester, D.J., Qian, J., Takahashi, S., Jenkins, R.B., Bostwick, D.G. and Thibodeau, S.N. (1996) Allelic imbalance and microsatellite instability in prostatic adenocarcinoma. *Cancer Res*, **56**, 4475-4482.

Damante, G., Fabbro, D., Pellizzari, L., Civitareale, D., Guazzi, S., Polycarpou-Schwartz, M., Cauci, C., Quadrifoglio, F., Formisano, S. and DiLauro, R. (1994) Sequence specific DNA recognition by the thyroid transcription factor-1 homeodomain. *Nucleic Acids Res*, **22**, 3075-3083.

de Carvalho, H.F. and Line, S.R. (1996) Basement membrane associated changes in the rat ventral prostate following castration. *Cell Biol Int*, **20**, 809-819.

Denti, S., Sirri, A., Cheli, A., Rogge, L., Innamorati, G., Putignano, S., Fabbri, M., Pardi, R. and Bianchi, E. (2004) RanBPM is a phosphoprotein that associates with the plasma membrane and interacts with the integrin LFA-1. *J Biol Chem*, **279**, 13027-13034.

Devys, D., Lutz, Y., Rouyer, N., Bellocq, J.P. and Mandel, J.L. (1993) The FMR-1 protein is cytoplasmic, most abundant in neurons and appears normal in carriers of a fragile X premutation. *Nat Genet*, **4**, 335-340.

Di Cristofano, A., De Acetis, M., Koff, A., Cordon-Cardo, C. and Pandolfi, P.P. (2001) Pten and p27KIP1 cooperate in prostate cancer tumor suppression in the mouse. *Nat Genet*, **27**, 222-224.

di Sant`Agnese, P.A. (1998) Neuroendocrine cells of the prostate and neuroendocrine differentiation in prostatic carcinoma: A review of morphologic aspects. *Urology*, **51**, 121-124.

Dillner, J., Knekt, P., Boman, J., Lehtinen, M., Af Geijersstam, V., Sapp, M., Schiller, J., Maatela, J. and Aroma, A. (1998) Sero-epidemiological association between human-papillomavirus infection and risk of prostate cancer. *Int J Cancer*, **75**, 564-567.

Dingwall, C. and Laskey, R.A. (1991) Nuclear targeting sequences--a consensus? *Trends Biochem Sci*, **16**, 478-481.

Dong, X., Wang, L., Taniguchi, K., Wang, X., Cunningham, J.M., McDonnell, S.K., Qian, C., Marks, A.F., Slager, S.L., Peterson, B.J., Smith, D.I., Cheville, J.C., Blute, M.L., Jacobsen, S.J., Schaid, D.J., Tindall, D.J., Thibodeau, S.N. and Liu, W. (2003) Mutations in CHEK2 associated with prostate cancer risk. *Am J Hum Genet*, **72**, 270-280.

Douglas, J., Hanks, S., Temple, I.K., Davies, S., Murray, A., Upadhyaya, M., Tomkins, S., Hughes, H.E., Cole, T.R. and Rahman, N. (2003) NSD1 mutations are the major cause of Sotos syndrome and occur in some cases of Weaver syndrome but are rare in other overgrowth phenotypes. *Am J Hum Genet*, **72**, 132-143.

Drasch, G., Schopfer, J. and Schrauzer, G.N. (2005) Selenium/cadmium ratios in human prostates: indicators of prostate cancer risk of smokers and nonsmokers, and relevance to the cancer protective effects of selenium. *Biol Trace Elem Res*, **103**, 103-107.

Droit, A., Poirer, G.G. and Hunter, J.M. (2005) Experimental and bioinformatic approaches for interrogating protein-protein interactions to determine protein function. *J Mol Endocrinology*, **34**, 263-280.

Durand, B., Saunders, M., Gaudon, C., Roy, B., Losson, R. and Chambon, P. (1994) Activation function 2 (AF-2) of retinoic acid receptor and 9-cis retinoic acid receptor: presence of a conserved autonomous constitutive activating domain and influence of the nature of the response element on AF-2 activity. *Embo J*, **13**, 5370-5382.

Elrick, L.J. and Docherty, K. (2001) Phosphorylation-dependent nucleocytoplasmic shuttling of pancreatic duodenal homeobox-1. *Diabetes*, **10**, 2244-2252.

Emes, R.D. and Ponting, C.P. (2001) A new sequence motif linking lissencephaly, Treacher Collins and oral-facial-digital type 1 syndromes, microtubule dynamics and cell migration. *Hum Mol Genet*, **10**, 2813-2820.

Emmert-Buck, M.R., Vocke, C.D., Pozzatti, R.O., Duray, P.H., Jennings, S.B., Florence, C.D., Zhuang, Z., Bostwick, D.G., Liotta, L.A. and Linehan, W.M. (1995) Allelic loss on chromosome 8p12-21 in microdissected prostatic intraepithelial neoplasia. *Cancer Res*, **55**, 2959-2962.

Enyenihi, A.H. and Saunders, W.S. (2003) Large-scale functional genomic analysis of sporulation and meiosis in Saccharomyces cerevisiae. *Genetics*, **163**, 47-54.

Esteller, M. (2005) Dormant hypermethylated tumour suppressor genes: questions and answers. *J Pathol*, **205**, 172-180.

Estojak, J., Brent, R. and Golemis, E.A. (1995) Correlation of two-hybrid affinity data with *in vitro* measurements. *Mol and Cell Biol*, **15**, 5820-5829.

Fahrenkrog, B. (2006) The nuclear pore complex, nuclear transport, and apoptosis. *Can J Physiol Pharmacol*, **84**, 279-286.

Faulkner, N.E., Dujardin, D.L., Tai, C.Y., Vaughan, K.T., O'Connell, C.B., Wang, Y. and Vallee, R.B. (2000) A role for the lissencephaly gene LIS1 in mitosis and cytoplasmic dynein function. *Nat Cell Biol*, **2**, 784-791.

Fehrenbacher, K.L., Boldogh, I.R. and Pon, L.A. (2005) A Role for Jsn1p in Recruiting the Arp2/3 Complex to Mitochondria in Budding Yeast. *Mol Biol Cell*, **11**, 5094-6102.

Feng, Y. and Walsh, C.A. (2004) Mitotic spindle regulation by Nde1 controls cerebral cortical size. *Neuron*, **44**, 279-293.

Ferlay, J., Bray, F., Pisani, P. and Parkin, D.M. (2004) GLOBOCAN 2002: Cancer Incidence, Mortality and Prevalence Worldwide. In *IARC CancerBase No. 5 version 2.0*. IARC*Press*, Lyon.

Ferrante, M.I., Giorgio, G., Feather, S.A., Bulfone, A., Wright, V., Ghiani, M., Selicorni, A., Gammaro, L., Scolari, F., Woolf, A.S., Sylvie, O., Bernard, L., Malcolm, S., Winter, R., Ballabio, A. and Franco, B. (2001) Identification of the gene for oral-facial-digital type I syndrome. *Am J Hum Genet*, **68**, 569-576.

Ferrante, M.I., Zullo, A., Barra, A., Bimonte, S., Messaddeq, N., Studer, M., Dolle, P. and Franco, B. (2006) Oral-facial-digital type I protein is required for primary cilia formation and left-right axis specification. *Nat Genet*, **38**, 112-117.

Fields, S. and Song, O. (1989) A novel genetic system to detect protein-protein interactions. *Nature*, **340**, 245-247.

Fields, S. and Sternglanz, R. (1994) The two-hybrid system: an assay for protein-protein interactions. *Trends Genet*, **10**, 286-292.

Figeys, D. (2003) Novel approaches to map protein interactions. *Curr Opin Biotechnol*, **14**, 119-125.

Fillmore, R.A., Dean, D.A. and Zimmer, W.E. (2002) The Smooth Muscle g-Actin Gene Is Androgen Responsive in Prostate Epithelia. *Gene Expr*, **10**, 201-211.

Formosa, T., Barry, J., Alberts, B.M. and Greenblatt, J. (1991) Using protein affinity chromatography to probe structure of protein machines. *Methods Enzymol*, **208**, 24-45.

Freeman, J.A., Esrig, D., Grossfeld, G.D., Stein, J.P., Chen, S.C., Young, L.L., Taylor, C.R., Skinner, D.G., Lieskovsky, G. and Cote, R.J. (1995) Incidence of occult lymph node metastases in pathological stage C (pT3N0) prostate cancer. *J Urol*, **154**, 474-478.

Garcia-Fernandez, J. (2005) The Genesis and Evolution of Homeobox Gene Clusters. *Nature Reviews Genetics*, **6**, 881-892.

Gardiner-Garden, M. and Frommer, M. (1987) CpG islands in vertebrate genomes. *J Mol Biol*, **196**, 261-282.

Garnick, M. and Fair, W. (1996) Prostate cancer: emerging concepts. Part II. *Ann Intern Med*, **125**, 205-212.

Gary, B., Azuero, R., Mohanty, G.S., Bell, W.C., Eltoum, I.E. and Abdulkadir, S.A. (2004) Interaction of Nkx3.1 and p27kip1 in prostate tumor initiation. *Am J Pathol*, **164**, 1607-1614.

Gehring, W.J., Qian, Y.Q., Billeter, M., Furukubo-Tokunaga, K., Schier, A.F., Resendez-Perez, D., Affolter, M., Otting, G. and Wuthrich, K. (1994) Homeodomain-DNA recognition. *Cell*, **78**, 211-223.

Gerlitz, G., Darhin, E., Giorgio, G., Franco, B. and Reiner, O. (2005) Novel functional features of the Lis-H domain: role in protein dimerization, half-life and cellular localization. *Cell Cycle*, **4**, 1632-1640.

Giege, P., Heazlewood, J.L., Roessner-Tunali, U., Millar, A.H., Fernie, A.R., Leaver, C.J. and Sweetlove, L.J. (2003) Enzymes of glycolysis are functionally associated with mitochondrion in Arabidopsis cells. *Plant Cell*, **15**, 2140-2151.

Gietz, R.D., Triggs-Raine, B., Robbins, A., Graham, K.C. and Woods, R.A. (1997) Identification of proteins that interact with a protein of interest: applications of the yeast two-hybrid system. *Mol Cell Biochem*, **172**, 67-79.

Gietz, R.D. and Woods, R.A. (2002) Screening for protein-protein interactions in the yeast two-hybrid system. *Methods Mol Biol*, **185**, 471-486.

Giovannucci, E. (2000) Gamma-tocopheral: A new player in prostate cancer prevention? *J Natl Cancer Inst*, **92**, 1966-1967.

Gleason, D. and Mellinger, G. (1974) Prediction of prognosis for prostatic adenocarcinoma by combined histological grading and clinical staging. *J Urol*, **111**, 58-64.

Goyal, P., Pandey, D. and Sless, W. (2006) Phosphorylation-dependent regulation of unique nuclear and nucleolar localization signals of lim-kinase 2 in endothelial cells. *J Biol Chem*, **281**, 25223-25230.

Gray, I.C., Phillips, S.M., Lee, S.J., Neoptolemos, J.P., Weissenbach, J. and Spurr, N.K. (1995) Loss of chromosomal region 10q23-25 in prostate cancer. *Cancer Res*, **55**, 4800-4803.

Greene, F.L., American Joint Committee on Cancer and American Cancer Society. (2002) *AJCC cancer staging handbook : from the AJCC cancer staging manual*. 6th ed. Springer, New York.

Gronberg, H. (2003) Prostate cancer epidemiology. *Lancet*, **361**, 859-864.

Gruschus, J.M., Tsao, D.H.H., Wang, L.-H., Nirenberg, M. and Ferretti, J.A. (1997) Interactions of the vnd/NK-2 Homeodomain with DNA by Nuclear Magnetic Resonance Spectroscopy: Basis of Binding Specificity. *Biochem*, **36**, 5372-5380.

Gupta, V. and Patel, R.C. (2002) Proapoptotic protein PACT is expressed at high levels in colonic epithelial cells in mice. *Am J Physiol Gastrointest Liver Physiol*, **283**, G801-G808.

Haggman, M.J., Wojno, K.J., Pearsall, C.P. and Macoska, J.A. (1997) Allelic loss of 8p sequences in prostatic intraepithelial neoplasia and carcinoma. *Urology*, **50**, 643-647.

Hancock, J.M. (2005) Gene factories, microfunctionalization and the evolution of gene families. *Trends Genet*, **21**, 591-595.

Hanspal, M., Smockova, Y. and Uong, Q. (1998) Molecular identification and functional characterization of a novel protein that mediates the attachment of erythroblasts to macrophages. *Blood*, **92**, 2940-2950.

Hartmann, C.M., Gehring, H. and Christen, P. (1993) The mature form of imported mitochondrial proteins undergoes conformational changes upon binding to isolated mitochondria. *Eur J Biochem*, **218**, 905-910.

Hattori, M., Arai, H. and Inoue, K. (1993) Purification and characterization of bovine brain platelet-activating factor acetylhydrolase. *J Biol Chem*, **268**, 18748-18753.

He, W.W., Sciavolino, P.J., Wing, J., Augustus, M., Hudson, P., Meissner, P.S., Curtis, R.T., Shell, B.K., Bostwick, D.G., Tindall, D.J., Gelmann, E.P., Abate-Shen, C. and Carter, K.C. (1997) A novel human prostate-specific, androgen-regulated homeobox gene (NKX3.1) that maps to 8p21, a region frequently deleted in prostate cancer. *Genomics*, **43**, 69-77.

Heger, P., Lohmaier, J., Schneider, G., Schweimer, K. and Stauber, R.H. (2001) Qualitative Highly Divergent Nuclear Export Signals Can Regulate Export by the Competition for Transport Cofactors *in Vivo*. *Traffic*, **2**, 544-555.

Herbrand, H., Pabst, O., Hill, R. and Arnold, H.H. (2002) Transcription factors Nkx3.1 and Nkx3.2 (Bapx1) play an overlapping role in sclerotomal development of the mouse. *Mech Dev*, **117**, 217-224.

Hillier, L.W., Miller, W., Birney, E., Warren, W., Hardison, R.C., Ponting, C.P., Bork, P., Burt, D.W., Groenen, M.A., Delany, M.E., Dodgson, J.B., Chinwalla, A.T., Cliften, P.F., Clifton, S.W., Delehaunty, K.D., Fronick, C., Fulton, R.S., Graves, T.A., Kremitzki, C., Layman, D., Magrini, V., McPherson, J.D., Miner, T.L., Minx, P., Nash, W.E., Nhan, M.N., Nelson, J.O., Oddy, L.G., Pohl, C.S., Randall-Maher, J., Smith, S.M., Wallis, J.W., Yang, S.P., Romanov, M.N., Rondelli, C.M., Paton, B., Smith, J., Morrice, D., Daniels, L., Tempest, H.G., Robertson, L., Masabanda, J.S., Griffin, D.K., Vignal, A., Fillon, V., Jacobbson, L., Kerje, S., Andersson, L., Crooijmans, R.P., Aerts, J., van der Poel, J.J., Ellegren, H., Caldwell, R.B., Hubbard, S.J., Grafham, D.V., Kierzek, A.M.,

McLaren, S.R., Overton, I.M., Arakawa, H., Beattie, K.J., Bezzubov, Y., Boardman, P.E., Bonfield, J.K., Croning, M.D., Davies, R.M., Francis, M.D., Humphray, S.J., Scott, C.E., Taylor, R.G., Tickle, C., Brown, W.R., Rogers, J., Buerstedde, J.M., Wilson, S.A., Stubbs, L., Ovcharenko, I., Gordon, L., Lucas, S., Miller, M.M., Inoko, H., Shiina, T., Kaufman, J., Salomonsen, J., Skjoedt, K., Wong, G.K., Wang, J., Liu, B., Yu, J., Yang, H., Nefedov, M., Koriabine, M., Dejong, P.J., Goodstadt, L., Webber, C., Dickens, N.J., Letunic, I., Suyama, M., Torrents, D., von Mering, C., Zdobnov, E.M., Makova, K., Nekrutenko, A., Elnitski, L., Eswara, P., King, D.C., Yang, S., Tyekucheva, S., Radakrishnan, A., Harris, R.S., Chiaromonte, F., Taylor, J., He, J., Rijnkels, M., Griffiths-Jones, S., Ureta-Vidal, A., Hoffman, M.M., Severin, J., Searle, S.M., Law, A.S., Speed, D., Waddington, D., Cheng, Z., Tuzun, E., Eichler, E., Bao, Z., Flicek, P., Shteynberg, D.D., Brent, M.R., Bye, J.M., Huckle, E.J., Chatterji, S., Dewey, C., Pachter, L., Kouranov, A., Mourelatos, Z., Hatzigeorgiou, A.G., Paterson, A.H., Ivarie, R., Brandstrom, M., Axelsson, E., Backstrom, N., Berlin, S., Webster, M.T., Pourquie, O., Reymond, A., Ucla, C., Antonarakis, S.E., Long, M., Emerson, J.J., Betran, E., Dupanloup, I., Kaessmann, H., Hinrichs, A.S., Bejerano, G., Furey, T.S., Harte, R.A., Raney, B., Siepel, A., Kent, W.J., Haussler, D., Eyras, E., Castelo, R., Abril, J.F., Castellano, S., Camara, F., Parra, G., Guigo, R., Bourque, G., Tesler, G., Pevzner, P.A., Smit, A., Fulton, L.A., Mardis, E.R. and Wilson, R.K. (2004) Sequence and comparative analysis of the chicken genome provide unique perspectives on vertebrate evolution. *Nature*, **432**, 695-716.

Hitti, E.G., Sallacz, N.B., Schoft, V.K. and Jantsch, M.F. (2004) Oligomerization activity of a double-stranded RNA-binding domain. *FEBS Lett*, **574**, 25-30.

Holland, P.W. and Takahashi, T. (2005) The evolution of homeobox genes: Implications for the study of brain development. *Brain Res Bull*, **66**, 484-490.

Holtz, A.E. and Zhu, L. (1995) *CLONTECHniques*, **X**, 20.

Huang, N., vom Baur, E., Garnier, J.M., Lerouge, T., Vonesch, J.L., Lutz, Y., Chambon, P. and Losson, R. (1998) Two distinct nuclear receptor interaction domains in NSD1, a novel SET protein that exhibits characteristics of both corepressors and coactivators. *Embo J*, **17**, 3398-3412.

Hughes, C., Murphy, A., Martin, C., Sheils, O. and O'Leary, J. (2005) Molecular pathology of prostate cancer. *J Clin Pathol*, **58**, 673-684.

Hutvagner, G., McLachlan, J., Pasquinelli, A.E., Balint, E., Tuschl, T. and Zamore, P.D. (2001) A cellular function for the RNA-interference enzyme Dicer in the maturation of the let-7 small temporal RNA. *Science*, **293**, 834-838.

Imai, T., Yamauchi, M., Seki, N., Sugawara, T., Saito, T., Matsuda, Y., Ito, H., Nagase, T., Nomura, N. and Hori, T. (1996) Identification and characterization of a new gene physically linked to the ATM gene. *Genome Res*, **6**, 439-447.

Ito, T., Ota, K., Kubota, H., Yamaguchi, Y., Chuba, T., Sakuraba, K. and Yoshida, M. (2002) Roles for the two-hybrid system in exploration of the yeast interactome. *Mol Cell Proteomics*, **1**, 561-566.

Ito, T., Yang, M. and May, W.S. (1999) RAX, a cellular activator for double-stranded RNA-dependent protein kinase during stress signaling. *J Biol Chem*, **274**, 15427-15432.

Iversen, P., Tyrrell, C.J., Kaisary, A.V., Anderson, J.B., Van Poppel, H., Tammela, T.L.J., Chamberlain, M., Carroll, K. and Melezinek, I. (2000) Bicalutamide monotherapy compared with castration in patients with nonmetastatic locally advanced prostate cancer: 6.3 years of follow up. *J Urol*, **164**, 1579-1582.

Iwamura, T., Yoneyama, M., Koizumi, N., Okabe, Y., Namiki, H., Samuel, C.E. and Fujita, T. (2001) PACT, a double-stranded RNA binding protein acts as a positive regulator for type I interferon gene induced by Newcastle disease virus. *Biochem Biophys Res Commun*, **282**, 515-523.

Jagla, K., Bellard, M. and Frasch, M. (2001) A cluster of *Drosophila* homeobox genes involved in mesoderm differentiation programs. *Bioessays*, **23**, 125-133.

James, P., Haliaday, J. and Craig, E.A. (1996) Genomic libraries and a host strain designed for highly efficient two-hybrid selection in yeast. *Genetics*, **144**, 1425-1436.

Jenkins, R., Takahashi, S., DeLacey, K., Bergstralh, E. and Lieber, M. (1998) Prognostic significance of allelic imbalance of chromosome arms 7q, 8p, 16q, and 18q in Stage T3N0M0 prostate cancer. *Genes Chromosomes Cancer*, **21**, 131-143.

Jiang, A.L., Hu, X.Y., Zhang, P.J., He, M.L., Kong, F., Liu, Z.F., Yuan, H.Q. and Zhang, J.Y. (2005a) Up-regulation of NKX3.1 expression and inhibition of LNCaP cell proliferation induced by an inhibitory element decoy. *Acta Biochim Biophys Sin (Shanghai)*, **37**, 335-340.

Jiang, A.L., Zhang, J.Y., Young, C., Hu, X.Y., Wang, Y.M., Liu, Z.F. and Hao, M.L. (2004) Molecular cloning and characterization of human homeobox gene *NKX3.1* promoter. *Acta Biochim Biophys Sin (Shanghai)*, **36**, 64-67.

Jiang, A.L., Zhang, P.J., Chen, W.W., Liu, W.W., Yu, C.X., Hu, X.Y., Zhang, X.Q. and Zhang, J.Y. (2006) Effects of 9-cis retinoic acid on human homeobox gene NKX3.1 expression in prostate cancer cell line LNCaP. *Asian J Androl*, **8**, 435-441.

Jiang, A.L., Zhang, P.J., Hu, X.Y., Chen, W.W., Kong, F., Liu, Z.F., Yuan, H.Q. and Zhang, J.Y. (2005b) Identification of a Positive *Cis*-Element Upstream of Human *NKX3.1* Gene. *Acta Biochim Biophys Sin (Shanghai)*, **37**, 773-778.

Johannsdottir, H.K., Jonsson, G., Johannesdottir, G., Agnarsson, B.A., Eerola, H., Arason, A., Heikkila, P., Egilsson, V., Olsson, H., Johannsson, O.T., Nevanlinna, H., Borg, A. and Barkardottir, R.B. (2006) Chromosome 5 imbalance mapping in breast tumors from BRCA1 and BRCA2 mutation carriers and sporadic breast tumors. *Int J Cancer*, **119**, 1052-1060.

Ju, J.H., Maeng, J.S., Zemedkun, M., Ahronovitz, N., Mack, J.W., Ferretti, J.A., Gelmann, E.P. and Gruschus, J.M. (2006) Physical and Functional Interactions between the Prostate Suppressor Homeoprotein NKX3.1 and Serum Response Factor. *J Mol Biol*, **360**, 989-999.

Kagan, J., Stein, J., Babaian, R.J., Joe, Y.S., Pisters, L.L., Glassman, A.B., von Eschenbach, A.C. and Troncoso, P. (1995) Homozygous deletions at 8p22 and 8p21 in prostate cancer implicate these regions as the sites for candidate tumor suppressor genes. *Oncogene*, **11**, 2121-2126.

Kasahara, H. and Benson, D.W. (2004) Biochemical analyses of eight NKX2.5 homeodomain missense mutations causing atrioventricular block and cardiac anomalies. *Cardiovasc Res*, **64**, 40-51.

Keller, L.C., Romijn, E.P., Zamora, I., Yates, J.R., 3rd and Marshall, W.F. (2005) Proteomic analysis of isolated chlamydomonas centrioles reveals orthologs of ciliary-disease genes. *Curr Biol*, **15**, 1090-1098.

Kellogg, D.E., Rybalkin, I., Chen, S., Mukhamedova, N., Vlasik, T., Siebert, P.D. and Chenchik, A. (1994) TaqStart Antibody: Hot start PCR facilitated by a neutralizing antibody directed against *Taq* DNA polymerase. *Bio Techniques*, **16**, 1134-1137.

Khaitovich, P., Weiss, G., Lachmann, M., Hellmann, I., Enard, W., Muetzel, B., Wirkner, U., Ansorge, W. and Paabo, S. (2004) A neutral model of transcriptome evolution. *PLoS Biol*, **2**, E132.

Kim, A.J., Lee, C.S. and Schlessinger, D. (2004a) Bex3 associates with replicating mitochondria and is involved in possible growth control of F9 teratocarcinoma cells. *Gene*, **343**, 79-89.

Kim, J.-w. and Dang, C.V. (2005) Multifaceted roles of glycolytic enzymes. *Trends Biochem Sci*, **30**, 142-150.

Kim, M., Bhatia-Gaur, R., Banach-Petrosky, W., Desai, N., Wang, Y., Hayward, S., Cunha, G., Cardiff, R., Shen, M. and Abate-Shen, C. (2002a) *Nkx3.1* Mutant Mice Recapitulate Early Stages of Prostate Carcinogenesis. *Cancer Research*, **62**, 2999-3004.

Kim, M.H., Cooper, D.R., Oleksy, A., Devedjiev, Y., Derewenda, U., Reiner, O., Otlewski, J. and Derewenda, Z.S. (2004b) The structure of the N-terminal domain of the product of the lissencephaly gene Lis1 and its functional implications. *Structure*, **12**, 987-998.

Kim, M.J., Cardiff, R.D., Desai, N., Banach-Petrosky, W.A., Parsons, R., Shen, M.M. and Abate-Shen, C. (2002b) Cooperativity of Nkx3.1 and Pten loss of function in a mouse model of prostate carcinogenesis. *Proc Natl Acad Sci U S A*, **99**, 2884-2889.

Kim, V.N. (2005) MicroRNA biogenesis: coordinated cropping and dicing. *Nat Rev Mol Cell Biol*, **6**, 376-385.

Kim, Y. and Nirenberg, M. (1989) *Drosophila* NK-homeobox genes. *Proc Natl Acad Sci U S A*, **86**, 7716-7720.

Kim, Y.H., Choi, C.Y., Lee, S.J., Conti, M.A. and Kim, Y. (1998) Homeodomain-interacting protein kinases, a novel family of co-repressors for homeodomain transcription factors. *J Biol Chem*, **273**, 25875-25879.

Kirby, R., Robertson, C., Turkes, A., Griffiths, K., Denis, L.J., Boyle, P., Altwein, J. and Schroder, F. (1999) Finasteride in association with either flutamide or goserelin as combination hormonal therapy in patients with stage M1 carcinoma of the prostate gland. International Prostate Health Council (IPHC) Trial Study Group. *Prostate*, **40**, 105-114.

Kitagawa, M., Umezu, M., Aoki, J., Koizumi, H., Arai, H. and Inoue, K. (2000) Direct association of LIS1, the lissencephaly gene product, with a mammalian homologue of a fungal nuclear distribution protein, rNUDE. *FEBS Lett*, **479**, 57-62.

Klotz, L. (2005) Active Surveillance for Prostate Cancer: For Whom? *J Clin Oncol*, **23**, 8165-8169.

Knauer, S.K., Carra, G. and Stauber, R.H. (2005) Nuclear Export Is Evolutionarily Conserved in CVC Paired-Like Homeobox Proteins and Influences Protein Stability, Transcriptional Activation, and Extracellular Secretion. *Mol and Cell Biol*, **25**, 2573-2582.

Korkmaz, C.G., Korkmaz, K.S., Manola, J., Xi, Z., Risberg, B., Danielsen, H., Kung, J., Sellers, W.R., Loda, M. and Saatcioglu, F. (2004) Analysis of androgen regulated homeobox gene NKX3.1 during prostate carcinogenesis. *J Urol*, **172**, 1134-1139.

Kos, L., Chiang, C. and Mahon, K.A. (1998) Mediolateral patterning of somites: multiple axial signals, including Sonic hedgehog, regulate Nkx-3.1 expression. *Mech Dev*, **70**, 25-34.

Koul, S., Houldsworth, J., Mansukhani, M.M., Donaldo, A., McKiernan, J.M., Reuter, V.E., Bosl, G.J., Chaganti, R.S. and Murty, V.V. (2002) Characteristic promoter hypermethylation signatures in male germ cell tumors. *Mol Cancer*, **1**, 8.

Kramer, S., Ozaki, T., Miyazaki, K., Kato, C., Hanamoto, T. and Nakagawara, A. (2005) Protein stability and function of p73 are modulated by a physical interaction with RanBPM in mammalian cultured cells. *Oncogene*, **24**, 938-944.

Krick, R., Aschrafi, A., Hasgum, D. and Arnemann, J. (2006) CK2-dependent C-terminal phosphorylation at T300 directs the nuclear transport of TSPY protein. *Biochem Biophys Res Commun*, **341**, 343-350.

Laggerbauer, B., Ostareck, D., Keidel, E.M., Ostareck-Lederer, A. and Fischer, U. (2001) Evidence that fragile X mental retardation protein is a negative regulator of translation. *Hum Mol Genet*, **10**, 329-338.

Lane, T.M., Ansell, W., Farrugia, D., Wilson, P., Williams, G., Chinegwundoh, F., Philp, T., Hines, J. and Oliver, R.T. (2004) Long-term outcomes in patients with prostate cancer managed with intermittent androgen suppression. *Urol Int*, **73**, 117-122.

Lang, S.H., Stower, M. and Maitland, N.J. (2000) *In vitro* modelling of epithelial and stromal interactions in non-malignant and malignant prostates. *Br J Cancer*, **82**, 990-997.

Lee, J.C. and Peter, M.E. (2003) Regulation of apoptosis by ubiquitination. *Immunol Rev*, **193**, 39-47.

Lee, Y., Hur, I., Park, S.Y., Kim, Y.K., Suh, M.R. and Kim, V.N. (2006) The role of PACT in the RNA silencing pathway. *EMBO J*, **25**, 522-532.

Lei, Q., Jiao, J., Xin, L., Chang, C.-J., Wang, S., Gao, J., Gleave, M.E., Witte, O.N., Liu, X. and Wu, H. (2006) NKX3.1 stabilizes p53, inhibits AKT activation, and blocks prostate cancer initiation caused by PTEN loss. *Cancer Cell*, **9**, 367-378.

Leibowitz, R.L. and Tucker, S.J. (2001) Treatment of localized prostate cancer with intermittent triple androgen blockade: Preliminary results in 110 consecutive patients. *Oncologist*, **6**, 177-182.

Leiros, G.J., Galliano, S.R., Sember, M.E., Kahn, T., Schwarz, E. and Eiguchi, K. (2005) Dection of human papillomavirus DNA and p53 codon 72 polymorphism in prostate carcinomas of patients from Argentina. *BMC Urol*, **5**, 15.

Lettice, L., Hecksher-Sorensen, J. and Hill, R. (2001) The role of Bapx1 (Nkx3.2) in the development and evolution of the axial skeleton. *J Anat*, **199**, 181-187.

Letunic, I., Copley, R.R., Pils, B., Pinkert, S., Schultz, J. and Bork, P. (2006) SMART 5: domains in the context of genomes and networks. *Nucleic Acids Res*, **34**, D257-260.

Li, D., Wang, F. and Samuels, H.H. (2001) Domain structure of the NRIF3 family of coregulators suggests potential dual roles in transcriptional regulation. *Mol Cell Biol*, **21**, 8371-8384.

Li, S., Peters, G.A., Ding, K., Zhang, X., Qin, J. and Sen, G.C. (2006a) Molecular basis for PKR activation by PACT or dsRNA. *PNAS*, **103**, 10005-10010.

Li, X., Guan, B., Maghami, S. and Bieberich, C.J. (2006b) NKX3.1 is regulated by protein kinase CK2 in prostate tumor cells. *Mol Cell Biol*, **26**, 3008-3017.

Liljestrom, P.L. (1985) The nucleotide sequence of the *MEL1* gene. *Nucleic Acids Res*, **13**, 7257-7268.

Lind, G.E., Skotheim, R.I., Fraga, M.F., Abeler, V.M., Henrique, R., Saatcioglu, F., Esteller, M., Teixeira, M.R. and Lothe, R.A. (2005) The loss of NKX3.1 expression in testicular-and prostate-cancers is not caused by promoter hypermethylation. *Mol Cancer*, **4**, 8.

Liu, A.Y., True, L.D., LaTray, L., Ellis, W.J., Vessella, R.L., Lange, P.H., Higano, C.S., Hood, L. and van den Engh, G. (1999) Analysis and sorting of prostate cancer cell types by flow cytometry. *Prostate*, **40**, 192-199.

Long, R.M., Morrissey, C., Fitzpatrick, J.M. and Watson, R.W.G. (2005) Prostate epithelial cell differentiation and its relevance to the understanding of prostate cancer therapies. *Clin Sci (Lond)*, **108**, 1-11.

Lopez-Beltran, A., Mikuz, G., Luque, R.J. and Mazzuccheli, R.M. (2006) Current practice of Gleason grading of prostate carcinoma. *Virchows Arch*, **448**, 111-118.

Louret, O.F., Doignon, F. and Crouzet, M. (1997) Stable DNA binding yeast vector allowing high bait expression for use in the two-hybrid system. *Bio Techniques*, **23**, 816-819.

Luke, G.N., Castro, L.F.C., McLay, K., Bird, C., Coulson, A. and Holland, P.W. (2003) Dispersal of NK homeobox gene clusters in amphioxus and humans. *Proc Natl Acad Sci U S A*, **100**, 5292-5295.

Lund, E., Guttinger, S., Calado, A., Dahlberg, J.E. and Kutay, U. (2004) Nuclear export of microRNA precursors. *Science*, **303**, 95-98.

Ma, K., Araki, K., Ichwan, S.J., Suganuma, T., Tamamori-Adachi, M. and Ikeda, M.A. (2003) E2FBP1/DRIL1, an AT-rich interaction domain-family transcription factor, is regulated by p53. *Mol Cancer Res*, **1**, 438-444.

Maatman, T.J., Gupta, M.K. and Montie, J.E. (1985) Effectiveness of castration versus intravenous estrogen therapy in producing rapid endocrine control of metastatic cancer of the prostate. *J Urol*, **133**, 620-621.

Maddali, K.K., Korzick, D.H., Tharp, D.L. and Bowles, D.K. (2005) PKCdelta mediates testosterone-induced increases in coronary smooth muscle Cav1.2. *J Biol Chem*, **280**, 43024-43029.

Magee, J.A., Abdulkadir, S.A. and Milbrandt, J. (2003) Haploinsufficiency at the Nkx3.1 locus. A paradigm for stochastic, dosage-sensitive gene regulation during tumor initiation. *Cancer Cell*, **3**, 273-283.

Malkowicz, S.B. (2001) The role of diethylstilbestrol in the treatment of prostate cancer. *Urology*, **58(Suppl 2A)**, 108-113.

Mandel, J.L. and Biancalana, V. (2004) Fragile X mental retardation syndrome: from pathogenesis to diagnostic issues. *Growth Horm IGF Res*, **14 Suppl A**, S158-165.

Mangelsdorf, D.J. and Evans, R.M. (1995) The RXR heterodimers and orphan receptors. *Cell*, **83**, 841-850.

Maru, Y., Afar, D.E., Witte, O.N. and Shibuya, M. (1996) The dimerization property of glutathione S-transferase partially reactivates Bcr-Abl lacking the oligomerization domain. *J Biol Chem*, **271**, 15353-15357.

Mateja, A., Cierpicki, T., Paduch, M., Derewenda, Z.S. and Otlewski, J. (2006) The Dimerization Mechanism of LIS1 and its Implication for Proteins Containing the LisH Motif. *J Mol Biol*, **357**, 621-631.

Matsuyama, H., Pan, Y., Yoshihiro, S., Kudren, D., Naito, K., Bergerheim, U.S. and Ekman, P. (2003) Clinical significance of chromosome 8p, 10q, and 16q deletions in prostate cancer. *Prostate*, **54**, 103-111.

McGinnis, W., Levine, M.S., Hafen, E., Kuroiwa, A. and Gehring, W.J. (1984) A conserved DNA sequence in homoeotic genes of the Drosophila Antennapedia and bithorax complexes. *Nature*, **308**, 428-433.

McKenzie, S. and Kyprianou, N. (2006) Apoptosis Evasion: The Role of Survival Pathways in Prostate Cancer Progression and Therapeutic Resistance. *J Cell Biochem*, **97**, 18-32.

McNeal, J.E. (1988) Normal histology of the prostate. *Am J Surg Pathol*, **12**, 619-633.

Mendelsohn, A.R. and Brent, R. (1994) Biotechnology applications of interaction traps/two-hybrid systems. *Curr Opin Biotechnol*, **5**, 482-486.

Mendelsohn, A.R. and Brent, R. (1999) Protein Interaction Methods-Toward an Endgame. *Science*, **284**, 1948-1950.

Mendes-da-Silva, P., Moreira, A., Duro-da-Costa, J., Matias, D. and Monteiro, C. (2000) Frequent loss of heterozygosity on chromosome 5 in non-small cell lung carcinoma. *Mol Pathol*, **53**, 184-187.

Menon, R.P., Gibson, T.J. and Pastore, A. (2004) The C terminus of fragile X mental retardation protein interacts with the multi-domain Ran-binding protein in the microtubule-organising centre. *J Mol Biol*, **343**, 43-53.

Mitelman, F., Johansson, B. and Mertens, F., (Eds). (2005) *Mitelman Database of Chromosome Aberrations in Cancer*. http://cgap.nci.nih.gov/Chromosomes/Mitelman, (Accessed 27.02.06).

Miyamoto, H., Messing, E.M. and Chang, C. (2004) Androgen Deprivation Therapy for Prostate Cancer: Current Status and Future Prospects. *The Prostate*, **61**, 332-353.

Mohanty, N.K., Saxena, S., Singh, U.P., Goyal, N.K. and Arora, R.P. (2005) Lycopene as a chemopreventive agent in the treatment of high-grade prostate intraepithelial neoplasia. *Urol Oncol*, **23**, 383-385.

Monti, M., Orru, S., Pagnozzi, D. and Pucci, P. (2005) Interaction Proteomics. *Biosci Rep*, **25**, 45-56.

Mootha, V.K., Bunkenborg, J., Olsen, J.V., Hjerrid, M., Wisniewski, J.R., Stahl, E., Bolouri, M.S., Ray, H.N., Sihag, S., Kamal, M., Patterson, N., Lander, E.S. and Mann, M. (2003) Integrated Analysis of Protein Composition, Tissue Diversity, and Gene Regulaton in Mouse Mitochondria. *Cell*, **115**, 629-640.

Mosse, Y.P., Greshock, J., Margolin, A., Naylor, T., Cole, K., Khazi, D., Hii, G., Winter, C., Shahzad, S., Asziz, M.U., Biegel, J.A., Weber, B.L. and Maris, J.M. (2005) High-resolution detection and mapping of genomic DNA alterations in neuroblastoma. *Genes Chromosomes Cancer*, **43**, 390-403.

Nakamura, M., Masuda, H., Horii, J., Kuma, K., Yokoyama, N., Ohba, T., Nishitani, H., Miyata, T., Tanaka, M. and Nishimoto, T. (1998) When overexpressed, a novel centrosomal protein, RanBPM, causes ectopic microtubule nucleation similar to gamma-tubulin. *J Cell Biol*, **143**, 1041-1052.

National Cancer Institute (NCI). (2002) *What You Need To Know About™Prostate Cancer*. NIH Publication No. 00-1576.

National Comprehensive Cancer Network (NCCN) and the American Cancer Society (ACS). (2005) Prostate Cancer. *Treatment Guidelines for Patients Version V/September 2005*. American Cancer Society, Inc., Vol. No. 9404.02.

NHMRC (National Health and Medical Research Council). (2006) *Making Decisions about Tests and Treatments: Principles for better communication between healthcare consumers and healthcare professionals*. Commonwealth of Australia, NHMRC, Canberra.

Nishitani, H., Hirose, E., Uchimura, Y., Nakamura, M., Umeda, M., Nishii, K., Mori, N. and Nishimoto, T. (2001) Full-sized RanBPM cDNA encodes a protein possessing a long stretch of proline and glutamine within the N-terminal region, comprising a large protein complex. *Gene*, **272**, 25-33.

Noonan-Wheeler, F.C., Wu, W., Roehl, K.A., Klim, A., Haugen, J., Suarez, B.K. and Kibel, A.S. (2006) Association of hereditary prostate cancer gene polymorphic variants with sporadic aggressive prostate carcinoma. *Prostate*, **66**, 49-56.

Nooren, I.M.A. and Thornton, J.M. (2003) Diversity of protein-protein interactions. *EMBO J*, **22**, 3486-3492.

Oefelein, M.G. (2003) Health related quality of life using serum testosterone as the trigger to re-dose long acting depot luteinizing hormone-releasing hormone agonists in patients with prostate cancer. *J Urol*, **169**, 251-255.

Ornstein, D.K., Cinquanta, M., Weiler, S., Duray, P.H., Emmert-Buck, M.R., Vocke, C.D., Linehan, W.M. and Ferretti, J.A. (2001) Expression studies and mutational analysis of the androgen regulated homeobox gene NKX3.1 in benign and malignant prostate epithelium. *J Urol*, **165**, 1329-1334.

Ouyang, X., DeWeese, T.L., Nelson, W.G. and Abate-Shen, C. (2005) Loss-of-Function of *Nkx3.1* Promotes Increased Oxidative Damage in Prostate Carcinogenesis. *Cancer Res*, **65**, 6773-6779.

Palanimurugan, R., Scheel, H., Hofmann, K. and Dohmen, R.J. (2004) Polyamines regulate their synthesis by inducing expression and blocking degradation of ODC antizyme. *Embo J*, **23**, 4857-4867.

Pathak, R., Bogomolnaya, L.M., Guo, J. and Polymeris, M. (2004) Gid8p (Dcr1p) and Dcr2p Function in a Common Pathway To Promote START Completion in *Saccharomyces cerevisiae*. *Eukaryotic Cell*, **3**, 1627-1638.

Patriotis, C., Russeva, M.G., Lin, J.H., Srinivasula, S.M., Markova, D.Z., Tsatsanis, C., Makris, A., Alnemri, E.S. and Tsichlis, P.N. (2001) Tpl-2 induces apoptosis by promoting the assembly of protein complexes that contain caspase-9, the adaptor protein Tvl-1, and procaspase-3. *J Cell Physiol*, **187**, 176-187.

Peeper, D.S., Shvarts, A., Brummelkamp, T., Douma, S., Koh, E.Y., Daley, G.O. and Bernards, R. (2002) A functional screen identifies hDRIL1 as an oncogene that rescues RAS-induced senescence. *Nat Cell Biol*, **4**, 148-153.

Pellegrinni, G., Dellambra, E., Golisano, O., Martinelle, E., Fantozzi, I., Bondanza, S., Ponzin, D., McKeon, F. and De Luca, M. (2001) p63 identifies keratinocyte stem cells. *Proc Natl Acad Sci U S A*, **98**, 3156-3161.

Pemberton, L.F. and Paschal, B.M. (2005) Mechanisms of receptor-mediated nuclear import and nuclear export. *Traffic*, **6**, 187-198.

Perissi, V., Aggarwal, A., Glass, C.K., Rose, D.W. and Rosenfeld, M.G. (2004) A corepressor/coactivator exchange complex required for transcriptional activation by nuclear receptors and other regulated transcription factors. *Cell*, **116**, 511-526.

Peters, G.A., Hartmann, R., Qin, J. and Sen, G.C. (2001) Modular structure of PACT: distinct domains for binding and activating PKR. *Mol Cell Biol*, **21**, 1908-1920.

Peters, G.A., Li, S. and Sen, G.C. (2006) Phosphorylation of specific serine residues in the PKR-activation domain of PACT is essential for its ability to mediate apoptosis. *J Biol Chem*, **281,** 35129-35136.

Peterziel, H., Mink, S., Schonert, A., Becker, M., Klocker, H. and Cato, A.C.B. (1999) Rapid signalling by androgen receptor in prostate cancer cells. *Oncogene*, **18**, 6322-6329.

Phizicky, E.M. and Fields, S. (1995) Protein-Protein Interactions: Methods for Detection and Analysis. *Microbiol Rev*, **59**, 94-123.

Poirier, M.B., Laflamme, L. and Langlois, M.F. (2006) Identification and characterization of RanBPM, a novel coactivator of thyroid hormone receptors. *J Mol Endocrinol*, **36**, 313-325.

Polek, T.C. and Weigel, N.L. (2002) Vitamin D and prostate cancer. *J Androl*, **23**, 9-17.

Pollard, S. and Holland, P.W.H. (2000) Evidence for 14 homeobox gene clusters in human genome ancestry. *Curr Biol*, **10**, 1059-1062.

Ponting, C., Schultz, J. and Bork, P. (1997) SPRY domains in ryanodine receptors (Ca(2+)-release channels). *Trends Biochem Sci*, **22**, 193-194.

Prescott, J.L., Blok, L. and Tindall, D.J. (1998) Isolation and androgen regulation of the human homeobox cDNA, NKX3.1. *Prostate*, **35**, 71-80.

Public Health Agency of Canada (PHAC). (2004) *Progress Report on Cancer Control in Canada*. Cat. No. H39-4/50-2004E-PDF.

Rao, M.A., Cheng, H., Quayle, A.N., Nishitani, H., Nelson, C.C. and Rennie, P.S. (2002) RanBPM, a nuclear protein that interacts with and regulates transcriptional activity of androgen receptor and glucocorticoid receptor. *J Biol Chem*, **277**, 48020-48027.

Regelmann, J., Schule, T., Josupeit, F.S., Horak, J., Rose, M., Entian, K.-D., Thumm, M. and Wolf, D.H. (2003) Catabolite Degradation of Fructose-1,6-bisphosphatase in the Yeast *Saccharomyces cerevisiae*: A Genome-wide Screen Identifies Eight Novel *GID* Genes and Indicates the Excistence of Two Degradation Pathways. *Mol Biol Cell*, **14**, 1652-1663.

Reiner, O., Carrozzo, R., Shen, Y., Wehnert, M., Faustinella, F., Dobyns, W.B., Caskey, C.T. and Ledbetter, D.H. (1993) Isolation of a Miller-Dieker lissencephaly gene containing G protein beta-subunit-like repeats. *Nature*, **364**, 717-721.

Richardson, K.S. and Zundel, W. (2005) The Emerging Role of the COP9 Signalosome in Cancer. *Mol Cancer Res*, **3**, 645-653.

Rihs, H.P., Jans, D.A., Fan, H. and Peters, R. (1991) The rate of nuclear cytoplasmic protein transport is determined by the casein kinase II site flanking the nuclear localization sequence of the SV40 T-antigen. *Embo J*, **10**, 633-639.

Robinson, P.N., Bohme, U., Lopez, R., Mundlos, S. and Nurnberg, P. (2004) Gene-Ontology analysis reveals association of tissue-specific 5` CpG-island genes with development and embryogenesis. *Hum Mol Genet*, **13**, 1969-1978.

Romio, L., Fry, A.M., Winyard, P.J., Malcolm, S., Woolf, A.S. and Feather, S.A. (2004) OFD1 is a centrosomal/basal body protein expressed during mesenchymal-epithelial transition in human nephrogenesis. *J Am Soc Nephrol*, **15**, 2556-2568.

Romio, L., Wright, V., Price, K., Winyard, P.J., Donnai, D., Porteous, M.E., Franco, B., Giorgio, G., Malcolm, S., Woolf, A.S. and Feather, S.A. (2003) OFD1, the gene mutated in oral-facial-digital syndrome type 1, is expressed in the metanephros and in human embryonic renal mesenchymal cells. *J Am Soc Nephrol*, **14**, 680-689.

Ruvolo, P.P., Gao, F., Blalock, W.L., Deng, X. and May, W.S. (2001) Ceramide regulates protein synthesis by a novel mechanism involving the cellular PKR activator RAX. *J Biol Chem*, **276**, 11754-11758.

Sakr, W.A., Haas, G.P., Cassin, B.F., Pontes, J.E. and Crissman, J.D. (1993) The frequency of carcinoma and intraepithelial neoplasia of the prostate in young male patients. *J Urol*, **150**, 379-385.

Sambrook, J. and Russell, D.W. (2001) *Molecular Cloning A Laboratory Manual*. Cold Spring Harbor Laboratory Press, New York.

Scher, H.I. and Sawyers, C.L. (2005) Biology of Progressive, Castration-Resistant Prostate Cancer: Directed Therapies Targeting the Androgen-Receptor Signaling Axis. *J Clin Oncol*, **23**, 8253-8261.

Schmitt, B., Wilt, T.J., Schellhammer, P.F., De Masi, V., Satror, O., Crawford, E.D. and Bennett, C.L. (2001) Combines androgen blockade with nonsteroidal antiandrogens for advanced prostate cancer: A systemic review. *Urology*, **57**, 727-732.

Schultz, J., Milpetz, F., Bork, P. and Ponting, C.P. (1998) SMART, a simple modular architecture research tool: identification of signaling domains. *Proc Natl Acad Sci U S A*, **95**, 5857-5864.

Schwartz, R.J. and Olsen, E.N. (1999) Building the heart piece by piece: modularity of cis-elements regulating Nkx2-5 transcription. *Development*, **126**, 4187-4192.

Schwechheimer, C. (2004) The COP9 signalosome (CSN): an evolutionary conserved proteolysis regulator in eukaryotic development. *Biochim Biophys Acta*, **1695**, 45-54.

Sciavolino, P.J., Abrams, E.W., Yang, L., Austenberg, L.P., Shen, M.M. and Abate-Shen, C. (1997) Tissue-specific expression of murine Nkx3.1 in the male urogenital system. *Dev Dyn*, **209**, 127-138.

Sèmon, M. and Duret, L. (2006) Evolutionary origin and maintenance of coexpressed gene clusters in mammals. *Mol Biol Evo*, **23**, 1715-1723.

Serebriiskii, I.G. and Golemis, E.A. (2001) Two-hybrid system and false positives. Approaches to detection and elimination. *Methods Mol Biol*, **177**, 123-134.

Serth, J., Panitz, F., Paeslack, U., Kuczyk, M.A. and Jonas, U. (1999) Increased Levels of Human Papillomavirus Type 16 DNA in a Subset of Prostate Cancers. *Cancer Res*, **59**, 823-825.

Sharifi, N., Gulley, J.L. and Dahut, W.L. (2005) Androgen deprivation therapy for prostate cancer. *Jama*, **294**, 238-244.

Shu, T., Ayala, R., Nguyen, M.D., Xie, Z., Gleeson, J.G. and Tsai, L.H. (2004) Ndel1 operates in a common pathway with LIS1 and cytoplasmic dynein to regulate cortical neuronal positioning. *Neuron*, **44**, 263-277.

Siepel, A., Bejerano, G., Pedersen, J.S., Hinrichs, A.S., Hou, M., Rosenbloom, K., Clawson, H., Spieth, J., Hillier, L.W., Richards, S., Weinstock, G.M., Wilson, R.K., Gibbs, R.A., Kent, W.J., Miller, W. and Haussler, D. (2005) Evolutionarily conserved elements in vertebrate, insect, worm, and yeast genomes. *Genome Res*, **15**, 1034-1050.

Silver, P.A., Brent, R. and Ptashne, M. (1986) DNA binding is not sufficient for nuclear localization of regulatory proteins in *Saccharomyces cerevisiae. Mol Biol Cell*, **12**, 4763-4766.

Silvestris, N., Leone, B., Numico, G., Vito, L. and De Lena, M. (2005) Present Status and Perspectives in the Treatment of Hormone-Refractory Prostate Cancer. *Oncology*, **69**, 273-282.

Simmons, S.O. and Horowitz, J.M. (2006) Nkx3.1 binds and negatively regulates the transcriptional activity of Sp-family members in prostate-derived cells. *Biochem J*, **393**, 397-409.

Skotheim, R.I., Abeler, V.M., Nesland, J.M., Fossa, S.D., Holm, R., Wagner, U., Florenes, V.A., Aass, N., Kallioniemi, O.P. and Lothe, R.A. (2003a) Candidate genes for testicular cancer evaluated by in situ protein expression analyses on tissue microarrays. *Neoplasia*, **5**, 397-404.

Skotheim, R.I., Korkmaz, K.S., Klokk, T.I., Abeler, V.M., Korkmaz, C.G., Nesland, J.M., Fossa, S.D., Lothe, R.A. and Saatcioglu, F. (2003b) NKX3.1 expression is lost in testicular germ cell tumors. *Am J Pathol*, **163**, 2149-2154.

Smith, D.B. and Johnson, K.S. (1988) Single-step purification of polypeptides expressed in *Escherichia coli* as fusions with glutathione S-transferase. *Gene*, **67**, 31-40.

Smith, D.S., Niethammer, M., Ayala, R., Zhou, Y., Gambello, M.J., Wynshaw-Boris, A. and Tsai, L.H. (2000) Regulation of cytoplasmic dynein behaviour and microtubule organization by mammalian Lis1. *Nat Cell Biol*, **2**, 767-775.

Soni, S., Bala, S., Gwynn, B., Sahr, K.E., Peters, L.L. and Hanspal, M. (2006) Absence of Erythroblast Macrophage Protein (Emp) Leads to Failure of Erythroblast Nuclear Extrusion. *J Biol Chem*, **281**, 20181-20189.

Sonpavde, G., Hutson, T.E. and Berry, W.R. (2006) Hormone refractory prostate cancer: Management and advances. *Cancer Treat Rev*, **32**, 90-100.

Steadman, D.J., Giuffrida, D. and Gelmann, E.P. (2000) DNA-binding sequence of the human prostate-specific homeodomain protein NKX3.1. *Nucleic Acids Res*, **28**, 2389-2395.

Strausberg, R.L., Feingold, E.A., Grouse, L.H., Derge, J.G., Klausner, R.D., Collins, F.S., Wagner, L., Shenmen, C.M., Schuler, G.D., Altschul, S.F., Zeeberg, B., Buetow, K.H., Schaefer, C.F., Bhat, N.K., Hopkins, R.F., Jordan, H., Moore, T., Max, S.I., Wang, J., Hsieh, F., Diatchenko, L., Marusina, K., Farmer, A.A., Rubin, G.M., Hong, L., Stapleton, M., Soares, M.B., Bonaldo, M.F., Casavant, T.L., Scheetz, T.E., Brownstein, M.J., Usdin, T.B., Toshiyuki, S., Carninci, P., Prange, C., Raha, S.S., Loquellano, N.A., Peters, G.J., Abramson, R.D., Mullahy, S.J., Bosak, S.A., McEwan, P.J., McKernan, K.J., Malek, J.A., Gunaratne, P.H., Richards, S., Worley, K.C., Hale, S., Garcia, A.M., Gay, L.J., Hulyk, S.W., Villalon, D.K., Muzny, D.M., Sodergren, E.J., Lu, X., Gibbs, R.A., Fahey, J., Helton, E., Ketteman, M., Madan, A., Rodrigues, S., Sanchez, A., Whiting, M., Young, A.C., Shevchenko, Y., Bouffard, G.G., Blakesley, R.W., Touchman, J.W., Green, E.D., Dickson, M.C., Rodriguez, A.C., Grimwood, J., Schmutz, J., Myers, R.M., Butterfield, Y.S., Krzywinski, M.I., Skalska, U., Smailus, D.E., Schnerch, A., Schein, J.E., Jones, S.J. and Marra, M.A. (2002) Generation and initial analysis of more than 15,000 full-length human and mouse cDNA sequences. *Proc Natl Acad Sci U S A*, **99**, 16899-16903.

Stricker, H.J. (2001) Luteinizing hormone-releasing hormone antagonists in prostate cancer. *Urology*, **58(Suppl 2A)**, 24-27.

Takacs, C.M., Amore, G., Oliveri, P., Poustka, A.J., Wang, D., Burke, R.D. and Peterson, K.J. (2004) Expression of an NK2 homeodomain gene in the apical ectoderm defines a new territory in the early sea urchin embryo. *Dev Biol*, **269**, 152-164.

Tamanini, F., Bontekoe, C., Bakker, C.E., van Unen, L., Anar, B., Willemsen, R., Yoshida, M., Galjaard, H., Oostra, B.A. and Hoogeveen, A.T. (1999) Different targets for the fragile X-related proteins revealed by their distinct nuclear localizations. *Hum Mol Genet*, **8**, 863-869.

Tanaka, M., Komuro, I., Inagaki, H., Jenkins, N.A., Copeland, N.G. and Izumo, S. (2000) Nkx3.1, a murine homolog of Ddrosophila bagpipe, regulates epithelial ductal branching and proliferation of the prostate and palatine glands. *Dev Dyn*, **219**, 248-260.

Tanaka, M., Lyons, G.E. and Izumo, S. (1999) Expression of the Nkx3.1 homobox gene during pre and postnatal development. *Mech Dev*, **85**, 179-182.

Tannock, I.F., de Wit, R., Berry, W.R., Horti, J., Pluzanska, A., Chi, K.N., Oudard, S., Theodore, C., James, N.D., Turesson, I., Rosenthal, M.A. and Eisenberger, M.A. (2004) Docetaxel plus prednisone or mitoxantrone plus prednisone for advanced prostate cancer. *N Engl J Med*, **351**, 1502-1512.

Tarricone, C., Perrina, F., Monzani, S., Massimiliano, L., Kim, M.H., Derewenda, Z.S., Knapp, S., Tsai, L.H. and Musacchio, A. (2004) Coupling PAF signaling to dynein regulation: structure of LIS1 in complex with PAF-acetylhydrolase. *Neuron*, **44**, 809-821.

Tassone, F. and Hagerman, P.J. (2003) Expression of the FMR1 gene. *Cytogenet Genome Res*, **100**, 124-128.

Tawfic, S. and Ahmed, K. (1994) Growth stimulus-mediated differential translocation of casein kinase 2 to the nuclear matrix. Evidence based on androgen action in the prostate. *J Biol Chem*, **269**, 24615-24620.

Taylor, S.W., Fahy, E., Zhang, B., Glenn, G.M., Warnock, D.E., Wiley, S., Murphy, A.N., Gaucher, S.P., Capaldi, R.A., Gibson, B.W. and Ghosh, S.S. (2003) Characterization of the human heart mitochondrial proteome. *Nat Biotech*, **21**, 281-286.

Thierry-Mieg, D., Thierry-Mieg, J., Potdevin, M. and Sienkiewicz, M. (2005) *AceView: Identification and functional annotation of cDNA-supported genes in higher organisms*. http://www.ncbi.nlm.nih.gov/IEB/Research/Acembly:, (Accessed 23.02.06).

Thomas, M.A., Hodgson, M.C., Loermans, S.D., Hooper, J., Endersby, R. and Bentel, J.M. (2006) Transcriptional regulation of the homeobox gene NKX3.1 by all-trans retinoic acid in prostate cancer cells. *J Cell Biochem*, **99,** 1409-1419.

Thompson, J.D., Higgins, D.G. and Gibson, T.J. (1994) CLUSTAL W: improving the sensitivity of progressive multiple sequence alignment through sequence weighting, position-specific gap penalties and weight matrix choice. *Nucleic Acids Res*, **22**, 4673-4680.

Tilley, W.D., Buchanan, G., Hickey, T.E. and Bentel, J.M. (1996) Mutations in the androgen receptor gene are associated with progression of human prostate cancer to androgen independence. *Clin Cancer Res*, **2**, 277-285.

Timms, B.G., Mohs, T.J. and Didio, L.J. (1994) Ductal budding and branching patterns in the developing prostate. *J Urol*, **151**, 1427-1432.

Tokar, E.J., Ancrile, B.B., Cunha, G.R. and Webber, M.M. (2005) Stem/progenitor and intermediate cell types and the origin of human prostate cancer. *Differentiation*, **73**, 463-473.

Tribioli, C., Frasch, M. and Lufkin, T. (1997) Bapx1: an evolutionary conserved homologue of the Drosophila bagpipe homeobox gene is expressed in splanchnic mesoderm and the embryonic skeleton. *Mech Dev*, **65**, 145-162.

Tsuchiya, N., Slezak, J., Lieber, M., Bergstralh, E. and Jenkins, R. (2002) Clinical Significance of Alterations of Chromosome 8 Detected by Fluorescence In Situ Hybridization Analysis in Pathologic Organ-Confined Prostate Cancer. *Genes, Chromosomes & Cancer*, **34**, 363-371.

Tsukada, S., Tanaka, Y., Maegawa, H., Kashiwagi, A., Kawamori, R. and Maeda, S. (2006) Intronic polymorphisms within TFAP2B regulate transcriptional activity and affect adipocytokine gene expression in differentiated adipocytes. *Mol Endocrinol*, **20**, 1104-1111.

Uetz, P. (2002) Two-hybrid arrays. *Curr Opin Chem Biol*, **6**, 57-62.

van Aelst, L., Barr, M., Marcus, S., Polverino, A. and Wigler, M. (1993) Complex formation between RAS and RAF and other protein kinases. *Proc Natl Acad Sci U S A*, **90**, 6213-6217.

van Leenders, G., Dijkman, H., Hulsbergen-van de Kaa, C., Ruiter, D. and Schalken, J. (2000) Demonstration of intermediate cells during human prostate epithelial differentiation *in situ* and *in vitro* using triple-staining confocal scanning microscopy. *Lab Invest*, **80**, 1251-1258.

Versteeg, R., van Schaik, B.D., van Batenburg, M.F., Roos, M., Monajemi, R., Caron, H., Bussemaker, H.J. and van Kampen, A.H. (2003) The human transcriptome map reveals extremes in gene density, intron length, GC content, and repeat pattern for domains of highly and weakly expressed genes. *Genome Res*, **13**, 1998-2004.

Vidalain, P.O., Boxem, M., Ge, H., Li, S. and Vidal, M. (2004) Increasing specificity in high-throughput yeast two-hybrid experiments. *Methods*, **32**, 363-370.

Vocke, C.D., Pozzatti, R.O., Bostwick, D.G., Florence, C.D., Jennings, S.B., Strup, S.E., Duray, P.H., Liotta, L.A., Emmert-Buck, M.R. and Lineham, W.M. (1996) Analysis of 99 microdissected prostate carcinomas reveals a high frequency of allelic loss on chromosome 8p12-21. *Cancer Res*, **56**, 2411-2416.

von Knobloch, R., Konrad, L., Barth, P.J., Brandt, H., Wille, S., Heidenreich, A., Moll, R. and Hofmann, R. (2004) Genetic Pathways and New Progression Markers for Prostate Cancer Suggested by Microsatellite Allelotyping. *Clin Can Res*, **10**, 1064-1073.

Waalkes, M.P. and Rehm, S. (1994) Cadmium and prostate cancer. *J Toxicol Environ Health*, **43**, 251-269.

Walhout, A.J. and Vidal, M. (1999) A genetic strategy to eliminate self-activator baits prior to high-throughput yeast two-hybrid screens. *Genome Res*, **9**, 1128-1134.

Wang, D., Li, Z., Messing, E.M. and Wu, G. (2002) Activation of Ras/Erk pathway by a novel MET-interacting protein RanBPM. *J Biol Chem*, **277**, 36216-36222.

Wang, S.-C. and Hung, M.-C. (2005) Cytoplasmic/Nuclear Shuttling and Tumor Progression. *Ann N Y Acad Sci*, **1059**, 11-15.

Watada, H., Mirmira, R.G., Kalamaras, J. and German, M.S. (2000) Intramolecular control of transcriptional activity by the NK2-specific domain in NK-2 homeodomain proteins. *Proc Natl Acad Sci U S A*, **97**, 9443-9448.

Watson, E., Jenkins, L., Bukach, C. and Austoker, J. (2002) *The PSA test and prostate cancer: information for primary care.* NHS Cancer Screening Programmes, Sheffield.

Wei, Y., Jin, J. and Harper, J.W. (2003) The cyclin E/Cdk2 substrate and Cajal body component p220(NPAT) activates histone transcription through a novel LisH-like domain. *Mol Cell Biol*, **23**, 3669-3680.

Wiklund, F., Jonsson, B.-A., Goransson, I., Bergh, A. and Gronberg, H. (2003) Linkage analysis of prostate cancer susceptibibty: confirmation of linkage at 8p22-23. *Hum Genet*, **112**, 414-418.

Willems, A.R., Schwab, M. and Tyers, M. (2004) A hitchhiker's guide to the cullin ubiquitin ligases: SCF and its kin. *Biochim Biophys Acta*, **1695**, 133-170.

Wilsker, D., Patsialou, A., Dallas, P.B. and Moran, E. (2002) ARID proteins: a diverse family of DNA binding proteins implicated in the control of cell growth, differentiation, and development. *Cell Growth Differ*, **13**, 95-106.

Xu, J., Dimitrov, L., Chang, B.-L., Adams, T.S., Turner, A.R., Meyers, D.A., Eeles, R.A., Easton, D.F., Foulkes, W.D., Simrad, J., Giles, G.C., Hopper, J.L., Mahle, L., Moller, P., Bishop, T., Evans, C., Edwards, S., Meitz, J., Bullock, S., Hope, Q., The ACTANE Consortium, Hsieh, C.-l., Halpern, J., Balise, R.N., Oakley-Girvan, O., Whittemore, A.S., Ewing, C.M., Gielzak, M., Isaacs, S.D., Walsh, P.C., Wiley, K.E., Isaacs, W.B., Thibodeau, S.N., McDonnell, S.K., Cunningham, J.M., Zarfas, K.E., Hebbring, S., Schaid, D.J., Friedrichsen, D.M., Deutsch, K., Kolb, S., Badzioch, M., Jarvik, G.P., Janer, M., Hood, L., Ostrander, E.A., Stanford, J.L., Lange, E.M., Beebe-Dimmer, J.L., Mohai, C.E., Cooney, K.A., Ikonen, T., Baffoe-Bonnie, A., Fredriksson, H., Matikainen, M.P., Tammela, T.L., Bailey-Wilson, J., Schleutker, J., Maier, C., Herkommer, K., Hoegel, J.J., Vogel, W., Paiss, T., Wiklund, F., Emanuelsson, M., Stenman, E., Jonsson, B.-A., Gronberg, H., Camp, N.J., Farnham, J., Cannon-Albright, L.A. and Seminara, D. (2005) A Combined Genomewide Linkage Scan of 1,233 Families for Prostate Cancer-Susceptibility Genes Conducted by the International Consortium for Prostate Cancer Genetics. *Am J Hum Genet*, **77**, 219-229.

Xu, L. and Massague, J. (2004) Nucleocytoplasmic shuttling of signal transducers. *Nat Rev Mol Cell Biol*, **5**, 209-219.

Xu, L.L., Srikantan, V., Sesterhenn, I.A., Augustus, M., Dean, R., Moul, J.W., Carter, K.C. and Srivastava, S. (2000) Expression profile of an androgen regulated prostate specific homeobox gene NKX3.1 in primary prostate cancer. *J Urol*, **163**, 972-979.

Yang, M., Ito, T. and May, W.S. (2003) A novel role for RAX, the cellular activator of PKR, in synergistically stimulating SV40 large T antigen-dependent gene expression. *J Biol Chem*, **278**, 38325-38332.

Yang, Y. and Yu, X. (2003) Regulation of apoptosis: the ubiquitous way. *Faseb J*, **17**, 790-799.

Ye, X., Wei, Y., Nalepa, G. and Harper, J.W. (2003) The cyclin E/Cdk2 substrate p220(NPAT) is required for S-phase entry, histone gene expression, and Cajal body maintenance in human somatic cells. *Mol Cell Biol*, **23**, 8586-8600.

Yip, I., Heber, D. and Aronson, W. (1999) Nutrition and prostate cancer. *Urol Clin North Am*, **26**, 403-411.

Yocum, R.R., Hanley, S., West, R.J. and Ptashne, M. (1984) Use of lacZ fusions to delimit regulatory elements of the inducible divergent GAL1-GAL10 promoter in *Saccharomyces cerevisiae. Mol Biol Cell*, **4**, 1985-1988.

Yoon, H.G., Chan, D.W., Huang, Z.Q., Li, J., Fondell, J.D., Qin, J. and Wong, J. (2003) Purification and functional characterization of the human N-CoR complex: the roles of HDAC3, TBL1 and TBLR1. *Embo J*, **22**, 1336-1346.

Yoon, H.-G. and Wong, J. (2005) The Corepressors Silencing Mediator of Retinoid and Thyroid Hormone Receptor and Nuclear Receptor Corepressor Are Involved in Agonist- and Antagonist-Regulated Transcription by Androgen Receptor. *Mol Endocrinol*, **20**, 1048-1060.

Yoon, K., Jang, H.D. and Lee, S.Y. (2004) Direct interaction of Smac with NADE promotes TRAIL-induced apoptosis. *Biochem Biophys Res Commun*, **319**, 649-654.

Zannini, M., Acebron, A., DeFelice, M., Arnone, M.I., Martin-Perez, J., Santisteban, P. and Di Lauro, R. (1996) Mapping and functional role of phosphorylation sites in the thyroid transcription factor-1 (TTF-1). *J Biol Chem*, **271**, 2249-2254.

Zhang, H.-G., Wang, J., Yang, X., Hsu, H.-C. and Mountz, J.D. (2004) Regulation of apoptosis proteins in cancer cells by ubiquitin. *Oncogene*, 2009-2015.

Zhang, J., Kalkum, M., Chait, B.T. and Roeder, R.G. (2002) The N-CoR-HDAC3 nuclear receptor corepressor complex inhibits the JNK pathway through the integral subunit GPS2. *Mol Cell*, **9**, 611-623.

Zhang, X., Li, L., Fourie, J., Davie, J.R., Guarcello, V. and Diasio, R.B. (2006) The role of Sp1 and Sp3 in the constitutive DPYD gene expression. *Biochim Biophys Acta*, **1759**, 247-256.

Zhao, X., Gan, L., Pan, H., Kan, D., Majeski, M., Adam, S.A. and Unterman, T.G. (2004) Multiple elements regulate nuclear/cytoplasmic shuttling of FOXO1: characterization of phosphorylation- and 14-3-3-dependent and -independent mechanisms. *Biochem J*, **378**, 839-849.

Zheng, L., Roeder, R.G. and Luo, Y. (2003) S phase activation of the histone H2B promoter by OCA-S, a coactivator complex that contains GAPDH as a key component. *Cell*, **114**, 255-266.

Zheng, S.L., Ju, J.-h., Chang, B.-l., Ortner, E., Sun, J., Isaacs, S.D., Sun, J., Wiley, K.E., Liu, W., Zemedkun, M., Walsh, P.C., Ferretti, J., Gruschus, J., Isaacs, W.B., Gelmann, E.P. and Xu, J. (2006) Germ-Line Mutation of *NKX3.1* Cosegregates with Hereditary Prostate Cancer and Alters the Homeodomain Structure and Function. *Cancer Res*, **66**, 69-77.

Zhu, Y.Y., Machleder, E.M., Chenchik, A., Li, R. and Siebert, P.D. (2001) Reverse transcriptase template switching: a SMART approach for full-length cDNA library construction. *Biotechniques*, **30**, 892-897.

Zou, Y., Lim, S., Lee, K., Deng, X. and Friedman, E. (2003) Serine/threonine kinase Mirk/Dyrk1B is an inhibitor of epithelial cell migration and is negatively regulated by the Met adaptor Ran-binding protein M. *J Biol Chem*, **278**, 49573-49581.

Appendices

Appendix 1 – Buffers and Solutions

1. 30% Acrylamide

58g Acrylamide
2g N,N'-Methylene-Bis-Acrylamide
Reagents were dissolved in 200mL ddH_2O and stored at 4°C.

2. 1/2% Agarose/TAE Gels

1-2g Agarose
100mL 1X TAE[134]
5µL Ethidium Bromide[39]
Agarose was dissolved in 1X TAE by heating in a microwave and ethidium bromide was added to give a final concentration of 0.5µg/mL.

3. 0.2% Adenine

200mg Adenine
100mL ddH_2O
Reagents were combined, autoclaved and stored at 4°C.

4. 100mM Adenosine 5' Triphosphate

1g ATP
18mL ddH_2O
Reagents were combined and stored in 1mL aliquots at -20°C.

5. 5M Ammonium Acetate

Supplied with the Poly (A) Pure™ mRNA Purification Kit.

6. 10% Ammonium Persulphate

100mg Ammonium Persulphate
1mL ddH_2O
Ammonium persulphate was dissolved in ddH_2O and stored at 4°C. Solution was made fresh for each polyacrylamide gel.

7. 100mg/mL Ampicillin

100mg Ampicillin Powder
1mL ddH_2O
Ampicillin powder was dissolved in ddH_2O and stored at -20°C.

8. Binding Buffer

Supplied with the Poly (A) Pure™ mRNA Purification Kit

9. 1% BSA/PBS

10mg BSA fraction V
1mL PBS[72]
Reagents were combined on day of use and stored at 4°C.

10. 1M Calcium Chloride

27g Calcium Chloride
100mL ddH_2O
Reagents were combined and the solution sterilised by passing through a 0.2µm filter then stored at -20°C in 5mL aliquots.

11. 100mM Co-Enzyme A

100mg Co-Enzyme A Lithium salt
1.3mL ddH_2O
Reagents were combined and the solution stored in 25µL aliquots at -20°C shielded from light.

12. Confocal Blocking Buffer

5mL Horse serum
500mg BSA fraction V
10mg Sodium Azide
45mL PBS[72]
Reagents were combined and the solution stored at 4°C shielded from light.

13. Coomassie Blue Staining Solution

1g Coomassie Brilliant Blue
450mL Methanol
450mL ddH_2O
100mL Glacial Acetic Acid
Coomassie brilliant blue was dissolved in methanol and the ddH_2O added. The glacial acetic acid was then added in a fume hood and the solution stored at room temperature.

14. Coomassie De-Stain Solution

450mL ddH_2O
450mL Methanol
100mL Glacial Acetic Acid
Methanol was combined with the ddH_2O and the glacial acetic acid was added in a fume hood. The solution was stored at room temperature.

15. DAB Staining Reagent

DAB staining reagent was prepared by adding 20µL of DAB reagent (DAKO) to 1mL of solvent immediately prior to use.

16. DEPC-Treated H_2O

1L ddH_2O
1mL Diethylpyrocarbonate (DEPC)
DEPC was added to ddH_2O in a fume hood, mixed and left at room temperature overnight to dissolve. Solution was then autoclaved and stored at room temperature.

17. 10^{-2}M DHT

2.904mg DHT
1mL Absolute Ethanol
Reagents were combined and the solution was stored at -20°C shielded from light.

18. 10^{-4}M DHT

10µL 10^{-2}M DHT[17]
990µL Absolute Ethanol
Reagents were combined and the solution was stored at -20°C shielded from light.

19. 10^{-6}M DHT

10µL 10^{-4}M DHT[18]
990µL Absolute Ethanol
Reagents were combined and the solution was stored at -20°C shielded from light.

20. Dilution Buffer

Supplied with the Poly (A) Pure™ mRNA Purification Kit (10mM Tris pH 7.5, 1mM EDTA).

21. 100mM D-Luciferin

25mg D-Luciferin Potassium Salt
785µL ddH_2O
Reagents were combined and the solution stored in 50µL aliquots at -20°C shielded from light.

22. 6X DNA Loading Dye

10mg Xylene Cyanol
10mg Bromophenol Blue
7g Sucrose
2mL 0.5M EDTA[34]
8mL ddH_2O
Reagents were combined and stored at room temperature.

23. 25mM dNTP (PCR)

25µL 100mM dATP
25µL 100mM dCTP
25µL 100mM dGTP
25µL 100mM dTTP
dNTPs were combined and stored at -20°C.

24. dNTP (Random Priming)

1µL 1.5mM dATP
1µL 1.5mM dGTP
1µL 1.5mM dTTP
dNTPs were combined immediately before use and stored on ice.

25. 1M DTT

5.0g Dithiothreitol
32mL ddH_2O
DTT powder was dissolved in ddH_2O, filter sterilised by passing through a 0.2µm filter and stored in 1mL aliquots at -20°C.

26. E1 Cell Suspension Buffer

Supplied with the Concert™ High Purity Plasmid Maxiprep Purification System (50mM Tris-HCl pH8.0, 10mM EDTA). RNaseA (also supplied with Concert™ High Purity Plasmid Purification System) was added according to the manufacturer's specifications prior to use and the solution was stored at 4°C.

27. E2 Cell Lysis Solution

Supplied with the Concert™ High Purity Plasmid Maxiprep Purification System (200mM NaOH, 1% SDS v/v)

28. E3 Neutralisation Buffer

Supplied with the Concert™ High Purity Plasmid Maxiprep Purification System (3.1M potassium acetate pH4.5)

29. E4 Equilibration Buffer

Supplied with the Concert™ High Purity Plasmid Maxiprep Purification System (600mM NaCl, 100mM sodium acetate pH 5.5, 0.15% Triton®X-100 v/v).

30. E5 Wash Buffer

Supplied with the Concert™ High Purity Plasmid Maxiprep Purification System (800mM NaCl, 100mM sodium acetate pH5.5).

31. E6 Elution Buffer

Supplied with the Concert™ High Purity Plasmid Maxiprep Purification System (1.25mM NaCl, 100mM Tris-HCl pH8.5).

32. ECL Detection Reagent

Supplied with ECL Western Blotting Detection Reagents (Amersham Pharmacia Biotech, Australia). ECL detection reagent was prepared by adding equal volumes of Solution 1 and Solution 2 immediately prior to use.

33. ECL Plus Detection Reagent

Supplied with ECL Western Blotting Detection Reagents (Amersham Pharmacia Biotech, Australia). ECL Plus detection reagent was prepared by adding Solutions A and B in a ratio of 40:1 immediately prior to use.

34. 0.5M EDTA pH 8.0

186.12g EDTA
20g Sodium Hydroxide Pellets
EDTA was dissolved in 500mL ddH_2O, pH adjusted to 8.0 with sodium hydroxide pellets, the volume adjusted to 1L with ddH_2O and the solution autoclaved and stored at room temperature.

35. 0.5M EDTA pH 8.0 (DEPC)

186.12g EDTA
20g Sodium Hydroxide Pellets
EDTA was dissolved in 500mL ddH_2O, pH adjusted to 8.0 with sodium hydroxide pellets, the volume adjusted to 1L with ddH_2O and 1mL of DEPC was added in a fume hood. The solution was mixed and left overnight, then autoclaved and stored at room temperature.

36. Elution Buffer

Supplied with the Poly (A) Pure™ mRNA Purification Kit (10mM Tris pH 7.5, 1mM EDTA).

37. 70% (v/v) Ethanol

70mL Ethanol (absolute)
30mL ddH_2O
Reagents were combined and stored at room temperature.

38. 95% (v/v) Ethanol

95mL Ethanol (absolute)
5mL ddH_2O
Reagents were combined and stored at room temperature.

39. 10mg/mL Ethidium Bromide

10mg Ethidium Bromide
1mL ddH_2O
Ethidium bromide was dissolved in 1mL of ddH_2O and stored in the dark at room temperature.

40. 4% Formaldehyde

200µL Formaldehyde
1800µL PBS[72]
Reagents were combined in a fume-hood on day of use and stored at room temperature shielded from light.

41. 40% Glucose

40g Glucose
100mL ddH_2O
Glucose was dissolved in ddH_2O and the solution filter sterilised and stored at 4°C.

42. 50% Glutathione Sepharose 4B

133µL 75% Sepharose/10mL Sonicate
Sepharose slurry was settled by centrifugation at 500 x g for 5 minutes, the supernatant was removed, the sepharose washed 3X using 1mL cold (4°C) PBS with centrifugation at 500 x g for 5 minutes, and the supernatant removed. Sepharose was resuspended in 100µL of cold (4°C) PBS to yield a 50% slurry. Glutathione Sepharose was prepared fresh immediately prior to use.

43. 50% Glycerol

5mL Glycerol
5mL ddH_2O
ddH_2O was added to glycerol and the reagents were thoroughly mixed.

44. 80% Glycerol

8mL Glycerol
2mL ddH_2O
ddH_2O was added to glycerol and the reagents were thoroughly mixed.

45. Glycerol Buffer

6mL 1M Calcium Chloride[10]
1mL 1M PIPES[78] pH 7.0
15mL Glycerol
100mL ddH_2O
Reagents were combined and the solution was sterilised by passing through a 0.2µm filter then stored at 4°C.

46. Herring Testes Carrier DNA

Supplied with the Yeastmaker™ Yeast Transformation System 2. Prior to use, ~15µL of herring DNA was incubated at 100°C for 5 minutes then immediately chilled on ice twice.

47. 100mM IPTG

500mg IPTG Powder
20mL ddH_2O
IPTG powder was dissolved in ddH_2O, filter sterilised by passing through a 0.2µm filter then stored in 1mL aliquots at -20°C.

48. 100mg/mL Kanamycin

100mg Kanamycin powder
1mL ddH_2O
Kanamycin powder was dissolved in ddH_2O and stored at -20°C.

49. LB Agar

5g Tryptone
2.5g Yeast Extract
5g Sodium Chloride
7.5g Agar Bacteriological
Reagents were dissolved in 400mL ddH_2O, the pH adjusted to 7.0 and the volume adjusted to 500mL with ddH_2O. Agar was added and the solution autoclaved then stored at room temperature.

50. LB Agar/Ampicillin

500mL LB Agar[49]
500µL Ampicillin[7]
Prior to use, LB agar was melted, allowed to cool to approximately 60°C and ampicillin added to a final concentration of 100µg/mL. LB agar/ampicillin was then poured into petri dishes and allowed to set.

51. LB Agar/Ampicillin/X-Gal Plates

15mL LB Agar/Ampicillin[50]
LB agar/ampicillin plates were prepared as usual and allowed to set. 40µL of X-Gal (50mg/mL) was spread over the top.

52. LB Agar/Kanamycin

500mL LB Agar[49]
500µL Kanamycin[48]
Prior to use, LB agar was melted, allowed to cool to approximately 60°C and kanamycin added to give a final concentration of 100µg/mL. LB agar/kanamycin was then poured into petri dishes and allowed to set.

53. LB Broth

10g Tryptone
5g Yeast Extract
10g Sodium Chloride
Reagents were dissolved in 900mL of ddH_2O, pH was adjusted to 7.0 and the volume was adjusted to 1L with ddH_2O. The solution was then autoclaved and stored at room temperature.

54. LB Broth/Ampicillin

One µL of 100mg/mL ampicillin[7] was added per 1mL of LB Broth[53] to give a final concentration of 100µg/mL ampicillin.

55. LB Broth/Kanamycin

One µL of 100mg/mL kanamycin[48] was added per 2mL of LB Broth to give a final concentration of 50µg/mL kanamycin.

56. 10% LB/Glycerol

9mL LB Broth[53]
1mL Glycerol
Glycerol was added to LB broth and reagents thoroughly mixed.

57.10X L-Histidine HCl Monohydrate

20mg L-Histidine HCl Monohydrate
100mL ddH_2O
Reagents were combined and the solution autoclaved and stored at 4°C.

58. 10X L-Leucine

100mg L-Leucine
100mL ddH_2O
Reagents were combined and the solution autoclaved and stored at 4°C.

59. 10X (1M) Lithium Acetate

51g LiAc

Lithium acetate was dissolved in 450mL ddH_2O, the pH adjusted to 7.5 using dilute acetic acid and the volume adjusted to 500mL. The solution was then autoclaved and stored at room temperature.

60. Low-Fade Mounting Media

5mL Tris-Phosphate Buffer[145]
75mL ddH_2O
2 drops 1% Phenol Red[77]
20g Polyvinyl Alcohol
30mL Glycerol
100mg Chlorobutanol
Tris-phosphate buffer, ddH_2O and phenol red were combined. The polyvinyl alcohol was added and the solution incubated at 60°C for 2-3 hours with occasional swirling until dissolved. The glycerol and chlorobutanol were added and the pH adjusted to below 8.2 with Tris-phosphate as necessary. The solution was stored in aliquots at -20° with the working aliquot stored at 4°C.

61. Luciferase Buffer

250µL 1M Tris HCl[144] pH 7.8
150µL 0.5M $MgSO_4$[65]
165µL 1M DTT[25]
1µL 0.5M EDTA[34]
12.5µL 100mM Co-Enzyme A[11]
25µL 100mM D-Luciferin[21]
25µL 100mM ATP[4]
250µL 10% Triton X-100[147]
4.2mL ddH_2O
Reagents were combined immediately prior to use and shielded from light.

62. Lysis Solution

Supplied with the Poly (A) Pure™ mRNA Purification Kit

63. Lysozyme 10mg/mL

100mg Lysozyme
2mL 1M Tris HCl[144] pH 8.0
8mL ddH_2O
Reagents were combined and the solution filter sterilised by passing through a 0.2µm filter. Lysozyme was then stored in 1mL aliquots at -20°C.

64. 1M Magnesium Chloride

203.3g $MgCl_3.6H_2O$
Magnesium chloride was dissolved in 800mL ddH_2O and the volume adjusted to 1L. The solution was then autoclaved and stored at room temperature.

65. 0.5M Magnesium Sulphate

12g $MgSO_4.7H_2O$
Magnesium sulphate was dissolved in 80mL ddH_2O and the volume adjusted to 100mL. The solution was then autoclaved and stored at room temperature.

66. Membrane Binding Solution

Supplied with the Wizard® SV Gel and PCR Clean-Up System (4.5M guanidine isothiocyanate, 0.5M potassium acetate pH 5.0).

67. Membrane Wash Solution

Supplied with the Wizard® SV Gel and PCR Clean-Up System (10mM potassium acetate pH 5.0, 80% ethanol, 16.7µM EDTA pH 8.0).

68. 1X MOPS Buffer

100mL 10X MOPS Buffer[69]
900mL DEPC-Treated H_2O[16]
Reagents were combined immediately prior to use.

69. 10X MOPS Buffer

41.2g MOPS
40mL 0.5M EDTA pH 8.0 (DEPC)[35]
6.56g Sodium Acetate
1mL DEPC
MOPS and sodium acetate were dissolved in 800mL of ddH_2O and the pH was adjusted to 7.0 using 10M sodium hydroxide. 0.5M EDTA pH 8.0 was added and the volume adjusted to 1L with ddH_2O. 1mL of DEPC was added and the solution was mixed and left overnight. 10X MOPS buffer was then autoclaved and stored in the dark at room temperature.

70. MOPS/Formaldehyde Gel

1g Agarose
72mL DEPC-Treated H_2O[16]
10mL 10X MOPS Buffer[69]
18mL Formaldehyde
Agarose was dissolved in DEPC-treated H_2O by heating in a microwave. 10X MOPS buffer was next added followed by formaldehyde in a fume hood. The gel was poured into a casting tray and allowed to set in a fume hood covered with plastic film.

71. 5X Passive Lysis Buffer (PLB)

(Supplied with Dual-Luciferase® Reporter Assay). Solution was diluted to 1X with ddH_2O immediately prior to use.

72. PBS (Phosphate Buffered Saline)

8g Sodium Chloride
0.2g Potassium Chloride
1.44g Disodium Hydrogen Orthophosphate
0.44g Potassium Dihydrogen Orthophosphate
Reagents were dissolved in 800mL of ddH_2O, pH was adjusted to 7.2 then the volume was adjusted to 1L with ddH_2O. The solution was autoclaved and stored at room temperature.

73. 5X PCR Buffer

5mL *Taq* 10X PCR Buffer minus $MgCl_2$ (Supplied with *Taq* DNA polymerase)
200µL 25mM dNTP[23]
4.8mL ddH_2O
Reagents were combined and stored at -20°C.

74. 10X PCR Buffer with $MgSO_4$

Supplied with *Pfu* DNA Polymerase (200mM Tris-HCl pH8.8, 100mM KCl, 100mM $(NH_4)_2SO_4$, 20mM $MgSO_4$, 1mg/mL nuclease-free BSA, 1% Triton® X-100)

75. 50% PEG 3550

250g PEG-3350

PEG-3350 was dissolved in 500mL ddH_2O and the solution stored at room temperature.

76. PEG/LiAc/TE

800µL 50% PEG-3350[75]
100µL 10X 1 M LiAc[59]
100µL 10X TE[141]
Reagents were combined immediately prior to use.

77. 1% Phenol Red

10mg Phenol Red Sodium Salt
1mL ddH_2O
Reagents were combined and stored at room temperature.

78. 1M PIPES

30.43g PIPES
100mL ddH_2O
Reagents were dissolved in 80mL of ddH_2O, the pH adjusted to 7.0 and the volume made to 100mL with ddH_2O. The solution was sterilised by passing through a 0.2µm filter then stored at room temperature.

79. 1Kb Plus™ Mol. Weight Marker

250µL 1Kb Plus Mol.Weight Marker
833.3µL 6X DNA Loading Dye[22]
Molecular weight marker was combined with freshly prepared DNA loading dye and the volume adjusted to 5mL with freshly prepared storage buffer[132]. Solution was dispensed into 1mL aliquots and stored at -20°C.

80. 200mM PMSF

348.4mg PMSF
10mL Isopropanol
PMSF was dissolved in isopropanol in a fume hood and the solution stored at room temperature.

81. 12% Polyacrylamide Separating Gel

6ml 30% Acrylamide[1]
5.03mL ddH_2O
3.75mL 1M Tris HCl[144] pH 8.8
75µL 20% SDS[110]
75µL 10% APS[6]
7.5µL TEMED
Tris HCl, acrylamide, SDS and ddH_2O were combined and mixed by inversion. APS and TEMED were added, the solution was mixed then immediately pipetted into the gel casting apparatus.

82. 6% Polyacrylamide Stacking Gel

2ml 30% Acrylamide[1]
6.65mL ddH_2O
1.25mL 1M Tris HCl[144] pH 8.8
50µL 20% SDS[110]
50µL 10% APS[6]
10µL TEMED
Tris HCl, acrylamide, SDS and ddH_2O, were combined and mixed by inversion. APS and TEMED were added. The solution was mixed then immediately pipetted into the gel casting apparatus.

83. 5M Potassium Acetate

24.5g Potassium Acetate
50mL ddH_2O
Potassium acetate was dissolved in 50mL of ddH_2O, and the solution was autoclaved and stored at room temperature.

84. 50% Protein A/G Sepharose

100µL Sepharose Slurry/mL Cell Lysate
Sepharose slurry was centrifuged at 4000rpm for 30 seconds and the supernatant removed. The sepharose was then washed 3X with 400µL cold (4°C) PBS followed by centrifugation at 4000rpm for 30 seconds and the supernatant removed. Sepharose was resuspended in an equal volume of cold (4°C) PBS to yield a 50% slurry. Protein A and Protein G were prepared fresh immediately prior to use.

85. RIPA Buffer

1.6mL ddH_2O
625µL 1% Sodium Deoxycholate
125µL 1M Tris-HCl[144] pH 7.4
93.8µL 4M Sodium Chloride[115]
25µL NP-40
12.5µL 200mM Na_3VO_4[121]
12.5µL 200mM PMSF[80]
5µL 0.5M EDTA[34]
5µL 0.5M Sodium Fluoride[119]
¼ Mini-protease inhibitor tablet
The mini-protease inhibitor tablet was dissolved in ddH_2O, then Tris HCl, NaCl, NP-40, Na-deoxycholate, EDTA, NaF, Na_3VO_4 were added, and the solution stored at 4°C for up to 5 days. Immediately before use, PMSF was added.

86. RNA Denaturing Buffer

1µL 10X MOPS[69]
1.75µL Formaldehyde
5µL Formamide
Reagents were combined then added to RNA samples.

87. RNA Loading Dye

5mL Glycerol
10µL 1M EDTA pH 8.0 (DEPC)[35]
25mg Bromophenol Blue
Reagents were combined, dispensed into 500µL aliquots and stored at –20°C. Prior to use, 0.5µL of ethidium bromide was added to 1µL of RNA loading dye for each RNA sample.

88. 10mg/mL RNaseA

100mg RNaseA
100µL 1M Tris-HCl[144] pH 7.5
37.5µL 4M Sodium Chloride[115]
Reagents were combined and the volume adjusted to 10mL with ddH_2O, heated to 100°C for 15 minutes then cooled slowly to room temperature. Solution was then dispensed into 1mL aliquots and stored at -20°C.

89. RPMI 1640 Medium

1 sachet RPMI 1640 with L-Glutamine
1L Baxter H_2O
2g Sodium Bicarbonate
RPMI 1640 powder was dissolved in Baxter H_2O, sodium bicarbonate was added, and the medium was filtered using a 0.2µm filter into sterilised bottles then stored at 4°C.

90. RPMI/5% CS-Fœtal Calf Serum

475m RPMI 1640 Medium[89]
25ml Charcoal Stripped-FCS
Reagents were combined and stored at 4°C.

91. RPMI/10% Fœtal Calf Serum

900ml RPMI 1640 Medium[89]
100ml Fœtal Calf Serum (FCS)
Reagents were combined and stored at 4°C.

92. RPMI/10% Fœtal Calf Serum/PS

900ml RPMI 1640 Medium[89]
100ml Fœtal Calf Serum
1000U Penicillin (100U/mL)
1mg Streptomycin (100µg/mL)
Reagents were combined and stored at 4°C.

93. 2X Sample Buffer (SDS-PAGE)

2.5mL 1M Tris-HCl[144] pH 6.8
1mL Glycerol
400µL 20% SDS[110]
200µL β-Mercaptoethanol
0.6mg Bromophenol Blue
Reagents were combined and the volume adjusted to 10mL with ddH_2O. The solution was dispensed into 1mL aliquots and stored at -20°C.

94. 10X Sample Buffer (SDS-PAGE)

12.5mL Glycerol
2.5mL 1M Tris HCl[144] pH 6.8
2.5mL 20% SDS[110]
2.5mL β-Mercaptoethanol
0.25g Bromophenol Blue
Reagents were combined and the volume adjusted to 25mL with ddH_2O. The solution was dispensed into 1mL aliquots and stored at -20°C.

95. SD/- Ade/-His/-Leu/-Trp Medium

300mg -Ade/-His/-Leu/-Trp Dropout
3.35g Yeast Nitrogen Base
25mL 40% Glucose[41]
Yeast nitrogen base and dropout supplement were dissolved in 475mL ddH_2O and the pH adjusted to 5.8. The solution was then autoclaved, allowed to cool to ~55°C, the glucose added and the solution stored at room temperature.

96. SD/-Ade/-His/-Leu/-Trp Agar

150mg -Ade/-His/-Leu/-Trp Dropout
1.675g Yeast Nitrogen Base
5g Agar Bacteriological
12.5mL 40% Glucose[41]
Yeast nitrogen base and dropout supplement were dissolved in 237.5mL ddH_2O and the pH adjusted to 5.8. Agar was then added and the solution autoclaved then allowed to cool to ~55°C. Glucose was added and 25mL per plate poured into petri dishes and allowed to set. Plates were stored inverted at 4°C.

97. SD/-Ade/-His/-Leu/-Trp-X-α-Gal Agar

SD/-Ade/-His/-Leu/-Trp Agar Plates[96]
X-α-Gal[157]
Prior to use, 100µL of X-α-Gal per plate was spread and plates were allowed to dry for 15 minutes at 30°C prior to use.

98. SD/-Ade/-Trp-X-α-Gal Agar

150mg -Ade/-His/-Leu/-Trp Dropout
1.675g Yeast Nitrogen Base
25mL 10X L-Histidine HCl Monohydrate[57]
25mL 10X L-Leucine[58]
5g Agar Bacteriological
12.5mL 40% Glucose[41]
Yeast nitrogen base and dropout supplement were dissolved in 187.5mL ddH_2O, the histidine and leucine were added and the pH adjusted to 5.8. Agar was added and the solution autoclaved then allowed to cool to ~55°C. Glucose was added and 25mL per plate poured into petri dishes and allowed to set. Prior to use, 100µL of X-α-Gal was spread and the plates dried for 15 minutes at 30°C.

99. SD/-His/-Leu/-Trp Agar

155mg -His/-Leu/-Trp Dropout
1.675g Yeast Nitrogen Base
5g Agar Bacteriological
12.5mL 40% Glucose[41]
Yeast nitrogen base and dropout supplement were dissolved in 237.5mL ddH_2O and the pH adjusted to 5.8. Agar was added and the solution was autoclaved then allowed to cool to ~55°C. Glucose was added and 25mL per plate poured into petri dishes and allowed to set. Plates were stored inverted at 4°C.

100. SD/-His/-Leu/-Trp-X-α-Gal Agar

SD/-His/-Leu/-Trp Agar Plates[99]
X-α-Gal[157]
Prior to use, 100µL of X-α-Gal per plate was spread and plates were dried for 15 minutes at 30°C prior to use.

101. SD/-His/-Trp-X-α-Gal Agar

155mg -His/-Leu/-Trp Dropout
25mL 10X L-Leucine[58]
1.675g Yeast Nitrogen Base
5g Agar Bacteriological
12.5mL 40% Glucose[41]
Yeast nitrogen base and dropout supplement were dissolved in 212.5mL ddH_2O, the leucine added and the pH adjusted to 5.8. Agar was added and the solution was autoclaved then allowed to cool to ~55°C. Glucose was added and 25mL per plate poured into petri dishes and allowed to set. Prior to use, 100µL of X-α-Gal was spread and the plates were dried for 15 minutes at 30°C.

102. SD/-Leu Agar

172.5mg -Leu Dropout
1.675g Yeast Nitrogen Base
5g Agar Bacteriological
12.5mL 40% Glucose[41]
Yeast nitrogen base and dropout supplement were dissolved in 237.5mL ddH_2O and the pH adjusted to 5.8. Agar was added and the solution was autoclaved then allowed to cool to ~55°C. Glucose was added and 25mL per plate poured into petri dishes and allowed to set. Plates were stored inverted at 4°C.

103. SD/-Leu Medium

172.5mg -Leu Dropout
1.675g Yeast Nitrogen Base
12.5mL 40% Glucose[41]
Yeast nitrogen base and dropout supplement were dissolved in 237.5mL ddH_2O and the pH adjusted to 5.8. The solution was then autoclaved, allowed to cool to ~55°C and the glucose added. Medium was stored at room temperature.

104. SD/-Leu/-Trp Agar

160mg -Leu/-Trp Dropout
1.675g Yeast Nitrogen Base
5g Agar Bacteriological
12.5mL 40% Glucose[41]
Yeast nitrogen base and dropout supplement were dissolved in 237.5mL ddH_2O and the pH adjusted to 5.8. Agar was added and the solution was autoclaved then allowed to cool to ~55°C. Glucose was added and 25mL per plate poured into petri dishes and allowed to set. Plates were stored inverted at 4°C.

105. SD/-Leu/-Trp Medium

160mg -Leu/-Trp Dropout
1.675g Yeast Nitrogen Base
12.5mL 40% Glucose[41]
Yeast nitrogen base and dropout supplement were dissolved in 237.5mL ddH_2O and the pH adjusted to 5.8. The solution was then autoclaved, allowed to cool to ~55°C and the glucose added. Medium was stored at room temperature.

106. SD/-Trp Agar

185mg -Trp Dropout
1.675g Yeast Nitrogen Base
5g Agar
12.5mL 40% Glucose[41]
Yeast nitrogen base and dropout supplement were dissolved in 237.5mL ddH_2O and the pH adjusted to 5.8. Agar was added and the solution autoclaved then allowed to cool to ~55°C. Glucose was added and 25mL per plate poured into petri dishes and allowed to set. Plates were stored inverted at 4°C.

107. SD/-Trp Medium

185mg -Trp Dropout
1.675g Yeast Nitrogen Base
12.5mL 40% Glucose[41]
Yeast nitrogen base and dropout supplement were dissolved in 237.5mL ddH_2O and the pH adjusted to 5.8. The solution was then autoclaved, allowed to cool to ~55°C and the glucose added. Medium was stored at room temperature.

108. SD/-Trp/Kan Medium

Ten µL of 100mg/mL kanamycin[48] was added per 50mL of SD/-Trp Medium[107] to give a final concentration of 20µg/mL kanamycin.

109. SD/-Trp-X-α-Gal Agar

SD/-Trp Agar Plates[106]
X-α-Gal[157]
Prior to use, 100µL of X-α-Gal per plate was spread and plates were allowed to dry for 15 minutes at 30°C

110. 20% SDS

10g SDS
50mL ddH_2O
SDS was dissolved in ddH_2O in a fume hood and the solution stored at room temperature.

111. 2M Sodium Acetate (pH 4.0)

32.8g Sodium Acetate
200mL DEPC-ddH_2O[16]
Sodium acetate was dissolved in 160mL of ddH_2O and the pH adjusted to 4.0 with glacial acetic acid. The volume was adjusted to 200mL with DEPC-ddH_2O, the solution autoclaved and stored at room temperature.

112. 3M Sodium Acetate (pH 4.6)

49.2g Sodium Acetate
200mL ddH_2O
Sodium acetate was dissolved in 160mL of ddH_2O and the pH was adjusted to 4.6 with glacial acetic acid. The volume was adjusted to 200mL with ddH_2O, and the solution was autoclaved and stored at room temperature.

113. 10mM Sodium Acetate (pH 5.2)

82mg Sodium Acetate
100mL ddH_2O
Sodium acetate was dissolved in 90mL of ddH_2O and the pH was adjusted to 5.2 with glacial acetic acid. The volume was adjusted to 100mL with ddH_2O, and the solution was autoclaved and stored at room temperature.

114. 0.9% Sodium Chloride

0.9g Sodium Chloride
100mL ddH_2O
Sodium chloride was dissolved in ddH_2O, the solution autoclaved then stored at room temperature.

115. 4M Sodium Chloride

117.2g Sodium Chloride
500mL ddH_2O
Sodium chloride was dissolved in ddH_2O, the solution autoclaved then stored at room temperature.

116. 5M Sodium Chloride

Supplied with the Poly (A) Pure™ mRNA Purification Kit.

117. 1% Sodium Deoxycholate

1g Sodium Deoxycholate
100mL ddH_2O
Sodium deoxycholate was dissolved in ddH_2O and the solution was autoclaved and stored in the dark at room temperature.

118. 1M Sodium Dihydrogen Orthophosphate

15.62g Sodium Dihydrogen Orthophosphate
100mL ddH_2O
Sodium dihydrogen orthophosphate was dissolved in ddH_2O and the solution autoclaved and stored at room temperature.

119. 0.5M Sodium Fluoride

2.1g Sodium Fluoride
100mL ddH_2O
Sodium fluoride was dissolved in ddH_2O in a fume hood, the solution autoclaved then stored at room temperature.

120. 10M Sodium Hydroxide

20g Sodium Hydroxide Pellets
50mL ddH_2O
Sodium hydroxide was dissolved in ddH_2O then stored at room temperature.

121. 200mM Sodium Orthovanadate

3.7g Sodium Orthovanadate
10mL ddH_2O
Reagents were combined and the pH adjusted to 10.0 with HCl. Solution was heated at 95°C until colourless (~10 minutes) then pH re-adjusted to 10.0. This procedure was repeated until solution remained colourless at pH10.0. Solution was then stored in 1mL aliquots at -20°C.

122. Solution I

0.9g Glucose
2.5mL 1M Tris HCL[144] pH 8.8
2mL 0.5M EDTA[34] pH 8.0
Reagents were combined, made up to 100mL with ddH_2O, autoclaved and stored at 4°C.

123. Solution II

1.86mL ddH_2O
100µL 20% SDS[110]
40µL 10M Sodium Hydroxide[120]
Sodium hydroxide and SDS were added to ddH_2O and mixed by inversion. Solution II was made fresh immediately prior to use.

124. Solution III

60mL 5M Potassium Acetate[83]
11.5mL Glacial Acetic Acid
28.5mL ddH_2O
Reagents were combined, autoclaved then stored at 4°C.

125. Sonication Buffer

25mL 1M Tris HCl[144] pH 8.0
5mL 5M Sodium Chloride[116]
1mL 0.5M EDTA[34]
469mL ddH_2O
Reagents were combined, autoclaved then stored at room temperature.

126. 1X SSC-DEPC

50mL 20X SSC-DEPC[128]
950mL DEPC-Treated ddH_2O[16]
Reagents were combined immediately prior to use.

127. 20X SSC

175.3g Sodium Chloride
88.2g Sodium Citrate
Sodium chloride and sodium citrate were dissolved in 900mL ddH_2O, pH adjusted to 7.0 and the volume was adjusted to 1L with ddH_2O. The solution was then autoclaved and stored at room temperature.

128. 20X SSC-DEPC

1L 20X SSC[127]
1mL DEPC
One mL of DEPC was added to 20X SSC, the solution was mixed, left overnight then autoclaved and stored at room temperature.

129. 1X Stop & Glo® Buffer

(Supplied with Dual-Luciferase® Reporter Assay). Buffer was stored at -20°C in the dark.

130. 1X Stop & Glo® Reagent

20µL of 50X Stop & Glo® Substrate was added to 1mL of 1X Stop & Glo® Buffer immediately prior to use.

131. 50X Stop & Glo® Substrate

(Supplied with Dual-Luciferase® Reporter Assay). Stop & Glo® Substrate was dissolved in Stop & Glo® Substrate solvent, vortexed for 10 seconds and stored at -80°C in the dark.

132. Storage Buffer

50µL 1M Tris HCl[144] pH 7.5
10µL 0.5M EDTA[34] pH 8.0
62.5µL 4M Sodium Chloride[115]
Reagents were combined and the volume made up to 5mL with ddH_2O.

133. 20% Sucrose

20g Sucrose
100mL ddH_2O
Sucrose was dissolved in 25mL ddH_2O and made up to 100mL then stored at room temperature.

134. 1X TAE (Tris Acetate EDTA)

100mL 50X TAE[135]
4.9L ddH_2O
Solutions were combined and stored at room temperature.

135. 50X TAE (Tris Acetate EDTA)

242g Tris Base
57.1mL Glacial Acetic Acid
100mL 0.5M EDTA[34] pH 8.0
Tris base was dissolved in ddH_2O, glacial acetic acid and EDTA were added and the volume was adjusted to 1L with ddH_2O. The solution was then autoclaved and stored at room temperature.

136. TBS (Tris Buffered Saline)

50mL 1M Tris HCl[144] pH 7.4
37.5mL 4M Sodium Chloride[115]
Reagents were combined, the volume was adjusted to 1L with ddH_2O and stored at room temperature.

137. TBS-3% Blotto

10mL TBS[136]
0.3g Skim Milk Powder
Milk powder was dissolved in TBS on the day of use.

138. TBST (TBS Tween)

500mL TBS[136]
1mL Tween 20
Reagents were combined, mixed by inversion and stored at room temperature.

139. TBST-1% Blotto

30mL TBST[138]
0.3g Skim Milk Powder
Milk powder was dissolved in TBST on the day of use.

140. TE Buffer

Supplied with the Concert™ High Purity Plasmid Purification System (10mM Tris-HCl pH 8.0, 0.1mM EDTA).

141. 10X TE Buffer

6.05g Tris Base
10mL 0.5M EDTA[34]
Tris base was dissolved in 450mL ddH_2O, the EDTA added and the pH adjusted to 7.5 using concentrated HCl. The volume was adjusted to 500mL with ddH_2O and the solution autoclaved and stored at room temperature.

142. 1X TE

1mL 10X TE Buffer[141]
9mL ddH_2O
Reagents were combined immediately prior to use.

143. 1X TE/LiAc

1mL 10X TE Buffer[141]
1mL 10X LiAc[59]
8mL ddH_2O
Reagents were combined immediately prior to use.

144. 1M Tris HCl (pH 6.8, 7.4, 7.5, 7.6, 8.0, 8.8)

121.1g Tris Base
1L ddH_2O
Tris base was dissolved in 800mL of ddH_2O, the pH was adjusted with concentrated HCl and the volume was adjusted to 1L with ddH_2O. The solution was then autoclaved and stored at room temperature.

145. Tris-Phosphate Buffer

50mL 1M Tris HCl[144]
1M Sodium dihydrogen orthophosphate[118] was added dropwise to Tris until a pH of 9.0 was obtained.

146. 0.2% Triton X-100

100µL 10% Triton X-100[147]
4.9mL PBS[72]
Reagents were combined immediately prior to use.

147. 10% Triton X-100

5mL Triton X-100
45mL PBS[72]
Reagents were combined and the solution stored at room temperature shielded from light.

148. Transformation Solution (BL21)

1.0g Tryptone
0.5g Yeast Extract
0.5g Sodium Chloride
10.0g PEG-3350
5.0mL DMSO
5.0mL 1M Magnesium Chloride[64]
Reagents were dissolved in 70mL ddH_2O, the pH adjusted to 6.5 and the volume made up to 100mL. The solution was then sterilised by passing through a 0.2µm filter and stored at 4°C for up to 6 months.

149. Wash Buffer

Supplied with the Poly (A) Pure™ mRNA Purification Kit

150. Wash Buffer I

5mL 20X SSC[127]
250µL 20% SDS[110]
44.75mL ddH_2O
Reagents were combined and the solution was made fresh prior to use.

151. Wash Buffer II

2.5mL 20X SSC[127]
250µL 20% SDS[110]
47.25mL ddH_2O
Reagents were combined and the solution was made fresh prior to use.

152. Wash Buffer III

250µL 20X SSC[127]
250µL 20% SDS[110]
49.5mL ddH_2O
Reagents were combined and the solution was made fresh prior to use.

153. Western Lysis Buffer

1.25mL 1M Tris HCL[144] pH 6.8
12.5mL 20% Sucrose[133]
2.5mL 20% SDS[110]
1.25mL β-Mercaptoethanol
7.5mL ddH_2O
Reagents were combined and stored in the dark at room temperature for up to one week.

154. 1X Western Running Buffer

180mL 5X Western Running Buffer[155]
720mL ddH_2O
Reagents were combined and the solution made fresh prior to use.

155. 5X Western Running Buffer

15g Tris Base
72g Glycine
5g SDS
1L ddH_2O
Reagents were dissolved in ddH_2O and stored at room temperature.

156. Western Transfer Buffer

3.03g Tris Base
14.4g Glycine
800mL ddH_2O
200mL Methanol
Tris base and glycine were dissolved in 600mL ddH_2O, methanol was added and the solution was made up to 1L with ddH_2O then stored at –20°C for at least three hours prior to transfer. The solution was made fresh on the day of use.

157. X-α-Gal/DMF

25mg X-α-Gal
6.25mL Dimethyl Formamide
Reagents were combined and stored in the dark at -20°C.

158. Yeast Lysis Buffer

0.5mL 1M Tris HCL[144] pH 8.0
2.5mL 20% SDS[110]
1.0mL Triton X-100
100µL 0.5M EDTA[34] pH8.0
290mg Sodium Chloride
Reagents were combined, the solution made up to 50mL with ddH_2O and stored at room temperature.

159. YPDA Agar

10g Peptone
5g Yeast Extract
7.5mL 0.2% Adenine[3]
25mL 40% Glucose[41]
10g Agar
Peptone and yeast were dissolved in 400mL ddH_2O, the pH adjusted to 6.5 and ddH_2O added to 475mL. The agar was added and the solution autoclaved then allowed to cool to ~55°C. The glucose and adenine were added and the YPDA agar stored at room temperature. Prior to use, agar was melted in a microwave and 15mL per plate was poured into 10cm petri dishes and allowed to set.

160. YPDA Medium

10g Peptone
5g Yeast Extract
7.5mL 0.2% Adenine[3]
25mL 40% Glucose[41]
Peptone and yeast were dissolved in 400mL ddH_2O, the pH adjusted to 6.5 and ddH_2O added to 467.5mL. The solution was then autoclaved, allowed to cool to ~55°C, the adenine and glucose added and the solution stored at room temperature.

161. YPD Plus Liquid Medium

Supplied with the Yeastmaker™ Yeast Transformation System 2.

Appendix 2 – Primers

PCR Primers	**Nucleotide Sequence**
ADLD Sense	$^{5'}$CTATTCGATGAAGATACCCCACCAAACCC$^{3'}$
ADLD Antisense	$^{5'}$AATCGTAGATACTGAAAAACCCCGCAAGTTCAC$^{3'}$
BAC Sense	$^{5'}$AGAAGGATTCCTATGTGGGCGACGA$^{3'}$
BAC Antisense	$^{5'}$CGAGTACATCACGATGCCAGTGGTA$^{3'}$
CDS III Oligo d(T)	$^{5'}$ ATTCTAGAGGCCGAGGCGGCCGACATG-d(T)$_{30}$VN-$^{3'}$[vii][4]
FLJBamHI Sense	$^{5'}$ATGGGATCCATGGAGCAGTGT$^{3'}$
FLJBamHI Antisense	$^{5'}$ATGGGATCCTCAGAATATGATGCG$^{3'}$
pCMV Sense	$^{5'}$ATGGTCGACTATGGAGCAGTGTGCG$^{3'}$
FLJSalI Sense	$^{5'}$ATGGTCGACTTATGGAGCAGTGTGCG$^{3'}$
FLJSalI Antisense	$^{5'}$ATGGTCGACTCAGAATATGATGCGTTT$^{3'}$
FLJTOPO Sense	$^{5'}$ATTATGGAGCAGTGTGCGTGCGTG$^{3'}$
FLJTOPO Antisense	$^{5'}$GAATATGATGCGTTTCCCATCTGC$^{3'}$
5' PCR Sense	$^{5'}$ TTCCACCCAAGCAGTGGTATCAACGCAGAGTGG$^{3'}$
3' PCR Anti-Sense	$^{5'}$ GTATCGATGCCCACCCTCTAGAGGCCGAGGCGGCCGACA$^{3'}$
pGEX Sense	$^{5'}$GGGCTGGCAAGCCACGTTTGGTG$^{3'}$
pGEX Antisense	$^{5'}$CCGGGAGCTGCATGTGTCAGAGG$^{3'}$
SMART III™ Oligo	$^{5'}$AAGCAGTGGTATCAACGCAGAGTGGCCATTATGGCCGGG$^{3'}$

Sequencing Primers	**Nucleotide Sequence**
BGHREV Antisense	$^{5'}$TAGAAGGCACAGTCGAGG$^{3'}$
DNA-BD Sense	$^{5'}$TCATCGGAAGAGAGTAG$^{3'}$
EGFP1266 Sense	$^{5'}$CATGGTCCTGCTGGAGTTCGTG$^{3'}$
FLJ789 Sense	$^{5'}$ATCTGTGAGACCTTTACCCGG$^{3'}$
FLJREV Antisense	$^{5'}$AAAGCTGACGCTAAGGGGGGA$^{3'}$
FLJREV2 Antisense	$^{5'}$CTGGAAGTGCCGAGCATAGCT$^{3'}$
pCMV Sense	$^{5'}$GATCCGGTACTAGAGGAACTGAAAAAC$^{3'}$
pGBREV Antisense	$^{5'}$GAAATTCGCCCGGAATTAGCT$^{3'}$

[viii] N = A, G, C, or T; V = A, G, or C.